Targeting IRAK1 in Tamoxifen-Resistant Breast Cancer

by

Devlin Wall-Coughlan

A thesis presented to

Maynooth University

for the degree of

Doctor of Philosophy

Kathleen Lonsdale Institute for Human Health Research

Department of Biology

Maynooth University

January 2021

Research Supervisor: Dr. Marion Butler

Head of Department: Prof. Paul Moynagh

Declaration of Authorship

I hereby declare that this thesis, submitted in candidature for the degree of Doctor of Philosophy of Biology with Maynooth University, has not been previously submitted for a degree to this or any other University. I further declare that work embodied in this thesis is my own and any assistance is acknowledged and clearly indicated.

Devlin Wall-Coughlan

Table of Contents

Acknowledgements

I would primarily like to take the opportunity to acknowledge two people.

Firstly, I would like to express my gratitude to my mother. Throughout my life, I have always been able to rely on your support towards everything that I do, irrespective of any ups and downs. You have always believed in my potential. Whilst it may not always be fully transparent, I am very appreciative of having your supportive presence in my life. You have inspired me to try to do something valuable with my existence.

Secondly, I would like to thank Dr. Marion Butler for providing me the opportunity to pursue this research. When I chose to undertake my final year undergraduate research project in your lab, I didn't really envisage pursuing a PhD. Your backing and support have been invaluable in my progression to this point. I feel like we have developed a very constructive working relationship, and you have pushed me to develop both my character and research career. I have really appreciated your enthusiasm and encouragement and it has been nice, through a challenging four years, to feel like my hard work is being valued.

Additionally, whilst they will probably never read this, I would like to thank several others. Ronan, you have been a real asset to my research and I've appreciated all of your advice throughout the last 3/4 years. Your random life perspectives have been almost as valuable as your technical expertise. Aisling, Jyotsna and Adam, you guys were all great to be around in the lab and made my time here more enjoyable. Camilla and Valentina, you were both wonderful to be around too and added a lot of charm to the lab in your brief time here. McCaffrey, can't believe you abandoned me after one year but the banter was great while it lasted. All other friends and family, I would hope that you are all aware of the value that you bring to my life already.

Finally, I would like to thank the Irish Research Council for funding me throughout this research, Dr. Karen English and Dr. Paul Dowling for their annual feedback and general advice throughout the 4 years as my advisor and assessor, and Dr. Sandra Roche and Dr. Denis Collins for providing valuable feedback at certain points during my PhD.

Summary

A role for Interleukin-1 receptor-associated kinase 1 (IRAK1) in promoting tumour growth and metastasis has been identified in recent years, across several aggressive cancer subtypes (Rhyasen *et al*. 2013, Wee *et al*. 2015, Dussiau *et al*. 2015). In certain cases, this has been linked to already recognized mechanisms associated with IRAK1 from its role in regulating immune responses, such as NF-κB activation (Wee *et al*. 2015). However, novel roles for IRAK1 in driving tumour growth have been identified that are unrelated to any previously defined role, including inhibiting PIDDosome-mediated apoptosis (Liu *et al*. 2019). This study showed that IRAK1 expression was elevated in tamoxifen-resistant (Tam-R) ER+ breast cancer, with IRAK1 knockdown significantly reducing the growth of Tam-R cells as assessed by 2D and 3D growth assays. Additionally, IRAK1 knockdown impaired the agonistic effects that tamoxifen has on the growth of Tam-R cells and re-sensitizes the cells to tamoxifen. This work identified a novel role for IRAK1 in regulating HER family expression in response to tamoxifen treatment, a significant finding as all members of the HER family have been linked to tamoxifen resistance previously (Britton *et al*. 2006, Cui *et al*. 2012, Thrane *et al*. 2013, Wege *et al*. 2018). Further, we identified an important role for IRAK1 in Aurora kinase A (Aurora-A) activation in response to tamoxifen treatment. Aurora-A activity has been linked to aggressive tumour growth and poor patient prognoses across a number of cancer subtypes, with Aurora-A inhibition being extensively studied as a potential therapeutic option (Bavetsias and Linardopoulos 2015). This study also examined the efficacy of using drugs that inhibit IRAK1 and JNK family kinases, alone or in combination, as novel therapeutic options for Tam-R breast cancer. JNK has already been linked to treatment resistance in TNBC and pancreatic cancer (Ebelt *et al*. 2017, Lipner *et al* 2020). We found that IRAK1 and JNK inhibition alone reduced Tam-R ER+ breast cancer cell growth, with less marked effects observed for tamoxifen-sensitive (Tam-S) cell lines with JNK specific inhibitors, as assessed by 2D and 3D cellular assays. However, combined inhibition of IRAK1 and JNK synergized to potently inhibit Tam-S and Tam-R ER+ breast cancer cell growth. These findings support progressing this research to *in-vivo* models of Tam-S and Tam-R ER+ breast cancer, as well as other breast and aggressive cancer subtypes. Overall, this work has identified a novel role for IRAK1 in

tamoxifen-resistant breast cancer and indicated the potential therapeutic benefits of targeting IRAK1 in this cancer subtype.

Abbreviations

5-FU: 5-fluorouracil

ABC-DLBCL: Activated B-Cell Diffuse Large B-Cell Lymphoma

AF: Activation Function

AIB1: Amplified In Breast cancer 1

AP1: Activator Protein 1

ATF4: cyclic AMP-dependent Transcription Factor 4

ATM: Ataxia Telangiectasia Mutated

ATP: Adenosine Tri-Phosphate

BAD: BCL2-associated Agonist of cell Death

BAK: BCL2 Antagonist/Killer

BCL2: B-Cell Lymphoma-2

Bcl-xl: BCL2-like extra large

BH3: B-cell Lymphoma-2 Homology-3

BID: BH3 Interacting-Domain death agonist

BIM: BCL2-Interacting Mediator of cell death

BSA: Bovine Serum Albumin

Ca2+: Calcium ion

cAMP: cyclic Adenosine Monophosphate

Cbl: E3 ubiquitin-protein ligase CBL

CCND1: Cyclin D1

CDK: Cyclin-Dependent Kinase

CDKI: Cyclin-Dependent Kinase inhibitor

cDNA: complementary Deoxyribonucleic Acid

ChIP-seq: Chromatin Immunoprecipitation – massively parallel DNA sequencing

CHK1: Checkpoint Kinase 1

CHOP: C/EBP Homologous Protein

CK: Casein Kinase

CSF: Charcoal-stripped FBS

CXCL: chemokine (C-X-C motif) Ligand

D: Aspartic Acid

DFS: Disease-Free Survival

DMEM: Dulbecco's Modified Eagle Medium

DMSO: Dimethyl Sulfoxide

DNA: Deoxyribonucleic Acid

DTT: Dithiothreitol

E2: Estradiol

EDTA: Ethylenediaminetetraacetic Acid

EF: helix-E-loop-helix-F

EGF: Epidermal Growth Factor

EGFR: Epidermal Growth Factor Receptor

EGR3: Early Growth Response 3

Elk-1: ETS domain-containing protein Elk-1

ERE: Estrogen Response Element

ERK: Extracellular signal-Regulated Kinase

FAK: Focal Adhesion Kinase

FBS: Fetal Bovine Serum

FKBP4: Peptidyl-Prolyl Cis-Trans Isomerase FKBP4

Flt3: Fms Like Tyrosine kinase 3

FOLFOX: Folinic Acid + 5-Fluorouracil + Oxaliplatin

FOXA1: Forkhead Box A1

FOXO: mammalian Forkhead transcription factors of the O class

GAPDH: Glyceraldehyde 3-phosphate dehydrogenase

GDP: Guanosine Diphosphate

GEM: Gemcitabine

Grb2: Growth factor receptor-bound protein 2

GREB1: Growth Regulation by Estrogen in Breast cancer 1

GSK3: Glycogen Synthase Kinase 3

GTP: Guanosine Triphosphate

HCC: Hepatocellular Carcinoma

HCL: Hydrochloric Acid

HDAC1: Histone Deacetylase 1

Mdm2: E3 ubiquitin-protein ligase MDM2

HER: Human Epidermal growth factor Receptor

HER4:ICD: Human Epidermal Growth Factor Receptor 4: Intracellular Domain

HNSCC: Head and Neck Squamous Cell Carcinoma

HRP: Horseradish Peroxidase

Hsp: Heat-shock protein

IGFR: Insulin-like Growth Factor Receptor

IgG: Immunoglobulin G

IKK: Inhibitor of κB Kinase

IL-1β: Interleukin-1 beta

IL-6: Interleukin 6

IL-8: Interleukin 8

IRAK: Interleukin-1 receptor-associated kinase 1

IκBα: Inhibitor of NF-κB alpha

JAK2: Janus Kinase 2

JM: Juxtamembrane region

JNK: c-Jun N-terminal Kinase

K: Lysine

LN+: Lymph Node positive

LVF: Linear Variable Filter

mAb: Monoclonal Antibody

MAPK: Mitogen-Activated Protein Kinase

MDS: Myelodysplastic Syndrome

MEM: Minimum Essential Medium

mRNA: messenger Ribonucleic Acid

mTOR: mammalian Target Of Rapamycin

mTORC1: mammalian Target Of Rapamycin/Raptor

mTORC2: mammalian Target Of Rapamycin/Rictor

MTS: 3-(4,5-dimethylthiazol-2-yl)-5-(3-carboxymethoxyphenyl)-2-(4-sulfophenyl)-2H-tetrazolium)

MYC: Myc proto-oncogene protein

MyD88: Myeloid Differentiation primary response 88

Na3VO4: Sodium Orthovanadate

NaCL: Sodium Chloride

NaF: Sodium Flouride

NCOR: Nuclear receptor Co-Repressor

NF-κB: Nuclear Factor kappa-light-chain-enhancer of activated B cells

NP-40: nonyl phenoxypolyethoxylethanol 40

Nrg-1: Neuregulin 1

OD: Optical Density

OS: Overall survival

p62: Sequestosome-1

PAK1: p21-Activated Kinase 1

PBS: Phosphate-Buffered Saline

PCNA: Proliferating Cell Nuclear Antigen

PDK1: 3-Phosphoinositide-Dependent protein Kinase 1

PH: Pleckstrin Homology

PI3K: Phosphoinositide 3-Kinase

PIDD: p53-induced Protein with a Death Domain

PIP2: Phosphatidylinositol 4,5-bisphosphate

PIP3: Phosphatidylinositol 3,4,5-trisphosphate

PKA: Protein Kinase A

PKC: Protein Kinase C

PLC: PhosphoLipase C

PLK1: Serine/Threonine-protein kinase PLK1

PMSF: phenylmethylsulfonyl flouride

PR: Progesterone Receptor

PTEN: Phosphatase and Tensin Homolog

PVDF: Polyvinylidene fluoride

qRT-PCR: quantitative Real-Time Polymerase Chain Reaction

RAD51: DNA repair protein RAD51

RFS: Relapse-Free Survival

RFU: Relative Flourescence Units

RLU: Relative Luminescence Units

ROS: Reactive Oxygen Species

ROX: carboxyrhodamine fluorescent dye

RSK: 90 kDa Ribosomal S6 Kinase

RT: Reverse Transcription

RTK: Receptor Tyrosine Kinase

S: Serine

S6K1: ribosomal protein S6 Kinase 1

SCID: Severe Combined Immunodeficiency

SDS-PAGE: Sodium Dodecyl Sulfate Polyacrylamide Gel Electrophoresis

SEM: Standard Error of the Mean

SERD: Selective Estrogen Receptor Degrader

SERM: Selective Estrogen Receptor Modulator

Shc: Src homology domain containing

shRNA: short hairpin Ribonucleic Acid

SIAH2: E3 ubiquitin-protein ligase SIAH2

siRNA: small interfering Ribonucleic Acid

SOS: Son Of Sevenless

SP1: Specificity Protein 1

SRC: Steroid Receptor Coactivator

STAT: Signal Transducer and Activator of Transcription

T: Threonine

TAB2: TGF-β-activated kinase 1 and MAP3K7-binding protein 2

T-ALL: T-cell Acute Lymphoblastic Leukemia

TAM: Tamoxifen

Tam-R: Tamoxifen-resistant

Tam-S: Tamoxifen-sensitive

TBS: Tris-buffered saline

TBST: TBS with Tween 20

TCF: T-Cell Factor

TEMED: Tetramethylethylenediamine

TFF1: TreFoil Factor 1

TGF-β: Transforming Growth Factor beta

TIR: Toll/Interleukin-1 Receptor

TKI: Tyrosine Kinase Inhibitor

TLR: Toll-Like Receptor

T_m: Melting Temperature

TNBC: Triple Negative Breast Cancer

TNF-α: Tumour Necrosis Factor alpha

TNM: Tumour, Nodes, Metastasis staging system

TRAF6: Tumour necrosis factor Receptor-Associated Factor 6

VP-16: Etoposide

XBP1: X-box Binding Protein 1

Y: Tyrosine

Chapter 1

General Introduction

1.1. Interleukin-1 receptor-associated kinase 1 (IRAK1).

1.1.1. IRAK1.

IRAK1 is a serine/threonine kinase that is recognised for its role in the innate immune response (Kawagoe *et al*. 2008, Gottipati *et al*. 2008, Flannery & Bowie 2010). The mammalian IRAK family consists of four members, IRAK1, IRAK2, IRAK-M and IRAK4 which all play important roles in regulating Interleukin-1 receptor (IL-1R) and Toll-like receptor (TLR) signalling pathways. IRAK1 was the first member of the family to be discovered, and is ubiquitously expressed in humans (Croston *et al*. 1995, Cao *et al*. 1996). The IRAK family only share around 30-40% sequence homology, although they are organised into similar structural domains. IRAK1 contains an N-terminal death domain (amino acids 1-103), followed by a proline-, serine- and threonine-rich region known as the ProST region (amino acids 104-198), a central kinase domain (amino acids 199-522) and a C-terminal domain that is separated into 2 sub-domains, C1 and C2 (amino acids 523-618 and 619-712, respectively). IRAK1 is catalytically active, with a lysine residue at K239 in the ATP-binding pocket and a critical aspartate residue at D340 believed to be essential for kinase function (Gottipati *et al*. 2008, Flannery and Bowie. 2010, Jain *et al*. 2014).

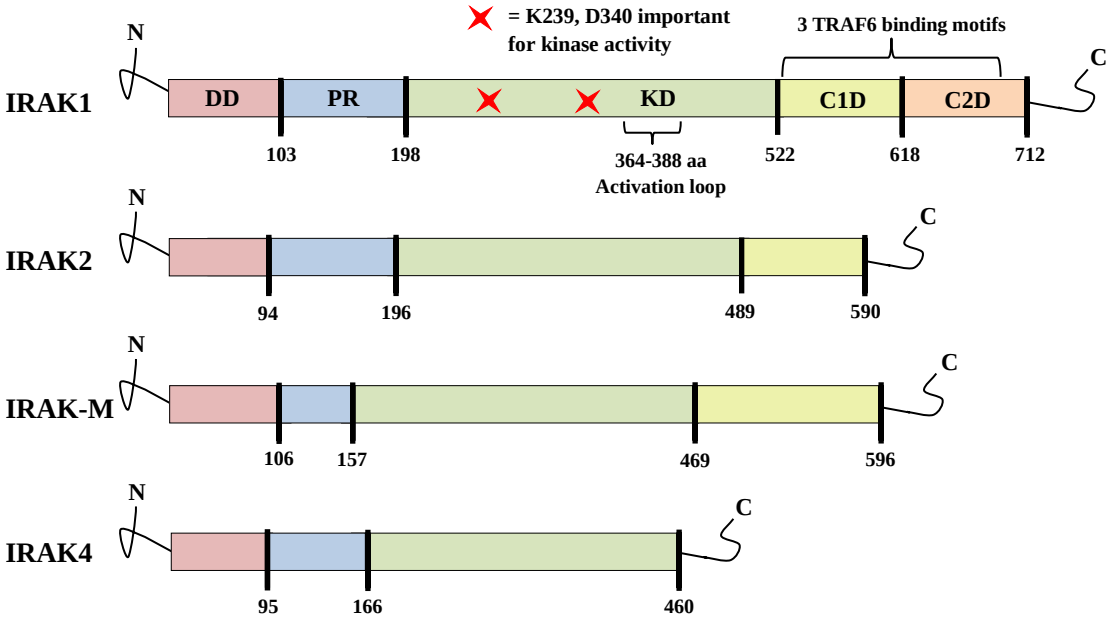

Figure 1.1. Structural representation of the IRAK1 family members. Image adapted from Gottipati *et al.* 2008 and Flannery & Bowie, 2010. DD = Death Domain; PR = ProST Region; KD = Kinase Domain; C1D = C-terminal Domain 1; C2D = C-terminal Domain 2.

Following the stimulation of IL-1R/TLR, a signalling cascade is initiated by the Toll/Interleukin-1 Receptor (TIR) adaptor myeloid differentiation primary response protein (MyD) 88. MyD88 is recruited to the intracellular TIR domain of the receptors after ligand binding and interacts with the receptors via its own TIR domain. MyD88 oligomerizes and then interacts with IRAKs through their death domains, with IRAK4 binding directly to MyD88 first (Jain *et al.* 2014). IRAK1 is then recruited to the complex, and subsequently undergoes a series of phosphorylation events leading to its full enzymatic activation. IRAK1 is initially phosphorylated at T209, which triggers a conformational change in the kinase domain allowing for subsequent phosphorylation to take place. Phosphorylation at T209 is essential to the kinase activity of IRAK1, with mutations of the residue resulting in loss of kinase function. Full activation of IRAK1 then requires phosphorylation at T387 in its activation loop. IRAK4 has been previously suggested to phosphorylate IRAK1 at both of these sites (Flannery and Bowie. 2010, Jain *et al.* 2014). However, more recent work has shown that both sites are also recognised to undergo autophosphorylation and a recent study found that the activation of IRAK1 does not require phosphorylation by IRAK4 (Vollmer *et al.* 2017). IRAK1 activation is completed through hyper-autophosphorylation in the ProST domain, which triggers the dissociation of IRAK1 from the complex. Subsequently, IRAK1 interacts with TNF-receptor associated factor 6 (TRAF6) through its C-terminal domain.

This allows for the activation of a signalling complex that can phosphorylate the inhibitor of κB kinase (IKK) complex (consisting of IKKα, IKKβ & IKKγ), resulting in NF-κB activation, or activate mitogen activated protein kinases (MAPKs) (Flannery & Bowie 2010, Jain *et al*. 2014).

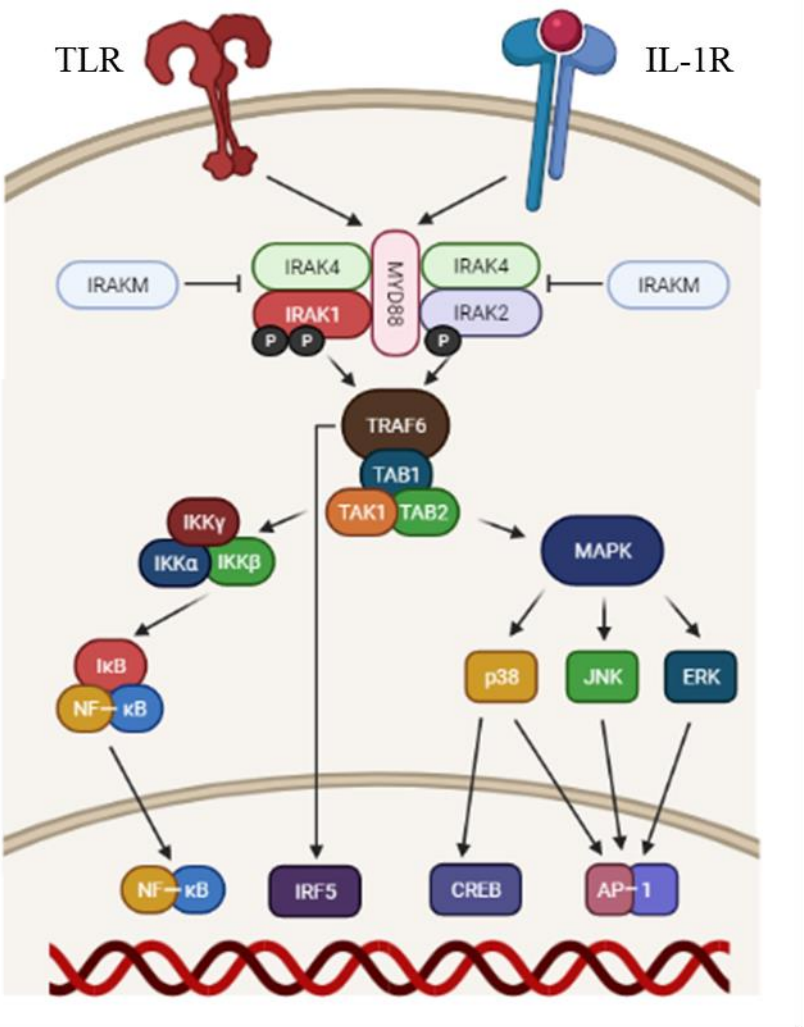

Figure 1.2. TLR/IL-1R signalling cascade. Image adapted from Jain et al. 2014. Ligand binding to the TLR/IL-1R triggers the recruitment of MyD88 and members of the IRAK family to the intracellular domain of the receptors. This leads to the activation of IRAK1, which can subsequently associate with TRAF6 resulting in the activation of NF-κB and MAPK signalling pathways. This results in the activation of transcription factors (NF-κB, AP-1) which regulate the expression of a broad array of genes involved in proliferation, apoptosis and inflammatory responses.

In mammals, the NF-κB transcription factor family consists of five members that form homo- and heterodimers: p65 (RELA), RELB, cREL, NF-κB1 (p50 and its precursor p105) and NF-κB2 (p52 and its precursor p110). In most quiescent cells NF-κB dimers are bound to inhibitory molecules of the IκB protein family, which attach to the DNA-binding domain rendering them transcriptionally inactive (Baud and Karin. 2009, Hoesel and Schmid. 2013). NF-κB signalling is separated into a classical canonical pathway, which mainly involves p65/p50 dimers, and an alternative pathway (Brasier 2006). IRAK1 is exclusively linked to the canonical pathway where, following IL-1R/TLR stimulation, the activation of the IKK complex triggers the phosphorylation of the IκB molecules at specific serine residues leading to their proteasome-mediated degradation (Baud and Karin. 2009). This frees the NF-κB dimers to translocate to the nucleus and regulate the transcription of a wide range of target genes involved in inflammation, proliferation and survival (Pahl 1999). The kinase activity of IRAK1 is dispensable in IL-1R mediated NF-κB activation, with the adaptor function of IRAK1 being essential in this process (Jain *et al*. 2014). Aberrations in the regulation of NF-κB are known to be involved in a vast amount of immune disorders, including psoriasis and Severe Combined Immunodeficiency (SCID) (Jordan *et al*. 2012, Stepensky *et al.* 2013). NF-κB is also recognised to have an oncogenic role in certain malignancies, most commonly lymphomas. The Activated B-cell subtype of Diffuse Large cell B-cell lymphoma (ABC-DLBCL) is highly dependent on constitutive NF-κB activation to maintain its transformed phenotype and disrupting NF-κB activity has been examined as a potential therapeutic strategy (Davis *et al*. 2001, Calado *et al*. 2010, Pulvino *et al*. 2012).

The mammalian MAPK family consists of extracellular signal-regulated kinase (ERK), c-Jun NH2-terminal kinase (JNK) and p38. ERK is activated downstream of growth factor receptors such as Epidermal Growth Factor Receptor (EGFR), while JNK and p38 are primarily activated by pro-inflammatory cytokines such as IL-1β or cellular stresses (Raman *et al*. 2007). The activation of these MAPKs leads to the phosphorylation of a diverse range of target proteins including the transcription factors c-Jun and c-Myc and proteins involved in regulating apoptosis such as Bcl-2 and Bad (Scheid *et al.* 1999, Boucher *et al*. 2000, Sabapathy *et al*. 2004, Alarcon-Vargas and Ronai 2004,). Signalling through p38 and JNK has been specifically linked to regulating stress responses, apoptosis, inflammation and autophagy while signalling through ERK has been associated with cell

proliferation, migration and survival (Dhanasekaran & Reddy 2008, Roskoski 2012, Koul *et al.* 2013). As a result, aberrant activity of MAPKs has been linked to numerous inflammatory disorders, with the hyperactivation of ERK and JNK also being detected in various cancers, particularly endometrial and colon cancers (Cheung *et al.* 2014, Kim and Choi. 2015, Braicu *et al*. 2019).

1.1.2. IRAK1 in cancer.

The data highlighting an important role for IRAK1 in the development and progression of cancer has been building in recent years. IRAK1 has been found to be overexpressed and/or hyperactivated in a variety of cancers, particularly in aggressive subtypes such as leukemia, lymphoma, hepatocellular carcinoma (HCC) and triple-negative breast cancer (TNBC) (Ngo *et al.* 2011, Rhyasen *et al*. 2013, Wee *et al*. 2015, Li *et al.* 2016). The changes in IRAK1 expression and activity in these cancers have been attributed to aberrations in IL-1R/TLR signalling cascades, but new mechanisms independent of these pathways have been found in recent years (Rhyasen *et al.* 2013, Liu *et al.* 2019). The subsequent role that IRAK1 plays in the oncogenesis of these cancers is also varied. Most research involving IRAK1 in cancer has focused on its immune-associated role in NF-κB and MAPK activation, but unique new roles are being identified for IRAK1 in other critical cellular mechanisms including cell cycle regulation and apoptosis (Ni *et al*. 2018, Liu *et al.* 2019).

IRAK1 has been associated with the growth and survival of several forms of leukemia, with targeted inhibition of IRAK1 showing promising results. Rhyasen *et al.* (2013) showed that IRAK1 expression is increased in ~20% of myelodysplastic syndrome (MDS) patients and a subset of acute myeloid leukemia (AML) patients. This has been attributed to the deletion of the miR-146a gene, a microRNA that targets IRAK1 and is commonly deleted in MDS (Rhyasen *et al*. 2013). IRAK1 was also found to be hyperphosphorylated in all MDS cell lines and patient samples tested, although the reasons for this are inconclusive (Rhyasen *et al*. 2013). Targeted inhibition of IRAK1 kinase activity, using a dual IRAK1/IRAK4 inhibitor, blocked TRAF6 and NF-κB activation in MDS cells and reduced cell growth *in-vitro*, while increasing survival in a xenograft model of human MDS. Interestingly, IRAK1 knockdown in MDS cells induced potent apoptosis in vitro, compared to the modest apoptotic effect of the IRAK1/4 inhibitor. In the xenograft model, IRAK1 knockdown reduced tumourigenicity and significantly delayed mortality in mice (Rhyasen *et al.* 2013).

IRAK1 overexpression is also common in T-cell acute lymphoblastic leukemia (T-ALL) regardless of the underlying oncogenetic abnormality or immunogenetic state of arrest, but phosphorylation of IRAK1 at T209 is not present in certain forms of the disease even in response to IL-1β stimulation (Dussiau *et al.* 2015). IRAK1 knockdown reduced

proliferation, increased apoptosis and disrupted the cell cycle in T-ALL cell lines (Dussiau *et al.* 2015). These findings would indicate a complex role for IRAK1 in T-ALL, wherein the structural role of IRAK1 may play a role in T-ALL cell growth. Similar to what was observed in MDS, pharmacological inhibition of IRAK1 using a dual IRAK1/4 inhibitor reduced proliferation and increased apoptosis in T-ALL cells that exhibit phosphorylated IRAK1 but was much less effective than IRAK1 knockdown (Dussiau *et al.* 2015).

A role for IRAK1 in Activated B-cell diffuse large B-cell lymphoma (ABC-DLBCL) and Waldenströms macroglobulinemia has also been identified. ABC-DLBCL is an aggressive form of lymphoma that has a very poor prognosis for patients. Ngo *et al*. (2011) identified a mutant form of MyD88, termed MyD88 L265P, that is present in 29% of ABC-DLBCL cases. Their analysis established that this mutation in MyD88 causes the hyperphosphorylation of IRAK1, contributing to elevated NF-κB activation and resulting in increased cell survival in this lymphoma type. Through an RNAi screen, they found that shRNA knockdown of IRAK1 was toxic to all 5 ABC-DLBCL cell lines tested. However, IRAK1 kinase activity was not required for cell survival (Ngo *et al.* 2011).

The same MyD88 mutation is observed in ~95% of Waldenströms macroglobulinemia. Here, inhibition of IRAK1 and IRAK4 using a dual IRAK1/4 inhibitor showed anti-tumour effects *in-vitro* and *in-vivo* (Ni *et al.* 2018). These effects included inhibition of NF-κB activation. Interestingly, several other molecular responses were identified. IRAK1/4 inhibition disrupted the cell cycle, with reductions in cyclin-dependent kinase (CDK) 4/6 expression, suppressed the Akt/mammalian target of rapamycin (mTOR) signalling pathway, reduced the expression of c-Myc and induced the endoplasmic reticulum (ER) stress response, with increases in the expression of the key ER stress markers cyclic AMP-dependent Transcription Factor 4 (ATF) 4, X-box Binding Protein (XBP) 1 and C/EBP Homologous Protein (CHOP) (Ni *et al.* 2018).

Hepatocellular carcinoma (HCC) is an inflammatory-associated cancer that is a leading cause of cancer-related mortality worldwide (Siegel *et al.* 2020). Su *et al.* (2015) identified a correlation between IRAK1 phosphorylation at T209 and patient survival. Eighty-four HCC patients were seprarated into phospho-IRAK1 high or low based on immunohistochemical staining, with 27% of patients exhibiting IRAK1

hyperphosphorylation. Patients that exhibited high IRAK1 activation showed significantly worse overall survival when compared to the phospho-IRAK1 low cohort. They found that elevated IRAK1 activity increased the expression of the oncoprotein Gankyrin, through IRAK1 activation of JNK, promoting oncogenesis (Su *et al.* 2015). Subsequent analysis of 33 clinical HCC samples showed that IRAK1 was overexpressed in ~66% of HCC samples compared to adjacent normal tissues (Li *et al*. 2016). IRAK1 knockdown using two independent siRNAs reduced HCC cell line growth and increased the sensitivity of HCC cells to cisplatin-induced apoptosis. Following up with an IRAK1/4 inhibitor, they found that inhibition of IRAK1 phosphorylation at T209 reduced cell growth and migration in vitro and tumour growth *in-vivo,* confirming previous findings of the importance of active IRAK1 to HCC cell growth (Li *et al.* 2016). IRAK1 has also been linked to HCC stemness and drug resistance. Sorafenib, Doxorubicin and Cisplatin are the chemotherapeutic drugs widely used in HCC treatment but all show very poor response rates. Cheng *et al*. (2018) showed that IRAK1 expression was increased in HCC cells in response to drug treatment and that IRAK1 knockdown increased the sensitivity of these cells to drug-induced apoptosis. In xenograft models of HCC, the combination of an IRAK1/4 inhibitor and sorafenib significantly reduced tumour volumes (Cheng *et al*. 2018).

1.2. Breast Cancer

Breast cancer is the most commonly diagnosed cancer in women and the second leading cause of cancer related mortality in women (Siegel *et al.* 2020). Human breast cancer has always displayed significant heterogeneity in terms of its characteristics and response to therapy. Extensive gene expression profiling has allowed for improved molecular classification of breast cancers and further understanding of how to provide beneficial targeted therapies to patients with specific tumours. This concept was initially developed by Perou *et al*. 2000, who examined variation in gene expression patterns in breast tumours using complementary DNA microarrays. Their work identified molecular patterns that correlated with cellular growth rate, activation of signalling pathways and cellular composition. Analysis allowed for the separation of tumours into clinically described estrogen receptor positive or negative cohorts, with the ER+ cohort exhibiting increased expression of genes expressed in breast luminal cells including FOXA1 and XBP1 (Perou *et al*. 2000). This correlation was further supported by immunohistochemical analysis of breast luminal cell keratins 8/18 in ER+ tumours, while all but one of these tumours did not express HER2 at high levels (Perou *et al*. 2000). The expression of genes characteristic of breast basal epithelial cells (CXCL1, PIK3CA, EGFR) were found to be elevated in a clustered group of tumours. Subsequent immunohistochemical analysis of breast basal cell keratins 5/6 and 17 supported the basal-like profile of these tumours, which also failed to express ER and most genes associated with the ER profile (Perou *et al*. 2000). Additionally, HER2 overexpressing tumours were associated with high expression of specific genes (TRAF4, TIAF1) while showing low levels of ER expression and ER-related gene expression (Perou *et al*. 2000). These findings provided early molecular framework for precisely categorizing newly diagnosed breast cancer patients.

The understanding of this framework has evolved through the years and culminated in breast cancer subtypes being defined into 4 categories; Luminal A, Luminal B, HER2-overexpressing and basal-like (Goldhirsch *et al*. 2013). Luminal A breast cancer is ER and progesterone receptor positive, HER2-negative and exhibits low Ki-67 levels. Ki-67 is a cellular proliferation marker, with a Ki-67 level <14% acting as the cut-off for luminal A classification. Additionally, multi-gene expression assay analysis (21-gene recurrence score

assay) indicating a low recurrence risk is further indication of the Luminal A subtype (Goldhirsch *et al*. 2013). Luminal B breast cancer is separated into two sub-classes; HER2 negative and HER2 positive. Luminal B (HER2-) shows ER positivity, HER2 negativity and at least one additional factor out of high Ki-67 levels, Progesterone receptor negative or low and a high risk of recurrence based on the previously mentioned multi-gene expression assay. Luminal B (HER2+) is ER positive and HER2-overexpressed or -amplified, while having any Ki-67 or progesterone receptor status. HER2-overexpressing breast cancer exhibits HER2 overexpression or amplification, while ER and progesterone receptor are both absent. Basal-like breast cancer is widely recognized as a 'triple-negative' subtype, where ER, progesterone receptor and HER2 expression are absent. The overlap between triple-negative status and the basal-like subtype is only ~80% as low ER staining tumours can cluster into basal-like based on gene-expression analysis, while triple-negative breast cancer also incorporates some additional histological types including adenoid cystic carcinoma (Goldhirsch *et al*. 2013).

These advancements in molecular classification of breast cancer have allowed for the optimization of targeted treatment strategies to improve patient outcomes. The standard of care for breast cancer patients classified as ER+ currently includes endocrine therapy with the selective ER modulator Tamoxifen (Premenopausal) or an aromatase inhibitor (Postmenopausal) which both serve to impair ER function (Curigliano *et al*. 2017). These drugs are both discussed in more detail in section 1.3.2. These treatments are further combined with ovarian function suppression or chemotherapy in more aggressive ER+ breast cancer cases (Curigliano *et al*. 2017). The standard treatment of breast cancer patients that have developed HER2-overexpressing disease includes the use of the monoclonal antibody trastuzumab in combination with chemotherapy. Trastuzumab binds to the extracellular domain of the HER2 receptor and impairs receptor dimerization. In cases that are ER+ and HER2+, endocrine therapy can be combined with HER2 targeted therapy to optimize patient treatment (Curigliano *et al*. 2017). TNBC patients are currently recommended to receive treatment that includes anthracycline and taxane-based chemotherapeutics, while BRCA1/2 mutated TNBC cancers should receive alkylating chemotherapy (Curigliano *et al*. 2017).

These advancements in breast cancer classification and treatment optimization has led to breast cancer patient prognoses improving to the point where 5-year survival rates for stage 1 ER+ breast cancer now stand at ~99%, 5-year survival for stage 1 HER2+ breast cancer is ~95% and 5-year survival for stage 1 TNBC is ~85%, although TNBC cases are associated with a much higher chance of recurrence. TNBC also tends to be more advanced and these cases are associated with significantly reduced overall patient survival (Waks and Winer 2019).

1.2.1. IRAK1 in breast cancer.

Most relevantly, IRAK1 has recently been implicated in the tumourigenicity of aggressive forms of breast cancer (Wee *et al.* 2015, Goh *et al*. 2017, Liu *et al.* 2019). An early study focused on miR-146a indicated a potential role for IRAK1 in breast cancer (Bhaumik *et al*. 2008). Research on the TNBC cell line MDA-MB-231 showed that overexpression of miR-146a, known to target IRAK1 and TRAF6, reduced the metastatic potential of the cell line *in-vitro*, with significant reductions observed in migration and invasion through a 3D matrix (Bhaumik *et al*. 2008).

Scheeren *et al.* (2014) further implicated IRAK1 in breast cancer growth. Through genomic analysis of breast cancer data, they were able to identify that IRAK1 amplifications are present in ~24% of breast cancers. Studying human breast xenograft Estrogen Receptor (ER)-negative tumours and ER-positive and –negative breast cancer cell lines, they found that IRAK1 knockdown reduced clonogenicity *in-vitro* and tumourigenicity *in-vivo* (Scheeren *et al.* 2014).

Analysis of The Cancer Genome Atlas indicated that IRAK1 expression is increased across all subtypes of breast cancer when compared to normal breast tissue, most significantly in the basal subtype, and high IRAK1 expression is associated with poorer patient prognosis (Wee *et al.* 2015). Wee *et al*. (2015) subsequently found that TNBC cells gain dependency on IRAK1 as they progress and metastasise, with IRAK1 expression and activity increased in higher grade metastatic tumours. Their findings showed that IRAK1 drives this aggressive tumour growth through NF-κB activation and a resultant increase in the expression of pro-inflammatory cytokines Interleukin (IL)-6 and IL-8. They also indicated that IRAK1 confers resistance to the chemotherapeutic paclitaxel. Interestingly, the role of IRAK1 here involves increasing p38 MAPK activation and not NF-κB. IRAK1 knockdown was sufficient to impair TNBC growth and metastasis *in-vivo*, and the use of an IRAK1/4 inhibitor in combination with paclitaxel was capable of inhibiting the growth of paclitaxel-resistant breast cancer cells (Wee *et al.* 2015).

The same group identified a 1q21.3 chromosome amplification that is present in a high percentage of breast tumours (Goh *et al*. 2017). The genes for several S100 family

members, a family of EF-hand Ca^{2+} binding proteins, are located at 1q21.3. They were able to identify a positive feedback loop involving S100A7/8/9 and IRAK1 that drives tumoursphere growth in cancers possessing this amplification. Pacritinib, a small molecule kinase inhibitor that inhibits the kinase activity of IRAK1, Janus Kinase (JAK) 2 and Fms-like tyrosine kinase (Flt) 3, was able to disrupt tumour growth *in-vitro* and *in-vivo*, showing increased efficacy in samples where the 1q21.3 amplification was present (Goh *et al.* 2017).

IRAK1 has also recently been associated with resistance to radiation therapy, a treatment course that ~60% of patients with cancer undergo, in cancers possessing mutant p53 (Liu *et al.* 2019). Mutation of the p53 transcription factor is present in ~50% of solid tumours and cells with mutant p53 fail to undergo apoptosis following radiation. Additionally, in a number of cancers including glioblastoma, colorectal and breast cancer, patients with mutant p53 have been shown to have significantly poorer outcomes following radiation therapy when compared to patients expressing wild-type p53 (Liu *et al.* 2019). Liu *et al*. (2019) identified a unique role for IRAK1 in mediating resistance to radiation therapy across cancers possessing p53 mutations, including breast. In cancers possessing mutant p53, IRAK1 was shown to inhibit PIDDosome mediated apoptosis in response to radiation independently of any association with MyD88. They found that targeted inhibition of IRAK1 kinase activity, using kinase inhibitors specifically targeting IRAK1 and not IRAK4, in mutant p53 tumour cell models re-sensitized these cells to radiation therapy (Liu *et al*. 2019).

These findings highlight the important role that IRAK1 has been indicated to play in breast cancer development and progression, and the relevance of investigating the potential of targeting IRAK1 to improve treatment responses in tamoxifen-resistant breast cancer.

1.2.2. Estrogen Receptor-positive (ER+) breast cancer.

1.2.2.1. Estrogen Receptor-alpha (ERα).

Breast cancer is the most commonly diagnosed cancer in women and the second leading cause of cancer related mortality in women (Siegel *et al.* 2020). Of newly diagnosed breast cancer cases, ~70% exhibit high expression of ERα and are defined as ER+ breast cancer. ERα, a member of the nuclear receptor superfamily, is a ligand-dependent transcription factor that is encoded by the ESR1 gene, and is differentially expressed across various tissues (Renoir *et al.* 2013). Structurally, the functional domains of ERα are separated into A/B, C, D and E/F regions. The A/B region represents the N-terminal domain, which contains a zinc finger and is involved in transactivation. The C region contains the central DNA-binding domain which facilitates dimerization and binding to specific Estrogen-Response Elements (EREs). The D region consists of a hinge segment that allows for structural rearrangement and can bind to chaperone proteins that support nuclear translocation following ligand-binding. The C-terminal E/F region contains the ligand-binding domain as well as binding sites for cofactors (Anbalagan and Rowan 2015, Fuentes and Silveyra 2019). ERα also contains two additional activation function (AF) domains that are critical to full receptor function termed AF-1 and AF-2. AF-1 is located within the N-terminal domain and is regulated by phosphorylation at key sites including S118 and S167, while AF-2 is contained within the ligand-binding domain and its activation is ligand-dependent. Full ERα transcriptional regulation requires synergistic AF-1 and AF-2 activity (Anbalagan and Rowan 2015, Fuentes and Silveyra 2019).

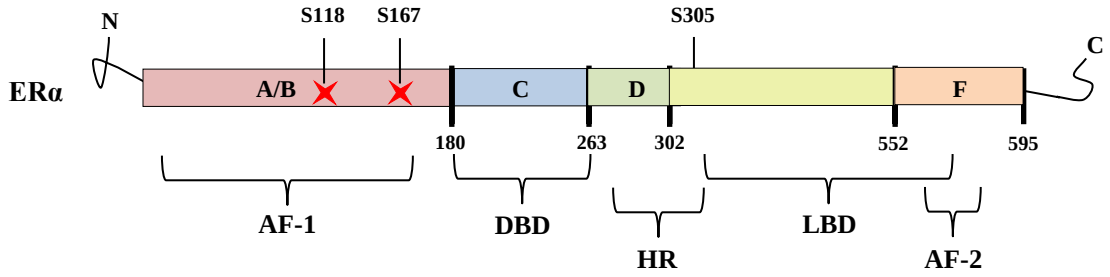

Figure 1.2. Structural representation of Estrogen Receptor alpha. Image adapted from Anbalagan and Rowan 2015. AF-1 = Activation Function Domain 1; DBD = DNA-Binding Domain; HR = Hinge Region; LBD = Ligand-Binding Domain; AF-2 = Activation Function Domain 2.

ERα is expressed at low levels in normal breast epithelia although it does have an essential, poorly-defined role in the breast, with ERα knockout mice showing dysfunctional mammary development (Tekmal *et al.* 2005). In the absence of ligand, ERα is believed to shuttle between the cytoplasm and nucleus as a monomer, maintained in a heat-shock protein (Hsp) complex primarily consisting of Hsp70 and Hsp90 family members. This complex keeps the receptor in an inactive state but is also important for maintaining the receptor in a conformation that is primed for ligand-binding (Dhamad *et al.* 2016).

There are three main physiological forms of estrogens in women, these being estrone, estradiol (E2) and estriol, with E2 being the predominant ERα agonist. In the canonical ERα pathway, ligand-binding results in conformational changes to the receptor, triggering the activation of the AF-2 domain and the release of ERα from its inhibitory heat-shock protein complex. The receptor also undergoes phosphorylation at several sites within the N-terminal, most importantly S118 and S167, which triggers the activation of the AF-1 domain (Anbalagan and Rowan 2015). The receptor can then dimerize and translocate to the nucleus. Here, ERα regulates the transcription of target genes directly through binding to DNA at specific EREs, recruiting cofactors (primarily members of the p160 co-activator family such as steroid receptor coactivator (SRC)-1 and amplified in breast cancer (AIB) 1) and transcriptional machinery, or indirectly by acting as a cofactor for other transcription factors including specificity protein (SP)-1 and activator protein (AP)-1 (Philips *et al.* 1993, Onate *et al.* 1995, Planas-Silva *et al.* 2001, Safe 2001, Fuentes and Silveyra 2019). ERα is recognised to target a wide-range of genes, which are well documented by Lin *et al.* (2004), involved in promoting proliferation, cell-cycle progression and cell survival.

Several post-translational modifications are important for ERα to fully function, mostly involving phosphorylation. As mentioned above, the role of phosphorylation at S118 and S167 has been most widely analysed and understood. A number of kinases have been identified to phosphorylate S118 including ERK1/2 (Kato *et al.* 1995), glycogen synthase kinase (GSK) 3 (Medunjanin *et al.* 2005), IKKα (Park *et al.* 2005) and cyclin-dependent kinase (CDK) 7 (Chen *et al.* 2002). Phosphorylation of ERα at S118 has been found to enhance dimerization and transactivation, increasing interactions with members of the p160 co-activator family and SRC3 (Dutertre *et al.* 2003, Likhite *et al.* 2006, Le Romancer *et al.*

2011). Kinases involved in phosphorylation at S167 include 90 kDa ribosomal S6 kinases (RSK, S6K1) (Yamnik and Holz 2010), Akt (Campbell *et al*. 2001), casein kinase (CK) 2 (Arnold *et al*. 1995), IKKε (Guo *et al.* 2010) and Aurora kinase A (Zheng *et al*. 2014) with S167 phosphorylation being associated with an increased DNA-binding capacity (Shah and Rowan 2005). Another important phospho-site is S305, which is phosphorylated by protein kinase A (PKA) (Michalides *et al*. 2004), Aurora kinase A (Zheng *et al*. 2014) and p21-activated kinase (PAK) 1 (Wang *et al*. 2002). S305 is located very close to the hinge region and its phosphorylation supports conformational changes to the receptor and subsequent dimerization and transactivation (Le Romancer *et al*. 2011, Anbalagan and Rowan 2015).

In addition to the genomic signalling of ERα, membrane-associated and cytoplasmic ERα signalling has been identified. These mechanisms trigger the activation of signalling cascades that allow for rapid responses to estrogen stimulation. ERα has been shown to activate subunits of the G protein-coupled estrogen receptor at the plasma membrane, conferring roles for membrane-associated ERα in activating important signalling cascades including the phospholipase C (PLC)/protein kinase A (PKA) pathway and the cyclic adenosine monophosphate (cAMP)/protein kinase C (PKC) pathway to indirectly regulate gene expression (Gu and Moss 1996, Marino *et al* 1998). This mechanism has also been indicated to contribute to enhanced Epidermal Growth Factor Receptor (EGFR) activation, and subsequent downstream activation of ERK1/2 (Filardo *et al*. 2000). Unique roles for ERα in the activation of cytoplasmic signalling complexes have also been identified. In response to estradiol stimulation, ERα was shown to quickly form a signalling complex with Src, focal adhesion kinase (FAK) and the p85 subunit of phosphoinositide-3 kinase (PI3K) leading to the activation of important downstream kinases such as ERK1/2 and Akt, allowing for rapid regulation of cell proliferation and survival (Le Romancer *et al*. 2008).

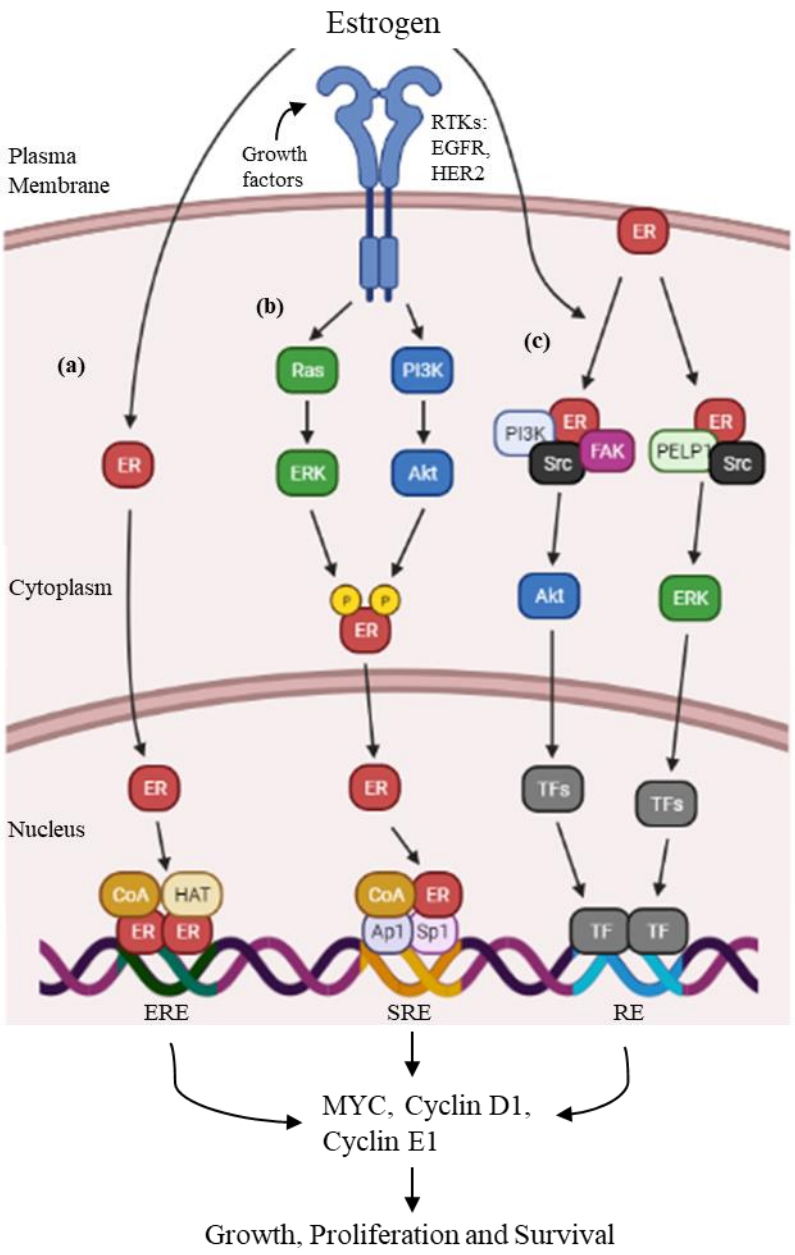

Figure 1.4. Estrogen signalling. Image adapted from Musgrove and Sutherland 2009 **(a)** In the canonical estrogen signalling pathway, estrogen binding to ERα triggers conformational changes, dimerization and translocation to the nucleus where ERα can regulate gene expression either through direct binding to DNA at specific estrogen response elements (EREs) in complexes with co-activators (CoAs) and histone acetyl transferases (HATs), or indirectly by acting as a cofactor for other transcription factors (Ap1, Sp1

families) to support binding to serum response elements (SREs) and subsequent transcription. **(b)** ERα activity can also be altered as a result of signalling downstream of receptor tyrosine kinases (RTKs) including EGFR and HER2. Here, ERK and Akt can phosphorylate ERα at important residues (Ser118, Ser167) that regulate the transactivation and DNA-binding capability of ERα, and has the potential to lead to ligand-independent ERα activity. **(c)** Signalling can also be mediated through non-genomic mechanisms by ER that is localized at the cell membrane or in the cytoplasm. Ligand binding triggers the formation of functional protein complexes including ERα that result in signalling cascades and the activation of downstream transcription factors (TFs).

1.2.2.2. Endocrine therapy and tamoxifen

The standard of care for ER+ breast cancers generally includes 5 years of adjuvant endocrine therapy, which has been found to reduce the rate of tumour recurrence by up to 50% (Levine *et al*. 1998). For ER+ breast cancer patients, there are several viable endocrine therapies that are prescribed based on the characteristics of the patient and the tumour.

Tamoxifen is a Selective Estrogen-Receptor Modulator (SERM) that was first approved for clinical use in 1973 and has remained the most commonly prescribed adjuvant treatment for ER+ breast cancer patients to this day. Adjuvant therapy with tamoxifen for 5 years was found to reduce contralateral breast cancer development by 50%, while reducing patient mortality by ~30% (Levine *et al*. 1998). SERMs like tamoxifen act by competing with estrogen for binding to the ligand-binding domain of ERα. When estrogen binds to ERα, the receptor undergoes conformational changes, with estrogen being sealed in the binding pocket by helix-12. These structural changes trigger AF-2 activation and allow for interactions with coactivators. When tamoxifen binds to the ligand-binding domain, ERα similarly undergoes structural rearrangements but the binding pocket cannot be sealed by helix-12. This disrupts the ability of ERα to interact with coactivators and inhibits AF-2 mediated transcription (Ring and Dowsett 2004, Arnal *et al*. 2017). However, the expression of AF-1 regulated genes, which include TFF1, XBP1, GREB1 & FKBP4, are not necessarily inhibited (Ring and Dowsett 2004). Tamoxifen can have a weak agonistic effect on the transcription of these genes, with the potential for enhanced S118 and/or S167 phosphorylation to drive their expression further (Berry *et al*. 1990, Feng *et al*. 2001, Caizzi *et al*. 2014). This has been suggested as a reason behind the tissue-specific effects of tamoxifen as, while it has inhibitory effects on growth in the breast, it can actually promote growth in other tissues, such as the uterus (Kedar *et al*. 1994, Wysowski *et al*. 2002).

While tamoxifen continues to be the most commonly prescribed adjuvant treatment for ER+ breast cancer patients, clinical trials over the past 20 years have identified that the use of more aggressive estrogen-targeted therapies alone or in combination with tamoxifen can improve patient outcomes, particularly in post-menopausal women. Fulvestrant is a Selective Estrogen-Receptor Degrader (SERD) that acts as a pure antagonist of ERα function. Unlike tamoxifen, which can have partial agonistic activity, fulvestrant binds to

ERα and impairs both AF-1 and AF-2 mediated transcriptional activity (Moverare-Skrtic *et al*. 2014). Further, the conformational changes to ERα following fulvestrant binding render it unstable and accelerate the degradation of the receptor (Osborne *et al*. 2004). Fulvestrant has not shown significantly increased efficacy compared to tamoxifen but has been indicated for patients with advanced ER+ breast cancer, where studies have shown that it can improve patient survival in both endocrine naïve patients and patients whose cancer has progressed following tamoxifen therapy (Howell *et al*. 2002, Robertson *et al*. 2009, Robertson *et al*. 2016).

Aromatase inhibitors, such as letrozole and anastrozole, have similarly shown the ability to enhance ER+ breast cancer patient survival. Aromatase inhibitors act by preventing the metabolization of androgen into estrogen, thus removing the receptor agonist (Smith and Dowsett 2003). They have been studied alone and in combination with tamoxifen as a treatment option, particularly for post-menopausal women, and have been shown to increase patient survival by up to 25% in comparison to tamoxifen therapy alone (Breast International Group (BIG) 1-98 Collaborative Group 2005, Howell *et al*. 2005, Arimidex 2008, Muss *et al*. 2008).

1.2.2.3. Tamoxifen resistance.

Tamoxifen has remained a highly effective treatment for ER+ breast cancer for nearly 50 years, but a significant percentage of patients will present with or develop resistance to tamoxifen therapy (Howell *et al*. 2005, Arimidex 2008). This is one of the major problems facing ER+ breast cancer patients, with limitations in other available treatment options for pre-menopausal women and significantly worse prognoses for patients that develop acquired resistance.

It has been suggested that approximately 20% of patients will present with *de novo* resistance to tamoxifen (Gutierrez *et al*. 2005, Hoskins *et al*. 2009). Two main mechanisms have been associated with *de novo* resistance to tamoxifen therapy, loss of ERα expression and loss of cytochrome p450 family member expression (Gutierrez *et al*. 2005, Hoskins *et al*. 2009). The expression of ERα is understandably very tightly linked to tamoxifen efficacy, and the majority of patients that lack ERα expression do not respond to tamoxifen (Kuukasjärvi *et al*. 1996). Members of the cytochrome p450 family are integral in metabolizing tamoxifen, and the lack of their expression limits the efficacy of the drug (Hoskins *et al*. 2009). Another mechanism is the presence of mutations in ERα but this is rarely seen in cases of *de novo* resistance (Clarke *et al*. 2003, Herynk & Fuqua 2004). These mutations have been reported in the ligand-binding domain and can promote ligand-independent activation of the receptor. Mutations have also been found to functionally inactivate the receptor. These mutational modifications of ERα inhibit tamoxifen function, despite the presence of an ER+ phenotype (Clarke *et al*. 2003, Herynk & Fuqua 2004).

The impact of ERα phosphorylation at S118 and S167 has been found to be complex with regards to patient responses to tamoxifen and overall patient prognosis. The presence of S118 and S167 phosphorylation has been associated both positively and negatively to tamoxifen responses in clinical trials (Murphy *et al*. 2004, Kirkegaard *et al*. 2005, Sarwar *et al*. 2006, Jiang *et al*. 2007). This may be linked to the phosphorylation status of ERα before and after tamoxifen treatment. The presence of S118 and S167 phosphorylation at the time of tamoxifen treatment indicates functional ERα, wherein tamoxifen can be effective. However, the presence of high S118 and S167 phosphorylation after tamoxifen treatment indicates potential ligand-independent receptor activity and resistance to tamoxifen therapy.

Research has shown that of patients that initially respond well to tamoxifen treatment, ~30% will present with a resistant recurrence within 10 years of finishing therapy (Howell *et al*. 2005, Arimidex 2008). These recurrences generally present an aggressive phenotype and a very poor patient prognosis, with an estimated 5-year survival rate of 20% (Robertson *et al*. 2003, Sotgia *et al*. 2017). Numerous mechanisms have been identified that can contribute to the development of acquired tamoxifen resistance. For the majority of cases, tamoxifen resistance has been linked to dysregulated expression and activity of human epidermal growth factor receptor (HER) family members (Refer to section 1.3 for detailed review) (Knowlden *et al*. 2003, Hutcheson *et al*. 2003). The expression of epidermal growth factor receptor (EGFR) and HER2 has been found to be increased in cells that are resistant to tamoxifen (Knowlden *et al*. 2003, Hutcheson *et al*. 2003). EGFR/HER2 can activate several signalling cascades that can impact on ERα activity through enhanced phosphorylation at S118 and S167, with the potential to trigger ligand-independent ERα activity (Kato *et al*. 1995, Campbell *et al*. 2001). The increased expression of EGFR/HER2 can also drive tumour growth independently of ERα and render anti-estrogens ineffective (Knowlden *et al*. 2003, Hutcheson *et al*. 2003). Similarly, the insulin-like growth factor receptor (IGFR) family has been associated with tamoxifen resistance by activating the same signalling cascades as HER family members. ERα has also been found to interact directly with IGFR-1 and promote the initiation of downstream signalling (Fagan and Yee 2008, Miller *et al*. 2009).

The increased expression and/or activity of members of the PI3K/Akt signalling pathway has been linked with acquired tamoxifen resistance. There is evidence that ERα can bind to PI3K and promote activation of Akt, a kinase that is recognised to promote cell proliferation and inhibit apoptosis. Akt is also active downstream of growth factor receptors including EGFR and HER2 and has been identified to phosphorylate ERα at S167, promoting ligand-independent receptor activity (Arpino *et al*. 2008).

The altered expression of co-regulators may also have a significant role in the development of resistance to tamoxifen therapy. Amplified in breast cancer (AIB) 1 is an ERα co-activator that is overexpressed in ~50% of breast tumours. Studies have shown that high AIB1 expression is associated with poorer response to tamoxifen therapy and worse

disease-free survival (Osborne *et al*. 2003). This would suggest that the overexpression of co-activators can overcome the transactivational limitations of ERα after tamoxifen binding. Similarly, the reduced expression of co-repressors such as nuclear receptor corepressor (NCOR) 1 can prevent tamoxifen from successfully repressing the expression of ERα target genes (Ring and Dowsett, 2004).

1.3. The human Epidermal Growth Factor receptor (HER) family.

1.3.1. HER family.

The HER family of receptor tyrosine kinases (RTKs) is one of the most widely studied in biology. It consists of four members (Epidermal Growth Factor Receptor (EGFR), HER2, HER3, HER4) that are ubiquitously expressed, and research in knockout mice has shown their critical importance in regulating the development of many organs (Miettinen *et al*. 1995, Gassmann *et al*. 1995, Lee *et al*. 1995, Riethmacher *et al*. 1997). The HER family members share significant structural similarities, with an extracellular ligand-binding domain, a small transmembrane region and an intracellular kinase domain. The extracellular region is divided into four domains, with leucine-rich domains I and III involved in ligand binding and cysteine-rich domains II and IV supporting dimerization through the formation of disulphide bonds. The intracellular component consists of a juxtamembrane (JM) region of around 40 residues, which has been identified to have a role in dimerization and protein kinase activation, a protein kinase domain and a c-terminal tail that contains various residues that undergo phosphorylation and further regulate the kinase activity of the receptor. The receptor family, like all receptor tyrosine kinases, requires dimerization and/or further oligomerization to function. A number of isoforms have been discovered for each receptor, which generates a wide array of potential dimer combinations and robust signalling regulation. There are eleven Epidermal Growth Factor (EGF)-related ligands that possess conserved EGF motifs and have affinity for specific receptors within the HER family. Two important characteristics of the family to take note of are the absence of a known ligand for HER2 and the presence of a functionally impaired kinase domain on HER3, which inhibits the signalling potential of HER3 homodimers. However, HER2 is the favoured dimerization partner for all the other members of the family and HER2 heterodimers with EGFR and HER3 are recognized to exhibit potent signalling activity. This is thought to be due to the HER2 extracellular domain remaining in a constitutively active conformation, while other members of the family require ligand binding to trigger structural rearrangements of their extracellular domains to ready them for dimerization (Cho *et al*. 2003). Dimerization initiates trans-phosphorylation of tyrosine residues which activates the kinase domain, while also triggering conformational changes in the c-terminal

tail to allow for interactions with adaptor proteins that promote downstream signalling cascades. These signalling pathways are often interconnected, with the Ras/Raf/MAPK cascade and the phosphatidylinositol 3-kinase (PI3K)/Akt pathway being the main cascades that are activated, conferring major roles for HER family signalling in mediating cell proliferation, cell survival, angiogenesis, and cell motility (Roskoski 2014).

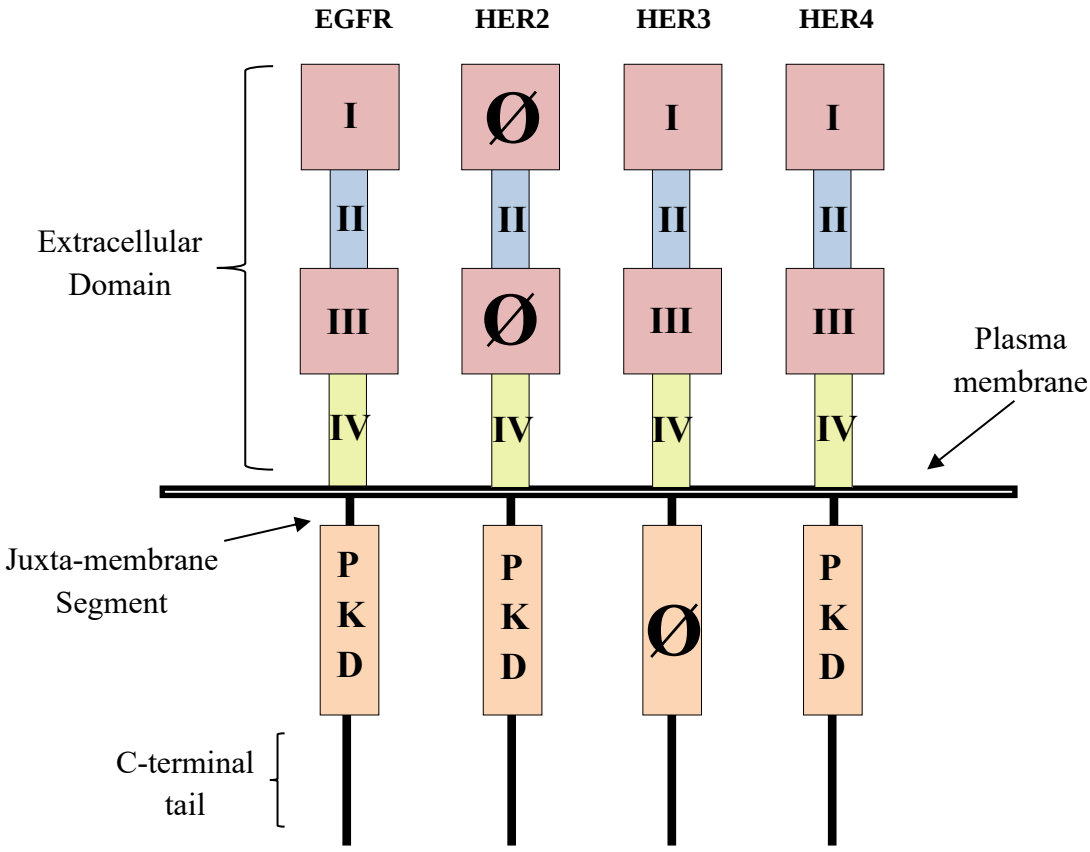

Figure 1.4. Structural representation of the HER family members. Image adapted from Roskoski 2014. The extracellular region of each receptor is separated into 4 domains (I-IV). Domains I & III have roles in regulating ligand binding while domains II and IV are involved in dimer formation. **Ø** = impaired function; PKD = protein kinase domain.

The MAPK signalling cascade can be initiated by all members of the HER family. The activation of this pathway is mediated by the adaptor proteins growth factor receptor-bound protein 2 (Grb2) and Src homology domain containing (Shc), which can bind to multiple phosphotyrosine sites on each HER receptor. These adaptor proteins are then able to recruit the guanine nucleotide exchange factor son of sevenless (SOS) which can catalyze the activation of Ras-GDP to Ras-GTP, the first component of the MAPK cascade, which leads to the activation of Raf kinases (Roskoski 2010). Raf kinases then catalyze the phosphorylation of MEK1/2, which can subsequently activate the effector kinases ERK1/2 by phosphorylation at T202 and Y204. Activated ERK1/2 can then translocate to the nucleus and regulate the activity of transcription factors such as the T-cell factor (TCF) family, Elk-1 and c-Fos. This confers an important role for ERK1/2 in regulating the expression of a wide array of genes involved in cell cycle regulation, cell proliferation, cell migration, cellular metabolism and cell survival (Roskoski 2012).

The PI3K/Akt pathway is activated in response to ligand binding of a number of RTKs including the HER family, but requires the presence of HER3 dimerization in each case as the c-terminal tail of HER3 contains multiple consensus sites for binding the p85 subunit of PI3K. This binding triggers the p110 subunit of PI3K to interact with its substrate phosphatidylinositol-4,5-bisphosphate (PIP2) at the plasma membrane. The p110 subunit can also be activated by Ras, due to the presence of a Ras-binding domain. PI3K phosphorylates PIP2 to generate phosphatidylinositol-3,4,5-trisphosphate (PIP3). Proteins containing a pleckstrin homology (PH) domain can then bind to PIP3, including Akt and phosphoinositide-dependent kinase (PDK) 1, leading to their activation. Akt activation requires phosphorylation at T308, located within the activation loop, by PDK1. This is sufficient to initiate Akt activity, but full enzymatic activation requires subsequent phosphorylation at S473 by a complex containing mammalian target of rapamycin (mTOR)/Rictor (mTORC2) (Garcia-Echeverria & Sellers 2008). Three isoforms of Akt have been identified in mammals and they play critical roles in regulating cell survival and the cell cycle through the phosphorylation of numerous proteins, including GSK3α/β, the FoxO family of transcription factors, BAD, p21 and p27 (Cross *et al*. 1995, Datta *et al*. 1997, Matsuzaki *et al*. 2003, Manning and Cantley 2007). The pathway is negatively regulated by phosphatase and tensin homologue (PTEN), which dephosphorylates PIP3.

Importantly, Akt can also phosphorylate and inactivate tuberin, leading to the activation of the mTOR/Raptor (mTORC1) complex. This complex is involved in the regulation of additional cellular processes including protein synthesis, autophagy and glucose metabolism (Mayer and Arteaga. 2016). The downstream substrate S6 kinase 1 (S6K1) is an important mediator of mTORC1 signalling and has been shown to phosphorylate ERα at S167 within the AF-1 domain and contribute to ligand-independent ERα signalling (Yamnik *et al*. 2009).

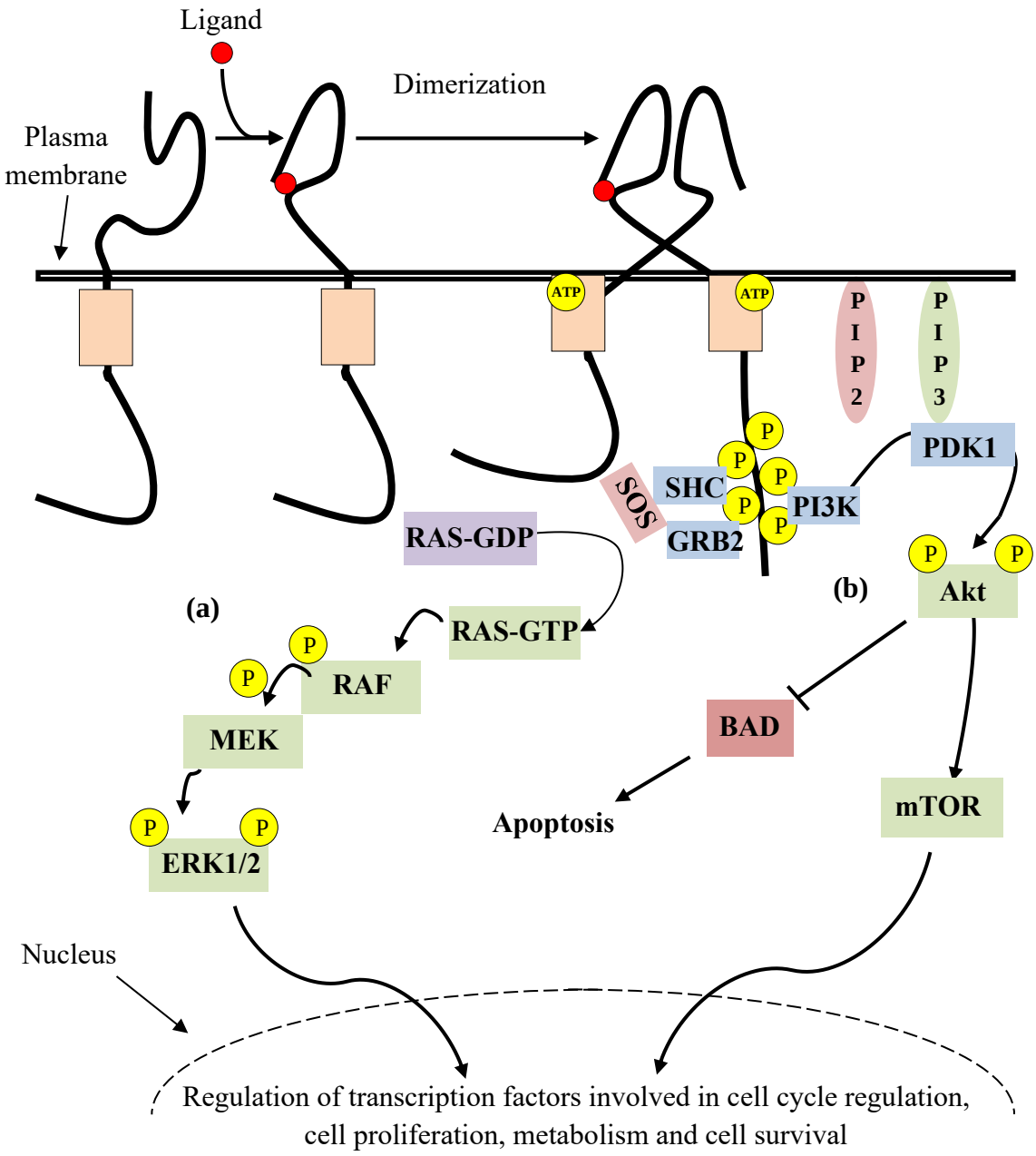

Figure 1.5. Overview of HER family signalling. Image adapted from Garcia-Etcheverria & Sellers 2008, Kol *et al*. 2014, Roskoski 2014. Image is representative of HER3 dimerization with HER2 (which has no known ligand). Ligand binding triggers a conformational change in the receptor, leading to subsequent homo- or heterodimerization. This results in the phosphorylation of several phosphotyrosine sites within the c-terminal tail. These sites act as docking points for adaptor proteins that can then initiate their

downstream signalling cascades. **(a)** The activation of the MAPK pathway is mediated by the adaptor proteins Grb2 and Shc, which can bind to multiple phosphotyrosine sites on each HER receptor. These adaptor proteins are then able to recruit SOS which can catalyze the activation of Ras-GDP to Ras-GTP, the first component of the MAPK cascade, which leads to the activation of Raf kinases. Raf kinases then catalyze the phosphorylation of MEK1/2, which can subsequently activate the effector kinases ERK1/2 by phosphorylation at T202 and Y204. Activated ERK1/2 can then translocate to the nucleus and regulate the activity of transcription factors. **(b)** The p85 subunit of PI3K binds to phosphosites on the c-terminal tail of HER3, triggering the p110 subunit of PI3K to interact with its substrate PIP2 at the plasma membrane. PI3K phosphorylates PIP2 to generate PIP3. Proteins containing a PH domain can then bind to PIP3, including Akt and PDK1. Akt activation requires phosphorylation at T308, located within the activation loop, by PDK1. Fully activated Akt can then phosphorylate a number of targets to regulate cell proliferation and survival.

In addition to their role as plasma membrane receptors, all members of the HER family have been found to translocate to the nucleus where they have further unique roles in regulating gene expression. These roles have not yet been fully elucidated, and are an area of ongoing research.

Nuclear localisation of full length EGFR has been identified in various cell and tissue types and while its roles are not fully understood, several mechanisms have been reported (Wang *et al*. 2006, Hadžisejdić *et al*. 2010, Brand *et al*. 2011). In breast cancer, patients that present with tumours possessing high levels of nuclear EGFR were found to have poorer overall survival (Lo *et al*. 2005). Here, nuclear EGFR has been suggested to interact with the Cyclin-D1 promoter, indicating a direct role in cell cycle regulation, while also having a role as a transcriptional co-activator of Cyclin-D1 expression (Lin *et al*. 2001). However, a correlation between EGFR and Cyclin-D1 expression has not been found across breast cancer patient cohorts (Lin *et al*. 2001, Lo *et al*. 2005, Hadžisejdić *et al*. 2010). Nuclear EGFR has been shown to associate with ataxia telangiectasia mutated (ATM) and mediate proliferating cell nuclear antigen (PCNA) phosphorylation, proteins that are important for DNA damage repair and DNA synthesis (Wang *et al*. 2006, Lee *et al*. 2015). Nuclear EGFR has also been found to bind to the promoter region of Aurora kinase A (Aurora-A), in a complex that also contains the transcription factor signal transducer and activator of transcription (STAT) 5, and enhance the expression of Aurora-A (Brand *et al*. 2011). Aurora-A is a serine/threonine kinase that associates with the centrosome and microtubules during mitosis to ensure precise spindle formation, chromatid separation and integrity of the spindle checkpoint (Brand *et al*. 2011).

CDK1 has been identified as a substrate of nuclear HER2, with phosphorylation of CDK1 at Y15 inhibiting its activity and delaying mitosis progression (Tan *et al*. 2002). Interestingly, nuclear HER2 has also been demonstrated to colocalize in the nucleus with CDK1, an interaction that has been linked with taxol resistance in breast cancer cells (Tan *et al*. 2002). Nuclear HER2 has been demonstrated to act as a transcriptional co-activator of STAT3, forming a complex with STAT3 at the Cyclin-D1 promoter and promoting growth in breast cancer cells (Beguelin *et al*. 2010). A role for nuclear HER3 in the formation of this complex, and subsequent regulation of Cyclin-D1, has been reported (Russo *et al*.

2015). High nuclear levels of HER3 have been linked to tumour progression and increased chance of metastasis in prostate cancer (Koumakpayi *et al*. 2006). These mechanisms have all been linked to resistance to HER2-targeted therapies.

In response to Neuregulin (Nrg)-1 binding, the Jma isoform of HER4 is cleaved to a soluble dimeric form of its intracellular domain termed HER4:ICD (Ni *et al*. 2001). HER4:ICD has been shown to form a complex with STAT5 at the β-casein promoter, implicating nuclear HER4 in regulating the STAT5 mediated expression of essential milk genes during lactation (Williams *et al*. 2004). Another study performed in glial cells identified that HER4:ICD formed a complex with the adaptor protein TGF-β-activated kinase 1 binding protein (TAB) 2 and the nuclear receptor co-repressor N-CoR, with this complex then translocating to the nucleus and inhibiting the expression of genes such as S100B (Sardi *et al*. 2006). This finding may be interesting due to the recent link between IRAK1 and S100 family members in driving tumour growth in the breast (Goh *et al*. 2017).

1.3.2. HER family in breast cancer.

1.3.2.1. HER2 in breast cancer.

Aberrant HER family expression and activity has been found to contribute to various cancers including lung and breast (Kobayashi *et al*. 2005, Mazieres *et al*. 2013, Loibl & Gianni 2017). HER2 has been most strongly associated with breast cancer, where HER2 overexpression with gene amplification is observed in ~20% of breast cancer cases (Loibl & Gianni 2017). This form of breast cancer was previously associated with an aggressive phenotype and poor prognosis for patients. However, the development of HER2-targeted therapies, such as the monoclonal antibody (mAb) trastuzumab which targets the extracellular domain and the dual tyrosine kinase inhibitor (TKI) Lapatinib which blocks EGFR and HER2 phosphorylation, have significantly improved patient survival (Rexer & Arteaga 2012). These treatments have been found to promote cell cycle arrest, with trastuzumab increasing p27 expression while reducing cyclin-D1 and CDK2 levels (Yakes *et al*. 2002). These drugs alone do not induce a significant level of apoptosis, however when used in combination (trastuzumab and lapatinib) the apoptotic effects are enhanced (Ahmed *et al*. 2015). They are also commonly used in combination with other drugs in the clinical setting where they have been shown to be synergistic with many chemotherapeutics, including docetaxel (Ahmed *et al*. 2015). It is generally accepted that the efficacy of HER2-targeted therapies is dependent on the resultant inhibition of the PI3K/Akt/mTOR signalling pathway, which is known for its role in cell survival (Rexer & Arteaga 2012).

Two variations in the HER2 receptor have been identified that significantly reduce responses to trastuzumab specifically. A truncated form of HER2, termed p95-HER2, which lacks the antibody binding region has been identified in patients (Anido *et al*. 2006). A splice variant that lacks exon 16 has also been found in HER2+ breast cancer patients and cell lines, and has been linked to trastuzumab resistance (Castiglioni *et al*. 2006).

A common observation in HER2-amplified breast cancer is the co-amplification of the onco-protein c-Myc. Studies have shown that the overexpression of these two oncogenes together enhances tumourigenesis significantly *in-vitro* and *in-vivo*, when compared to the

overexpression of either oncogene alone, and these tumours resemble the aggressive basal-HER2 phenotype. The co-expression of HER2 and c-Myc in breast cancer patients has been associated with poor prognosis (Nair *et al*. 2014).

A number of combined therapies have also been trialled in an attempt to improve the efficacy of HER2-targeted therapy. Heat-shock protein 90 (Hsp90) is a chaperone protein that has a role in folding proteins and maintaining their structural integrity in response to cellular stresses. HER2 is known to interact with Hsp90 in this way, and inhibition of Hsp90 function promotes the proteasomal degradation of HER2 (Basso *et al*. 2002). In a phase II clinical trial, the combination of trastuzumab with a Hsp90 inhibitor showed enhanced anti-tumour activity in patients with progressing metastatic HER2+ breast cancer (Modi *et al*. 2011). Sequestosome 1 (SQSTM1 or p62) is a scaffold protein that has been shown to correlate with HER2 overexpression. p62 has been implicated in the activation of several signalling pathways including NF-κB, PI3K/Akt & Wnt/β-catenin signalling pathways. Recently, studies have shown that p62 is involved in HER2-mediated mammary tumourigenesis *in-vivo* with p62-null, HER2-overexpressing mice exhibiting impaired HER2 signalling and delayed HER2-induced tumourigenesis (Cai-McRae *et al*. 2015). HER2 overexpressing breast cancer cells have been shown to enhance IL-6 secretion, which subsequently increases the activation of STAT3. Enhanced STAT3 activity has also been observed in HER2+/ER+ breast cancer cell lines and primary tumours, with targeted inhibition of STAT3 reducing cell growth and enhancing trastuzumab efficacy *in-vitro* (Chung *et al*. 2014).

1.3.2.2. EGFR in breast cancer.

EGFR expression has been observed in all subtypes of breast cancer but EGFR overexpression is most commonly found in TNBC, a subtype that is defined by the absence of ER, progesterone receptor and HER2 expression, and is highly proliferative. EGFR overexpression is observed in up to 70% of TNBC cases and is associated with large, poorly differentiated, aggressive tumours in breast cancer patients, and increased development of distant metastases (Foley *et al*. 2010). The presence of limited therapeutic options for TNBC has led to studies on the potential of targeted EGFR inhibition. EGFR-targeted therapies have been developed in the form of TKIs (gefitinib) and mAbs (cetuximab), but phase II clinical trials in advanced metastatic breast cancer were disappointing (von Minckwitz *et al*. 2005, Baselga *et al* 2005, Dickler *et al*. 2009, Carey *et al*. 2012). The use of gefitinib and cetuximab as monotherapies showed very little effect on patient response rates, although these trials didn't select for patients that were EGFR-positive. Subsequently, when TNBC cohorts were tested, the use of EGFR-targeted therapies in combination with other chemotherapeutics (carboplatin, cisplatin) seemed to improve patient outcomes and provide significant clinical benefits (Baselga *et al*. 2013). However, these therapies have not been approved for the treatment of TNBC patients and have not progressed beyond phase II clinical trials (Nakai *et al*. 2016).

Mutations to the EGFR have been linked to oncogenesis in certain cancers, particularly lung cancer and glioblastoma (Kobayashi *et al*. 2005, Liu *et al*. 2015). Many of these mutations can affect the E3 ubiquitin-protein ligase CBL (c-Cbl)-binding site, impairing c-Cbl mediated degradation of the EGFR. One of the most commonly observed mutations, L858R, exhibits enhanced phosphorylation at Y1045, the c-Cbl-binding site, but shows impaired c-Cbl recruitment and receptor degradation which is explained by enhanced EGFR heterodimerization with HER2 (Shtiegman *et al*. 2007). The L858R mutant was found to dimerize with HER2 prior to ligand-binding, and HER2 is recognized to have reduced interaction with c-Cbl, allowing the L858R mutant to evade c-Cbl (Shtiegman *et al*. 2007). In contrast, several other mutations can result in hypo-phosphorylation of the Cbl-binding site, similarly disrupting receptor ubiquitination and degradation, sustaining EGFR signalling (Sigismund *et al*. 2018). The EGFR is also recognized to have an

important role in negatively regulating autophagy, the process of recycling defective components of the cell, a process that is commonly altered in cancer (Wei *et al*. 2013, Tan *et al*. 2016). EGFR inhibits autophagy, directly through phosphorylation and inhibition of Beclin-1 and indirectly through activation of the PI3K/Akt/mTOR signalling pathway (Wei *et al*. 2013, Tan *et al*. 2016).

Increased EGFR expression in ER+ breast cancer has been associated with enhanced tumour growth and tamoxifen resistance (Ciupek *et al*. 2015). Elevated EGFR expression drives ERK1/2 mediated phosphorylation of ERα at S118 and promotes an agonistic function for tamoxifen (Ciupek *et al*. 2015).

1.3.2.3. HER3 in breast cancer.

The role of HER3 in breast cancer has been primarily studied in the HER2+ and TNBC subtypes, where high HER3 expression has been specifically associated with tumour progression and poor patient prognoses (Bae *et al*. 2013). Interestingly, analysis of the cancer genome atlas identified that HER3 copy number gains are present in 12.3 % of luminal A, 21.1% of luminal B and 27.6% of HER2-amplified breast tumours. However, HER3 copy number losses were much more common in basal (33.3%) and claudin-low (25%) breast tumours (Morrison *et al*. 2013) The role of HER3 in HER2-amplified breast tumours has been linked to the ability of HER3 to potently activate the PI3K/Akt signalling pathway, with HER3 being the preferential dimer partner for HER2 (Roskoski 2014). HER3 overexpression has been associated with resistance to HER2 targeted therapies and reduced survival in HER2+ breast cancer patients (Berghoff *et al*. 2014). Targeted knockdown of HER3 significantly reduced the proliferation of HER2-amplified breast tumours *in-vitro* and *in-vivo,* implying that the HER2-HER3 heterodimer is essential for HER2-driven oncogenesis (Lee-Hoeflich *et al*. 2008). A negative feedback loop has been identified between the PI3K/Akt pathway and HER3 expression in breast cancer cell lines, wherein Akt limits the expression of HER3 and other RTKs (Chandarlapaty *et al*. 2011). Targeted inhibition of the PI3K/Akt has been explored as a therapeutic option for breast cancer patients, but the presence of this negative feedback mechanism indicates limitations to the efficacy of this type of treatment. Akt inhibition was shown to induce HER3 expression and enhance phosphorylation of HER3, along with several other RTKs, indicating that combination treatments targeting Akt and HER3 would provide more benefit to patients (Chandarlapaty *et al*. 2011).

Pertuzumab, a drug targeted towards the extracellular domain of HER2, has been shown to inhibit HER2-HER3 dimerization. This drug showed promise *in-vivo* for the treatment of HER2+ breast cancer, with enhanced efficacy compared to trastuzumab (Lee-Hoeflich *et al*. 2008). Pertuzumab has since been approved for the treatment of HER2+ metastatic breast cancer, and is given in combination with trastuzumab and chemotherapy where it has improved progression free survival by 6 months over the combination of trastuzumab and chemotherapy (Blumenthal *et al*. 2013).

There have been some contradictory findings in relation to the potential of using HER3 status as a prognostic factor. Several publications have shown that high HER3 expression correlates with improved disease-free survival in breast cancer patients (Pawlowski *et al*. 2000, Lee *et al*. 2007) while others have shown the converse (Chiu *et al*. 2010). A suggestion for this has been the subcellular localisation of HER3, with the receptor having a different impact on cell responses dependent on its location. Nuclear HER3 has been shown to activate the transcription of Cyclin D1, through directly binding to the Cyclin D1 promoter, in lung and breast cancer cells (Brand *et al*. 2013). The presence of high nuclear levels of HER3 have been linked to tumour progression and increased chance of metastasis in prostate cancer (Koumakpayi *et al*. 2006). HER3 expression has also been correlated with ERα expression, indicating a potential role for HER3 in ER+ breast cancer. However, ERα expression has been found to correlate with reduced dimerization of HER3 with other HER family members (Green *et al*. 2014). HER3 has also been linked to HER2-mediated tamoxifen-resistance (Liu *et al*. 2007). In a HER2-overexpressing cell model of tamoxifen-resistant breast cancer, siRNA knockdown of HER3 was shown to reduce cell growth and colony formation while increasing the sensitivity of these cells to tamoxifen treatments (Liu *et al*. 2007). These results were primarily associated with disruption to the PI3K/Akt signalling pathway (Liu *et al*. 2007).

1.3.2.4. HER4 in breast cancer.

HER4 expression is less studied in breast cancer and has been mostly associated with an anti-proliferative and pro-apoptotic role in the breast (Naresh *et al*. 2006, Muraoka-Cook *et al*. 2006). HER4 expression is primarily observed in the luminal subtypes, and high HER4 levels have generally been found to correlate with improved patient survival (Thor *et al*. 2009). The loss of HER4 expression, which is observed in most HER2+ and TNBC breast cancer cases, has been associated with high tumour grade and an increased chance of tumour recurrence and metastasis (Sundvall *et al*. 2008, Kreike *et al*. 2009, Das *et al*. 2010).

Loss of HER4 expression has also been suggested as an independent marker of resistance to tamoxifen in breast cancer patients (Guler *et al*. 2007). In ER+ breast cancer patients, HER4 is commonly co-expressed with ERα in ~90% of cases. The role of HER4 in ER+ breast cancer appears to predominantly involve the JMa isoform of HER4. which has been found to be cleaved to a soluble intracellular HER4:ICD form (Wang *et al*. 2016). The presence of HER4:ICD in the nucleus has been shown to directly enhance ligand-bound ERα activity by acting as a potent co-activator, and upregulating the expression of many estrogen response genes including the progesterone receptor (PR) and CXCL12, and driving ER+ breast cancer growth and progression (Han & Jones 2014, Göthlin Eremo *et al*. 2015, Wang *et al*. 2016). Tamoxifen treatment was found to impair the formation of the HER4:ICD-ERα transcriptional complex and stimulates mitochondrial accumulation of HER4:ICD which induces apoptosis in a BH3-domain dependent manner through the activation of BAK (Naresh *et al*. 2006, Rokicki *et al*. 2010, Han and Jones 2014). Another novel role for HER4:ICD has been demonstrated in the regulation of Mdm2, a negative regulator of the tumour suppressor p53. Stimulation of HER4 and translocation of HER4:ICD to the nucleus resulted in increased phosphorylation of Mdm2 through a direct interaction with HER4:ICD, subsequently enhancing the ubiquitin-mediated degradation of Mdm2. This led to elevated levels of p53 and the CDK inhibitor (CDKI) p21, a transcriptional target of p53 (Arasada and Carpenter 2005).

However, there have been contradictory findings in relation to the prognostic value of HER4, most likely related to the breast cancer subtype studied and the existence of multiple

HER4 isoforms with diverse signalling activities (Pawlowski *et al*. 2000, Suo *et al*. 2002, Bieche *et al*. 2003, Lodge *et al*. 2003, Thor *et al*. 2009, Nafi *et al*. 2014). Subsequent meta-analysis of past HER4 studies in breast cancer were unable to identify a significant correlation between nuclear HER4 levels and overall or relapse-free survival. In contrast, the presence of elevated levels of cytoplasmic HER4 was associated with significantly prolonged relapse-free survival in breast cancer patients (Wang *et al*. 2016).

1.4. Aurora kinase A

The Aurora kinase family consists of three highly conserved serine/threonine kinases, termed Aurora kinase A, B and C which are primarily recognised for their role during mitosis (Vader and Lens 2008). Aurora kinase A (Aurora-A) has important roles in centrosome maturation, spindle assembly and spindle damage recovery. Aurora-A localises to the centrosome during G2 phase and is also present on the mitotic spindle during mitosis. Targeting to the centrosome requires several kinases, including p21-activated kinase (PAK) 1 which is known to directly bind and phosphorylate Aurora-A. Aurora-A activation is dependent on phosphorylation at T288, located within its activation loop. Activation is essential in triggering the assembly of a large Aurora-A complex on the mitotic spindle, which supports chromatin-driven spindle assembly (Vader and Lens. 2008).

Aurora-A has been identified as an upstream regulator of polo like kinase (PLK) 1, a mitotic kinase that stimulates cell cycle progression. Aurora-A can directly and indirectly, through the phosphorylation of PLK1 at T210, phosphorylate and activate the phosphatase cell division cycle (CDC) 25B which is required for initial cyclinB/CDK1 activation during the G2/M transition (Dutertre *et al*. 2004). A role for Aurora-A in mediating cellular responses to DNA double strand breaks has also been shown, through inhibition of RAD51 recruitment to the damaged site (Sourisseau *et al*. 2010). This process is linked to the activity of PLK1 which inhibits the checkpoint kinase (CHK) 1, implicating Aurora-A in tumourigenesis (Sourisseau *et al*. 2010).

The aurora kinases are overexpressed in a number of cancers, including breast, and have been associated with poor patient prognoses (Tanaka *et al*. 1999, Gritsko *et al*. 2003, Dauch *et al*. 2016, Shah *et al*. 2019). Aurora-A overexpression has been linked to override of the spindle assembly checkpoint and abrogation of DNA damage-induced apoptosis which leads to the development of genetic instability and aneuploidy (Katayama *et al*. 2012, Do *et al*. 2014). As a result, the therapeutic potential of targeted aurora kinase inhibition has been investigated in recent years and has shown promise. Aurora-A inhibition disrupts mitotic spindle assembly and potentiates both p53-dependent and –independent mechanisms of cell death (Kaestner *et al*. 2009). Alisertib is a selective Aurora-A inhibitor that has shown potent anti-proliferative effects *in-vitro* and *in-vivo* across a variety of cancer subtypes.

Alisertib has progressed to clinical trials for lymphomas but has shown only modest efficacy and has not been approved for treatment at this point (Bavetsias and Linardopoulos 2015).

The MYC family of transcription factors have been implicated in the tumourigenesis of various cancers, and a link has recently been established between Aurora-A and members of the MYC family. In neuroblastoma, a kinase-independent function of Aurora-A was found to be stabilizing MYCN, with targeted disruption of the native conformation of Aurora-A enhancing MYCN degradation (Otto *et al.* 2009, Brockmann *et al.* 2013) . This finding is of particular relevance to cancers that present with altered p53, where the development of MYC dependency is common. Studies have recently shown the potential of targeting Aurora-A in the mutant p53 subset of liver cancer (Dauch *et al*. 2016). In p53 altered liver cancer, Aurora-A was found to be activated by the tumour suppressor p19 in response to oncogenic stress and contribute to G2/M cell cycle arrest (Dauch *et al*. 2016). However, the presence of high levels of MYC in these tumours resulted in tumour progression and was dependent on Aurora-A mediated MYC stabilization (Dauch *et al*. 2016). The use of conformation-altering Aurora-A inhibitors prevented the formation of the Aurora-A-MYC complex, resulting in increased MYC degradation and reduced tumour growth (Dauch *et al*. 2016). The efficacy of Aurora-A inhibition was observed *in-vivo*, where 50% of mice harbouring an aggressive liver tumour presented with reduced tumour size and improved long-term survival following treatment (Dauch *et al*. 2016).

Interestingly, Aurora-A has also been shown to functionally inactivate p53 in cells expressing wild-type p53. Aurora-A can phosphorylate p53 at S315, which promotes Mdm2-mediated degradation of p53, and at S215, which inhibits the DNA-binding ability of p53 (Katayama *et al*. 2004). In ovarian cancer cells, the inhibition of p53 function by Aurora-A was shown to enhance Akt activation and drive resistance to several chemotherapeutics including paclitaxel (Yang *et al*. 2006). Aurora-A has also been found to regulate the activity of p73, a tumour suppressor with a similar role to p53 (Katayama *et al*. 2012). Aurora-A can phosphorylate p73 at S235, diminishing p73 DNA-binding and transactivation activity by sequestering p73 in the cytoplasm. This phosphorylation of p73

was found to directly contribute to the abrogation of DNA damage-induced apoptosis and impaired the role of p73 at the spindle assembly checkpoint (Katayama *et al*. 2012).

Studies in gastric cancer have indicated a role for Aurora-A in NF-κB signalling. Analysis of gastric cancer cell lines showed that Aurora-A overexpression resulted in increased phosphorylation of IκBα, indicating that Aurora-A has a direct role in NF-κB activation. The potential of targeted inhibition of Aurora-A in gastric cancer was demonstrated in vivo in both a mouse model of gastric cancer and a xenograft model, with a significant reduction in tumour growth and enhanced apoptosis observed (Katsha *et al*. 2013).

Importantly, Aurora-A has recently been linked to tamoxifen resistance, with Aurora-A inhibition showing the ability to impair the growth of tamoxifen-resistant (Tam-R) breast cancer cells (Zheng *et al*. 2014, Thrane *et al*. 2015). The overexpression of forkhead box protein (FOX) A1 has been identified in metastatic ER+ breast cancer and has been linked to driving Tam-R cell growth (Hurtado *et al*. 2011, Ross-Innes *et al*. 2012). Inhibition of Aurora-A in Tam-R breast cancer cells was shown to impair cell growth, and reduced FOXA1 levels were observed in inhibitor treated Tam-R cells (Thrane *et al*. 2015). The inhibition of Aurora kinase was found to cause G2 arrest and induce apoptosis in Tam-R cells (Thrane *et al*. 2015). Furthermore, knockdown of Aurora-A decreased the growth of Tam-R cells and improved the efficacy of tamoxifen treatment (Thrane *et al*. 2015). Similarly, Zheng *et al*. (2014) found that Aurora-A inhibition worked synergistically with tamoxifen and overcame tamoxifen resistance. Their work also showed that Aurora-A can phosphorylate ERα at S167 and S305, driving ERα activity in the absence of estrogen (Zheng *et al*. 2014).

1.5 c-Jun N-terminal kinase (JNK) signalling in cancer.

The JNK family of MAPKs consists of three proteins JNK1, JNK2 and JNK3 whose genes are alternatively spliced resulting in at least ten isoforms (Gupta *et al*. 1996). JNK1 and JNK2 are thought to be expressed in all tissue types, while JNK3 is primarily expressed in the brain. JNKs are primarily activated by pro-inflammatory cytokine signalling and environmental stresses, with active JNK having a significant role in regulating cell proliferation, survival and migration in specific cell types (Weston and Davis. 2007, Rincon and Davis. 2009). JNKs require phosphorylation at both T183 and Y185 for full activation (Fleming *et al*. 2000). c-Jun is a substrate of JNK kinases, with phosphorylation of c-Jun at S73 supporting the activation of Activating protein (AP)-1, a master transcription factor consisting of homo- and heterodimers of jun, fos and activating transcription factor (ATF) family members (Karin *et al*. 1997). This confers a role for JNK in controlling the expression of an array of target genes (CyclinD1, p53, p21) that contain AP-1 binding sites, genes that are involved in cell cycle regulation, survival and apoptosis (Shaulian and Karin. 2002).

However, the actual role that JNK signalling can play in these cellular processes can vary depending on the cell type, the form and duration of stimuli and the isoform of JNK that is activated. For example, JNK has been indicated to have pro- and anti-apoptotic roles in cells through differential phosphorylation of Bcl-2 family members. JNK can promote apoptosis by phosphorylating the pro-apoptotic Bcl-2 family member BIM, while also supporting the cleavage and pro-apoptotic role of BID. Conversely, JNK can phosphorylate the pro-apoptotic BAD, leading to its sequestration and preventing the inactivation of the pro-survival protein Bcl-xL (Zha *et al*. 1996, Lei & Davis, 2003, Deng *et al*. 2003). Similarly, JNK has been found to have a significant role in balancing autophagy, the process of recycling old proteins and dysfunctional cell organelles, between contributing to cell survival or cell death depending on cell type and stimulus (Sui *et al*. 2014). A study in Head and Neck Sqaumous Cell Carcinoma (HNSCC) found that the drug bortezomib induces JNK activation and autophagy induction, leading to apoptotic cell death (Li and Johnson, 2012). Conversely, increased JNK activation and JNK driven autophagy in

myeloid leukemia cells was shown to promote cell survival and render cells resistant to treatment with chemotherapeutic drugs including Vincristine and VP-16 (Zhao *et al*. 2011).

As a result, JNK has been found to have a complex role in cancer, with both tumour-promoting and tumour-suppressing effects. JNK1 has been associated with driving HCC tumour growth and progression. JNK1 downregulation was shown to disrupt liver tumour formation and proliferation in mouse models, with observed increases in the expression of the CDK inhibitor p21 (Hui *et al*, 2008). Additionally, pharmacological inhibition of JNKs was shown to impair HCC development in xenograft studies (Chen *et al*. 2009). Conversely, JNK1 has been linked to a tumour suppressive role in skin cancer, with JNK1-deficient mice exhibiting increased susceptibility to skin tumour formation. However, in skin cancer JNK2 was shown to promote tumour development, with JNK2-deficient mice showing significantly reduced carcinogenesis (Chen *et al*. 2001, She *et al*. 2002). Importantly, high JNK2 expression has been associated with reduced survival of patients with basal like breast cancer, while JNK2 has been linked to tumour migration and metastasis in murine mammary tumour models (Nasrazadani and Van Den Berg 2010, Mitra *et al*. 2011).

Altered JNK activation has also been linked to chemotherapeutic resistance across multiple cancer subtypes (Sui *et al*. 2014, Suzuki *et al*. 2015, Ebelt *et al*. 2017, Lipner *et al*. 2020). JNK activation has been shown to contribute to 5-fluorouracil (5-FU) and gemcitabine (GEM) resistance of pancreatic cancer stem cells, due to JNKs ability to reduce intracellular reactive oxygen species (ROS) accumulation (Suzuki *et al*. 2015). JNK inhibition was shown to re-sensitize pancreatic cancer stem cells to 5-FU and GEM, promoting ROS-induced apoptosis (Suzuki *et al*. 2015). Similarly, JNK activation has been associated with 5-FU resistance in colon cancer by upregulating pro-survival autophagic signalling, with increased JNK phosphorylation of Bcl-2 observed. JNK inhibition impaired the autophagic responses and returned sensitivity of colon cancer cells to 5-FU treatment (Sui *et al*, 2014). JNK-IN-8 is an irreversible inhibitor of JNK1-3 family kinases. Lipner *et al*. (2020) showed that JNK-IN-8 treatment enhanced the sensitivity of 5-FU/FOLFOX(Folinic Acid + 5-Fluorouracil + Oxaliplatin)–resistant pancreatic ductal adenocarcinoma to 5-FU/FOLFOX, producing growth arrest of tumours *in-vivo* and tumour

regression in some cases (Lipner *et al*. 2020). Ebelt *et al*. (2017) were similarly able to show a synergistic role for JNK inhibition in TNBC using JNK-IN-8. Gefitinib, an EGFR inhibitor, and Lapatinib, a dual EGFR/HER2 inhibitor, have shown minimal efficacy in treating TNBC despite the presence of EGFR signalling. In breast cancer, EGFR signalling correlates significantly with JNK activation. Combining JNK-IN-8 with Lapatinib was found to synergize to promote cell death in TNBC cells (Ebelt *et al*. 2017). Here, JNK1 was indicated to be driving resistance to lapatinib treatment by limiting reactive oxygen species accumulation and supporting cell survival. Combining JNK-IN-8 treatment with lapatinib led to 10-fold increases in reactive oxygen species and enhanced cellular apoptosis (Ebelt *et al*. 2017). Overall, these research findings highlight the potential of JNK inhibition as a combination therapeutic option in tumours that have developed chemotherapeutic resistance.

1.6. Aims and Objectives

The aim of this work was to examine the role of IRAK1 in Tam-R ER+ breast cancer cells, determine whether targeted inhibition of IRAK1, alone or in combination with JNK family kinase inhibition, had an impact on the growth of Tam-R ER+ breast cancer cells and whether this inhibition re-sensitized Tam-R cells to tamoxifen treatments.

Chapter 2

Materials and Methods

2.1. Standard Laboratory Procedures.

Good laboratory practices were followed in all activities. All tissue culture materials and reagents were kept sterile and used in a class II (laminar flow) biological safety cabinet. Nucleic acid-free pipettes and nuclease-free solutions were used for all RNA work. Composition of all solutions, reagent and product sources, qRT-PCR primers and ImageJ analyses are outlined in Appendix I, II, III, and IV, respectively.

2.2. Cell culture.

2.2.1. Cell lines.

The ER+ tamoxifen-sensitive breast cancer cell line MCF-7 (Adenocarcinoma patient) was purchased from the American Type Culture Collection (ATCC) and gifted from the Young group (Royal College of Surgeons in Ireland) while its tamoxifen-resistant subline LY2 was gifted from Prof. Robert Clarke (Georgetown University). MCF-7 cells were established in 1973 from the pleural effusion of a 69-year old female breast cancer patient who had developed metastatic disease (Soule *et al*. 1973). MCF-7 cells have an epithelial phenotype whilst being ER+, progesterone receptor positive and belong to the luminal A molecular subtype (Brandes and Hermonat 1983, Comşa *et al*. 2015). This cell-line has subsequently been used worldwide as a model for studying ER+ breast cancer (Comşa *et al*. 2015). The LY2 cell line was established in 1985, by gradually increasing the concentration of LY117018 in the growth media of MCF-7 cells from 10^{-8} to 10^{-6} M as the cells became resistant (Bronzert *et al*. 1985). LY117018 is a raloxifene analog, a selective estrogen receptor modulator that exerts anti-proliferative effects in ER+ breast cancer cells. LY2 cells were subsequently found to exhibit resistance to the similar anti-estrogens tamoxifen and 4-OH hydroxytamoxifen (Bronzert *et al*. 1985). The ER+ tamoxifen-sensitive breast cancer cell line T47D (Ductal carcinoma patient) along with its tamoxifen-resistant subline TR-1 were purchased from the European Collection of Authenticated Cell Cultures (ECACC). T47D cells were isolated from the pleural effusion of a 54-year old female breast cancer patient (Keydar *et al*. 1979). T47D cells have an epithelial phenotype and are ER+, progesterone receptor positive and belong to the luminal A molecular subtype (Yu *et*

al. 2017). Thus, they have been widely used as a model to research ER+ breast cancer. The TR-1 cell line was established in 2014 from the T47D subline T47D/S2, T47D cells that had been adapted to grow in 2% FBS. These cells were treated long-term with 1uM Tamoxifen and after ~10 months the growth of TR-1 cells was similar to that of parental cells (Thrane *et al*. 2015).

2.2.2. Reagents for cell passage and treatment.

Z-(4)-hydroxytamoxifen was purchased from Tocris. JNK-IN-7 and JNK-IN-8 were purchased from MedChemExpress Europe. Pacritinib was purchased from SelleckChem. AS602801 was purchased from MedChemExpress Europe. Fetal Bovine Serum (FBS) was purchased from Sigma-Aldrich, with specific batches that had been tested for any excessive hormonal responses used. FBS was briefly inactivated prior to use by incubating at 56^0C for 30 minutes. The FBS that was used for the tamoxifen-resistant cell lines was first stripped of hormones using Charcoal, dextran coated (Sigma-Aldrich). 1% (w/v) Charcoal was added to a bottle of FBS, which was then incubated overnight at 4^0C with gentle agitation on a rocker. The charcoal was then removed by centrifugation at 1500g for 30 minutes, followed by sterile filtration using 0.20μm filters (Sarstedt).

The MCF-7 cell line was cultured in DMEM High-Glucose (Sigma-Aldrich) supplemented with 10% FBS and 0.1% Gentamicin. The LY2 cell line was cultured in Gibco™ phenol-free MEM (ThermoFisher Scientific) supplemented with 10% charcoal-stripped FBS (CSF), 1% L-Glutamine (Sigma-Aldrich), 10nM Z-(4)-hydroxytamoxifen (Tocris) and 0.1% Gentamicin (Sigma-Aldrich). The T47D cell line was cultured in Gibco™ RPMI-1640 (ThermoFisher Scientific) supplemented with 10% FBS and 0.1% Gentamicin. The TR-1 cell line was cultured in phenol-free RPMI-1640 (Sigma-Aldrich) supplemented with 10% CSF, 2.5mM Alanyl-Glutamine (Sigma-Aldrich), 8μg/ml Insulin (Sigma-Aldrich), 5nM Z-(4)-hydroxytamoxifen and 0.1% Gentamicin. Cells were maintained in an incubator at 37^0C and 5% CO_2 in a humidified atmosphere. All cells were passaged using 2% trypsin-EDTA in PBS when reaching approximately 90% confluency. Cell number was determined

using a haemocytometer. Briefly, cells were loaded onto the chamber by capillarity, and then visualised and counted using a microscope.

2.2.3. Lentiviral shRNA knockdown.

HEK293T cells were seeded at a density of $2x10^5$ cells/ml (3mls) in 6-well plates to reach a confluency of 70-80% for next day transfection. Cells were transfected using Lipofectamine 2000 (Invitrogen) according to the manufacturer's instructions with the packaging plasmid psPAX2 (1μg), envelope plasmid pMD2.G (1μg) and IRAK1 sh-pLKO.1 vector (2μg; Sigma-Aldrich), or control short-hairpin RNA (shRNA) (SigmaAldrich). The control shRNA was a non-targeting shRNA vector. Medium was replaced 24 hours post-transfection with a 30% (v/v) FBS-containing medium for a further 24 hours. The lentivirus-containing medium was then harvested, fresh medium was added, and lentiviral particles were collected again 24 h later. Collected lentiviral medium was centrifuged at 1200rpm for 5 minutes before transfer to falcon tubes for long-term storage at -20^0C. For transduction, cells were seeded into T75 flasks and at a confluency of ~70%, cells were transduced with 2mls of lentivirus-containing medium with hexadimethrine bromide (8 mg/ml). The following day medium was removed and replaced with fresh medium supplemented with the selective agent puromycin (InvivoGen) at a final concentration of 5μg/ml. Results shown are from IRAK1sh-1 unless otherwise stated.

Human IRAK1 Sequence (IRAK1sh-1)

CCGGGCCACCGCAGATTATCATCAACTCGAGTTGATGATAATCTGCGGTGGCTTTTTG

Human IRAK1 Sequence (IRAK1sh-2):

CCGGCCGCTTCTACAAAGTGATGGACTCGAGTCCATCACTTTGTAGAAGCGGTTTTTG

Dr. Marion Butler (PhD supervisor) generated the control and IRAK1 knockdown cell lines for MCF-7, LY2, T47D and TR-1 that were used in this project.

2.2.4. Cryopreservation of cells.

Cells were trypsinized and pelleted by centrifugation at 1500rpm for 5 minutes at room temperature and re-suspended in pre-cooled (4^0C) freezing medium (Complete culture medium containing 15% FBS and 10% DMSO) at a concentration of $1x10^6$ cells/ml. Cells were then transferred to cryotubes (Nunc) and placed in a Mr. Frosty (Sigma-Aldrich) in a -70^0C freezer overnight. This container has a cooling rate of approximately 1^0C/minute. Vials were then transferred to liquid nitrogen for long term storage.

2.2.5. Recovery of cells from liquid nitrogen.

Cells were quickly thawed at 37^0C and transferred to a 50ml Falcon tube for centrifugation at 1500g for 5 minutes at room temperature. The freezing medium was removed and the cell pellet was re-suspended in the relevant complete media. Cells were then transferred to a sterile tissue culture flask and placed in an incubator as detailed previously.

2.3. Cell Growth and Migration assays.

2.3.1. 2D cell proliferation assays.

Knockdown assays

Cells were seeded in two individual 12-well plates at $4x10^4$ cells/ml in their relevant complete media. Cells were then incubated for either 4 or 7 days. One plate was counted after 4 days and the other after 7 days. Here, media was removed and 200µl of 2X trypsin was added for ~5 minutes. 800µl of PBS was then added, wells were resuspended and counted using a haemocytometer to determine the cell concentration/ml. Cells were seeded in quadruplicate and counted in triplicate. Whole cell lysate was collected from the extra well to confirm that knockdown was present. These results can be seen in Appendix V.

Inhibitor assays.

Cells were seeded in two individual 12-well plates at $4x10^4$ cells/ml in their relevant complete media. Cells were treated after 24 hours with the indicated inhibitor or DMSO (vehicle control). Cells were then incubated for 7 days. One plate was counted after 4 days and the other after 7 days. Here, media was removed and 200µl of 2X trypsin was added for ~5 minutes. 800µl of PBS was then added, wells were resuspended and counted using a haemocytometer to determine the cell concentration/ml. All treatment conditions were counted in triplicate.

MTS assays for tamoxifen-resistant cell lines.

Tamoxifen-resistant (Tam-R) cells were seeded at 2000 cells/well (150µl) in relevant media containing no supplementary tamoxifen in a 96-well plate. After 24 hours, cells were treated with 30µl of the indicated concentrations of tamoxifen or DMSO (vehicle control). After 72 hours, 20µl of MTS reagent (abcam) was added to the wells and the plate was returned to the CO_2 tissue culture incubator for 2 hours. The plate was then placed on a rocker at 50rpm for 2 minutes to equilibrate and absorbance was then read at OD=490nm (Biotek Synergy HTX plate reader).

2.3.2. Colony-formation assays.

Knockdown assays.

Cells were seeded in 6-well plates at 3000 cells/well (MCF-7 and LY2) or 9000 cells/well (T47D and TR-1) in relevant media (Section 2.2.2). After ~17 days, media was removed and wells were gently rinsed with PBS. Colonies were then fixed in methanol (Sigma-Aldrich) for 5 minutes. Methanol was removed and colonies were stained with 0.5% (v/v) Crystal Violet (Sigma-Aldrich) diluted in 20% Methanol. Colonies were counted using the OpenCFU software.

Tamoxifen response assays.

Cells were seeded in 6-well plates at 3000 cells/well (LY2) or 9000 cells/well (TR-1) in relevant media containing no supplementary tamoxifen. Wells were treated with tamoxifen after 24 hours and left for ~1 days. At this point, media was removed and wells were gently rinsed with PBS. Colonies were then fixed in methanol for 5 minutes. Methanol was removed and colonies were stained with 0.5% (v/v) Crystal Violet diluted in 20% Methanol. Colonies were counted using the OpenCFU software.

2.3.3. 3D Matrigel assays.

Flat-bottom 96-well plates (Corning) were coated with 50µl of 5mg/ml PolyHEMA (Sigma) diluted in 96% ethanol to inhibit the ability of cells to adhere to the well surface. PolyHEMA was solubilised by heating overnight in a water bath at 50^0C and vortexing multiple times. Following the coating, plates were dried for 2 days at 50^0C.

Knockdown assays.

Cells were seeded at $5x10^4$ cells/ml in complete media with 2% (v/v) Matrigel® Basement Membrane Matrix, growth factor reduced (Corning). 90µl of the cell suspension was added to each well. Plates were wrapped in parafilm and incubated for 10 days, supplemented with 30µl of fresh media every 3 days. On Day 10, 50µl of CellTiter-Glo® 3D viability reagent (Promega) was added to the wells. The plate was wrapped in tin foil and rotated at 150rpm for 5 minutes to induce cell lysis, followed by incubation at room temperature for 25 minutes. Luminescence was then read using a CLARIOstar® plus microplate reader (BMG Labtech).

Inhibitor assays.

Cells were seeded at $5x10^4$ cells/ml in complete media with 2% (v/v) Matrigel. 90µl of the cell suspension was added to each well. Wells were treated with indicated inhibitors on Day 4 to allow for colony formation before the addition of inhibitors. Plates were wrapped in

parafilm and incubated for a further 3 days. On Day 7, 12µl of PrestoBlue Cell Viability (Invitrogen) was added to the wells and plates were returned to the incubator for 7 hours. Fluorescence was then read using a CLARIOstar® plus microplate reader (BMG Labtech).

2.3.4. 3D spheroid assays.

Knockdown assays.

Cells were seeded at 500cells/well in complete media in 96-well U-bottom ultra-low attachment plates (Greiner Bio-One). Spheroids were allowed to develop for 24 hours, and then imaged at 10X magnification (Optika Vision Pro) and the diameter measured (Olympus EP50) under a microscope using EP-view software to record spheroid diameter at Day 1. Spheroids were left to develop for 10 days in total with spheroids being imaged and the diameter measured at Day 6 and Day 10. Day 1 diameter was subtracted from the Day 6 or Day 10 measurement to determine spheroid progression.

Inhibitor assays.

Cells were seeded at 500cells/well in hormone-deplete media in 96-well U-bottom ultra-low attachment plates (Greiner Bio-One). Spheroids were allowed to develop for 24 hours, and then imaged at 10X magnification (Optika Vision Pro) and the diameter measured (Olympus EP50) under a microscope using EP-view software to record spheroid diameter at Day 1. Wells were then treated with the indicated concentration of tamoxifen or DMSO (vehicle control). Spheroids were then left to develop for 10 days in total with spheroids being imaged and the diameter measured at Day 6 and Day 10. Day 1 diameter was subtracted from the Day 6 or Day 10 measurement to determine spheroid progression.

2.3.5. 2D Migration assays.

4-chamber inserts (IBIDI) were placed in the centre of the wells of a 6-well plate. Cells were seeded into the individual chambers at 6-8x10^5 cells/ml and left for 24 hours. 200µl of cell suspension was added to each chamber. After 24 hours the inserts were removed and the wells were gently rinsed with PBS. 3mls of fresh complete media was gently added to the wells and the gap left between the cells was immediately imaged and measured at ~500µm at 10X magnification on an Optika Vision Pro camera using Optika Vision Pro software. Images were then taken twice daily until the gap closed.

2.4 Western Blot.

2.4.1. Preparation of samples.

Whole Cell Lysates.

Cells were seeded into 6-well plates at a density of 4x10^5 cells/ml (3mls/well) for next day harvest. For inhibitor treatments, cells were seeded at 1-2x10^5 cells/ml for 24 hours prior to treatment. The details for each experiment are described in the correspondent results section and figure legends.

When harvesting cell lysates, plates were placed on ice. Media was removed and the cells were gently washed once with ice-cold PBS. 200µl of Lysis Buffer (Appendix I) was added to each well, and the plates were incubated at 4^0C on a rocker at 35rpm for 35 minutes. Lysates were then collected into 1.5ml tubes and centrifuged at 12000g at 4^0C for 10 minutes. The supernatants were transferred into new 1.5ml tubes and the appropriate amount of 4X Sample buffer (Appendix I) was added. Samples were then boiled for 10 minutes at 95^0C, before being stored at -20^0C.

Nuclear Extraction.

Cells were seeded in 10cm dishes at 4x10^5 cells/ml (10mls/dish). After 24 hours, the medium was removed from the wells and nuclear and cytosolic fractionation was performed a Nuclear Extraction Kit (Active Motif - MyBio) as per manufacturer's

instructions. Dishes were gently washed with ice-cold PBS containing phosphatase inhibitors. 1ml of PBS with phosphatase inhibitors was then added to the dishes and cells were collected with a scraper into 1.5ml tubes, then centrifuged at 500g for 5 minutes at 4^0C. Supernatant was removed and the cell pellet was re-suspended in 400µl 1X hypotonic buffer and left for 15 minutes on ice. 20µl of detergent (10% NP-40) was added and each tube was vortexed for 10 seconds, prior to centrifugation at 12000g for 30 seconds at 4^0C. The supernatant (cytoplasmic fraction) was collected in a new 1.5ml tube. The cell pellet was washed in 500µl of PBS containing protease inhibitors three times, with centrifugation at 12000g for 1 minute at 4^0C. All supernatant was removed and the cell pellet was re-suspended in nuclear lysis buffer, with samples then placed on a rocker at 70rpm for 30 minutes. All samples were re-suspended every 10 minutes while on the rocker. All tubes were then vortexed for 30 seconds, followed by centrifugation at 12000g for 10 minutes at 4^0C. The supernatant (nuclear fraction) was transferred to a fresh 1.5ml tube. The appropriate amount of 4X sample buffer was added to cytoplasmic and nuclear samples and they were subsequently boiled at 95^0C for 10 minutes, followed by storage at -20^0C.

2.4.2. SDS-PAGE.

SDS-polyacrylamide gel electrophoresis (SDS-PAGE) was conducted in a Biorad Mini-Protean® Tetra System, according to the method of Laemmli (Laemmli, 1970), as modified by Studier (Studier, 1973). Typically, 10% gels were used with alterations made depending on the size of the protein of interest. Details about the preparation of all gels are displayed in Table 2.1, whilst all the buffers used can be found in Appendix I. Ultra-pure Protogel® was purchased from National Diagnostics; APS and TEMED from Sigma-Aldrich. Samples and pre-stained protein marker (PageRuler^{TM} Pre-stained Protein Ladder, 15-250kDa, ThermoFisher Scientific) were loaded into separate wells. They were then run in 1X Running buffer at 90V through the 5% stacking gel, followed by 120V through the resolving gel for between 2-3 hours depending on the size of the protein of interest

Lower Resolving Gels:

% Total Acrylamide		8%	10%	12%	15%
H_20	ml	12.1	10.5	8.75	6.25
4X Lower Tris Buffer	ml	6.25	6.25	6.25	6.25
Protogel	ml	6.67	8.35	10	12.5
10% (w/v) APS	µl	130	130	130	130
TEMED	µl	14	14	14	14
Total Volume	ml	25	25	25	25

Upper Stacking Gel:

% Total Acrylamide		5%
H_20	ml	5.8
4X Upper Tris Buffer	ml	2.5
Protogel	ml	1.7
10% (w/v) APS	µl	40
TEMED	µl	20
Total Volume	ml	10

Table 2.1. Composition of the polyacrylamide gels used.

2.4.3. Immunoblotting (Western Blot).

Following the electrophoretic separation, the proteins were transferred onto Immobilon-P PVDF membranes (0.45µm pore size) (Merck-Millipore) in a Biometra FastBlot™ semi-dry transfer unit at 90mA/gel (4 gels maximum, correspondent to 360mA) for 25-35 minutes, depending on the size of the protein of interest, using PVDF and whatman paper

(Sigma-Aldrich) pre-soaked in transfer buffer (Appendix I). Amersham^{TM} nitrocellulose membranes (GE Healthcare) were used when probing for smaller proteins (<50kDa). All membranes were activated prior to use in methanol (PVDF) or water (Nitrocellulose) for 1 minute. At the end of the transfer, the membranes were quickly washed in TBST (Appendix I), and their non-specific binding sites blocked for 1 hour using TBST containing 5% (w/v) powdered milk (Marvel). The membranes were then quickly washed in TBST, prior to overnight incubation at 4^0C with the appropriate primary antibody, diluted in 5% milk-TBST or 5% BSA-TBST. The specificity and dilution used for the various antibodies are listed in Table 2.2. After overnight incubation, membranes were washed in TBST for three 5 minute washes, length and number of washes varying slightly depending on the antibody being used. Following washing, the membranes were incubated for 2 hours at room temperature with the HRP-conjugated secondary antibody. Anti-Mouse or Anti-Rabbit IgG-HRP (Cell Signalling Technology Inc. (7076S) and Sigma-Aldrich (A6154), respectively) was diluted 1:2000 in 5% milk-TBST. The membranes were finally washed three times for 5 minutes in TBST, transferred to an autoradiography cassette and covered with either Luminata Forte Western HRP substrate (Sigma-Aldrich) or a 1:1 mix of Solution A and Solution B (Appendix I). The cassette was then transferred to a dark room, where autoradiograph film (Santa Cruz Biotechnology) was placed on top of the membranes, left to expose for 1-60 minutes and developed using developer and fixer solutions (LabTech). Blots were scanned and the relative abundance of protein quantified by densitometric analysis using ImageJ software (NIH, Bethesda, MD). All Western Blot densitometry data were normalized to β-actin.

Primary Ab	Source	Dilution	Secondary Ab
β-actin (A5441)	Sigma	1:2000	Anti-mouse IgG-HRP
IRAK1 (D51G7)	Cell Signaling	1:1000	Anti-rabbit IgG-HRP
pERα (Ser118) (16J4)	Cell Signaling	1:1000	Anti-mouse IgG-HRP
pERα (Ser167) (D5W3Z)	Cell Signaling	1:1000	Anti-rabbit IgG-HRP
Total ERα (D8H8)	Cell Signaling	1:1000	Anti-rabbit IgG-HRP
PCNA (D3H8P)	Cell Signaling	1:1000	Anti-rabbit IgG-HRP
Tubulin (DM1A)	Cell Signaling	1:2000	Anti-mouse IgG-HRP
EGFR (D38B1)	Cell Signaling	1:1000	Anti-rabbit IgG-HRP
HER2 (D8F12)	Cell Signaling	1:1000	Anti-rabbit IgG-HRP
HER3 (D22C5)	Cell Signaling	1:1000	Anti-rabbit IgG-HRP
HER4 (111B2)	Cell Signaling	1:1000	Anti-rabbit IgG-HRP
HDAC1 (10E2)	Cell Signaling	1:1000	Anti-mouse IgG-HRP
p21 Waf1/Cip1 (DCS60)	Cell Signaling	1:1000	Anti-mouse IgG-HRP
p27 Kip1 (SX53G8.5)	Cell Signaling	1:1000	Anti-mouse IgG-HRP
pAurora A (Thr288) (C39D8)	Cell Signaling	1:1000	Anti-rabbit IgG-HRP
Total Aurora A (D3E4Q)	Cell Signaling	1:1000	Anti-rabbit IgG-HRP
pJNK (Thr183/Tyr185) (81E11)	Cell Signaling	1:1000	Anti-rabbit IgG-HRP
Total JNK (9252)	Cell Signaling	1:1000	Anti-rabbit IgG-HRP
pc-Jun (Ser73) (D47G9)	Cell Signaling	1:1000	Anti-rabbit IgG-HRP
Total c-Jun (60A8)	Cell Signaling	1:1000	Anti-rabbit IgG-HRP

Table 2.2. Specificity, source, dilution and correspondent secondary antibody of all primary antibodies used.

2.5. RNA isolation and cDNA synthesis.

All plasticware in use was certified RNAse-free.

2.5.1. Preparation of samples.

Cells were seeded in 12-well plates at a density of $4x10^5$ cells/ml (1.5ml/well) and left overnight. The details about each individual experiment are described in the relevant results section and figure legend. When ready, cells were gently washed with 1ml of ice-cold PBS, harvested in 500µl TRIzol® reagent (Sigma-Aldrich) and transferred to 1.5ml tubes. The samples were then subjected to RNA isolation or frozen at -70^0C until ready for RNA isolation procedure.

2.5.2. RNA isolation procedure.

Total RNA extraction was performed according to the manufacturer's instructions (TRIzol® reagent - Sigma-Aldrich). 50µl of 1-bromo-3-chloropropane (Sigma-Aldrich) was added to each sample, which were each then vortexed briefly and allowed to sit for 5 minutes at room temperature, followed by centrifugation at 12000g for 15 minutes at 4^0C. Here, the mixture separates into a lower red phenol phase, an interphase and a colourless upper aqueous phase; the RNA remains exclusively in the aqueous phase which was transferred to fresh 1.5ml tubes, avoiding any contact with the interphase or phenol layers. 250µl of Isopropanol (Sigma-Aldrich) was added to each sample, they were briefly vortexed and allowed to sit for 10 minutes at room temperature, followed by centrifugation at 12000g for 10 minutes at 4^0C. The supernatant was then decanted and 500µl of 75% ethanol (Sigma-Aldrich) was added. Samples were inverted 5 times, followed by centrifugation at 8000g for 5 minutes at 4^0C. Ethanol was removed and the pellet was left to air dry in a laminar flow hood for 7/8 minutes. 25µl of nuclease-free water was added and the samples were heated for 10 minutes at 60^0C. Samples were then briefly mixed and centrifuged to return all of samples to bottom of tubes. The quality and quantity of the isolated RNA was then determined using a Nanodrop 1000 spectrophotometer v3.3 (ThermoScientific).

2.5.3. cDNA synthesis.

400ng of RNA was converted into cDNA using the 5X All-In-One RT MasterMix (NBS Biologicals), according to the manufacturer's instructions. 2µl of the MasterMix was added to 8µl of 50ng/µl RNA, for a final volume of 10µl. Samples were gently mixed and then placed in a thermal cycler (G-Storm, Gene Technologies). Samples were incubated at 4^0C for 5 minutes, 25^0C for 10 minutes, 42^0C for 50 minutes, 85^0C for 5 minutes and then held at 4^0C prior to retrieval.

2.5.4. Real-time PCR.

The real-time PCR was performed on cDNAs using the FastStart Universal SYBR Green Master (ROX) (Roche Diagnostic). The mix used for the quantification of the target genes included 5µl of the Master mix, 0.5µM of each primer (forward and reverse), 2µl of cDNA and water up to a final volume of 10µl. The sequence and T_m of the primers used is shown in Appendix II. The thermal cycling conditions are shown in Table 2.3. The annealing temperature was selected based on the primer set being used, and was generally 2^0C less than the lower T_m value. Real-time PCR was performed on a StepOnePlus Real-Time PCR System (Applied Biosystems) using MicroAmp Fast 96-well reaction plates (0.1ml, Applied Biosystems). All Real-time PCR experiments included a negative control to ensure the absence of contaminating DNA. The data was analysed using the $2^{-\Delta\Delta CT}$ method, with all samples normalised to *GAPDH*.

Step	Temperature, ^{0}C	Time	Number of cycles
Initial denaturation	95	10 min	1
Denaturation	95	15 s	40
Annealing	52-60	1 min	
Extension	72	15 s	

Table 2.3. Thermal cycling protocol followed for real-time PCR experiments.

2.6. Statistical analysis.

Data analysis was carried out using paired or unpaired Student t tests using GraphPad Prism. Statistically significant differences are indicated by the asterisks: *, $P<0.05$; **, $P<0.01$; ***, $P<0.001$.

Chapter 3

Targeting IRAK1 in Tamoxifen-Resistant Breast Cancer

3.1. Introduction.

IRAK1 has been extensively researched in innate immunology, where it is recognized as an important mediator of signalling downstream of the IL-1 and Toll-like receptors (Flannery and Bowie 2010). In the innate immune response, IRAK1 plays a crucial role in regulating cellular responses to various infections, influencing processes including cell cycle progression, apoptosis and inflammatory responses (Flannery & Bowie 2010, Jain *et al*. 2014). The predominant mechanisms by which IRAK1 modulates the innate immune response is through the activation of the NF-kB and MAPK signalling cascades. Given the role that aberrant NF-kB and MAPK activity can play in cancer development and progression, a potential oncogenic role for IRAK1 has subsequently been studied in various cancers (Zhang *et al*. 2017, Braicu *et al*. 2019).

In recent years, IRAK1 has been found to be overexpressed in Myelodysplastic Syndrome (Rhyasen *et al*. 2013), T-cell Acute Lymphoblastic Leukemia (Dussiau *et al*. 2015) and Hepatocellular Carcinoma (HCC) (Su *et al*. 2015) while hyperphosphorylation of IRAK1 has also been identified in HCC and Activated B-cell like Diffuse Large B-cell Lymphoma (Ngo *et al*. 2011, Su *et al*. 2015). In each of these cases, targeted inhibition of IRAK1 through shRNA knockdown and/or the use of an IRAK1/4 kinase inhibitor showed potential therapeutic benefits, reducing cancer cell growth *in-vitro* and increasing survival in xenograft models (Rhyasen *et al*. 2013, Li *et al*. 2016).

Wee *et al*. (2015) investigated the role of IRAK1 in breast cancer where, through analysis of The Cancer Genome Atlas, they were able to identify that IRAK1 expression was elevated across breast cancer subtypes when compared to normal breast epithelium, most significantly in the basal subtype. Their research focused on TNBC, where they found that blocking IRAK1 kinase activity reduced cell growth and migration *in-vitro*. Their findings indicated that the inhibition of IRAK1 kinase activity was sufficient to reduce NF-κB activation and the subsequent production of the pro-inflammatory cytokines IL-6 and IL-8 (Wee *et al*. 2015). They were subsequently able to show that IRAK1 knockdown impaired the growth of TNBC xenograft models and reduced lung metastasis while IRAK1 kinase inhibition was also capable of impairing lung metastasis *in-vivo* (Wee *et al*. 2015). Additionally, their research revealed a role for IRAK1 in the development of resistance to

the chemotherapeutic paclitaxel, with both IRAK1 knockdown and IRAK1 kinase inhibition reducing the growth of paclitaxel-resistant cells and re-sensitizing cells to paclitaxel treatments *in-vitro* (Wee *et al*, 2015).

Recently, two further publications have expanded on the role of IRAK1 in breast cancer. Research by Goh *et al*. (2017) was able to identify the presence of a chromosome amplification at 1q21.3 in a high percentage of breast tumours. The genes for several S100 family members are located here and their findings showed that IRAK1, through a positive feedback loop with S100A7/8/9, was driving tumoursphere growth in 1q21.3-amplified breast cancer cell lines. The inhibition of IRAK1 using pacritinib, a small molecule kinase inhibitor that also targets JAK2 and Flt3, reduced cancer cell growth *in-vitro* and *in-vivo*, showing enhanced efficacy in 1q21.3-amplified cells (Goh *et al*. 2017). Liu *et al*. (2019) identified a unique role for IRAK1 in mediating radiation resistance across cancers containing mutant p53, including breast cancer. Their research on mutant p53 cancers showed that, in response to radiation therapy, IRAK1 was inhibiting PIDDosome-mediated apoptosis. They were subsequently able to show that targeted inhibition of IRAK1 kinase activity in mutant p53 tumour cell models was able to re-sensitize cells to radiation therapy at the *in vitro* and *in-vivo* level (Liu *et al*. 2019).

However, the role of IRAK1 in ER+ endocrine-resistant breast cancer has not yet been studied. A role for IRAK1 in the growth of tamoxifen-sensitive (Tam-S) ER+ cells was demonstrated with the use of pacritinib, which impaired the growth of the 1q21.3-amplified ER+ breast cancer cell lines MCF-7 and T47D (Goh *et al*. 2017).

This work assessed the role of IRAK1 in ER+ breast cancer, with particular focus on the part that IRAK1 may play in the tamoxifen-resistant phenotype. Additionally, we studied whether targeting IRAK1 would re-sensitize tamoxifen-resistant (Tam-R) ER+ cells to tamoxifen treatments. Our findings show that targeting IRAK1 impairs the growth of Tam-R ER+ breast cancer cells and re-sensitizes Tam-R cells to tamoxifen *in-vitro*, supporting progression to animal models to assess the efficacy of targeting IRAK1 in Tam-R xenografts.

3.2. Results.

3.2.1. High IRAK1 expression is a significant negative prognostic marker in Luminal A breast cancer.

Analysis of data from The Cancer Genome Atlas database previously identified that IRAK1 is overexpressed across breast cancer subtypes when compared to normal breast epithelium (Wee *et al*. 2015). Subsequent analysis of breast cancer patient outcomes found that higher IRAK1 expression correlated with reduced survival and an increased chance of developing metastatic disease (Wee *et al*, 2015).

Analysis of the COSMIC database, provided by the Sanger institute, showed that IRAK1 is overexpressed in 12.23% of breast cancer samples tested while IRAK1 point mutations and copy number variations are rare in the breast (0.78% and 0.47% respectively) (https://cancer.sanger.ac.uk/cosmic/gene/analysis?ln=IRAK1). We analysed breast cancer patient survival data from the Kaplan-meier cancer survival database (kmplot.com) (Győrffy *et al*. 2010) to assess how IRAK1 expression affects the survival of Luminal A breast cancer patients specifically. For this analysis, we compared the survival of patients with upper quartile IRAK1 expression with patients with lower quartile IRAK1 expression (Q1 vs. Q4). We found that high IRAK1 expression correlated with significantly reduced relapse-free survival (RFS) of Luminal A breast cancer patients (Figure 3.1 (A), P=0.00088, n=966), with this correlation enhanced further when the lymph node positive Luminal A cohort was isolated (Figure 3.1 (B), P=0.0018, n=264). Additionally, high IRAK1 expression was a significant negative prognostic marker for overall survival (OS) of Luminal A breast cancer patients (Figure 3.2, P=0.0043, n=307).

Taken together, these findings implied that high IRAK1 expression is associated with tumour recurrence, cancer progression and reduced survival in patients with Luminal A breast cancer.

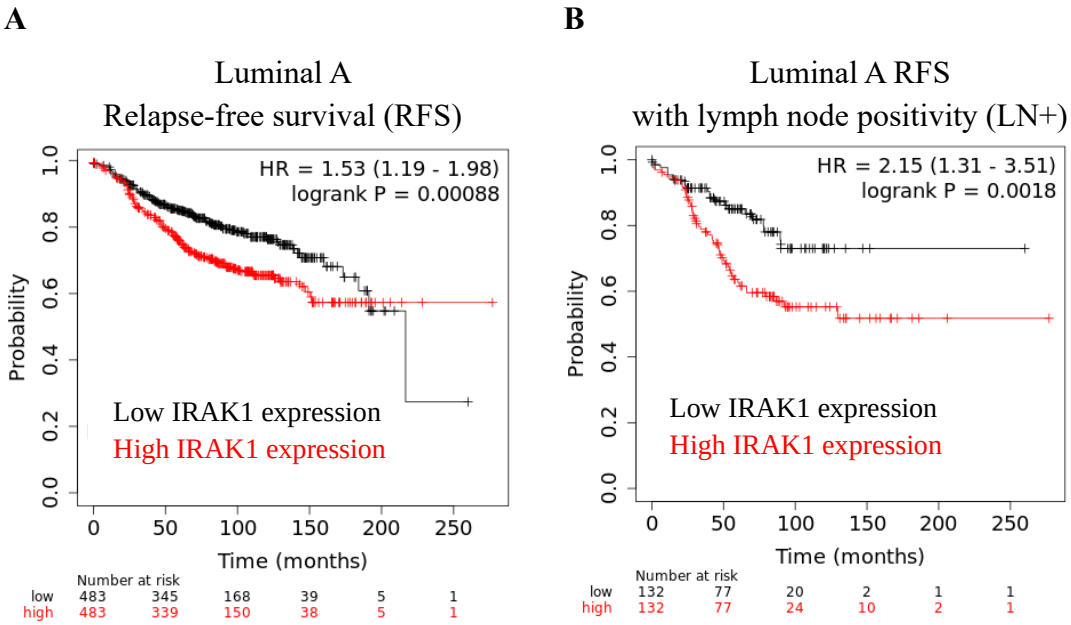

Figure 3.1. High IRAK1 expression correlates with significantly reduced relapse-free survival of Luminal A breast cancer patients, particularly in those patients where the cancer has progressed to the lymph nodes. Analysis of breast cancer survival data from kmplot.com separated into upper quartile IRAK1 expression vs lower quartile IRAK1 expression patients (Q1 vs Q4) (A) High IRAK1 expression correlates with significantly reduced RFS of Luminal A breast cancer patients (P=0.00088, n=1933). (B) High IRAK1 expression correlates with significantly reduced RFS of Luminal A breast cancer patients that present with lymph node positivity (P=0.0018, n=530).

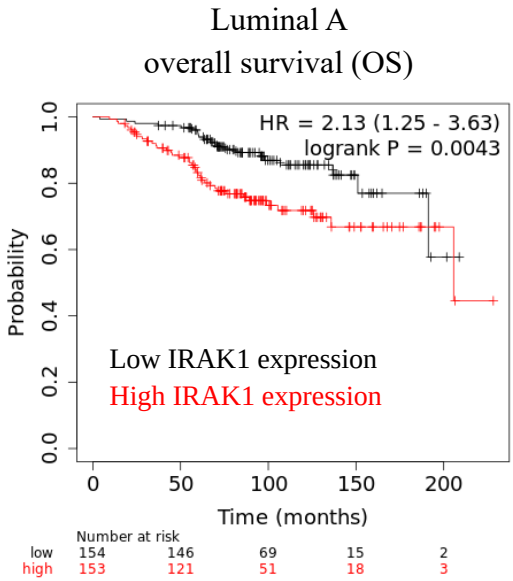

Figure 3.2. High IRAK1 expression correlates with significantly reduced overall survival of Luminal A breast cancer patients. Analysis of breast cancer survival data from kmplot.com separated into upper quartile IRAK1 expression vs lower quartile IRAK1 expression (Q1 vs Q4). High IRAK1 expression correlates with significantly reduced OS of Luminal A breast cancer patients (P=0.0043, n=611).

3.2.2. IRAK1 mRNA and protein levels are elevated in tamoxifen-resistant breast cancer cell lines when compared to their tamoxifen-sensitive parental cell lines, and this correlates with increased ERα expression and/or activity.

We analysed the expression of IRAK1 in the Tam-S Luminal A breast cancer cell lines MCF-7 and T47D, along with their Tam-R sublines LY2 and TR-1, respectively. We first measured mRNA levels in these cell lines by quantitative real-time PCR (qRT-PCR). As shown in Figure 3.3. (A), IRAK1 mRNA levels were significantly higher in both Tam-R cell lines when compared to their Tam-S parental cell lines. Similarly, we observed increases in IRAK1 protein levels in both Tam-R cell lines (Figure 3.3. (C), Supplementary Figure AIV.1). The presence of elevated IRAK1 levels in both tamoxifen-resistant cell lines together with the kmplot.com data (Figure 3.1 and Figure 3.2) supported an investigation into the role of IRAK1 in the growth of Tam-R ER+ breast cancer cell lines.

We next assessed the expression and activity of ERα in both Tam-S and Tam-R ER+ breast cancer cell lines. ERα expression is significantly increased in ER+ breast cancer and is recognised to drive ER+ tumour growth. We found that ERα mRNA levels were significantly increased in the LY2 cell line, when compared to the MCF-7 cell line. However, this result was not mirrored when we compared the T47D and TR-1 cell lines, where there was no discernible difference in ERα expression (Figure 3.3. (B)). When we looked at the protein level, the same results were observed (Figure 3.3. (C), Supplementary Figure AIV.1). To expand further, we subsequently sought to analyse the activity of ERα by looking at the phosphorylation of ERα at S118 and S167. Phosphorylation at these sites is important for the full activation of the receptor, and its ability to regulate transcription of target genes. Figure 3.3. (C) shows that the phosphorylation of ERα at both sites is increased in both Tam-R LY2 and TR-1 cells, when compared to their tamoxifen-sensitive parental cell lines. These findings indicated that there may be a link between IRAK1 and ERα activity in Tam-R cells

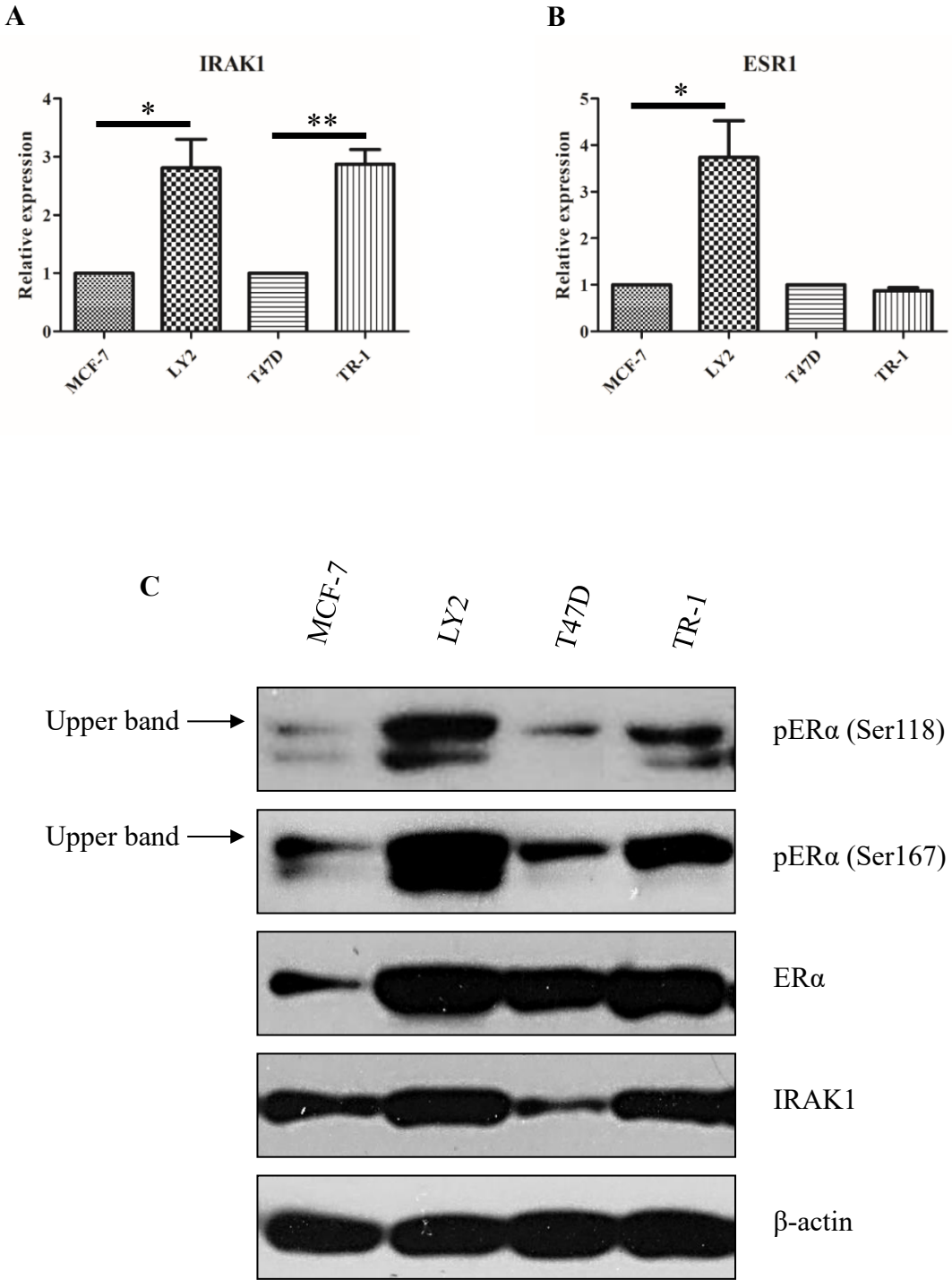
A
IRAK1
Relative expression
*
**
MCF-7
LY2
T47D
TR-1
B
ESR1
Relative expression
*
MCF-7
LY2
T47D
TR-1
C
MCF-7
LY2
T47D
TR-1
Upper band
Upper band
pERα (Ser118)
pERα (Ser167)
ERα
IRAK1
β-actin

Figure 3.3. IRAK1 mRNA and protein expression is increased in tamoxifen-resistant ER+ breast cancer cell lines and correlates with increased phosphorylation of ERα at S118 and S167. (A-B) Cells were seeded at $4x10^5$ cells/ml in 12-well plates overnight. LY2 cells were cultured in relevant media supplemented with 10nM Z-(4)-hydroxytamoxifen. TR-1 cells were cultured in relevant media supplemented with 5nM Z-(4)-hydroxytamoxifen. After 24 hours, cells were harvested in TriZol, RNA was isolated and subsequently subjected to reverse transcription, as previously described. The transcript levels of IRAK1 and ESR1 were determined by qRT-PCR and normalised against GAPDH mRNA. Results shown are the mean (±SEM) of three independent experiments performed in triplicate. (C) Cells were seeded at $4x10^5$ cells/ml in 6-well plates overnight. After 24 hours, whole cell lysates were extracted and subjected to Western blot. The resulting membranes were probed with phospho-ERα (S118), phospho-ERα (S167), total ERα, total IRAK1 and β-actin. Similar results were obtained in three independent experiments. Densitometric analysis comparing the expression of each protein (LY2 relative to MCF-7, TR-1 relative to T47D) was performed using ImageJ software (Figure AIV.1). The upper band was shown to be relevant to ERα in regard to Western blots involving pERα antibodies (Figure AVI.1). P value was calculated using the paired Student t test. Statistically significant differences are indicated by the asterisks: *, $P<0.05$; **, $P<0.01$.

As there were major differences observed in ERα expression and/or activity in the Tam-R LY2 and TR-1 breast cancer cell lines, we next analysed the expression of a number of ERα target genes (Figure 3.4). The most significant changes we observed were in the expression of EGR3 and GREB1, which were significantly reduced in both Tam-R cell lines (Figure 3.4. (A) & (C)). These genes are commonly used to assess ERα function in response to estrogen stimulation, while the loss of GREB1 expression has been linked to reduced tamoxifen efficacy previously (Ghosh *et al*. 2000, Inoue *et al*. 2004, Mohammed *et al*. 2013). The changes observed in the expression of other ERα target genes varied between the Tam-R cell lines (Figure 3.4). The expression of TFF1 and CCND1 was reduced in LY2 cells when compared to their parental MCF-7 cells, while their expression was increased in TR-1 cells when compared to their parental T47D cells (Figure 3.4. (B) & (E)). Conversely, the expression of SIAH2 was increased in LY2 cells whilst being reduced in TR-1 cells (Figure 3.4. (G)). Overall, these findings show that there are major alterations in ERα function following the development of resistance to tamoxifen treatment. The expression of CDK1 was also altered in both Tam-R cell lines (Figure 3.4. (F)). Combining this result with the changes in CCND1 expression would indicate that significant modifications are made in cell cycle regulation during the development of tamoxifen-resistance.

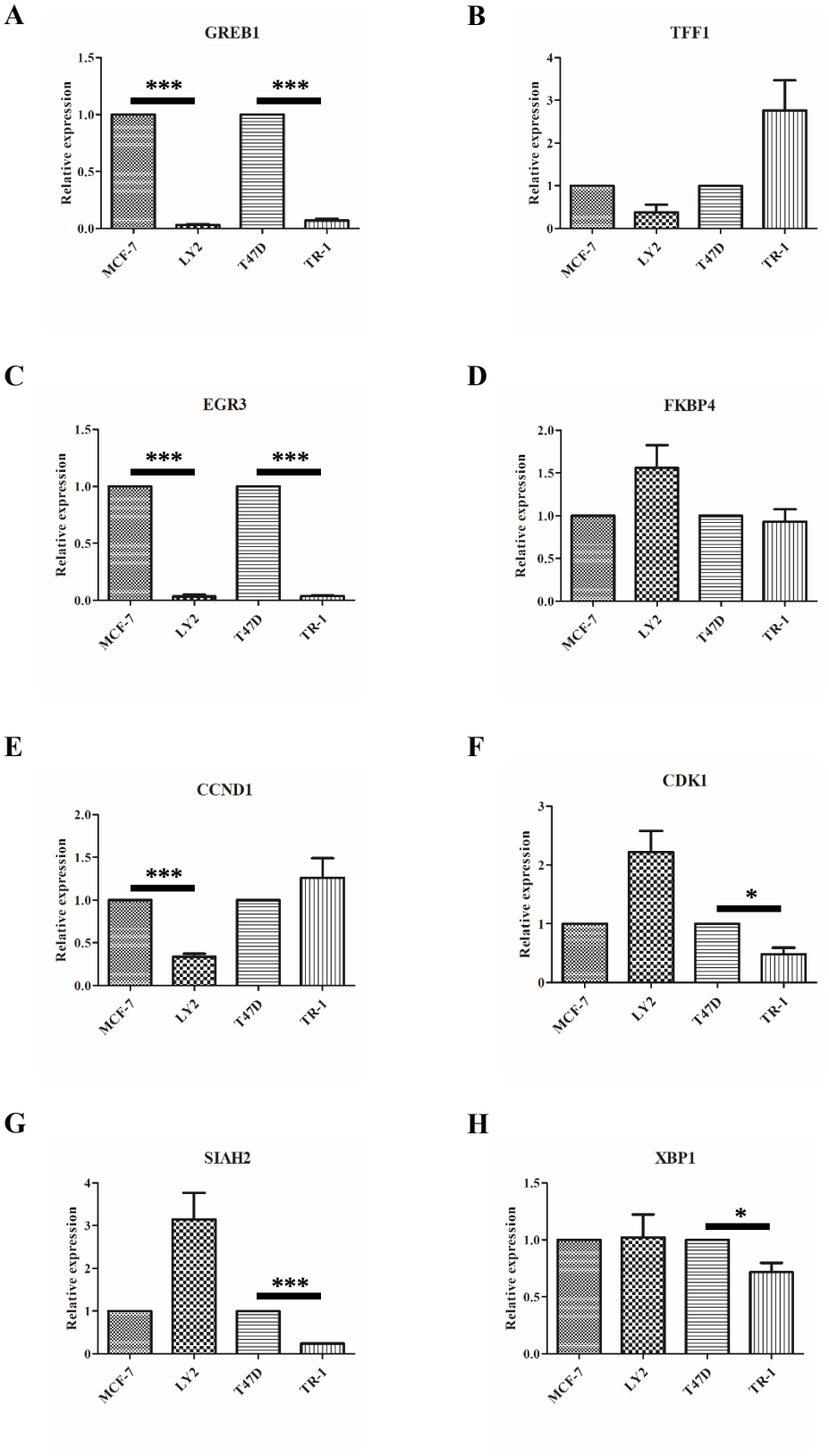
A
GREB1
Relative expression
1.5
1.0
0.5
0.0
***
***
MCF-7
LY2
T47D
TR-1
B
TFF1
Relative expression
4
3
2
1
0
MCF-7
LY2
T47D
TR-1
C
EGR3
Relative expression
1.5
1.0
0.5
0.0
***
***
MCF-7
LY2
T47D
TR-1
D
FKBP4
Relative expression
2.0
1.5
1.0
0.5
0.0
MCF-7
LY2
T47D
TR-1
E
CCND1
Relative expression
2.0
1.5
1.0
0.5
0.0
***
MCF-7
LY2
T47D
TR-1
F
CDK1
Relative expression
3
2
1
0
*
MCF-7
LY2
T47D
TR-1
G
SIAH2
Relative expression
4
3
2
1
0
***
MCF-7
LY2
T47D
TR-1
H
XBP1
Relative expression
1.5
1.0
0.5
0.0
*
MCF-7
LY2
T47D
TR-1

Figure 3.4. The expression of ERα target genes is significantly altered in tamoxifen-resistant ER+ breast cancer cells. Cells were seeded at $4x10^5$ cells/ml in 12-well plates overnight. LY2 cells were cultured in relevant media supplemented with 10nM Z-(4)-hydroxytamoxifen. TR-1 cells were cultured in relevant media supplemented with 5nM Z-(4)-hydroxytamoxifen. After 24 hours, cells were harvested in TriZol, RNA was isolated and subsequently subjected to reverse transcription, as previously described. The transcript levels of (A) GREB1, (B) TFF1, (C) EGR3, (D) FKBP4, (E) CCND1, (F) CDK1, (G) SIAH2 and (H) XBP1 were determined by qRT-PCR and normalised against GAPDH mRNA. Results shown are the mean (±SEM) of at least three independent experiments performed in triplicates. P value was calculated using the paired Student t test. Statistically significant differences are indicated by the asterisks: *, $P<0.05$; **, $P<0.01$; ***, $P<0.001$.

3.2.3. IRAK1 knockdown disrupts the growth of tamoxifen-resistant ER+ breast cancer cell lines across several *in-vitro* growth models, with reductions in cell growth also observed in the tamoxifen-sensitive T47D cell line.

IRAK1 has been identified to be overexpressed and/or hyperactivated in a number of cancers. These findings have led other researchers to assess the effects that targeted inhibition of IRAK1 has on the growth of these cancers. Wee *et al*. (2015) have already shown that both kinase inhibition and IRAK1 knockdown reduce the growth of TNBC cells.

Knowledge that high-IRAK1 expressing Luminal A breast cancers show poorer RFS and OS (Figure 3.1 and Figure 3.2), together with our data on higher IRAK1 expression in Tam-R cells (Figure 3.3), prompted us to address whether targeting IRAK1 would have an effect on the growth of both Tam-R and Tam-S ER+ breast cancer cell lines. We first generated stable knockdown of IRAK1, using two independent shRNAs targeting IRAK1, through a lentiviral approach in Tam-S breast cancer cell lines MCF-7 and T47D and their Tam-R sublines LY2 and TR-1, respectively. We performed proliferation assays, seeding cells at $4x10^4$ cells/ml in triplicate and counting on day 4 and day 7. We found that IRAK1 knockdown significantly reduced the proliferation of Tam-R LY2 and TR-1 cells (Figure 3.5. (B & D)). IRAK1 knockdown also significantly reduced the growth of Tam-S T47D cells but had no impact on the growth of MCF-7 cells as assessed by this 2D proliferation assay (Figure 3.5 (A & C)).

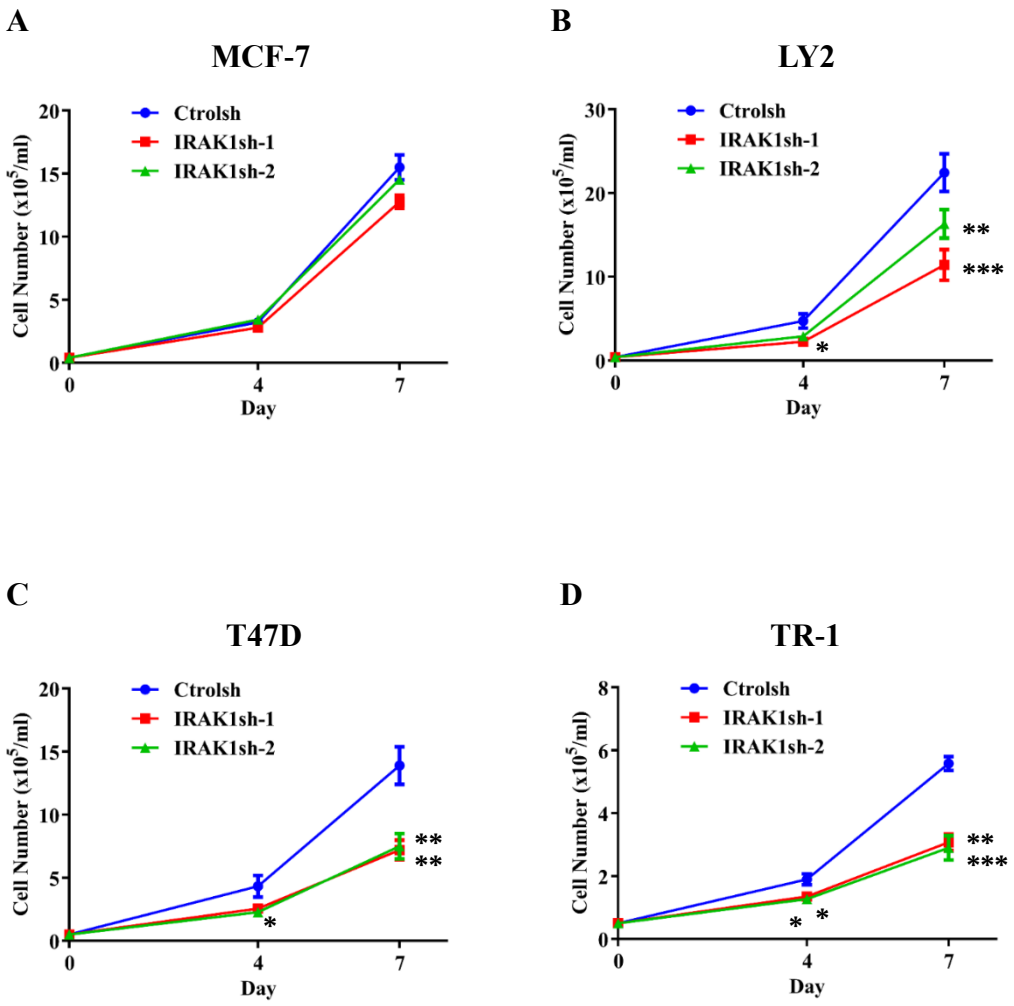

Figure 3.5. IRAK1 knockdown reduced 2D proliferation of Tam-R LY2 and TR-1 cells, while also reducing the growth of Tam-S T47D cells. Cells were seeded in two 12-well plates at 4x10^{4}cells/ml in quadruplicate. LY2 cells were cultured in relevant media supplemented with 10nM Z-(4)-hydroxytamoxifen. TR-1 cells were cultured in relevant media supplemented with 5nM Z-(4)-hydroxytamoxifen. Wells were counted in triplicate on day 4 and day 7 using a haemocytometer. Whole cell lysates were generated from the extra well on day 7 and subjected to Western Blot analysis to confirm IRAK1 knockdown (Appendix V). Results were obtained from at least 4 independent experiments. (A.) MCF-7 (B.) LY2 (C.) T47D (D.) TR-1. P value was calculated using the paired Student t test. Statistically significant differences are indicated by the asterisks: *, P<0.05; **, P<0.01; ***, P<0.001. **Dr. Marion Butler (PhD supervisor) generated the control and IRAK1 knockdown cell lines for MCF-7, LY2, T47D and TR-1 that were used in this project.**

We next addressed whether IRAK1 knockdown impacted colony-formation in Tam-R and Tam-S ER+ breast cancer cell lines. IRAK1 knockdown impaired the ability of Tam-R LY2 and TR-1 cells to form colonies, with pronounced differences observed between TR-1 control and IRAK1 knockdown cells (Figure 3.6. (B & D)). Similar to that observed in our 2D growth assays, colony-formation was decreased in T47D IRAK1sh cells compared to control cells while no differences were observed for MCF-7 IRAK1sh cells (Figure 3.6 (A & C)).

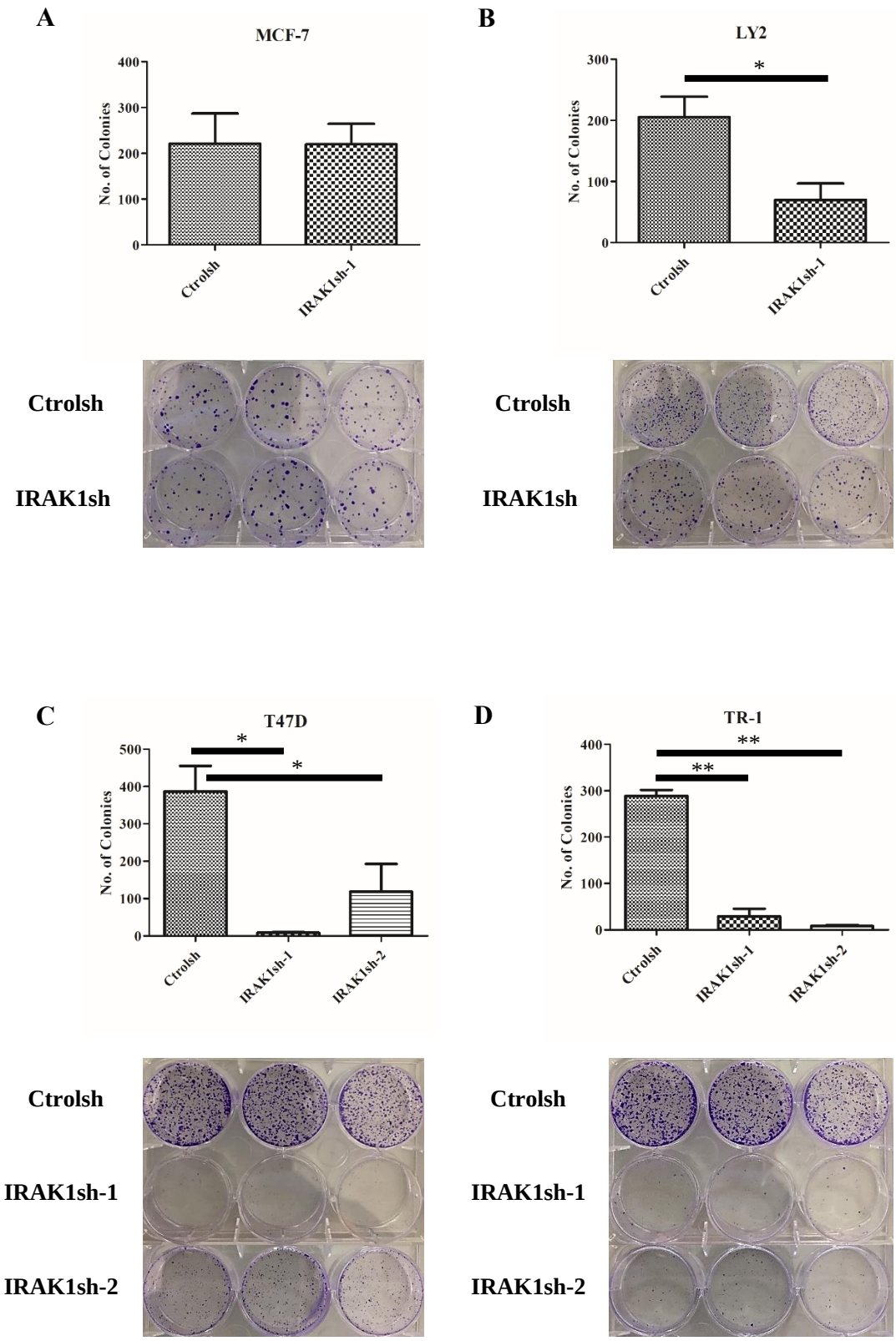
A
MCF-7
No. of Colonies
400
300
200
100
0
Ctrolsh
IRAK1sh-1
Ctrolsh
IRAK1sh
B
LY2
*
No. of Colonies
300
200
100
0
Ctrolsh
IRAK1sh-1
Ctrolsh
IRAK1sh
C
T47D
*
*
No. of Colonies
500
400
300
200
100
0
Ctrolsh
IRAK1sh-1
IRAK1sh-2
Ctrolsh
IRAK1sh-1
IRAK1sh-2
D
TR-1
**
**
No. of Colonies
400
300
200
100
0
Ctrolsh
IRAK1sh-1
IRAK1sh-2
Ctrolsh
IRAK1sh-1
IRAK1sh-2

Figure 3.6. IRAK1 knockdown reduced colony-formation of Tam-R LY2 and TR-1 cells, while also reducing the colony growth of Tam-S T47D cells. Cells were seeded in 6-well plates at 3000cells/well (MCF-7, LY2) and 9000cells/well (T47D, TR-1) to generate single-cell derived colonies. LY2 cells were cultured in relevant media supplemented with 10nM Z-(4)-hydroxytamoxifen. TR-1 cells were cultured in relevant media supplemented with 5nM Z-(4)-hydroxytamoxifen. Colony formation was assessed at day 17-21, at which point colonies were fixed in methanol and stained with 0.5% crystal violet. Analysis was done using the OpenCFU software tool. Results were obtained from at least 3 independent experiments. (A.) MCF-7 (B.) LY2 (C.) T47D (D.) TR-1. P value was calculated using the paired Student t test. Statistically significant differences are indicated by the asterisks: *, $P<0.05$; **, $P<0.01$.

To build on these findings, we wanted to address whether the results from these cellular assays would translate to a 3D *in-vitro* growth assay. 3D growth models more closely mimic *in-vivo* growth.

Firstly, we used a 3D Matrigel growth model. Results showed a modest reduction in the growth of Tam-R LY2 and TR-1 IRAK1sh cells compared to control cells. However, images captured at the time of analysis clearly showed growth differences between control and IRAK1 knockdown for LY2, TR-1 and T47D cells, whereas no differences were observed for MCF-7 cells (Figure 3.7).

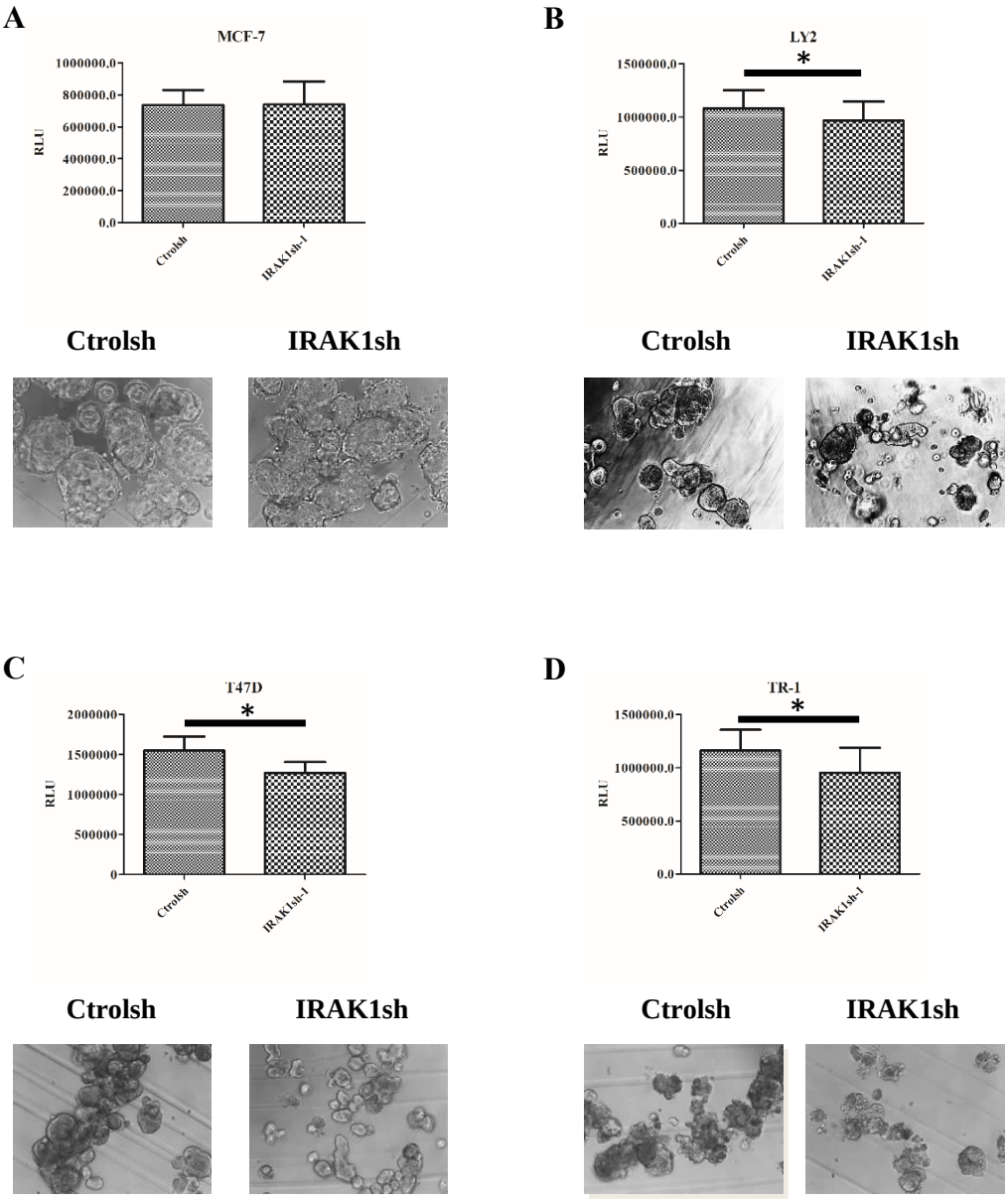

Figure 3.7. IRAK1 knockdown reduced the 3D growth of Tam-R LY2 and TR-1 cells in a 3D Matrigel model, while also reducing the growth of Tam-S T47D cells. Cells were seeded at $5x10^4$/ml (90µl/well) in Polyhema coated flat-bottom 96-well plates in their respective media containing 2% Matrigel. LY2 cells were cultured in relevant media supplemented with 10nM Z-(4)-hydroxytamoxifen. TR-1 cells were cultured in relevant media supplemented with 5nM Z-(4)-hydroxytamoxifen. Cells were then allowed to grow

out for 10 days, whilst being supplemented with 30µl of complete media every 3 days. On Day 10, 50µl of CellTiter Glo 3D viability reagent (Promega) was added. Plates were covered in tin foil before being placed on a rotator at 150rpm for 5 minutes, and subsequently allowed to sit at room temperature for 25 minutes. Luminescence was then read on a CLARIOstar® plus microplate reader (BMG Labtech). Wells were imaged using an Optika Vision Pro camera at 10X magnification. Results were obtained from at least 3 independent experiments. (A.) MCF-7 (B.) LY2 (C.) T47D (D.) TR-1. P value was calculated using the paired Student t test. Statistically significant differences are indicated by the asterisks: *, $P<0.05$.

To strengthen our 3D growth findings, we also used a 3D spheroid growth model (Figure 3.8). IRAK1 knockdown significantly reduced the growth of Tam-R LY2 and TR-1 spheroids, with a marked effect on Tam-R TR-1 spheroids (Figure 3.8 B & D) IRAK1 knockdown significantly reduced the growth of Tam-S T47D spheroids, but had no impact on the growth of the MCF-7 spheroids which is in agreement with our 2D proliferation, colony-forming assay and 3D Matrigel results for IRAK1sh T47D and MCF-7 cells.

A

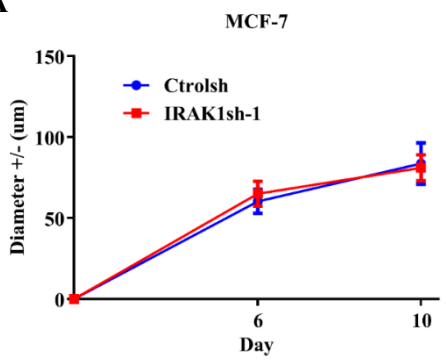

MCF-7 Ctrolsh
Day 10

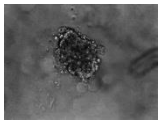

MCF-7 IRAK1sh
Day 10

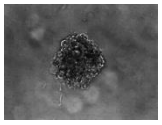

B

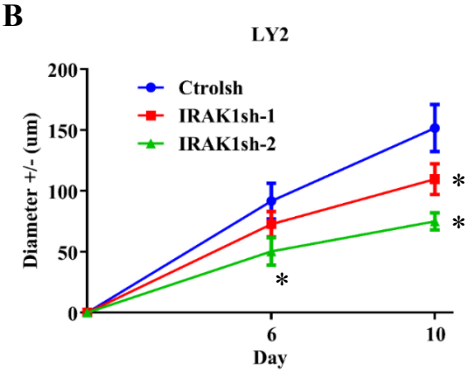

LY2 Ctrolsh
Day 10

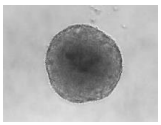

LY2 IRAK1sh-1
Day 10

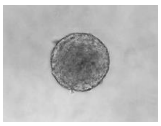

LY2 IRAK1sh-2
Day 10

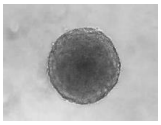

C

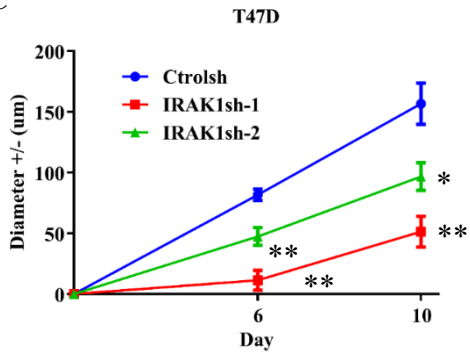

T47D Ctrolsh
Day 10

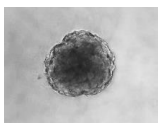

T47D IRAK1sh-1
Day 10

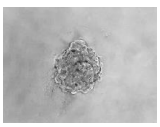

T47D IRAK1sh-2
Day 10

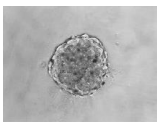

D

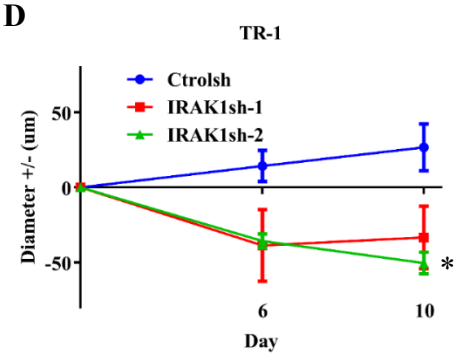

TR-1 Ctrolsh
Day 10

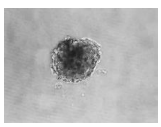

TR-1 IRAK1sh-1
Day 10

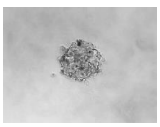

TR-1 IRAK1sh-2
Day 10

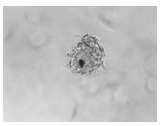

Figure 3.8. IRAK1 knockdown reduced the growth of Tam-R LY2 and TR-1 cells in a 3D spheroid growth model, while also reducing the growth of Tam-S T47D cells. Cells were seeded at 500cells/well in ultra-low attachment U-bottom 96-well plates (Greiner Bio-One). LY2 cells were cultured in relevant media supplemented with 10nM Z-(4)-hydroxytamoxifen. TR-1 cells were cultured in relevant media supplemented with 5nM Z-(4)-hydroxytamoxifen. The diameter of the resultant spheroids was measured using an Olympus EP50 camera after 24 hours and spheroids were imaged using an Optika Vision Pro camera at 10X magnification. Spheroid measurements and images were taken at day 6 and day 10. Results were obtained by subtracting the day 1 spheroid diameter from the day 6 and day 10 measurements to determine spheroid growth progression over that period. Results were obtained from at least 3 independent experiments. (A.) MCF-7 (B.) LY2 (C.) T47D (D.) TR-1. P value was calculated using the paired Student t test. Statistically significant differences are indicated by the asterisks: *, $P<0.05$; **, $P<0.01$.

Altogether, our results from these 2D and 3D assays showed consistent findings for IRAK1 knockdown in the Tam-R and Tam-S ER+ breast cancer cell lines used in this study. Firstly, IRAK1 knockdown has no significant effect on the growth of Tam-S MCF-7 cells, whilst significantly reducing the growth of Tam-S T47D cells, highlighting the existence of growth-pathway differences between these two most commonly studied Tam-S ER+ breast cancer cell lines. In contrast, IRAK1 knockdown significantly reduced the growth of Tam-R LY2 and TR-1 cells, which are the Tam-R sublines of MCF-7 and T47D, respectively. It is interesting that IRAK1 has a growth promoting role in Tam-R LY2 cells, given our findings for the parental cell line, MCF-7. These findings suggest that IRAK1 has a major role in maintaining the growth of Tam-R ER+ breast cancer cells.

We next assessed the impact of IRAK1 knockdown on 2D migration in the Tam-S and Tam-R ER+ breast cancer cell lines used in this study. There was no significant change in migration observed in IRAK1sh MCF-7 cells when compared to control cells (Figure 3.9. (A)). In contrast, IRAK1 knockdown significantly impaired the migration of LY2 and T47D cells when compared to control cells in this 2D migration assay (Figure 3.9. (B) & (C)). Interestingly, in disparity with the results from our growth analysis, IRAK1 knockdown had no significant effect on the migration of Tam-R TR-1 cells (Figure 3.9. (D)). The TR-1 cells migrated slower than the other Tam-S and Tam-R cells, as gap closure time was 5 days for TR-1 cells compared to 2/3 days for the other ER+ breast cancer cells used in this study.

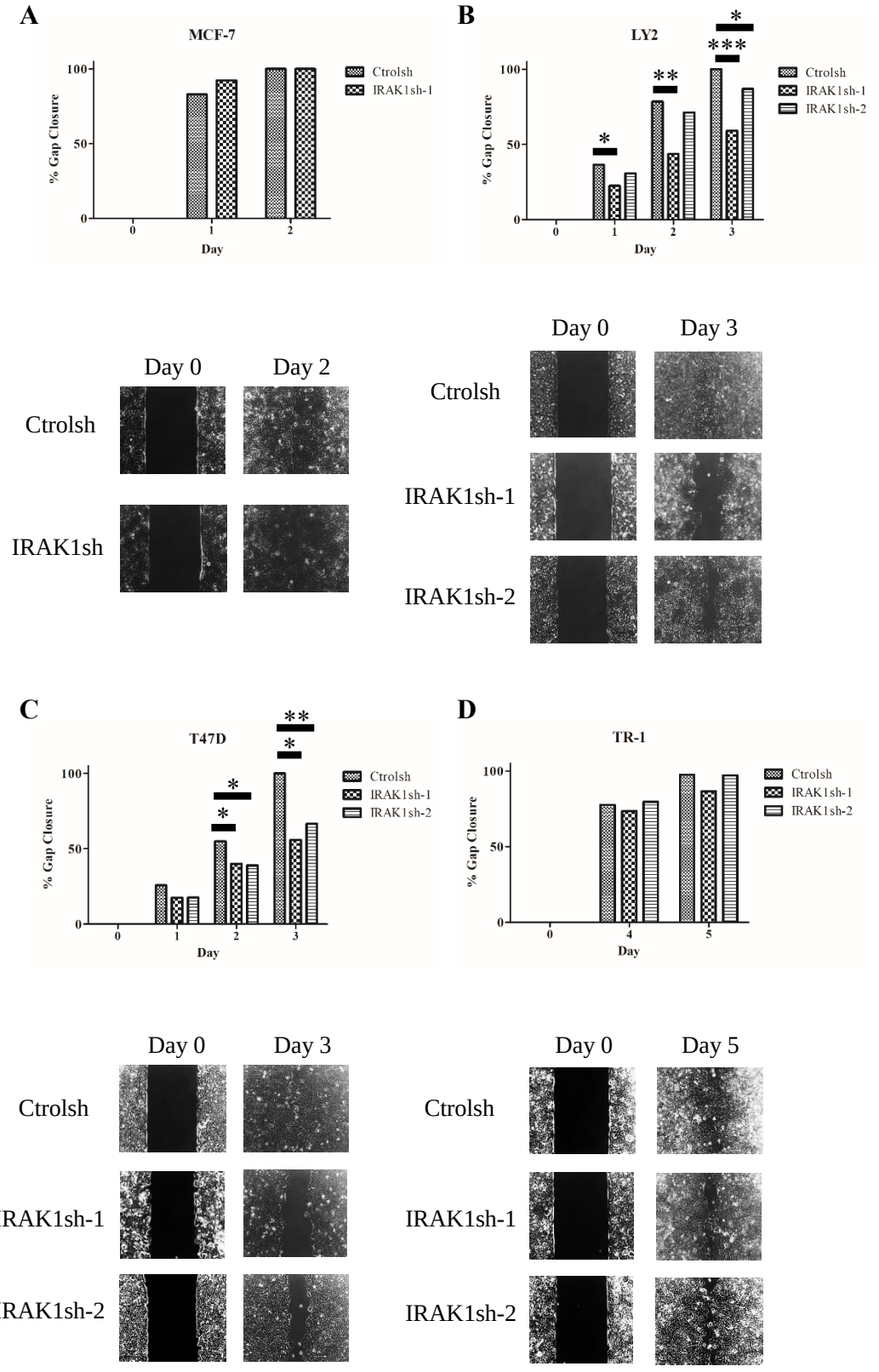
A
MCF-7
% Gap Closure
Day
Ctrolsh
IRAK1sh-1
B
LY2
% Gap Closure
Day
Ctrolsh
IRAK1sh-1
IRAK1sh-2
Day 0
Day 2
Ctrolsh
IRAK1sh
Day 0
Day 3
Ctrolsh
IRAK1sh-1
IRAK1sh-2
C
T47D
% Gap Closure
Day
Ctrolsh
IRAK1sh-1
IRAK1sh-2
D
TR-1
% Gap Closure
Day
Ctrolsh
IRAK1sh-1
IRAK1sh-2
Day 0
Day 3
Ctrolsh
IRAK1sh-1
IRAK1sh-2
Day 0
Day 5
Ctrolsh
IRAK1sh-1
IRAK1sh-2

Figure 3.9. IRAK1 knockdown impairs the migration of Tam-R LY2 cells and Tam-S T47D cells. 4-chamber inserts (IBIDI) were placed in the centre of the wells of a 6-well plate. Cells were seeded into the individual chambers at 6-8x10^5 cells/ml and left for 24 hours. 200µl of cell suspension was added to each chamber. After 24 hours the inserts were removed, leaving a gap of ~500µm and the wells were gently rinsed with PBS. 3mls of fresh complete media was added to the wells and the gap left between the cells was immediately imaged and measured using an Optika Vision Pro camera. LY2 cells were cultured in relevant media supplemented with 10nM Z-(4)-hydroxytamoxifen. TR-1 cells were cultured in relevant media supplemented with 5nM Z-(4)-hydroxytamoxifen. Images were then taken twice daily until the gap closed. Measurements were made using the Optika Vision Pro software. Results were obtained from at least 3 independent experiments. (A.) MCF-7 (B.) LY2 (C.) T47D (D.) TR-1. P value was calculated using the paired Student t test. Statistically significant differences are indicated by the asterisks: *, $P<0.05$; **, $P<0.01$; ***, $P<0.001$.

3.2.4. IRAK1 knockdown alters ERα expression and/or activity in tamoxifen-resistant ER+ breast cancer cell lines, and in the T47D cell line.

Given the correlations observed between IRAK1 expression and ERα activity in the parental cell lines, we wanted to see what impact IRAK1 knockdown had on ERα activity and function. We initially measured the mRNA levels of IRAK1 through RT-PCR and confirmed successful knockdown of ~70-90% when compared to respective control cells (Figure 3.10 (A)). Subsequently, we analysed mRNA levels of ESR1 and found that the expression of ERα was differentially altered in the T47D and TR-1 cells following IRAK1 knockdown. Interestingly, we found that IRAK1 knockdown significantly reduced ESR1 mRNA levels in T47D cells, whereas the opposite trend was seen in TR-1 cells (Figure 3.10. (B)). No change in ESR1 expression was observed between the MCF-7 or LY2 cell lines at the mRNA level.

Using whole cell lysates, we next sought to assess changes in the expression and activity of ERα through Western blot analysis (Figure 3.10. (C)). The changes observed at the mRNA level in T47D and TR-1 IRAK1sh cells matched total ERα levels as assessed by Western blot analysis. Reduced phosphorylation of ERα at S118 and S167 was detected in IRAK1 knockdown T47D cells compared to control cells, whilst increased phosphorylation of ERα at these same phospho-sites was found in IRAK1 knockdown TR-1 cells.

In the case of MCF-7 and LY2 cells, IRAK1 knockdown reduced phosphorylation of ERα at S118 in MCF-7 cells, while IRAK1 knockdown did not significantly alter ERα expression or activity in LY2 whole cell lysates as assessed by Western blot (Figure 3.10 (C), Figure AIV.2). However, when we isolated the nuclear fraction in these same cells, we found a pronounced increase in nuclear levels of active ERα (S118/S167) in IRAK1sh LY2 cells compared to control cells (Figure 3.11 (A)). In IRAK1sh TR-1 cells, the increase in nuclear levels of phospho-ERα showed a less marked change compared to control cells, with slight increases in both nuclear and cytoplasmic phospho-ERα (Figure 3.11 (B)). In the case of Tam-S T47D cells, IRAK1 knockdown showed a marked reduction in cytoplasmic levels of phospho-ERα (S118/S167), with modest reductions seen in phospho-ERα levels in the nuclear fraction (Figure 3.11 (B)).

We used qRT-PCR to assess the impact of IRAK1 knockdown on the expression of ERα target genes (Figure 3.12). Specifically focusing on the expression of the ERα target genes GREB1, EGR3 and TFF1, which are frequently used to assess ERα activity, we found that IRAK1 knockdown increased the mRNA levels of two or more of these ERα target genes in both LY2 and TR-1 Tam-R cells. Having previously observed (Figure 3.4) the dramatically reduced levels of both GREB1 and EGR3 in the Tam-R LY2 and TR-1 cells when compared to their Tam-S parental cells, the increased expression of these genes in IRAK1 knockdown cells points to increased ligand-independent ERα activity in these Tam-R cells (Figure 3.12 (A) & (F)). Increased GREB1 expression has been linked to tamoxifen responsiveness previously (Wu *et al*. 2018). These Tam-R cells are cultured in estrogen-deplete media and in low levels of tamoxifen with the purpose of maintaining tamoxifen resistance. Previous work in LY2 cells identified GREB1, EGR3 and TFF1 as steroid-independent ER-regulated genes (Vareslija *et al*. 2016). Further work was needed to clarify whether this finding translates to a higher sensitivity to tamoxifen using increasing tamoxifen concentrations in cellular growth assays. IRAK1 knockdown also increased the expression of TFF1 in Tam-R LY2 and TR-1 cells, and in Tam-S T47D cells (Figure 3.12. (B)). Increased TFF1 expression has been positively correlated with tumour migration and metastasis in breast cancer previously (Prest *et al*. 2002). However, studies in TFF1 knockout mice showed that the absence of TFF1 actually increased breast tumour incidence and breast tumour growth, indicating that our result may contribute to the reduced growth we observed in these cell lines (Buache *et al*. 2011).

Subtle variations were observed across the other ERα target genes. Interestingly, the expression of the estrogen-regulated cell cycle protein CDK1 was reduced in both the LY2 and T47D cell lines following IRAK1 knockdown (Figure 3.12. (D)). Additionally, we observed that IRAK1 knockdown reduced the expression of XBP1 in T47D cells compared to control cells. The expression of XBP1 and its splice variant XBP1s are upregulated by ERα. XBP1 can act as a cofactor for ERα transcriptional activity, whilst also having a major role in the endoplasmic reticulum (ER) stress response (Ding *et al*. 2003, Sengupta *et al*. 2010).The ER stress response is commonly upregulated in cancers to cope with the increased protein turnover associated with aberrant tumour growth (Koong *et al*. 2006).

Overall, these findings indicate that IRAK1 has an important role in regulating ERα function in Luminal A breast cancer cells and further work is needed to fully explain these intriguing findings.

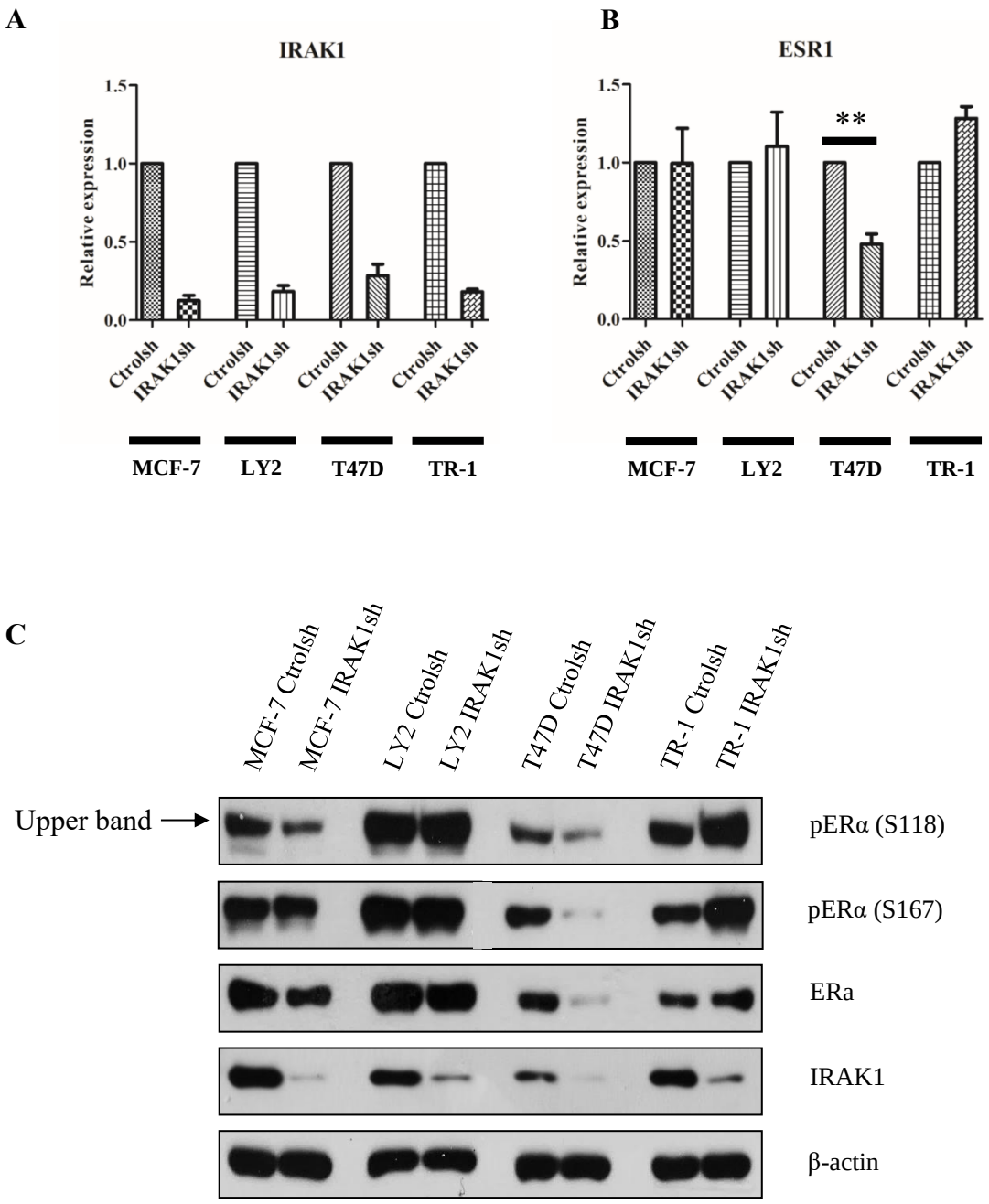

Figure 3.10. IRAK1 knockdown alters ERα expression and/or activity in ER+ breast cancer cell lines. (A-B) Cells were seeded at $4x10^5$ cells/ml in 12-well plates overnight. LY2 cells were cultured in relevant media supplemented with 10nM Z-(4)-hydroxytamoxifen. TR-1 cells were cultured in relevant media supplemented with 5nM Z-

(4)-hydroxytamoxifen. After 24 hours, cells were harvested in TriZol, RNA was isolated and subsequently subjected to reverse transcription, as previously described. The transcript levels of IRAK1 and ESR1 were determined by qRT-PCR and normalised against GAPDH mRNA. Results shown are the mean (±SEM) of at least three independent experiments performed in triplicates. (C) Cells were seeded at $4x10^5$cells/ml in 6-well plates overnight. LY2 cells were cultured in relevant media supplemented with 10nM Z-(4)-hydroxytamoxifen. TR-1 cells were cultured in relevant media supplemented with 5nM Z-(4)-hydroxytamoxifen. After 24 hours, whole cell lysates were extracted and subjected to Western blot. The resulting membranes were probed with phospho-ERα (S118), phospho-ERα (S167), total ERα, total IRAK1 and β-actin. Phospho-ERα (S167) image contains two exposures of the same blot. Similar results were obtained in three independent experiments. Densitometric analysis comparing the expression of each target (IRAK1sh compared to controlsh for each cell line) was performed using ImageJ software (Figure AIV.2). P value was calculated using the paired Student t test. Statistically significant differences are indicated by the asterisks: *, $P<0.05$; **, $P<0.01$.

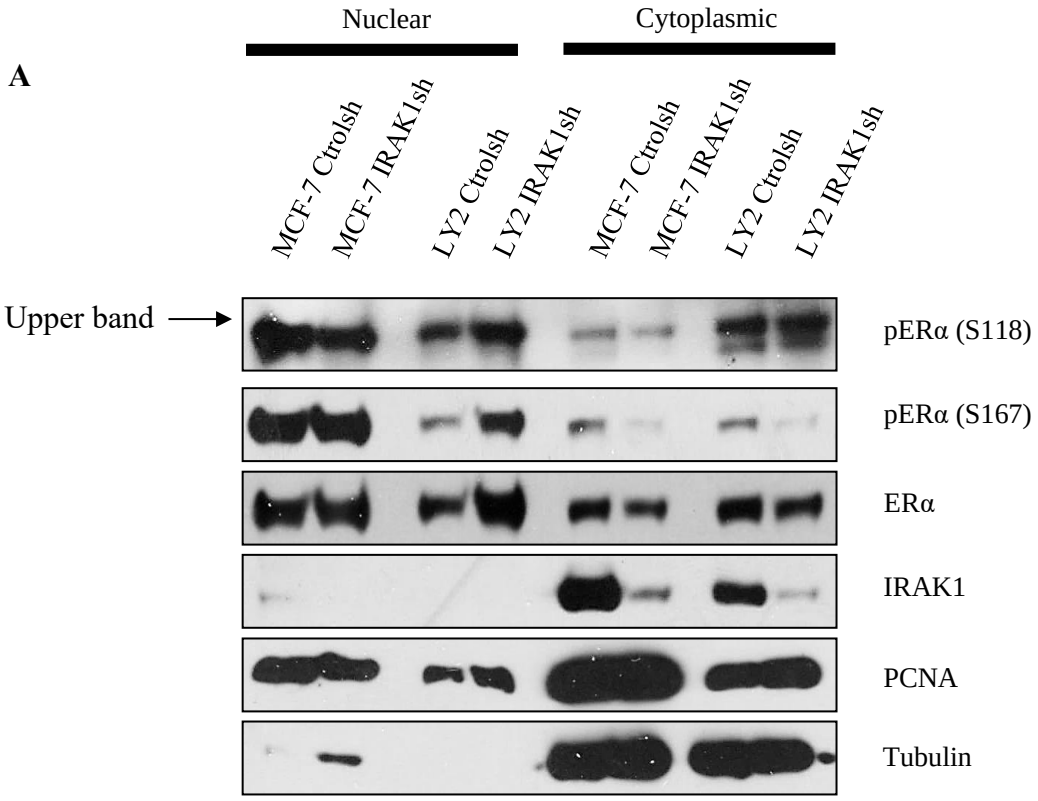
A
Nuclear
Cytoplasmic
MCF-7 Ctrolsh
MCF-7 IRAK1sh
LY2 Ctrolsh
LY2 IRAK1sh
MCF-7 Ctrolsh
MCF-7 IRAK1sh
LY2 Ctrolsh
LY2 IRAK1sh
Upper band
pERα (S118)
pERα (S167)
ERα
IRAK1
PCNA
Tubulin

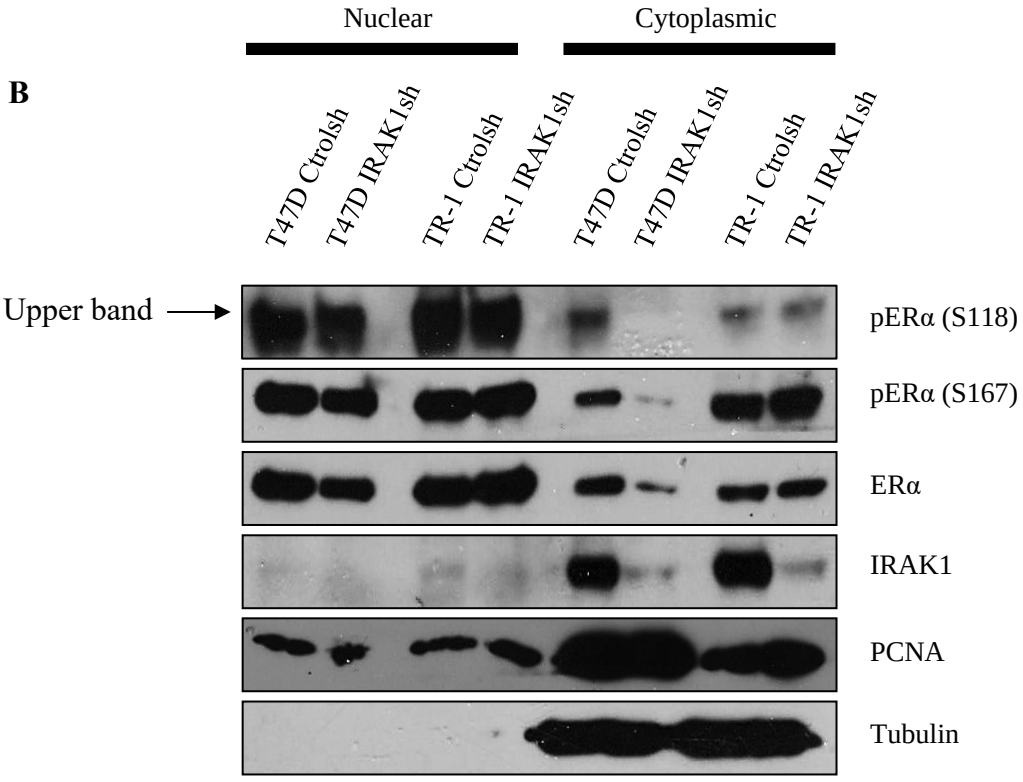
B
Nuclear
Cytoplasmic
T47D Ctrolsh
T47D IRAK1sh
TR-1 Ctrolsh
TR-1 IRAK1sh
T47D Ctrolsh
T47D IRAK1sh
TR-1 Ctrolsh
TR-1 IRAK1sh
Upper band
pERα (S118)
pERα (S167)
ERα
IRAK1
PCNA
Tubulin

Figure 3.11. IRAK1 knockdown results in an increase in nuclear levels of active ERα in the Tam-R LY2 cell line. Cells were seeded in 10cm dishes at $4x10^5$ cells/ml (10mls/dish). LY2 cells were cultured in relevant media supplemented with 10nM Z-(4)-hydroxytamoxifen. TR-1 cells were cultured in relevant media supplemented with 5nM Z-(4)-hydroxytamoxifen. Nuclear and cytoplasmic fractions were subsequently extracted using the Active Motif Nuclear Extract Kit (MyBio) in accordance with the recommended protocol. Nuclear and cytosolic lysates were then subjected to Western blot. The resulting membranes were probed with phospho-ERα (S118), phospho-ERα (S167), total ERα, total IRAK1, PCNA and tubulin. Similar results were obtained in two independent experiments. (A) MCF-7 and LY2 (B) T47D and TR-1.

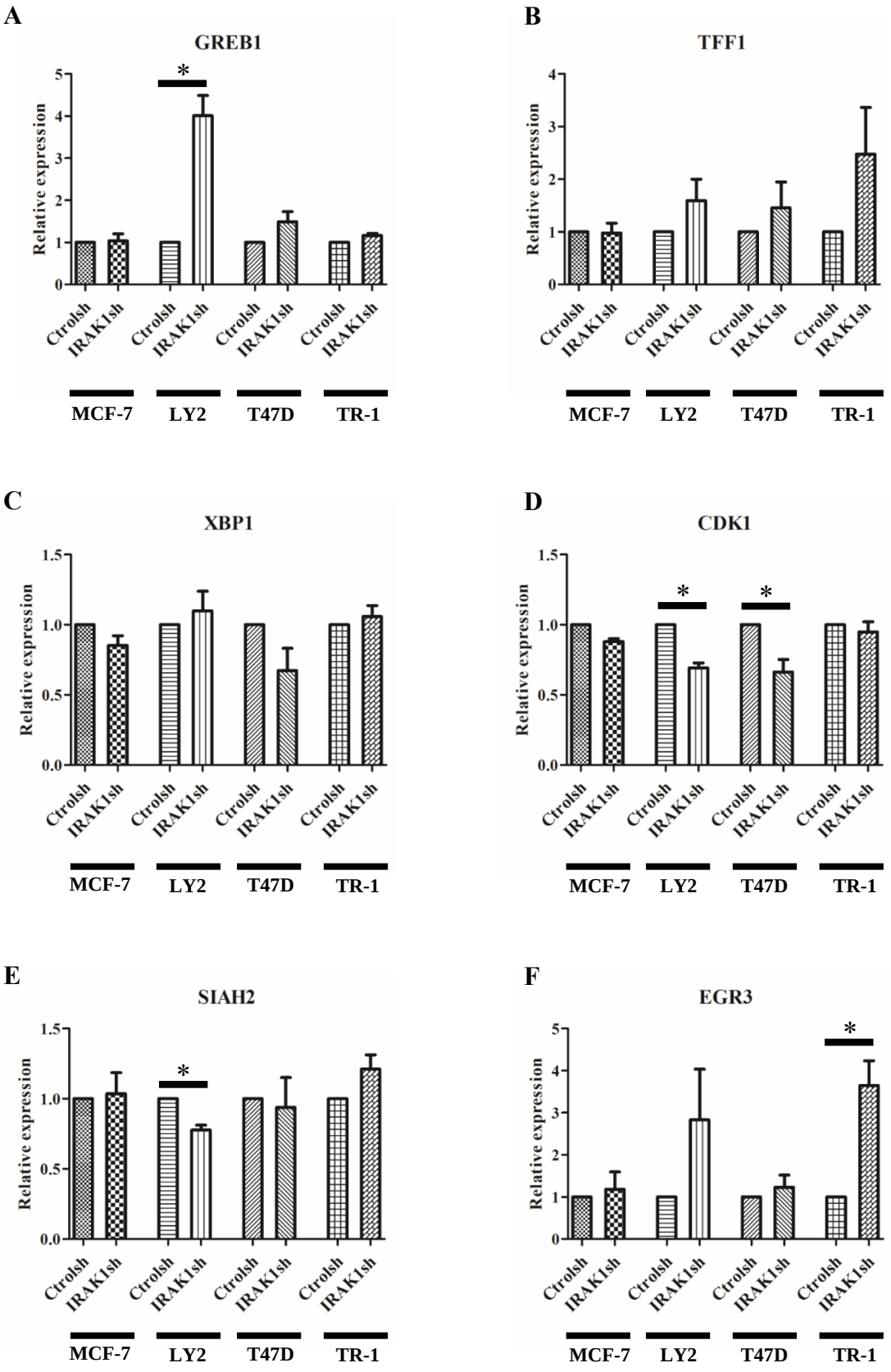
A
GREB1
Relative expression
Ctrolsh
IRAK1sh
MCF-7
LY2
T47D
TR-1
B
TFF1
C
XBP1
D
CDK1
E
SIAH2
F
EGR3

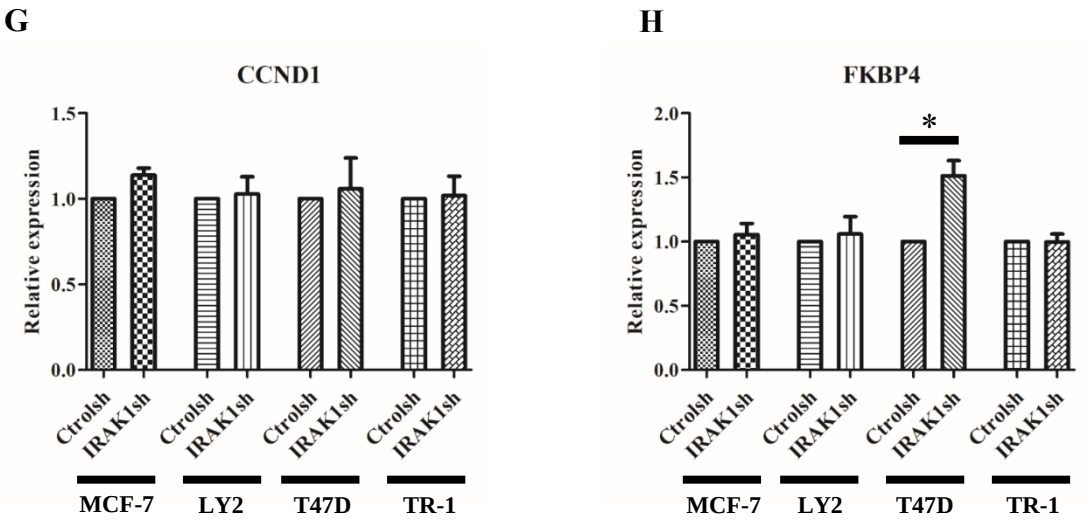

Figure 3.12. IRAK1 knockdown results in changes to the expression of ERα target genes in tamoxifen-resistant ER+ breast cancer cell lines, and the tamoxifen-sensitive T47D cell line. Cells were seeded at $4x10^5$cells/ml in 12-well plates overnight. LY2 cells were cultured in relevant media supplemented with 10nM Z-(4)-hydroxytamoxifen. TR-1 cells were cultured in relevant media supplemented with 5nM Z-(4)-hydroxytamoxifen. After 24 hours, cells were harvested in TriZol, RNA was isolated and subsequently subjected to reverse transcription, as previously described. The transcriptional levels of (A) GREB1, (B) TFF1, (C) EGR3, (D) FKBP4, (E) CCND1, (F) CDK1, (G) SIAH2 and (H) XBP1 were determined by qRT-PCR and normalised against GAPDH mRNA. Results shown are the mean (±SEM) of at least three independent experiments performed in triplicates. P value was calculated using the paired Student t test. Statistically significant differences are indicated by the asterisks: *, $P<0.05$.

3.2.5. IRAK1 knockdown increases the sensitivity of tamoxifen-resistant cells to tamoxifen treatment.

The Tam-R LY2 and TR-1 cell lines were generated through long-term culture in low concentrations of tamoxifen. Interestingly, for the TR-1 cells we have shown that treating these Tam-R cells with increasing concentrations of tamoxifen has an agonistic effect on their growth. We next wanted to examine whether IRAK1 knockdown would sensitize Tam-R cells to tamoxifen.

We analysed whether IRAK1 knockdown affected the growth of tamoxifen-resistant breast cancer cells in response to tamoxifen treatments through 2D MTS assays, colony-forming assays and 3D spheroid assays. Initially, using an MTS assay we found that IRAK1 knockdown significantly increased the potency of increasing concentrations of tamoxifen in both resistant cell lines (Figure 3.13). Importantly, in IRAK1 knockdown Tam-R LY2 and TR-1 cells the agonistic growth action of tamoxifen, which can be clearly observed in Tam-R controlsh cells, was lost (Figure 3.13).

Subsequently, we studied whether IRAK1 knockdown could lead to similar findings in colony-formation assays. Here, IRAK1 knockdown did similarly increase the responsiveness of Tam-R cells to tamoxifen. The agonistic effect of tamoxifen on cell growth was limited for both LY2 and TR-1 cells following IRAK1 knockdown, with reduced colony formation seen in response to increasing concentrations of tamoxifen in IRAK1 knockdown cells when compared to control tamoxifen treated cells. Tamoxifen treatments had a potent agonistic effect on the growth of TR-1 control cells, with this response being diminished following IRAK1 knockdown (Figure 3.14). The OpenCFU analysis tool was used to count the colonies, software that had difficulty precisely counting colonies in wells with a high-density of colonies as observed in LY2 control cells.

We next progressed to the 3D spheroid assay, where findings for the LY2 cell line were different to that observed for the 2D and colony formation assays. The agonistic effects of tamoxifen were absent, with tamoxifen treatment reducing the growth of control cells at low concentrations. However, IRAK1 knockdown did increase the inhibitory effects of tamoxifen (Figure 3.15 (A)). We found that the growth of IRAK1sh-1 LY2 spheroids was

significantly lower at DMSO treatment conditions when compared to control LY2 spheroids, while tamoxifen treatments had a more pronounced effect on the growth of IRAK1sh-1 LY2 spheroids when compared to control spheroids. Interestingly, the growth of IRAK1sh-2 LY2 spheroids was not impaired as much at DMSO treatment conditions when compared to control LY2 spheroids but did show increased responsiveness to tamoxifen treatment (Figure 3.15 (A)). We plan to repeat this assay in future, assessing the growth of spheroids over a longer period of time to further study the effects of IRAK1 knockdown on tamoxifen sensitivity in this 3D spheroid assay.

Results for TR-1 cells using this 3D spheroid assay aligned with results from both the MTS and colony-formation assays, with tamoxifen treatments showing an agonistic role on the growth of TR-1 control spheroids, which was lost in IRAK1 knockdown TR-1 cells. In IRAK1 knockdown TR-1 cells, spheroid growth regressed in response to tamoxifen treatment (Figure 3.15 (B)). Similarly, we plan to repeat this assay to assess spheroid growth up to 21 days, with measurements and images taken at day 6, 10, 14 and 21. Additionally, we want to measure the diameter of TR-1 spheroids on day 2 and day 3. TR-1 cells did not condense into clean spheroids as quickly as LY2 cells, which may have added some variance to the day 1 measurements.

Results coming from these 2D and 3D assays show that IRAK1 knockdown can re-sensitize Tam-R ER+ breast cancer cells to tamoxifen treatments and provides the rationale to test whether targeting IRAK1 could reduce tumour burden in xenograft models of Tam-R ER+ breast cancer.

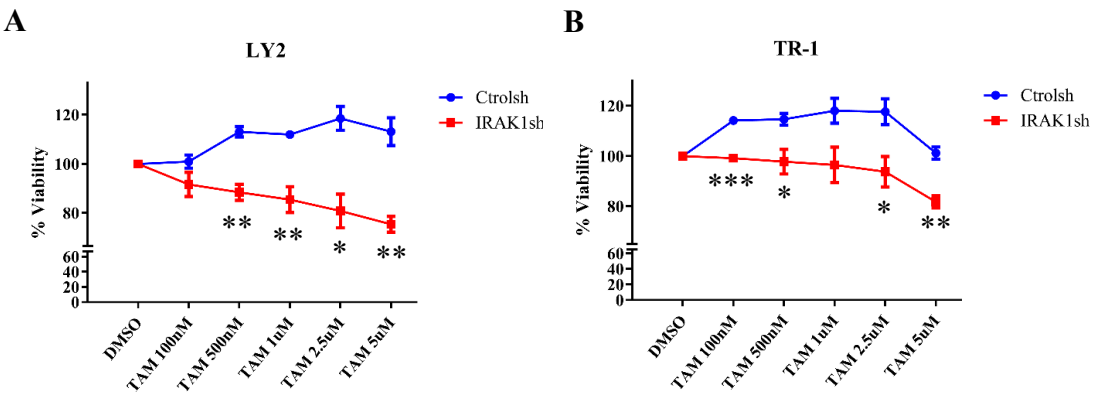

Figure 3.13. IRAK1 knockdown re-sensitizes tamoxifen-resistant LY2 and TR-1 breast cancer cells to tamoxifen in 2D growth model. Cells were seeded in 96-well plates in triplicate at 5000 cells/well in relevant media containing no supplementary tamoxifen for 24 hours. Cells were then treated with the indicated concentrations of tamoxifen or DMSO (vehicle control). Following 72 hour tamoxifen treatment, 20µl MTS cell viability reagent was added for 2 hours. Plates were then briefly placed on a rocker at medium speed to equilibrate and absorbance was subsequently read at 490nm (Biotek Synergy HTX plate reader). Data was represented as a percentage of vehicle control, with DMSO absorbance readings considered as 100% for each respective cell line. Results shown are the mean (±SEM) of at least three independent experiments performed in triplicates. P value was calculated using the unpaired Student t test. Statistically significant differences are indicated by the asterisks: *, $P<0.05$; **, $P<0.01$;***, $P<0.001$.

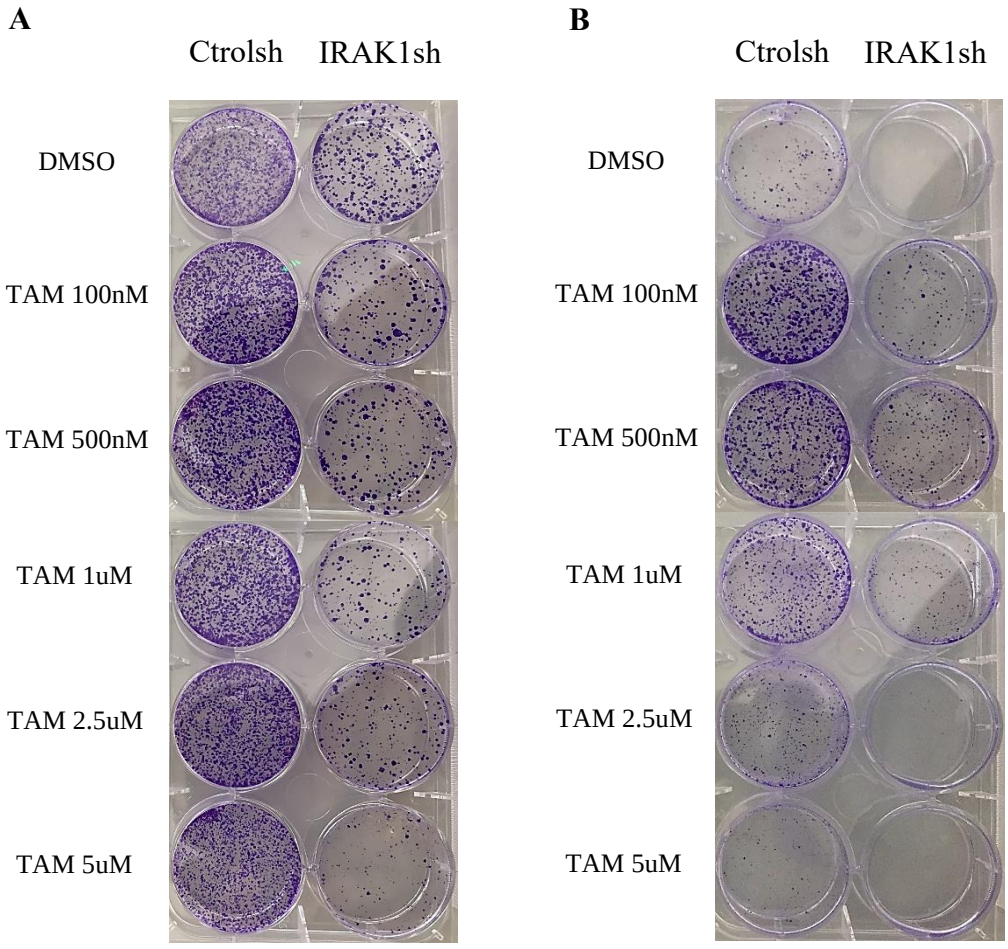
A
Ctrolsh
IRAK1sh
DMSO
TAM 100nM
TAM 500nM
TAM 1uM
TAM 2.5uM
TAM 5uM
B
Ctrolsh
IRAK1sh
DMSO
TAM 100nM
TAM 500nM
TAM 1uM
TAM 2.5uM
TAM 5uM

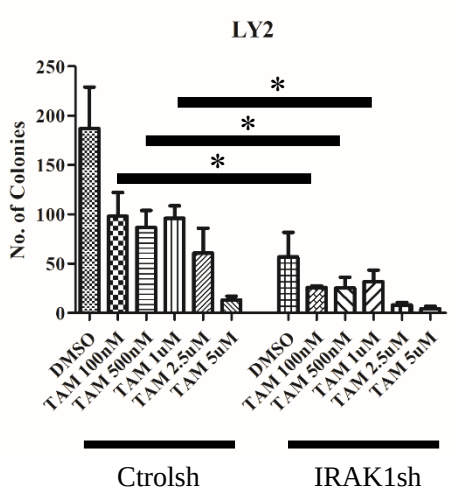
LY2
No. of Colonies
250
200
150
100
50
0
*
*
*
DMSO
TAM 100nM
TAM 500nM
TAM 1uM
TAM 2.5uM
TAM 5uM
DMSO
TAM 100nM
TAM 500nM
TAM 1uM
TAM 2.5uM
TAM 5uM
Ctrolsh
IRAK1sh

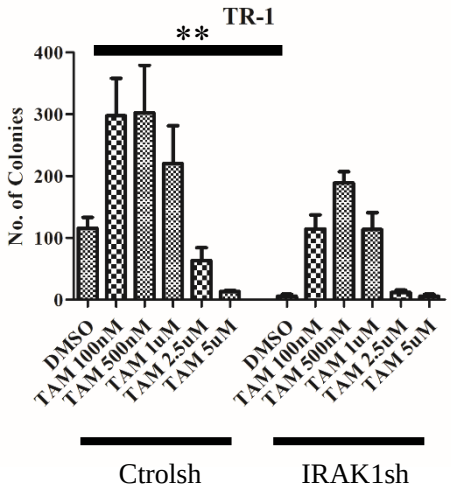
TR-1
No. of Colonies
400
300
200
100
0
**
DMSO
TAM 100nM
TAM 500nM
TAM 1uM
TAM 2.5uM
TAM 5uM
DMSO
TAM 100nM
TAM 500nM
TAM 1uM
TAM 2.5uM
TAM 5uM
Ctrolsh
IRAK1sh

Figure 3.14. IRAK1 knockdown reduces colony formation of Tam-R LY2 and TR-1 cells in response to tamoxifen. Cells were seeded in 6-well plates at 3000cells/well (LY2) and 9000cells/well (TR-1) to generate single-cell colonies. Cells were seeded in relevant media containing no supplementary tamoxifen for 24 hours prior to treatment with the indicated concentration of tamoxifen or DMSO (vehicle control). Colonies were allowed to form for ~17 days, at which point they were fixed in methanol and stained with 0.5% crystal violet. Analysis was done using the OpenCFU software tool. Results were obtained from at least 3 independent experiments. (A.) LY2 (B.) TR-1. P value was calculated using the unpaired Student t test. Statistically significant differences are indicated by the asterisks: *, $P<0.05$; **, $P<0.01$; ***, $P<0.001$.

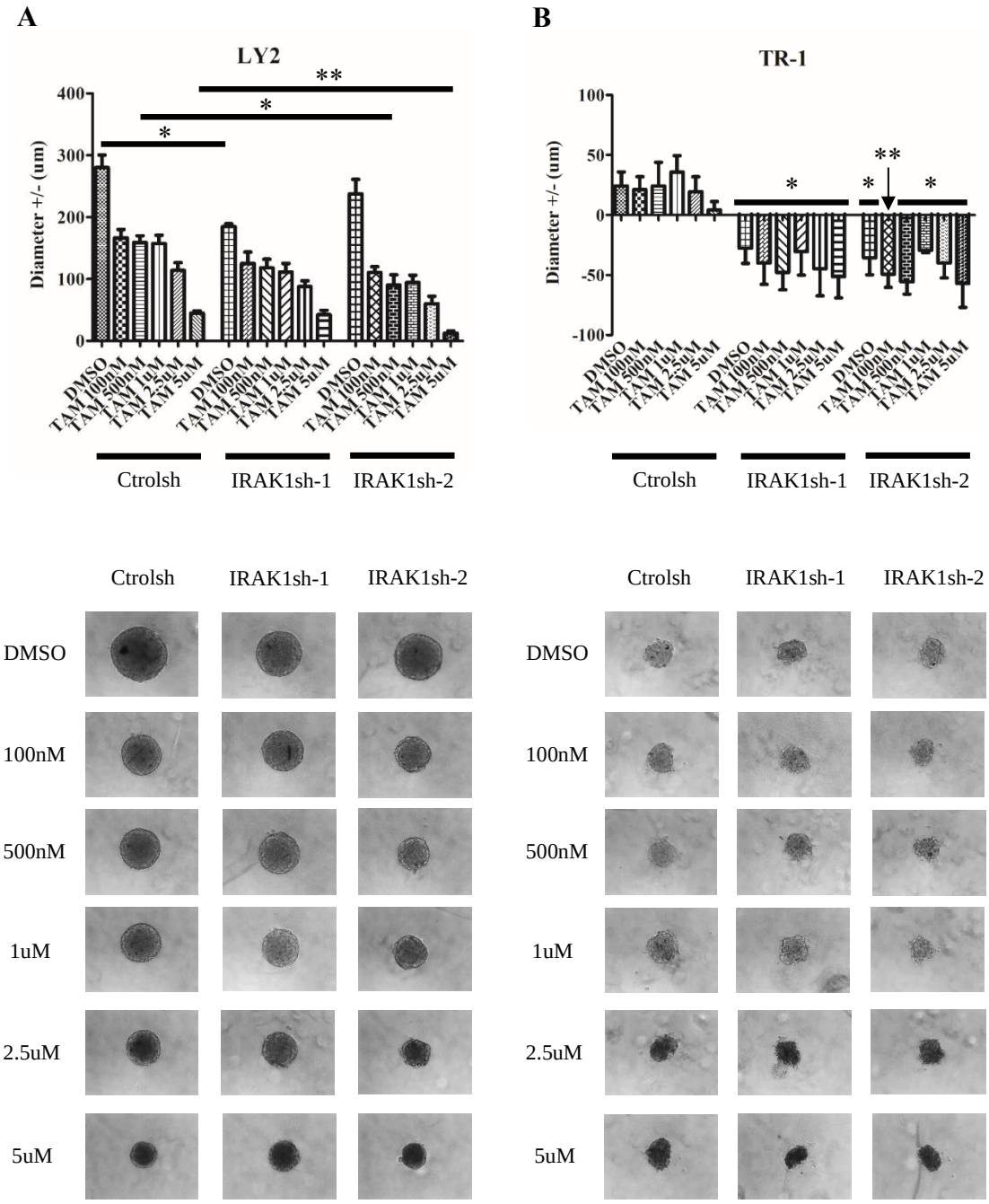
A
LY2
Diameter +/- (um)
400
300
200
100
0
*
*
**
DMSO
TAM 100nM
TAM 500nM
TAM 1uM
TAM 2.5uM
TAM 5uM
Ctrolsh
IRAK1sh-1
IRAK1sh-2
B
TR-1
Diameter +/- (um)
100
50
0
-50
-100
*
*
**
*
Ctrolsh
IRAK1sh-1
IRAK1sh-2
Ctrolsh
IRAK1sh-1
IRAK1sh-2
DMSO
100nM
500nM
1uM
2.5uM
5uM
Ctrolsh
IRAK1sh-1
IRAK1sh-2
DMSO
100nM
500nM
1uM
2.5uM
5uM

Figure 3.15. IRAK1 knockdown enhances the efficacy of tamoxifen in treating Tam-R LY2 and TR-1 cells in a 3D spheroid growth model. Cells were seeded at 500cells/well in ultra-low attachment U-bottom 96-well plates (Greiner Bio-One). Cells were seeded in relevant media containing no supplementary tamoxifen for 24 hours prior to treatment with the indicated concentration of tamoxifen or DMSO (vehicle control). The diameter of the resultant spheroids that were generated was measured just prior to treatment and spheroids were imaged (Optika Vision Pro, Olympus EP50). This process was repeated after 10 days to determine how much the spheroids had grown over that time period. Results were obtained from at least 3 independent experiments. (A.) LY2 (B.) TR-1. P value was calculated using the unpaired Student t test. Statistically significant differences are indicated by the asterisks: *, $P<0.05$; **, $P<0.01$.

3.2.6. IRAK1 has a role in regulating the expression of HER family members in tamoxifen-resistant cells.

Following on from our observation that IRAK1 knockdown increases the efficacy of tamoxifen in inhibiting the growth of Tam-R LY2 and TR-1 cell lines (Figure 3.13, Figure 3.14 and Figure 3.15), we attempted to gain further insight into the mechanism behind these results.

We started by studying the expression of the HER family members, which have been extensively studied across breast cancer subtypes and have previously been linked to tamoxifen resistance (Britton *et al*. 2006, Cui *et al*. 2012, Thrane *et al*. 2013, Wege *et al*. 2018). Initially, we analysed the basal expression of HER family members in Tam-R LY2 and TR-1 cells. We found that the expression of all HER family members was higher basally in TR-1 cells when compared to LY2 cells, with EGFR and full length HER4 expression very low in LY2 cells.

In the Tam-R LY2 cell line, HER 4 was undetectable in control cells by Western blot analysis (Figure 3.17). We found that IRAK1 knockdown triggered a dramatic increase in HER4 expression levels, at both the mRNA and protein levels (Figure 3.16 & 3.17). Tamoxifen treatments increased the expression of HER4 even further in IRAK1 knockdown LY2 cells. Another important finding was the presence of high levels of HER4:ICD in IRAK1 knockdown LY2 cells, when compared to control cells. The levels of HER4:ICD increased further with tamoxifen treatment, mirroring what was observed with full-length HER4 protein. This response was absent in control cells. This finding may have particular significance as HER4:ICD has been linked to driving ER+ breast cancer growth previously (Wang *et al*. 2016). However, tamoxifen treatment can impair the function of HER4:ICD and stimulate mitochondrial accumulation of HER4:ICD, inducing apoptosis through the activation of BAK (Naresh *et al*. 2006, Rokicki *et al*. 2010, Han and Jones 2014). Studying the subcellular localisation of HER4:ICD will be an important part of future work.

HER2 and HER3 expression was detected in both control and IRAK1 knockdown LY2 cells (Figure 3.16 & 3.17). Interestingly, when we look at their expression at the protein

level, we observed some differences in HER3 expression. Tamoxifen treatments gradually increased the protein levels of HER3 in control cells, while reducing HER3 protein levels in IRAK1 knockdown cells at later timepoints (Figure 3.17). We failed to detect EGFR expression by Western blot analysis in control and IRAK1 knockdown LY2 cells.

For TR-1 cells, EGFR expression was detectable by Western blot analysis. The expression of EGFR, HER2 and HER3 was increased basally in IRAK1 knockdown TR-1 cells compared to control cells, with HER4 expression being reduced basally in IRAK1 knockdown TR-1 cells. Interestingly, tamoxifen treatments triggered a dose dependent increase in EGFR, HER2 and HER3 expression in control TR-1 cells, while full-length HER4 expression was reduced in response to tamoxifen treatments with increased cleavage to HER4:ICD (Figure 3.18 & 3.19). Importantly, these responses were disrupted following IRAK1 knockdown. EGFR levels in IRAK1 knockdown TR-1 cells remained unchanged in response to tamoxifen (Figure 3.19). HER2 and HER3 expression was reduced in IRAK1 knockdown TR-1 cells following tamoxifen treatment, with a more pronounced reduction seen for HER3 (Figure 3.19). HER4 expression was very low basally in IRAK1 knockdown TR-1 cells, with low levels seen in response to tamoxifen treatments, while HER4:ICD levels are almost completely absent (Figure 3.19)

Next, we analysed the nuclear and cytoplasmic levels of HER3 and HER4 in Tam-R LY2 and TR-1 control and IRAK1 knockdown cells (Figure 3.20). For the LY2 cells, nuclear levels of HER3 were increased in IRAK1 knockdown cells. Nuclear HER4 levels were undetectable in control and IRAK1 knockdown LY2 cells, while increased cytoplasmic HER4 levels were detected in IRAK1 knockdown cells when compared to control cells (Figure 3.20). Nuclear HER4 levels were reduced in IRAK1 knockdown TR-1 cells (Figure 3.20). We were unable to cleanly assess HER4:ICD nuclear levels across these experiments.

Overall, these findings indicate that IRAK1 and the HER family may synergize to play important roles in supporting the tamoxifen-resistant phenotype seen in Tam-R LY2 and TR-1 cells. Importantly, IRAK1 knockdown appears to disrupt this dynamic, although the impact varies between the cell lines. The most interesting observation may be the HER3 levels, as the profiles are very similar for both Tam-R cell lines. HER3 overexpression has

been linked to poorer patient outcomes in breast cancer previously, including in response to tamoxifen treatment, and our findings indicate that IRAK1 knockdown can impair HER3 expression (Tovey *et al*. 2005, Chiu *et al*. 2010). Additionally, the increases observed in HER4 and HER4:ICD expression in IRAK1 knockdown LY2 cells following tamoxifen treatment may be significant, given that HER4 has generally been associated with an anti-proliferative and pro-apoptotic role (Naresh *et al*. 2006, Sundvall *et al*. 2008). Studying the subcellular localisation of HER4:ICD will also be an important part of future work, given that HER4:ICD has been linked to driving ER+ breast cancer growth but mitochondrial accumulation of HER4:ICD in response to tamoxifen treatment can induce apoptosis (Naresh *et al*. 2006, Rokicki *et al*. 2010, Han and Jones 2014, Wang *et al*. 2016).

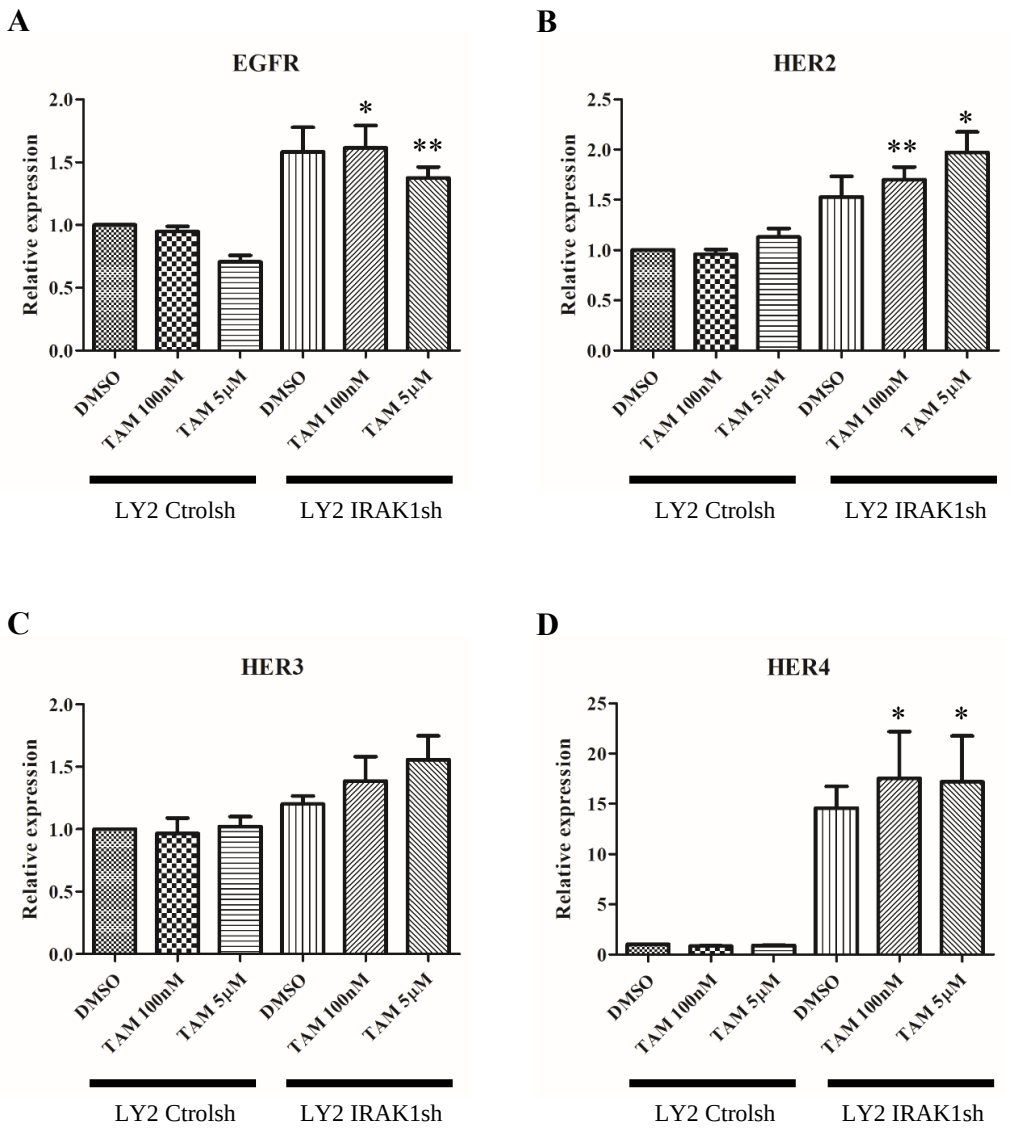

Figure 3.16. IRAK1 knockdown alters HER family mRNA expression in Tam-R LY2 ER+ breast cancer cells. Cells were seeded at $2x10^5$ cells/ml in 12-well plates in relevant media containing no supplementary tamoxifen for 24 hours. Cells were then treated with the indicated concentrations of tamoxifen or DMSO (vehicle control) for 24 hours. At that point, cells were harvested in TriZol, RNA was isolated and subsequently subjected to reverse transcription, as previously described. The mRNA levels of (A) EGFR, (B) HER2, (C) HER3, (D) HER4 were determined by qRT-PCR and normalised against GAPDH. Results shown are the mean (±SEM) of at least three independent experiments performed

in duplicates. P value was calculated using the unpaired Student t test. Statistically significant differences are indicated by the asterisks: *, $P<0.05$; **, $P<0.01$.

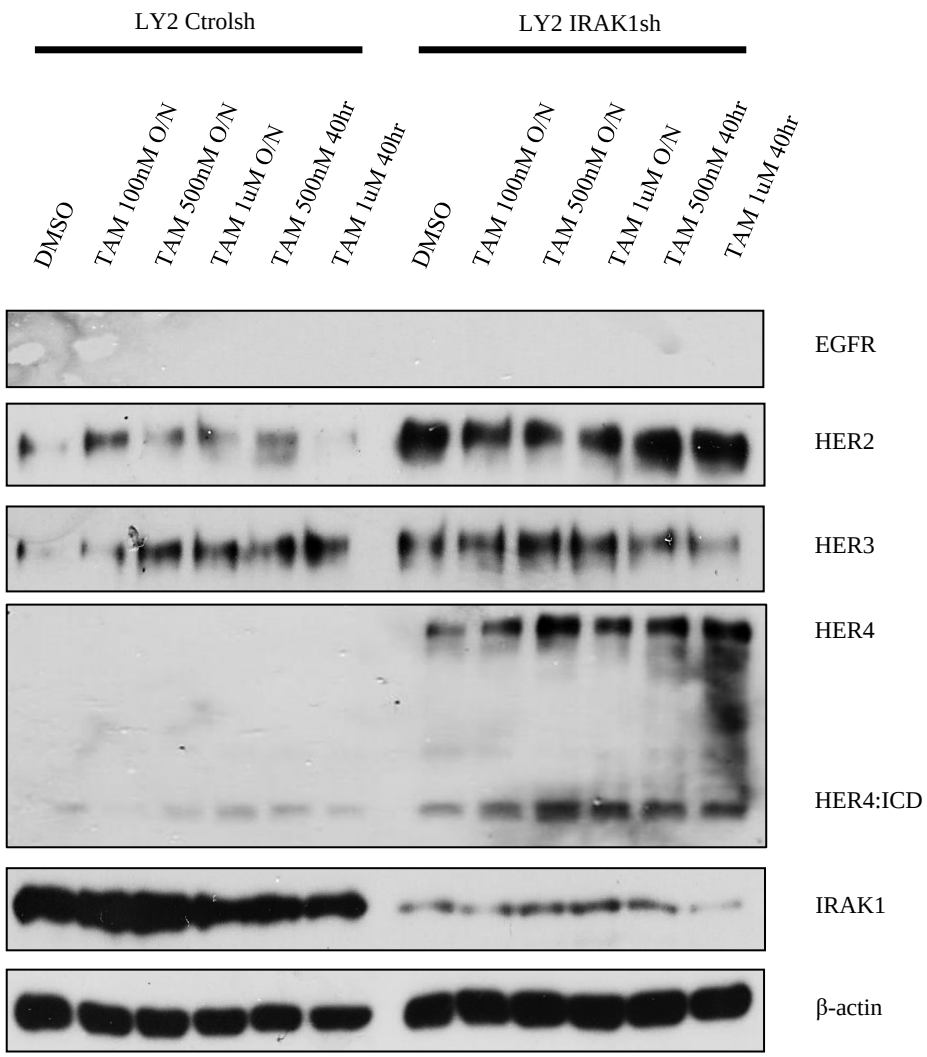

Figure 3.17. IRAK1 knockdown alters HER family protein expression in Tam-R LY2 ER+ breast cancer cells. Cells were seeded at $2x10^5$ cells/ml in 6-well plates in relevant media containing no supplementary tamoxifen for 24 hours. Cells were then treated with the indicated concentrations of tamoxifen or DMSO (vehicle) control overnight or for 40hrs. Whole cell lysates were extracted and subjected to Western blot analysis. The resulting membranes were probed for total levels of the following antibodies; EGFR, HER2, HER3, HER4, IRAK1 and β-actin. Similar results were obtained in two independent experiments. Densitometric analysis comparing the expression of each protein (relative to LY2 Ctrolsh DMSO) was performed using ImageJ software (Figure AIV.3).

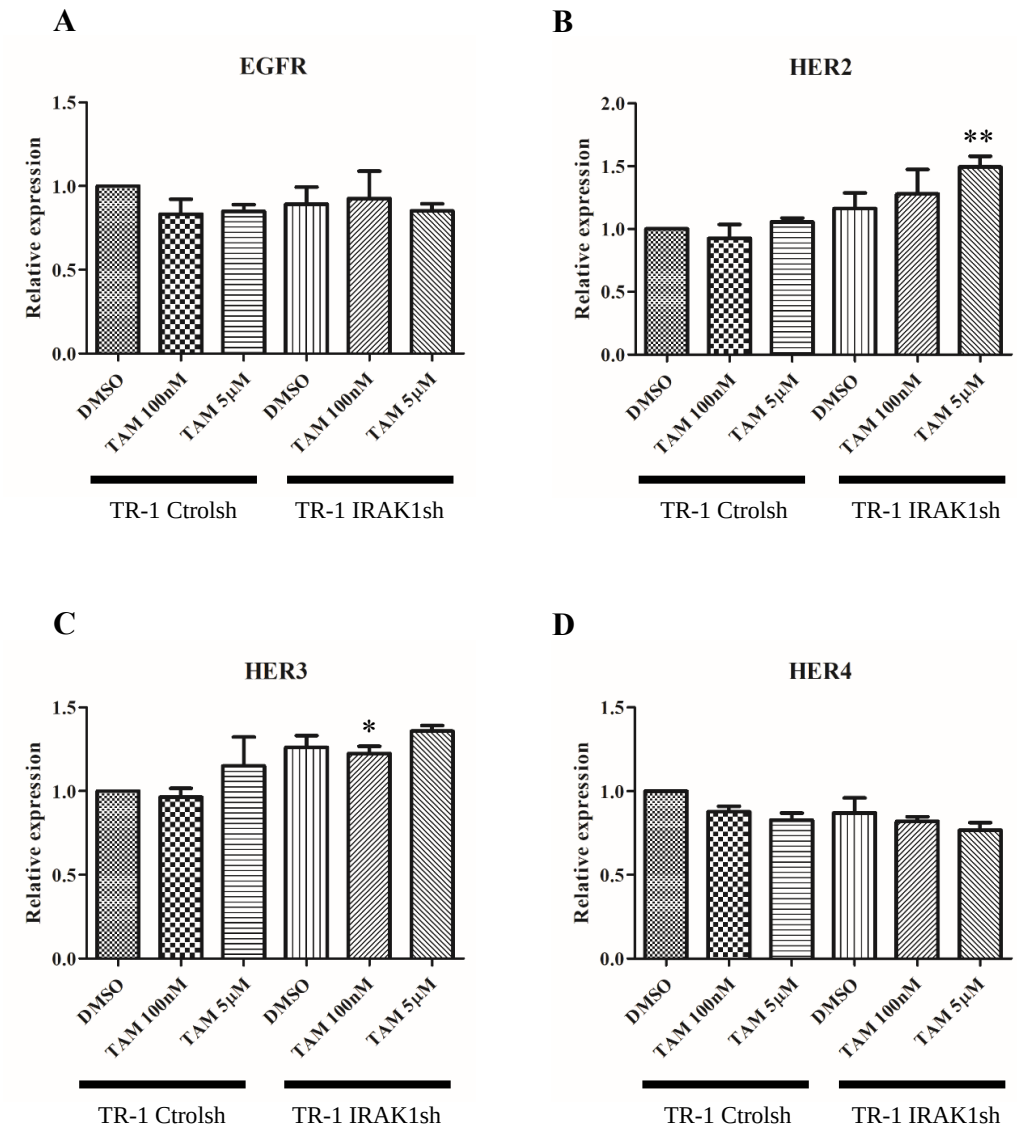

Figure 3.18. IRAK1 knockdown alters HER family mRNA expression in Tam-R TR-1 breast cancer cells. Cells were seeded at $2x10^5$ cells/ml in 12-well plates in relevant media containing no supplementary tamoxifen for 24 hours. Cells were then treated with the indicated concentrations of tamoxifen or DMSO (vehicle control) for 24 hours. At that point, cells were harvested in TriZol, RNA was isolated and subsequently subjected to reverse transcription, as previously described. The mRNA levels of (A) EGFR, (B) HER2, (C) HER3, (D) HER4 were determined by qRT-PCR and normalised against GAPDH.

Results shown are the mean (±SEM) of at least three independent experiments performed in duplicates. P value was calculated using the unpaired Student t test. Statistically significant differences are indicated by the asterisks: *, $P<0.05$; **, $P<0.01$.

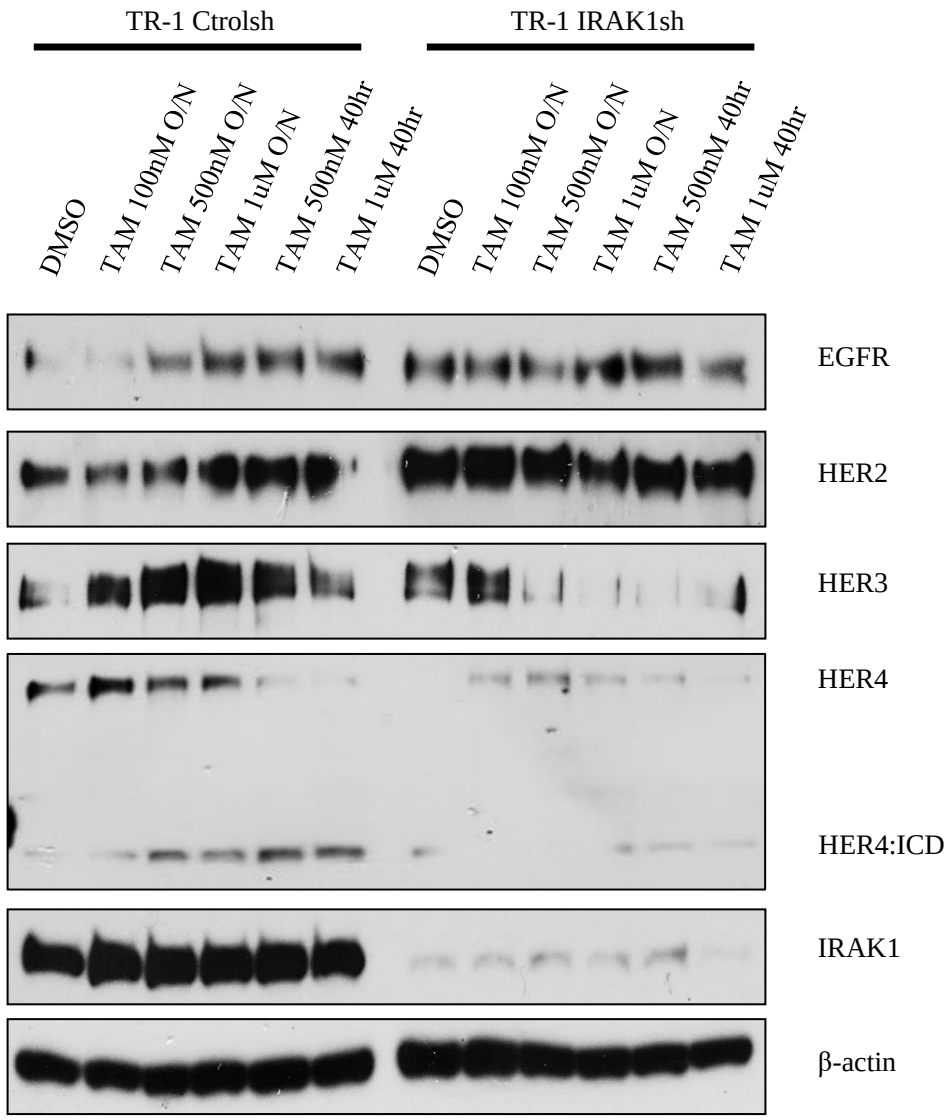

Figure 3.19. IRAK1 knockdown alters HER family protein expression in Tam-R TR-1 breast cancer cells. Cells were seeded at $2x10^5$ cells/ml in 6-well plates in relevant media containing no supplementary tamoxifen for 24 hours. Cells were then treated with the indicated concentrations of tamoxifen or DMSO (vehicle control) overnight or for 40hrs. Whole cell lysates were extracted and subjected to Western blot analysis. The resulting membranes were probed for total levels of the following antibodies; EGFR, HER2, HER3, HER4, IRAK1 and β-actin. Similar results were obtained in two independent experiments. Densitometric analysis comparing the expression of each protein (relative to TR-1 Ctrolsh DMSO) was performed using ImageJ software (Figure AIV.4).

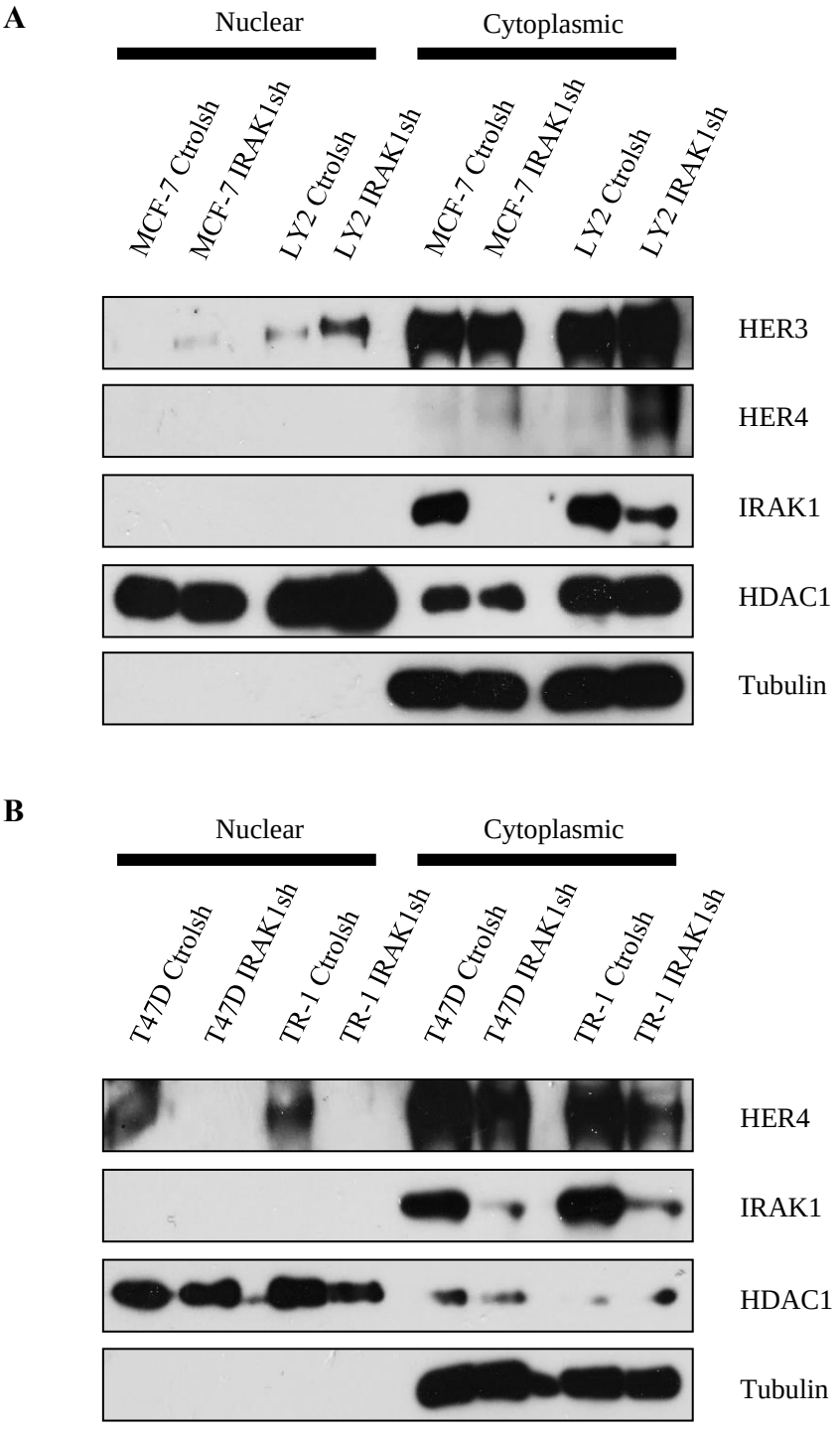
A
Nuclear
Cytoplasmic
MCF-7 Ctrolsh
MCF-7 IRAK1sh
LY2 Ctrolsh
LY2 IRAK1sh
MCF-7 Ctrolsh
MCF-7 IRAK1sh
LY2 Ctrolsh
LY2 IRAK1sh
HER3
HER4
IRAK1
HDAC1
Tubulin
B
Nuclear
Cytoplasmic
T47D Ctrolsh
T47D IRAK1sh
TR-1 Ctrolsh
TR-1 IRAK1sh
T47D Ctrolsh
T47D IRAK1sh
TR-1 Ctrolsh
TR-1 IRAK1sh
HER4
IRAK1
HDAC1
Tubulin

Figure 3.20. IRAK1 knockdown alters the nuclear and cytoplasmic levels of HER3 and HER4 in LY2 and TR-1 cells. Cells were seeded in 10cm dishes at $4x10^5$ cells/ml (10mls/dish). LY2 cells were cultured in relevant media supplemented with 10nM Z-(4)-hydroxytamoxifen. TR-1 cells were cultured in relevant media supplemented with 5nM Z-(4)-hydroxytamoxifen. Nuclear and cytoplasmic fractions were subsequently prepared using the Active Motif Nuclear Extract Kit (MyBio) in accordance with the recommended protocol and subsequently subjected to Western blot analysis. The resulting membranes were probed with phospho-ERα (S118), phospho-ERα (S167), total ERα, total IRAK1, HDAC1 and Tubulin. Results are from a single experiment. (A) MCF-7 and LY2 (B) T47D and TR-1.

3.2.7. IRAK1 has an important role in regulating cell cycle proteins in Tam-R ER+ breast cancer cells.

Given the reduced CDK1 expression detected in IRAK1 knockdown LY2 and T47D cells (Figure 3.12 (D)), we wanted to expand on our analysis of the role of IRAK1 on the cell cycle in the Tam-R LY2 and TR-1 ER+ breast cancer cells.

We examined the expression of the CDK inhibitors p21 and p27 by qRT-PCR and Western blot analysis of whole cell lysates in Tam-R LY2 and TR-1 cells. In LY2 cells, IRAK1 knockdown increased the basal expression of both p21 and p27 at the mRNA and protein levels (Figure 3.21). The expression of p21 at the mRNA level increased further in response to tamoxifen in IRAK1 knockdown LY2 cells. However, tamoxifen had no visible influence on p21 protein levels in IRAK1 knockdown LY2 cells, with p21 levels already being very high basally. The levels of p27 were found to decrease slightly following tamoxifen treatment conditions in IRAK1 knockdown LY2 cells as assessed by Western blot analysis (Figure 3.21). Interestingly, control cells showed a dose-dependent increase in the expression of both p21 and p27 at the protein level. However, the level of both CDK inhibitors in control cells never reached the basal levels that were observed in IRAK1 knockdown cells.

In TR-1 cells, the expression of both CDK inhibitors was again increased basally in IRAK1 knockdown cells (Figure 3.22). However, the response profiles of p21 and p27 to tamoxifen treatments in TR-1 cells presented some interesting results. p21 and p27 expression increased in a dose dependent manner in control cells in response to tamoxifen treatment, while the opposite profile was observed in IRAK1 knockdown cells with a dose-dependent reduction in the levels of both CDK inhibitors. These results were very clear but present some challenges to understand as they contradict what would be expected, based on the outcome of our growth experiments on the sensitivity of these cell lines to tamoxifen. We plan to assess the expression and activity of Akt, an important kinase that is activated downstream of HER3, which can phosphorylate and inhibit the function of p21 and p27 (Manning and Cantley 2007). Given the increased HER3 expression following tamoxifen treatment of control Tam-R LY2 and TR-1 cells (Figure 3.17 and Figure 3.19), examining subsequent changes in downstream Akt activity may provide further mechanistic insight.

Using flow cytometry for cell cycle analysis will also be essential to future work, allowing us to further understand how IRAK1 knockdown may be disrupting the cell cycle.

Subsequently, we studied the expression and activity of Aurora kinase A (Aurora-A) by Western blot analysis in untreated and tamoxifen treated Tam-R LY2 and TR-1 IRAK1sh and control cells. In IRAK1 knockdown LY2 cells, Aurora-A expression was slightly increased basally when compared to control LY2 cells, but Aurora-A activity levels were very low in IRAK1 knockdown LY2 cells even in response to tamoxifen treatment (Figure 3.21. (B)). However, in control LY2 cells, while expression and activity of Aurora-A were very low basally, the expression and activity of Aurora-A increased in response to tamoxifen treatments (Figure 3.21 (B)).

In Tam-R TR-1 cells, this result was even more defined. Control TR-1 cells showed a very clear dose-dependent increase in Aurora-A activation following tamoxifen treatments, a response that was completely abolished by IRAK1 knockdown in TR-1 cells (Figure 3.22. (B)). Additionally, we assessed the phosphorylation of ERα at S167 in these same lysates. Aurora-A has been shown to phosphorylate ERα at S167 previously (Zheng *et al*. 2014). While phosphorylation of ERα at this phospho-site did appear to increase in response to tamoxifen treatment in both cell lines, there was no correlation with the activation of Aurora-A (Figure 3.23). This would indicate that Aurora-A is not involved in regulating ERα in these cell lines. Several other kinases including S6K1 (Yamnik and Holz 2010), Akt (Campbell *et al*. 2001) and IKKε (Guo *et al*. 2010) have been shown to phosphorylate ERα at S167 and their activity would be worth assessing in future work.

Overall, these results suggest that IRAK1 has a major role in regulating the cell-cycle in Tam-R LY2 and TR-1 cells. Our findings indicate that IRAK1 has an integral role in Aurora-A activation in response to tamoxifen treatment, which is very clearly defined in the TR-1 cell line, implicating IRAK1 in driving cell cycle progression and sustaining the growth of tamoxifen-resistant cells. Aurora-A has important roles in centrosome maturation, spindle assembly and spindle damage recovery during G2/M phase of the cell cycle (Vader and Lens 2008). Increased Aurora-A expression has recently been linked to tamoxifen resistance, with Aurora-A inhibition inducing G2 arrest and apoptosis in Tam-R cells (Thrane *et al*. 2015). IRAK1 also has an impact on the expression of the CDK

inhibitors p21 and p27, although this role is not as well defined due to variations in CDK inhibitor expression between the two cell lines in response to tamoxifen treatment. Future work assessing the expression and activity of Akt may help us to gain a better understanding of how IRAK1 knockdown is affecting p21 and p27 activity (Manning and Cantley 2007).

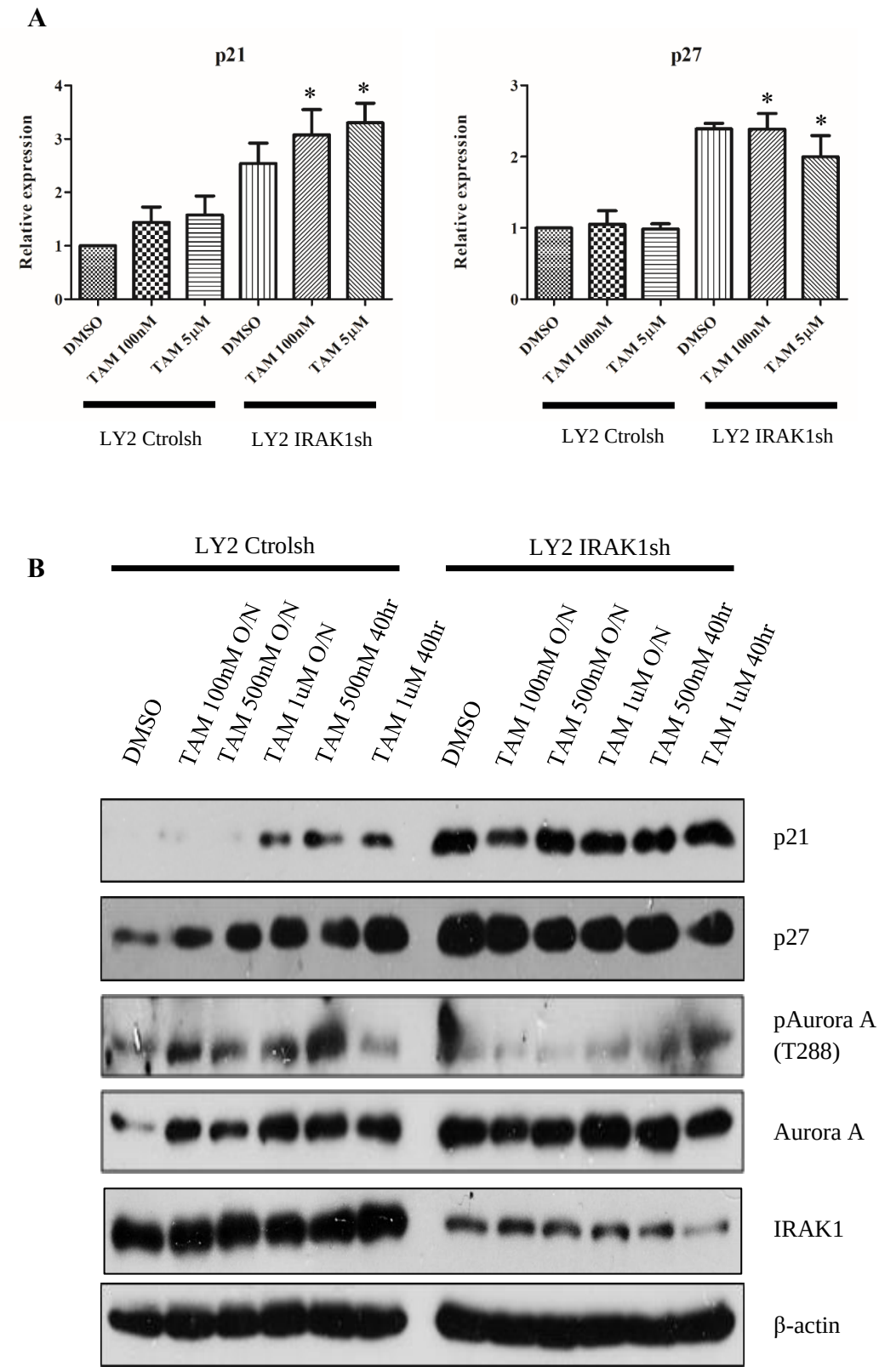
A
p21
p27
Relative expression
DMSO
TAM 100nM
TAM 5μM
LY2 Ctrolsh
LY2 IRAK1sh
B
LY2 Ctrolsh
LY2 IRAK1sh
DMSO
TAM 100nM O/N
TAM 500nM O/N
TAM 1uM O/N
TAM 500nM 40hr
TAM 1uM 40hr
p21
p27
pAurora A (T288)
Aurora A
IRAK1
β-actin

Figure 3.21. IRAK1 knockdown increases the expression of the CDK inhibitors p21 and p27 in Tam-R LY2 cells. (A) Cells were seeded at $2x10^5$cells/ml in 12-well plates in relevant media containing no supplementary tamoxifen for 24 hours. Cells were then treated with the indicated concentrations of tamoxifen or DMSO (vehicle control) for 24 hours. Cells were harvested in TriZol, RNA was isolated and subsequently subjected to reverse transcription, as previously described. The mRNA levels of p21 and p27 were determined by qRT-PCR and normalised against GAPDH. Results shown are the mean (±SEM) of three independent experiments performed in duplicates. (B) Cells were seeded at $2x10^5$cells/ml in 6-well plates and starved of tamoxifen for 24 hours. Cells were then treated with the indicated concentrations of tamoxifen or DMSO (vehicle control) for 24 hours. Whole cell lysates were extracted and subjected to Western blot analysis. The resulting membranes were probed with p21, p27, phospho-Aurora A (T288), total Aurora A, total IRAK1 and β-actin. Similar results were obtained in two independent experiments. Densitometric analysis comparing the expression of each target (relative to LY2 Ctrolsh DMSO) was performed using ImageJ software (Figure AIV.5). P value was calculated using the unpaired Student t test. Statistically significant differences are indicated by the asterisks: *, $P<0.05$.

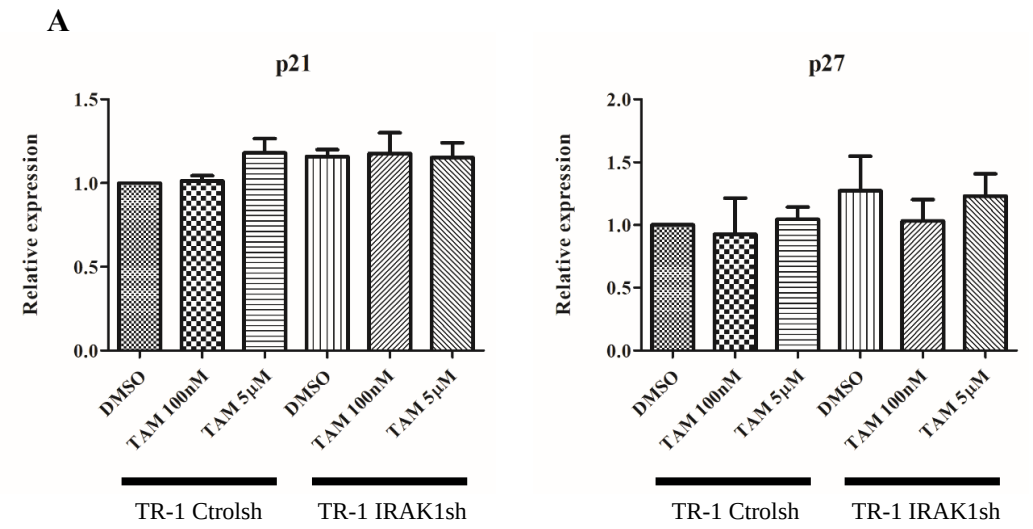
A
p21
p27
Relative expression
1.5
1.0
0.5
0.0
2.0
1.5
1.0
0.5
0.0
DMSO
TAM 100nM
TAM 5μM
DMSO
TAM 100nM
TAM 5μM
TR-1 Ctrolsh
TR-1 IRAK1sh
TR-1 Ctrolsh
TR-1 IRAK1sh

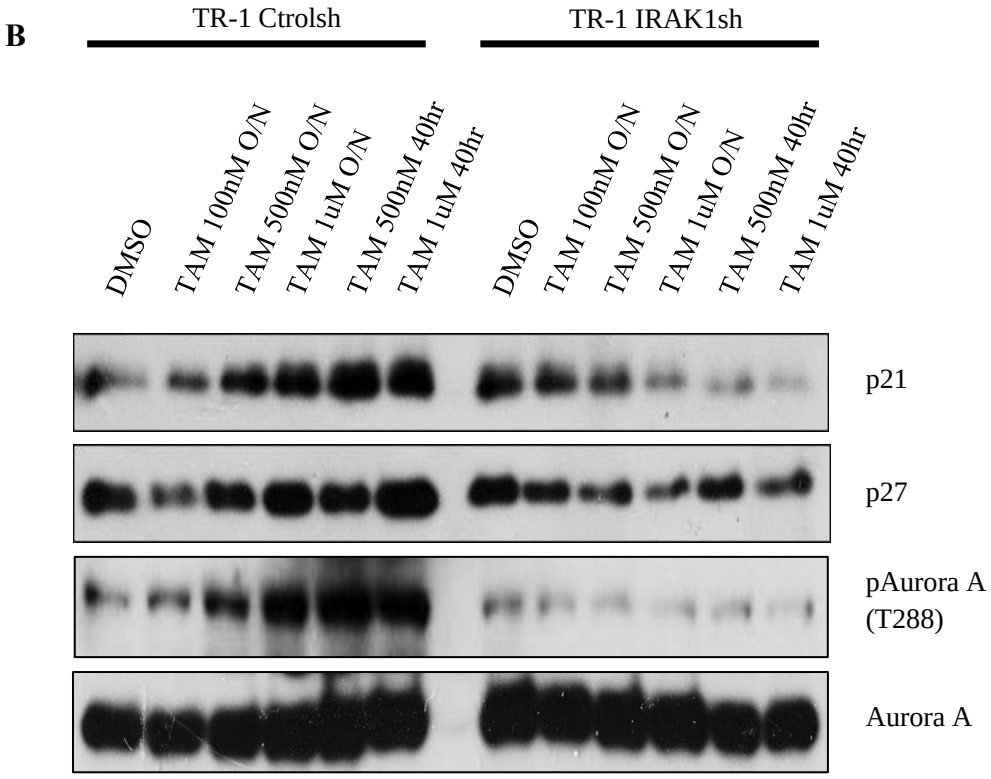
B
TR-1 Ctrolsh
TR-1 IRAK1sh
DMSO
TAM 100nM O/N
TAM 500nM O/N
TAM 1uM O/N
TAM 500nM 40hr
TAM 1uM 40hr
DMSO
TAM 100nM O/N
TAM 500nM O/N
TAM 1uM O/N
TAM 500nM 40hr
TAM 1uM 40hr
p21
p27
pAurora A
(T288)
Aurora A

Figure 3.22. IRAK1 knockdown impairs Aurora-A activity and alters the expression of the CDK inhibitors p21 and p27 in Tam-R TR-1 cells. (A) Cells were seeded at $2x10^5$ cells/ml in 12-well plates in relevant media containing no supplementary tamoxifen for 24 hours. Cells were then treated with the indicated concentrations of tamoxifen or DMSO (vehicle control) for 24 hours. Cells were harvested in TriZol, RNA was isolated and subsequently subjected to reverse transcription, as previously described. The mRNA levels of p21 and p27 were determined by qRT-PCR and normalised against GAPDH. Results shown are the mean (±SEM) of three independent experiments performed in duplicates. (B) Cells were seeded at $2x10^5$ cells/ml in 6-well plates and starved of tamoxifen for 24 hours. Cells were then treated with the indicated concentrations of tamoxifen or DMSO (vehicle control) for 24 hours. Whole cell lysates were extracted and subjected to Western blot analysis. The resulting membranes were probed with p21, p27, phospho-Aurora A (T288), total Aurora A, total IRAK1 and β-actin. The total IRAK1 and β-actin for these lysates blots are shown in Figure 3.19. Similar results were obtained in two independent experiments. Densitometric analysis comparing the expression of each target (relative to TR-1 Ctrolsh DMSO) was performed using ImageJ software (Figure AIV.6).

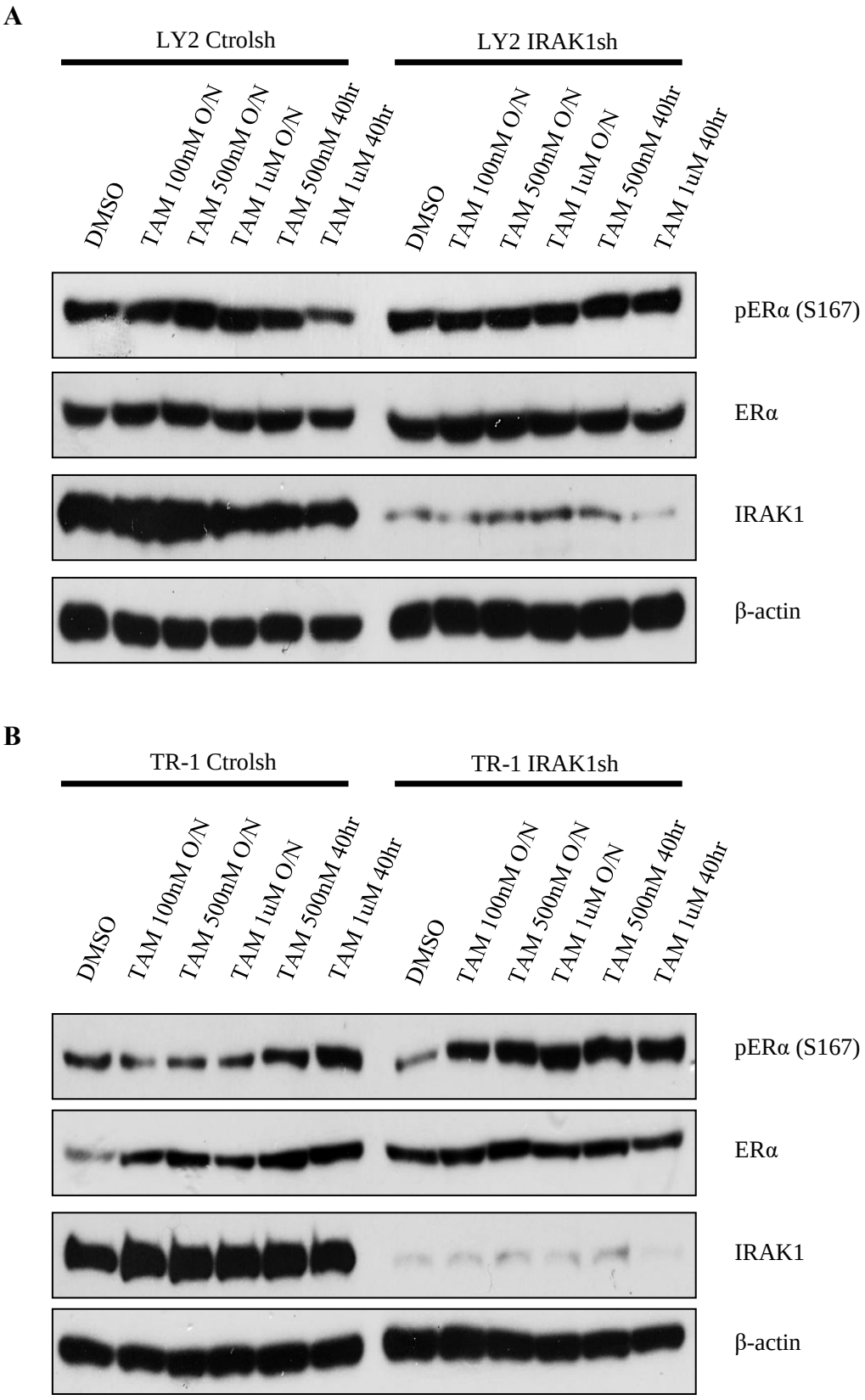
A
LY2 Ctrolsh
LY2 IRAK1sh
DMSO
TAM 100nM O/N
TAM 500nM O/N
TAM 1uM O/N
TAM 500nM 40hr
TAM 1uM 40hr
DMSO
TAM 100nM O/N
TAM 500nM O/N
TAM 1uM O/N
TAM 500nM 40hr
TAM 1uM 40hr
pERα (S167)
ERα
IRAK1
β-actin
B
TR-1 Ctrolsh
TR-1 IRAK1sh
DMSO
TAM 100nM O/N
TAM 500nM O/N
TAM 1uM O/N
TAM 500nM 40hr
TAM 1uM 40hr
DMSO
TAM 100nM O/N
TAM 500nM O/N
TAM 1uM O/N
TAM 500nM 40hr
TAM 1uM 40hr
pERα (S167)
ERα
IRAK1
β-actin

Figure 3.23. Examining ERα phosphorylation at S167 in response to tamoxifen treatment in Tam-R LY2 and TR-1 cells. Cells were seeded at $2x10^5$ cells/ml in 6-well plates in relevant media containing no supplementary tamoxifen for 24 hours. Cells were then treated with the indicated concentrations of tamoxifen or DMSO (vehicle control) for 24 hours. Whole cell lysates were prepared and subjected to Western blot analysis. The resulting membranes were probed with phospho-ERα (S167), total ERα, total IRAK1 and β-actin. The total IRAK1 and β-actin for these same lysates are shown in Figure 3.19. Similar results were obtained in two independent experiments.

3.3. Discussion.

IRAK1 has become a target of interest in recent years for several cancers, particularly in aggressive cancers such as ABC-DLBCL, T-ALL, HCC and TNBC (Ngo *et al*. 2011, Dussiau *et al*. 2015, Wee *et al*. 2015, Li *et al*. 2016). In each of these cancers, targeted inhibition of IRAK1 kinase activity and/or IRAK1 knockdown has reduced tumour growth and, in several cases, re-sensitized tumour cells to certain chemotherapeutics, indicating the potential of targeting IRAK1 for therapeutic benefit (Ngo *et al*. 2011, Dussiau *et al*. 2015, Wee *et al*. 2015, Li *et al*. 2016). To this point, there has been limited research into any role for IRAK1 in ER+ breast cancer. Goh *et al*. (2017) did show as part of their research that treatment of the ER+ breast cancer cell lines MCF-7 and T47D with pacritinib, which targets IRAK1 along with JAK2 and Flt3, reduced the growth of both MCF-7 and T47D cells *in-vitro*, while also impairing the growth of MCF-7 xenografts. However, there has not been any insight into the mechanistic role of IRAK1 in ER+ breast cancer.

ER+ breast cancer accounts for approximately 70% of newly diagnosed breast cancer cases and is generally associated with a good prognosis. Treatment for this type of breast cancer generally includes the use of estrogen-targeted therapies, including the SERM tamoxifen. Five years of adjuvant therapy with tamoxifen has been shown to reduce the rate of tumour recurrence by up to 50% (Levine *et al*. 1998). However, approximately one-third of patients that initially respond to tamoxifen treatment will develop a resistant recurrence within 10 years of finishing therapy (Howell *et al*. 2005, Arimidex 2008). Understandably, patients that develop a resistant recurrence currently have limited treatment options and a very poor prognosis, with an estimated 5-year survival rate of 20% (Robertson *et al*. 2003, Sotgia *et al*. 2017).

The aim of this work was to investigate the role of IRAK1 in ER+ tamoxifen-sensitive (Tam-S) and tamoxifen-resistant (Tam-R) breast cancer subtypes and to determine whether targeting IRAK1 re-sensitizes Tam-R ER+ breast cancer cells to tamoxifen.

Initially, we analysed survival data of Luminal A breast cancer patients from kmplot.com (Győrffy *et al*. 2010) to determine whether IRAK1 expression levels had an impact on RFS and OS of Luminal A breast cancer patients. We found that high IRAK1 expression was

correlated with significantly reduced RFS in Luminal A breast cancer patients (Figure 3.1 (A), P=0.00088, n=1933), with this correlation becoming very distinct when the lymph node positive Luminal A cohort was isolated (Figure 3.1 (B), P=0.0018, n=530). We also found that high IRAK1 expression was a significant negative prognostic marker for OS in Luminal A breast cancer patients (Figure 3.2, P=0.0043, n=611). These findings indicated the significance of high IRAK1 expression to Luminal A breast cancer recurrence and tumour progression.

These findings are further supported by recently published data by Yang *et al*. (2019), who examined data from The Cancer Genome Atlas on IRAK1 expression across Luminal A, Luminal B, HER2-positive and basal subtypes of breast cancer. Their analysis of patient data across these breast cancer subtypes indicated a relationship between IRAK1 expression and lymph node status and metastasis. Using the TNM classification system, tumours were graded from N0 to N3 based on the degree of spread to the lymph nodes and M0 or M1 based on whether the cancer had spread to distant parts of the body. Statistically, it was found that 9% of N0 patients showed IRAK1 expression compared to 20% of N3 patients, while 14% of M0 patients exhibited IRAK1 expression compared to 81% of M1 patients (Yang *et al*. 2019).

Having established that IRAK1 has a significant role in luminal A breast cancer recurrence and progression based on our analysis of luminal A breast cancer patient RFS and OS, we focused our research on the Tam-S luminal A breast cancer cell lines MCF-7 and T47D and their Tam-R sublines, LY2 and TR-1, respectively. Our results showed that IRAK1 expression was increased in both Tam-R cell lines at both the mRNA and protein level when compared to their parental cell lines (Figure 3.3). This finding built on the results that we had gained from our data analysis, indicating that increased IRAK1 expression may be contributing to tamoxifen resistance. IRAK1 has previously been linked to drug resistance across a variety of cancers, including resistance to paclitaxel in TNBC and radiation resistance across breast cancer subtypes including ER+ (Wee *et al*. 2015, Liu *et al*. 2019). This is the first study to address whether high IRAK1 expression found in Tam-R ER+ breast cancer cells affects their sensitivity to tamoxifen.

The increase observed in IRAK1 expression in both Tam-R cell lines correlated with increased ERα phosphorylation at both S118 and S167. These sites lie within the AF-1 domain and are important for full ERα activation, with phosphorylation at S118 associated with enhanced dimerization and transactivation and phosphorylation at S167 increasing the DNA-binding capability of the receptor (Shah and Rowan. 2005, Le Romancer *et al*. 2011, Anbalagan and Rowan. 2015). Increased phosphorylation at S118 and S167 has been linked both positively and negatively to tamoxifen responsiveness (Yamashita *et al*. 2005, Sarwar *et al*. 2006). The reason for this may be that phosphorylation at these sites prior to tamoxifen treatment is indicative of a functionally active estrogen receptor, which is obviously necessary for tamoxifen to be efficacious, while high levels of phosphorylation at these residues after tamoxifen treatment has been suggested to be indicative of ligand-independent ERα activity and resistance to tamoxifen (Murphy *et al*. 2004, Zoubir *et al*. 2008). Given the correlation that we observed between increased IRAK1 expression and enhanced ERα activity in these tamoxifen-resistant cell lines, our results suggested that IRAK1 may have a role in regulating ERα through phosphorylation at S118 and S167, supporting the resistant phenotype.

Additionally, when we looked at the expression of ERα target genes we were able to confirm major alterations to ERα signalling following the development of resistance to tamoxifen (Figure 3.4). This was most apparent when we analysed the expression of GREB1 and EGR3, two early estrogen response genes that are commonly used to assess estrogen signalling (Ghosh *et al*. 2000, Inoue *et al*. 2004). The expression of both genes is generally increased by estrogen stimulation and inhibited by tamoxifen treatment in ER+ Tam-S breast cancer cells. Our findings showed that the expression of GREB1 and EGR3 was significantly reduced in both Tam-R cell lines when compared to their parental cells. Recent publications, particularly in relation to GREB1, have pointed to reduced expression of these genes contributing to the development of tamoxifen-resistance (Mohammed *et al*. 2013, Wu *et al*. 2018). Interestingly, siRNA silencing of GREB1 expression has been shown to prevent the inhibitory effects of tamoxifen on ER+ cells (Wu *et al*. 2018). Mohammed *et al*. (2013) found that GREB1 expression correlated with improved patient outcome. They found that GREB1 expression in their tamoxifen-resistant cell model was lost, and re-expression of GREB1 resulted in reduced growth of the cells in the presence of

tamoxifen (Mohammed *et al*. 2013). Our finding on GREB1 matches these recent findings, wherein loss of GREB1 expression has been associated with tamoxifen-resistance. GREB1 is recognized as an important cofactor for ERα-mediated gene regulation (Mohammed *et al*. 2013). While reduced GREB1 may be indicative of the inhibitory effects of tamoxifen, the significantly lower levels of GREB1 in Tam-R cells may also be limiting the ability of tamoxifen-bound ERα to regulate the expression of genes associated with the inhibitory profile (Mohamed *et al*. 2013, Wu *et al*. 2018). The same may be true for EGR3, which is a transcription factor that acts as a secondary signalling factor in ERα transcriptional regulation and may similarly act as a cofactor for ERα-mediated gene regulation, but the significance of EGR3 expression to tamoxifen-resistance has not yet been shown (Drabovich *et al*. 2016). We also observed variations in the expression of the ERα target genes TFF1, CCND1 and SIAH2, further indicating the disruptions to ERα signalling in tamoxifen-resistant cells (Lin *et al*. 2004).

Expression Levels	**IRAK1**	**Active ERα**	**GREB1**	**EGR3**
Tam-S	Moderate	Moderate	High	High
Tam-R	High	High	Low	Low

Table 3.1. Expression levels in parental Tam-S and Tam-R ER+ breast cancer cell lines. IRAK1 expression is increased in Tam-R cells when compared to parental Tam-S cells, which correlates with elevated ERα activity as measured by phosphorylation at Ser118 and Ser167. However, despite ERα activity being increased in Tam-R cells, the expression of the estrogenic genes GREB1 and EGR3 is significantly lower in Tam-R cells.

Summarizing, increased IRAK1 levels were detected in Tam-R ER+ breast cancer cell lines, and this correlated with changes in ERα expression levels and/or activity. This prompted us to investigate the role of IRAK1 in Tam-R ER+ breast cancer. To do this, we first generated stable IRAK1 knockdown in both Tam-S Luminal A breast cancer cell lines (MCF-7, T47D) and their respective Tam-R sublines (LY2, TR-1). Subsequently, we examined whether the knockdown of IRAK1 impacted the growth of these Tam-S and Tam-R cell lines in cellular assays including 2D proliferation, colony-formation assays and 3D growth assays. We found that IRAK1 knockdown impaired the growth of both LY2 and TR-1 Tam-R cell lines across all growth models.

This result pointed to a key role for IRAK1 in regulating the growth of these Tam-R cells, a novel finding. Interestingly, IRAK1 has been shown to play an integral role in resistance to the chemotherapeutic paclitaxel in TNBC (Wee *et al*. 2015) and radiation resistance in mutant p53 cancers (Liu *et al*. 2019). This data provides further evidence that IRAK1 plays an important role in cellular adaptations towards survival and growth progression in response to therapy in breast cancer, and across multiple cancer subtypes (Dussiau *et al*. 2015, Cheng *et al*. 2018). Interestingly, IRAK1 knockdown potently inhibited the growth of Tam-S T47D cells but had no effect on the growth of Tam-S MCF-7 cells. A recognised difference between these cells would be the presence of wild-type p53 in MCF-7 cells, while T47D cells express mutant p53 (Liu *et al*. 2019). IRAK1 has recently been shown to drive resistance to radiotherapy in mutant p53 cancers, including T47D cells, through inhibition of PIDDosome-mediated apoptosis (Goh *et al*. 2017).

We also examined the impact of IRAK1 knockdown on cell migration in Tam-S and Tam-R ER+ cell lines at the 2D level. IRAK1 knockdown significantly reduced migration in tamoxifen-resistant LY2 cells and tamoxifen-sensitive T47D cells but did not disrupt the migration of either the MCF-7 or TR-1 cells. The lack of impairment in cell migration of the MCF-7 cell line supports the findings from our growth models, wherein IRAK1 appears to have no significant role in these cells. However, the TR-1 result diverges from the consistent results that we obtained in relation to the Tam-R TR-1 cells from the growth model. Gap closure took five days for TR-1 cells compared to two to three days for the other breast cancer cells used in this study. As a result, the health of TR-1 cells throughout

this assay deteriorated and may have affected the results. TFF1 expression in the TR-1 cell line by qRT-PCR show that TFF1 expression increases significantly (~2.5 fold) following IRAK1 knockdown, compared to more modest increases in the LY2 (~1.6 fold) and T47D (~1.4 fold) cell lines. High TFF1 expression is widely recognised to correlate positively with increased tumour migration and metastasis in breast cancer (Prest *et al*. 2002). The significant increase in TFF1 levels in TR-1 cells following IRAK1 knockdown may be preventing any impairment of cell migration.

Assay	**IRAK1 knockdown**			
	MCF-7	**LY2**	**T47D**	**TR-1**
2D Growth	No impact	Growth Impaired	Growth Impaired	Growth Impaired
Colony Formation	No impact	Growth Impaired	Growth Impaired	Growth Impaired
3D Growth	No impact	Growth Impaired	Growth Impaired	Growth Impaired
2D Migration	No Impact	Migration Impaired	Migration Impaired	No Impact

Table 3.2. The effects of shRNA IRAK1 knockdown on the growth and migration of Tam-S and Tam-R ER+ breast cancer cell lines across in-vitro growth models. IRAK1 knockdown impaired the growth of both Tam-R cell lines (LY2 and TR-1), while also disrupting the growth of Tam-S T47D cells. IRAK1 knockdown had no significant impact on Tam-S MCF-7 cell growth.

An important part of future work would be to build on these 2D migration findings using other cell migration analysis techniques, such as transwell migration assays, which could clarify the migration data that we have obtained during this project. Transwell migration assays examine migration of cells through a 3D matrix, and as such should be a better representation of what could be expected at the *in-vivo* level. Based on the outcome of these experiments, it may be valuable to try to expand on our mechanistic understanding of changes to migration in these cells by examining the expression of other migratory factors. Wee *et al*. (2015) showed that IRAK1 knockdown reduced Interleukin (IL)-6, IL-8 and Chemokine (C-X-C motif) ligand (CXCL)1 levels in TNBC cells, cytokines that have major roles in TNBC growth and metastasis. Future work could begin by assessing whether similar effects are seen in tamoxifen-resistant ER+ breast cancer.

We next investigated how IRAK1 knockdown impacted ERα expression and activity in our Tam-S and Tam-R ER+ breast cancer cells. We found that IRAK1 knockdown was altering ERα function in the cell lines that were exhibiting growth inhibition while having minimal impact in MCF-7 cells. We observed that ERα expression was significantly reduced in T47D cells following IRAK1 knockdown while, conversely, expression of ERα was slightly increased in TR-1 cells. Similarly, when we studied ERα activity we saw that phosphorylation at S118 and S167 was reduced in T47D cells and increased in TR-1 cells. When we analysed ERα function in MCF-7 cells we saw that ERα expression and activity was reduced slightly, but not reduced to the same degree as what was observed in T47D cells. This finding may explain the differences we observed in the growth of these cells in our cellular assays following IRAK1 knockdown. ERα expression and activity is not impaired in MCF-7 cells following IRAK1 knockdown, and ERα driven cell growth is not disrupted in these cells. When we looked at the whole cell level in the LY2 cell line, we observed minor increases in ERα expression and activity following IRAK1 knockdown. However, Western blots examining nuclear and cytoplasmic fractions of LY2 cells showed that IRAK1 knockdown resulted in an increase in levels of active ERα in the nuclear fraction of LY2 cells.

Considering these findings, IRAK1 has an important role in regulating ERα activity across luminal A breast cancer cell lines. However, this regulation diverges in tamoxifen-

resistance and leads to converse effects of IRAK1 on ERα signalling. In Tam-S cells, IRAK1 appears to support ERα expression and activation, with IRAK1 knockdown limiting ERα function in Tam-S cells, particularly the activation of cytoplasmic ERα. Cytoplasmic ERα has been shown to form signalling complexes with Src and PI3K to drive rapid estrogen responses, and our data indicates that IRAK1 may have a role in cytoplasmic ERα function (Cabodi *et al*. 2004, Greger *et al*. 2007).

We did not observe any reduction in the growth of MCF-7 cells following IRAK1 knockdown, but the mechanistic changes observed in ERα function do appear to overlap in MCF-7 and T47D cells. This overlap was confirmed with qRT-PCR data which looked at the expression of ERα target genes. Changes in the expression of ERα target genes in MCF-7 cells is altered similarly, but to a lesser extent to that observed in the T47D cell line. This is most clearly observed with XBP1 and CDK1 (Figure 3.12 (C) & (D)). These findings further support IRAK1 knockdown having minimal effects on ERα activity in MCF-7 cells. Interestingly, the impairment we observed in ERα signalling in T47D cells did not reduce the expression of known positively regulated estrogen response genes such as EGR3 and GREB1 (Ghosh *et al*. 2000, Inoue *et al*. 2004). This might be explained by the fact that these cells are cultured in low estrogen conditions, and as a result the expression levels of EGR3 and GREB1 is not high enough basally to observe a clear reduction in their expression following the inhibition of ERα activity in T47D cells. Treating these cells with increasing concentrations of estradiol to examine dose-dependent estrogen responses in these cells following IRAK1 knockdown will address this possibility. Additionally, culturing these cells in high estrogen conditions for an extended period of time and re-analysing the impact of IRAK1 knockdown could similarly address this.

Conversely, increased ligand-independent ERα activity was observed in both of the tamoxifen-resistant cell lines following IRAK1 knockdown. Specifically, IRAK1 knockdown increased phosphorylation of ERα at both S118 and S167, which corresponded with increased expression of GREB1, TFF1 and EGR3 in Tam-R LY2 and TR-1 cells. Previous work has shown that unliganded ERα binds to the estrogen response element of GREB1 and TFF1 (Caizzi *et al*. 2014). Additionally, Vareslija *et al*. (2016) showed that the expression of GREB1, EGR3 and TFF1 is dysregulated in LetR aromatase inhibitor (AI)

resistant breast cancer cells, and they identified these genes as steroid-independent ER-regulated genes in LetR cells. These same genes formed part of a gene signature for predicting disease-free survival and overall survival in response to neoadjuvant AI therapy (Vareslija *et al*. 2016). ChIP-seq data in LY2 cells similarly demonstrated that these genes are also steroid-independent ER target genes in Tam-R cells (Vareslija *et al*. 2016). We first showed reduced expression of GREB1 and EGR3 in Tam-R LY2 and TR-1 cells, as assessed by qRT-PCR, when compared to their parental MCF-7 and T47D cells, respectively. This supports previous studies on GREB1 which showed significantly downregulated GREB1 expression in endocrine-resistant cell lines and xenograft tumours (Mohammed *et al*. 2013, Cottu *et al*. 2014, Wu *et al*. 2018)

IRAK1 knockdown led to an increase in ERα activity (S118/S167) coupled to an increase in the expression of GREB1, TFF1 and EGR3 in Tam-R cells, as measured by qRT-PCR. The increase in phosphorylation that we observed in ERα (S118/S167) following IRAK1 knockdown may trigger this increase in ligand-independent ERα activity accounting for the increased expression of GREB1, EGR3 and TFF1. The increased expression of a subset of ERα-regulated genes in Tam-R IRAK1 knockdown cells, including GREB1 and EGR3, may be contributing to the reduced growth observed in Tam-R IRAK1 knockdown cells. GREB1 acts to recruit coactivators required for full ERα transcriptional activity in response to estrogen (Mohammed *et al*. 2013). In contrast, GREB1 has been shown to have a role in the formation of inactive ERα complexes in response to tamoxifen through blocking the association of coactivators with tamoxifen-liganded ERα (Wu *et al*. 2018). EGR3 is a transcription factor that acts as a secondary signalling factor in estrogen-mediated gene expression and may similarly act as a cofactor for ERα-mediated gene regulation, but EGR3 has not been associated with tamoxifen resistance at this point (Drabovich *et al*. 2016).

Additionally, we found that TFF1 expression was increased following IRAK1 knockdown in both of our tamoxifen-resistant cell lines. While TFF1 has been positively linked to migration and metastasis, TFF1 has also been negatively correlated with tumour growth *in-vitro* and *in-vivo* (Prest *et al*. 2002). Buache *et al*. (2011) showed that TFF1 knockdown enhanced MCF-7 soft agar colony-formation and increased tumourigenicity *in-vivo* in nude

mice. Follow-up experiments, where tumourigenesis was induced in TFF1 -/- mice, found that tumour incidence and size were increased in TFF1 -/- mice when compared to wild type. These results would further indicate that the increases we observed in GREB1 and TFF1 expression following IRAK1 knockdown are positively contributing to the subsequent inhibition of Tam-R ER+ breast cancer cell growth. Examining how IRAK1 knockdown affects the expression of GREB1, EGR3 and TFF1 in response to tamoxifen treatment in Tam-R LY2 and TR-1 cells will be important to future work. Furthermore, future work on EGR3 in the tamoxifen-resistant setting will add to our understanding of the significance of our finding that EGR3 levels were increased in IRAK1-deficient Tam-R cells.

ERα signalling	**IRAK1 Knockdown**			
	MCF-7	**LY2**	**T47D**	**TR-1**
ERα expression	Slight reduction	Slight increase	Reduced	Increased
ERα phosphorylation	Slight reduction	Slight increase	Reduced	Increased
GREB1 expression	No change	Increased	Slight increase	Slight increase
EGR3 expression	Slight increase	Increased	Slight increase	Increased
TFF1 expression	No change	Increased	Increased	Increased

Table 3.3. The effects of IRAK1 knockdown on ERα signalling in Tam-S and Tam-R ER+ breast cancer cells. IRAK1 knockdown altered ERα signalling in both Tam-R cell lines (LY2 and TR-1), while also impacting on ERα activity in Tam-S T47D cells. IRAK1 knockdown had minimal impact on ERα function in Tam-S MCF-7 cells.

Assessing how IRAK1 is altering ERα function would also be an essential part of future work. Firstly, endogenous co-immunoprecipitation could be used to examine whether

IRAK1 is interacting with ERα in Tam-S and Tam-R Luminal A breast cancer cells. Subsequently, we could investigate whether there are changes in the activity of several upstream kinases that have previously been shown to phosphorylate these residues. ERK1/2 is recognised to phosphorylate ERα at S118, while Akt is known to phosphorylate ERα at S167 (Kato *et al*. 1995, Campbell *et al*. 2001). IRAK1 has already been shown to have links to ERK1/2 and Akt activity (Kim *et al*. 2012, Zhang *et al*. 2018), so this would be a logical first step. IKKε has previously been shown to phosphorylate ERα at S167 (Guo *et al*. 2010). Our lab has previously identified an association between IRAK1 and IKKε, so this may represent an interesting target to investigate.

The role of IRAK1 in luminal A breast cancer may also be separate from any previously identified role within a signalling cascade. We have yet to look at S6K1 expression or activity. S6K1 is active downstream of Akt and has been suggested as the primary kinase to phosphorylate ERα at S167 (Yamnik *et al*. 2009). Additional relevant kinases that could be examined in future work in relation to the changes in S118 phosphorylation include CDK7 and IKKα. IKKα has previously been suggested to be the main kinase to phosphorylate S118 in response to estrogen stimulation, and our lab has previously observed a signalling link between IRAK1 and another member of the IKK family, IKKε (Park *et al*. 2005). CDK7 has also been shown to phosphorylate S118 and, given the changes we observed in CDK1 expression following IRAK1 knockdown, assessing whether CDK7 expression and activity is similarly disrupted by IRAK1 knockdown could provide further mechanistic insight (Chen *et al*. 2002).

Having established that IRAK1 has an important role in maintaining the growth of Tam-R cells, we next sought to address whether IRAK1 knockdown would increase the responsiveness of these cells to tamoxifen treatments. Our results show that IRAK1 knockdown not only reduces the growth of these cells but re-sensitizes them to tamoxifen. The agonistic role that tamoxifen showed on the growth of Tam-R TR-1 cells was reduced by IRAK1 knockdown. This result was seen in 2D MTS assays, colony formation assays and 3D spheroid assays. The agonistic role of tamoxifen treatment on Tam-R LY2 cell growth was observed in 2D MTS assays, with IRAK1 knockdown impairing this agonistic effect and reducing cell viability. Tamoxifen did not have the same agonistic action on the

growth of LY2 cells in colony formation assays or 3D spheroid assays. However, in these cases, IRAK1 knockdown led to decreased cell growth with increasing concentrations of tamoxifen.

We next sought to investigate the mechanism behind the increased sensitivity of Tam-R cells to tamoxifen treatments following IRAK1 knockdown, initially focusing on the HER family of receptor tyrosine kinases. All HER family members have been linked to tamoxifen resistance previously but no relationship to IRAK1 has been examined (Britton *et al*. 2006, Cui *et al*. 2012, Thrane *et al*. 2013, Wege *et al*. 2018). The clearest result we observed was in relation to HER3 expression. HER3 overexpression has been linked to poorer patient outcomes in breast cancer previously, including in response to tamoxifen treatment (Tovey *et al*. 2005, Chiu *et al*. 2010). In both Tam-R cell lines, HER3 expression was slightly increased in IRAK1 knockdown cells when compared to control cells. However, when control cells were treated with tamoxifen, a clear dose-dependent increase in HER3 expression was observed in both LY2 and TR-1 cells. This profile was not seen following IRAK1 knockdown, where overnight treatment with low concentrations of tamoxifen reduced HER3 expression in TR-1 cells and at a later timepoint (40h) for LY2 cells tamoxifen led to reduced HER3 protein levels. This finding suggests that HER3 is important in supporting the resistant phenotype and that IRAK1 has a role in regulating HER3 expression. The significance of this finding on HER3 may be associated with the subcellular localisation of the receptor. Increased levels of nuclear HER3 have been correlated with tumour progression and metastasis in prostate cancer patients (Koumakpayi *et al* 2006). We found that nuclear HER3 levels were elevated in IRAK1 knockdown LY2 cells. However, tamoxifen induced changes in nuclear levels of HER3 in LY2 cells was not assessed. This will be an important part of future work to further our understanding of the role that IRAK1 plays in HER3 regulation following tamoxifen treatments since tamoxifen led to reduced expression of HER3 in both Tam-R LY2 and TR-1 IRAK1 knockdown cells.

HER2 has been linked to tamoxifen-resistance in breast cancer (Shou *et al*. 2004, Osborne *et al*. 2005, Liu *et al*. 2007, Massarweh *et al*, 2008). We found that IRAK1 knockdown increased the levels of HER2 in Tam-R LY2 and TR-1 cell lines. Tamoxifen treatments led to increases in HER2 levels in control LY2 and TR-1 cells. However, tamoxifen treatments

reduced HER2 levels slightly in IRAK1 knockdown LY2 and TR-1 cells was reduced slightly. Previously published work showed that, in a HER2-overexpressing model of tamoxifen-resistant breast cancer, HER3 in combination with HER2 was driving tumour growth in this resistant phenotype (Liu *et al*. 2007). In this case, siRNA knockdown of HER3 reduced cell growth and re-sensitized cells to tamoxifen. This may highlight the significance of IRAK1 knockdown reducing HER2/HER3 expression in response to tamoxifen treatment, which we observed in our experiments.

Additionally, we examined the expression of EGFR and HER4 in Tam-R LY2 and TR-1 cell lines where we observed some contrasting results. HER4 expression was not detectable by Western blot analysis in LY2 control cells, with highly elevated expression seen in IRAK1 knockdown LY2 cells. HER4:ICD levels mirrored the levels of full-length HER4. This is significant given that HER4 has generally been associated with an anti-proliferative and pro-apoptotic role, with loss of HER4 expression being associated with aggressive tumour growth (Naresh *et al*. 2006, Sundvall *et al*. 2008). Tamoxifen treatment had no significant impact on the expression of HER4 or HER4:ICD in LY2 control cells while the expression of HER4 and importantly HER4:ICD increased slightly in IRAK1 knockdown LY2 cells in response to tamoxifen. Conversely, HER4 levels were higher basally in TR-1 control cells, but expression of full-length HER4 gradually reduced in response to tamoxifen treatment. This corresponded with a sequential increase in the levels of HER4:ICD, indicating that tamoxifen treatment is triggering increased cleavage of HER4 to HER4:ICD. In IRAK1 knockdown TR-1 cells, HER4 and HER4:ICD levels were low but increased slightly in response to tamoxifen treatment. The significance of HER4 in ER+ breast cancer has been associated with the level of HER4:ICD in the nucleus versus in the cytoplasm. HER4:ICD has been shown to act as a potent co-activator of ligand-bound ERα activity (Han & Jones 2014, Göthlin Eremo *et al*. 2015, Wang *et al*. 2016). However, tamoxifen treatment has been shown to impair the formation of the HER4:ICD-ERα transcriptional complex, promoting the accumulation of HER4:ICD in the cytoplasm and promoting mitochondria-associated apoptosis (Naresh *et al*. 2006). Despite the differences in basal HER4 expression between our two tamoxifen-resistant cell lines, these results may support each other in relation to the importance of HER4 expression in breast cancer.

Reduced HER4 expression has been suggested as a marker of tamoxifen resistance in breast cancer patients previously (Guler *et al*. 2007).

Expression	Condition	LY2	TR-1
EGFR	**Basal**	Absent	Higher in IRAK1sh.
	Response to Tam treatments	Absent	Expression increases slightly in Ctrolsh, no change in IRAK1sh
HER2	**Basal**	Higher in IRAK1sh	Higher in IRAK1sh
	Response to Tam treatments	Increases slightly in Ctrolsh, no change in IRAK1sh	Increases in Ctrolsh, decreases slightly in IRAK1sh
HER3	**Basal**	Higher in IRAK1sh	Higher in IRAK1sh
	Response to Tam treatments	Increases in Ctrolsh, reduces in IRAK1sh at later timepoints	Increases in Ctrolsh, decreases in IRAK1sh
HER4	**Basal**	High in IRAK1sh, absent in Ctrolsh	Higher in Ctrolsh
	Response to Tam treatments	Increased further in IRAK1sh, remains absent in Ctrolsh	Decreases in Ctrolsh, Increases in IRAK1sh
HER4:ICD	**Basal**	Higher in IRAK1sh.	Low basally in Ctrolsh and IRAK1sh
	Response to Tam treatments	Increased further in IRAK1sh, very low levels present in Ctrolsh	Increases in Ctrolsh, remains very low in IRAK1sh

Table 3.4. IRAK1 knockdown alters the expression of HER family receptors in Tam-R ER+ breast cancer cells, both basally and in response to tamoxifen treatments.

Given the potential significance of the subcellular localisation of HER4:ICD to our work, assessing nuclear and cytoplasmic levels of HER4:ICD in response to tamoxifen treatments in Tam-R LY2 and TR-1 cells would be an important part of future work.

EGFR protein levels were not detectable in LY2 cells by Western blot analysis, despite IRAK1 knockdown increasing EGFR mRNA levels slightly. In TR-1 cells, IRAK1 knockdown increased basal expression. However, following tamoxifen treatment we observed a dose-dependent increase in EGFR expression in control TR-1 cells but no response in IRAK1 knockdown TR-1 cells. Overall, our findings begin to indicate a consistent trend in Tam-R cells. In response to tamoxifen treatment, control Tam-R cells showed a dose-dependent increase in the expression of EGFR, HER2, HER3 and HER4:ICD, while full length HER4 levels were absent or decreased. In IRAK1 knockdown cells, tamoxifen treatments lead to reductions in HER2 and HER3 expression, EGFR levels remain unchanged and full length HER4 and HER4:ICD levels increase slightly. These findings indicate that the role of IRAK1 in maintaining the tamoxifen-resistant phenotype involves the regulation of HER family member expression.

As mentioned above, elevated expression of these HER family members has been associated with tamoxifen-resistance but our results indicate a novel role for IRAK1 in regulating HER family expression in tamoxifen-resistant breast cancer. We have not investigated the activity of the HER family in Tam-R LY2 and TR-1 cells. However, examining receptor phosphorylation and downstream signalling cascade activation would provide a much deeper understanding of the role of IRAK1 in regulating HER family expression/activity. Future work using inhibitors specific to HER family members would allow us to confirm which member/s of the HER family are supporting the tamoxifen-resistant phenotype. Examining whether HER inhibition mimics the effects of IRAK1 knockdown on ERα activity would add to the mechanism by which IRAK1 is regulating ERα activity in Tam-R cells. Additionally, we need to fully investigate nuclear levels of all HER family members due to the unique roles that nuclear HER family expression can have on tumour growth and progression (Wang *et al*. 2006, Tan *et al*. 2002, Sardi *et al*. 2006, Brand *et al*. 2013).

We investigated whether IRAK1 was playing a role in cell cycle regulation within our tamoxifen-resistant cell lines. We found the expression of both CDK inhibitors p21 and p27 was increased basally following IRAK1 knockdown, most clearly in the LY2 cell line (Figure 3.21 and Figure 3.22). Interestingly, the expression of p21 and p27 increased in response to tamoxifen treatment in control cells despite the cells exhibiting enhanced growth. Conversely, the expression of p21 and p27 in IRAK1 knockdown cells did not increase in a dose-dependent manner, with expression falling in response to tamoxifen treatments in IRAK1 knockdown TR-1 cells. The basal increase in the expression of p21 and p27 following IRAK1 knockdown is likely contributing to the growth inhibition observed in Tam-R LY2 and TR-1 cells.

We have not investigated the phosphorylation of p21 or p27. Investigating the activity of Akt in Tam-R LY2 and TR-1 cells in response to tamoxifen treatment would be valuable in future work, with Akt being linked to p21 and p27 regulation previously (Manning and Cantley, 2007). Given the changes we observed in HER3 expression, downstream Akt activity may be similarly altered in these cell lines and leading to impaired p21 and p27 activity. Phosphorylation of p21 and p27 by Akt has been shown to promote cytosolic sequestration of both CDK inhibitors, disrupting their ability to inhibit cell cycle progression (Manning and Cantley, 2007).

In addition, our finding in relation to the mitosis-associated Aurora-A may highlight our most significant result in relation to the role of IRAK1 in sustaining resistance to tamoxifen. Aurora-A has been found to be overexpressed in a number of cancers, including breast, where it has been associated with forcing the cell through the spindle assembly checkpoint even in the presence of genetic instability (Dauch *et al*. 2016, Shah *et al*. 2019). Aurora-A has also recently been linked to tamoxifen resistance, with Aurora-A inhibition showing promise in working synergistically with tamoxifen and overcoming resistance (Zheng *et al*. 2014). We found that Aurora-A activation was increased in control cells following tamoxifen treatment, most markedly in the TR-1 cell line where we saw a very clear dose-dependent increase in phosphorylation at T288 in response to tamoxifen. However, following IRAK1 knockdown, activation of Aurora-A was impaired in untreated cells and failed to increase in response to tamoxifen. This finding may highlight the

primary mechanism by which Tam-R cell lines are re-sensitized to tamoxifen in the absence of IRAK1.

Protein levels		**LY2**	**TR-1**
Aurora-A expression	**Basal**	Higher in IRAK1sh	High in both Ctrolsh and IRAK1sh
	Response to Tam	Increases in Ctrolsh, no change in IRAK1sh	Increases slightly in Ctrolsh, decreases slightly in IRAK1sh
Aurora-A phosphorylation	**Basal**	Slightly higher in Ctrolsh	Moderate levels in both Ctrolsh and IRAK1sh
	Response to Tam	Increases in Ctrolsh, remains low in IRAK1sh	Increases in Ctrolsh, remains low in IRAK1sh
p21	**Basal**	Higher in IRAK1sh	Slightly higher in IRAK1sh
	Response to Tam	Increases in Ctrolsh, remains high in IRAK1sh	Increases in Ctrolsh, decreases in IRAK1sh
p27	**Basal**	Higher in IRAK1sh	Slightly higher in IRAK1sh
	Response to Tam	Increases in Ctrolsh, remains high in IRAK1sh	Increases in Ctrolsh, decreases slightly in IRAK1sh

Table 3.5. IRAK1 knockdown impairs the activation of Aurora kinase A in Tam-R cells, while also altering the expression of CDK inhibitors p21 and p27 basally and in response to tamoxifen treatments.

We have not examined whether IRAK1 is directly interacting with Aurora-A. Endogenous co-immunoprecipitation would be valuable to future work, to determine whether IRAK1 is directly regulating Aurora-A activation in these cells. Following on from this result, we could proceed to look for changes in the activity of other kinases that have been shown to phosphorylate Aurora-A. p21-activated kinase 1 (PAK1) is one of the primary kinases to phosphorylate Aurora-A at T288 (Zhao *et al*. 2005). The impairment of Aurora-A activity following IRAK1 knockdown is a very valuable novel finding, given the research that has been carried out on the efficacy of Aurora-A inhibitors in cancers, including breast (Bavetsias and Linardopoulos 2015). Similar disruption of PAK1 activity would really highlight the potential therapeutic benefits of targeting IRAK1 in tamoxifen-resistant breast cancer (Korobeynikov *et al*. 2019). Future work would also need to assess the phosphorylation status of ERα at S305. Phosphorylation at this residue has been linked to ligand-independent ERα activity and tamoxifen-resistance previously, and it is recognised as a target of both PAK1 and Aurora-A (Wang *et al*. 2002, Michalides *et al*. 2004, Zheng *et al*. 2014).

Given the changes we have observed in the expression of CDK1, p21 and p27, as well as the activation of Aurora-A, cell cycle analysis using flow cytometry will be carried out in future work. Cell cycle analysis would confirm that the changes in the expression/activity of these proteins following IRAK1 knockdown are limiting cell cycle progression. This type of analysis would also highlight where in the cell cycle IRAK1 is playing the most significant role. An increase in the number of cells in the G2 phase would strengthen the idea that inhibition of Aurora-A activity is the main contributor to growth inhibition, preventing progression through mitosis. Significant research has been carried out to assess the efficacy of cell cycle inhibition as a potential therapeutic option for cancer patients, particularly using CDK4/6 inhibitors. Palbociclib, a CDK4/6 inhibitor, has undergone extensive clinical trials for the treatment of advanced ER+ breast cancer and has shown some promise in improving patient survival (Turner *et al*. 2015, Finn *et al*. 2016). However, increases to patient survival has not always been found to be significant (Turner *et al*. 2018). Our data may indicate the potential of combining CDK4/6 inhibition with IRAK1 inhibition to further impair the cell cycle and improve patient outcomes.

Overall, our research is the first to identify that IRAK1 has a significant role in maintaining the growth of Tam-R luminal A breast cancer cells, with IRAK1 knockdown reducing the growth of Tam-R cells in 2D growth assays, colony formation assays and 3D growth assays. We found that targeting IRAK1 can re-sensitize Tam-R cells to tamoxifen. Our findings indicate that IRAK1 has an important role in regulating HER family expression in Tam-R cells in response to tamoxifen treatment. We also show that IRAK1 has a role in cell cycle regulation in Tam-R cells. This is indicated to be most significant towards the G2/M phase where IRAK1 is involved in the activation of the key mitotic kinase Aurora-A. This research has highlighted the potential therapeutic benefits of targeting IRAK1 alone or in combination with tamoxifen in tamoxifen-resistant luminal A breast cancer.

Chapter 4

Targeting IRAK1 and JNK kinases synergizes to potently inhibit ER+ breast cancer growth

4.1 Introduction.

Given the growing body of evidence indicating that IRAK1 has a significant role in aggressive tumour growth and metastasis, the effect of targeted inhibition of IRAK1 in cancer has become an area of major interest. Numerous research groups have begun to assess the impact of using IRAK1 inhibitors as a potential therapeutic option across several cancer subtypes including breast, where they have shown potential, particularly in aggressive cancers (Rhyasen *et al*. 2013, Dussiau *et al*. 2015, Li *et al*. 2016, Goh *et al*. 2017).

Rhyasen *et al*. (2013) studied the efficacy of a dual IRAK1/4 inhibitor in Myelodysplastic Syndromes (MDS), a form of leukaemia where IRAK1 has been found to be overexpressed in ~20% of cases. Their results showed that treating MDS cells with the IRAK1/4 inhibitor reduced cell growth *in-vitro* and increased survival in a xenograft model of MDS (Rhyasen *et al*. 2013). Similar has been observed in T-cell Acute Lymphoblastic Leukemia (T-ALL), where use of an IRAK1/4 inhibitor reduced T-ALL cell growth and increased apoptosis (Dussiau *et al*. 2015). However, in this case the impact was isolated to cells that exhibit high levels of IRAK1 activity. In Hepatocellular carcinoma (HCC) an IRAK1/4 inhibitor was found to reduce cell growth and migration *in vitro* and tumour growth *in-vivo* (Li *et al*. 2016). Additionally, a separate drug pacritinib, a small molecule inhibitor that targets IRAK1, JAK2 and Flt3, has shown promise in breast cancer (Goh *et al*. 2017). Goh *et al*. (2017) identified a chromosome amplification at 1q21.3 that is present in a high percentage of breast tumours, including the Tam-S MCF-7 and T47D cell lines. Subsequently, they showed that pacritinib was able to specifically reduce tumour burden in xenograft studies of 1q21.3 amplified breast cancer cell lines.

The aim of this work was to build on the data we had obtained from our previous research on IRAK1 knockdown. We wanted to examine whether IRAK1 kinase inhibition would yield similar results, while additionally assessing whether it may synergize with JNK inhibition. The JNK family kinases (JNK1, JNK2, JNK3) are primarily recognised as stress-response kinases and, with the unique and complex roles they play in balancing cell survival, they have been studied across various cancers (Wagner and Nebreda, 2009). JNKs have been shown to have both tumour promoting and tumour suppressing roles (Chen *et al*.

2001, Hui *et al*. 2008). There have been several suggestions as to why this occurs. JNKs have been found to have tissue-specific roles, the mechanism by which JNKs are being dysregulated in these cancers affects their impact, and the specific isoforms of JNK that exhibit altered activity as at least ten isoforms have been identified (Wagner and Nebreda, 2009). JNK1 appears to have an oncogenic role in HCC, where increased JNK1 activity has been correlated with elevated tumour growth while JNK2 has not been associated with HCC (Hui *et al*. 2008). Conversely, JNK2-knockout mice show reduced susceptibility to papilloma formation, indicating that JNK2 has an oncogenic role in skin tumours (Chen *et al*. 2001). Additionally, increases in stress-induced JNK activation can promote tumour survival and progression, while conversely, reduced JNK activity through growth factor signalling has been linked to increased tumour susceptibility due to dysfunctional activation of mitochondria-associated apoptosis (Bubici and Papa, 2014). This is particularly relevant in relation to treatment resistance, as JNK activity can be upregulated by cancer cells to try to compensate for the cellular stresses induced by chemotherapy (Ebelt *et al*. 2017, Lipner *et al*. 2020).

To assess whether combined IRAK1 and JNK inhibition could synergize to inhibit the growth of ER+ breast cancer cells, we tested several inhibitors that target these proteins and have shown promising results in disrupting cancer growth. Pacritinib, has already shown encouraging results in inhibiting growth of breast cancer cells and is currently in phase 3 clinical trials as a myelofibrosis treatment option (Goh *et al*. 2017, Mesa *et al*. 2017). We aimed to examine how this drug impacts on the growth of Tam-R ER+ breast cancer cells, while additionally assessing the potential of combining this drug with AS602801. AS602801 is a JNK family kinase inhibitor that has shown inhibitory effects in several cancer subtypes and has undergone phase 2 clinical trials for the treatment of endometriosis (Okada *et al*. 2016). Additionally, we used another combination of drugs to try to assess the same targeted inhibition. JNK-IN-7 is a dual-kinase inhibitor which inhibits both IRAK1 and the JNK family kinases, while JNK-IN-8 inhibits JNK family kinase only (Zhang *et al*. 2012). These drugs have been shown to potently inhibit JNK activity and limit downstream c-Jun activation. The use of JNK-IN-8 in combination with Lapatinib was found to significantly increase TNBC cell death and increase the survival of mice with TNBC xenografts, with Lapatinib having minimal effect on its own (Ebelt *et al*. 2017). Similarly,

JNK-IN-8 was shown to potently enhance the efficacy of 5-fluorouracil based chemotherapy in pancreatic cancer models, with combination therapy reducing tumour growth *in-vitro* and *in-vivo* (Lipner *et al*. 2020).

This work has shown that JNK has a particularly important role in Tam-R cells, where JNK inhibition alone was able to significantly reduce cell growth in 2D and 3D *in-vitro* growth models. Furthermore, combined inhibition of IRAK1 and JNK family kinases was found to synergize to potently inhibit tamoxifen-resistant cell growth. Based on this work, future plans to carry out xenograft studies to test the potential of targeting IRAK1 and JNK as a potential therapeutic option for patients with this aggressive form of disease is warranted.

4.2. Results.

4.2.1. c-Jun expression and activity are increased in tamoxifen-resistant ER+ breast cancer cell lines.

The JNK family kinases are known to play a role in regulating important cellular processes, particularly in relation to cell survival. Previous findings have identified roles for JNK family kinases in supporting tumour survival and promoting tumour growth, with their activity being shown to be upregulated in response to certain chemotherapeutics (Ebelt *et al*. 2017, Lipner *et al*. 2020). These findings indicate the potential role that JNK family kinases could play in supporting the resistant phenotype that can develop in response to tamoxifen treatment.

Through analysis of the breast cancer databank BreastMark (Madden *et al.* 2010), we found that high JNK2 expression correlated with significantly reduced overall survival (OS) of ER+ breast cancer patients as a whole (P=3.562e-06, n=934, Figure 4.1 (A)), whereas no significant differences in OS were found for high c-Jun expressing tumours (Figure 4.1 (B)). Interestingly, when we selected for the patient cohort who had received tamoxifen treatment, we found that high levels of JNK2 and c-Jun significantly reduced OS of ER+ breast cancer patients (P=6.346e-05, n=210, Figure 4.1 (C) and P=0.0046682, n=210, Figure 4.1 (D) respectively). Using Western blot analysis, we initially investigated the levels and activity of JNK1-3 kinases (T183/Y185) and c-Jun (Ser73), a known substrate of JNK kinases, in Tam-S and Tam-R ER+ breast cancer cells. Using an antibody that cross-reacts against all 3 JNK family members, elevated total levels of JNK were detected in Tam-R LY2 cells, when compared to the respective parental MCF-7 cells (Figure 4.2). Interestingly, the amount of active JNK in these cells showed a different profile, with JNK activity being higher in MCF-7 cells (Figure 4.2). However, the levels and activation of c-Jun was markedly increased in LY2 cells, when compared to MCF-7 cells (Figure 4.2). Our findings in Tam-R TR-1 cells showed an increase in both phospho- and total levels of JNK and c-Jun when compared to parental T47D cells (Figure 4.2). These results show that c-Jun activity is increased in Tam-R ER+ breast cancer cells.

A Overall survival (OS) of ER+ breast cancer patients (High cut-off)

n= 934, number of events= 216
Hazard ratio = 1.89 (1.438 - 2.486)
Score (logrank) test = 21.49 on 1 df, p=3.562e-06

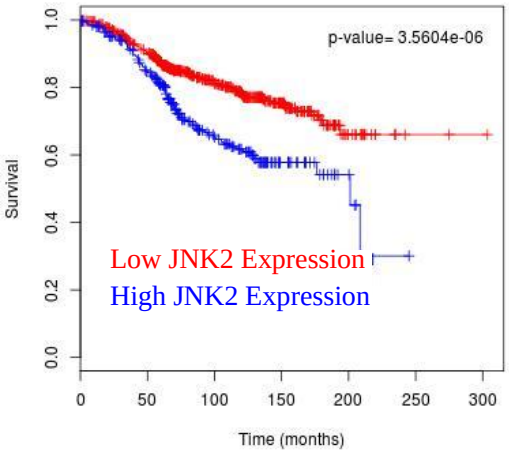

B OS of ER+ breast cancer patients (High cut-off)

n= 934, number of events= 216
Hazard ratio = 0.8843 (0.6459 - 1.211)
Score (logrank) test = 0.59 on 1 df, p=0.4428

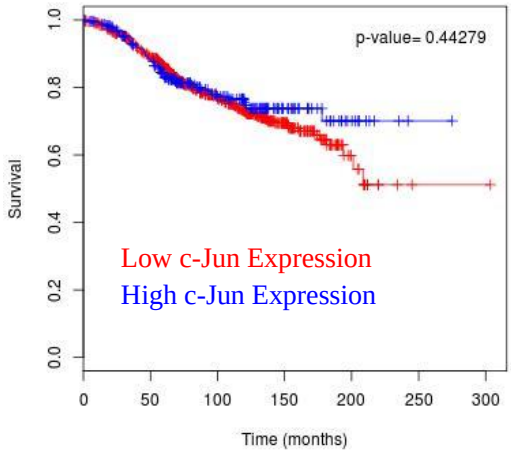

C OS of ER+ breast cancer patients that received tamoxifen (High cut-off)

n= 210, number of events= 49
Hazard ratio = 2.978 (1.699 - 5.222)
Score (logrank) test = 16 on 1 df, p=6.346e-05

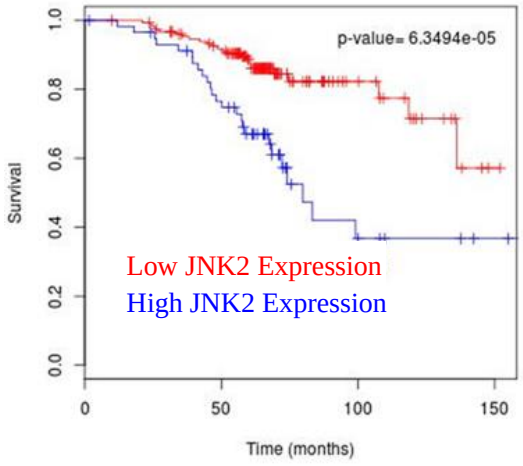

D OS of ER+ breast cancer patients that received tamoxifen (High cut-off)

n= 210, number of events= 49
Hazard ratio = 2.235 (1.262 - 3.961)
Score (logrank) test = 8.01 on 1 df, p=0.004664

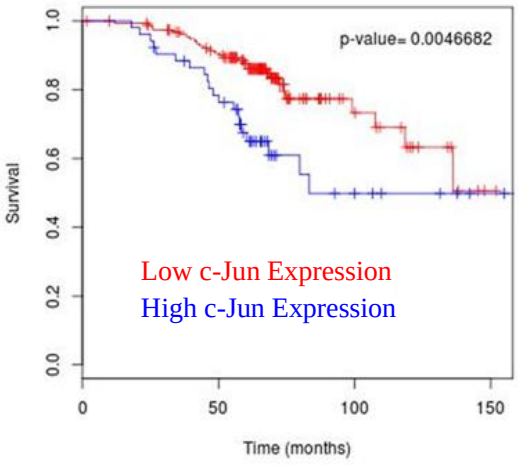

Figure 4.1. High JNK2 and c-Jun expression correlates with reduced survival of ER+ breast cancer patients who have received tamoxifen treatment. Analysis of breast cancer survival data from BreastMark separated into high and low expression based on the high cut-off. (A) OS of ER+ breast cancer patients, based on JNK2 expression (B) OS of ER+ breast cancer patients, based on c-Jun expression (C) OS of ER+ breast cancer patients that have received tamoxifen treatment, based on JNK2 expression levels. (D) OS analysis of ER+ breast cancer patients that have received tamoxifen treatment, based on c-Jun expression levels.

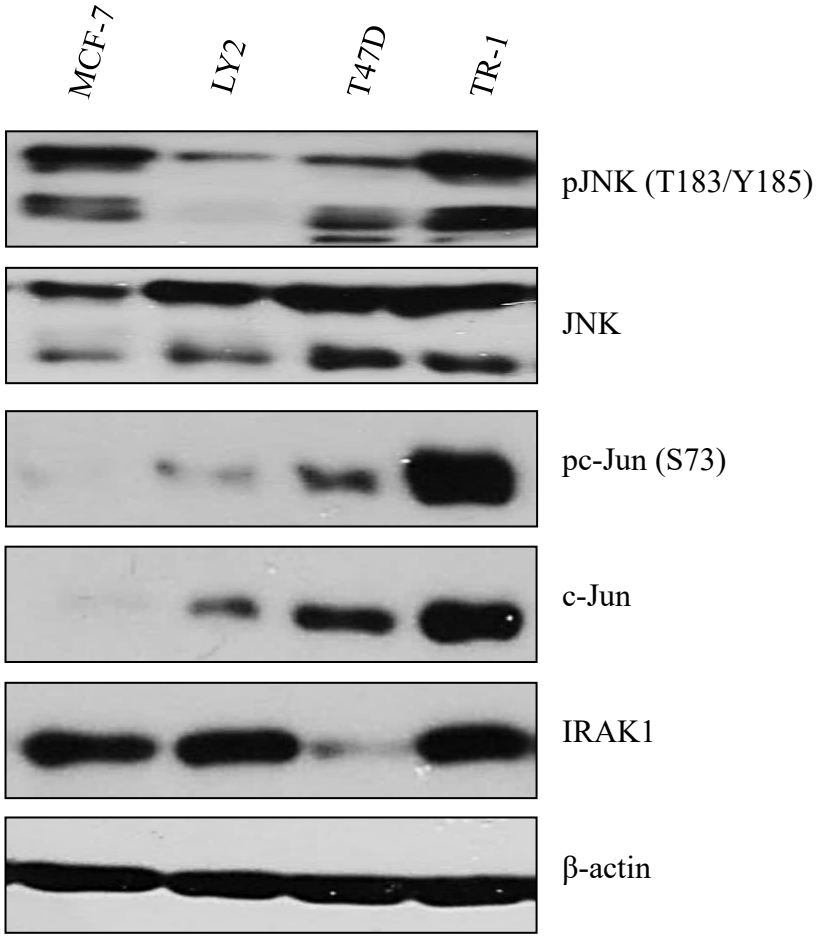

Figure 4.2. JNK and c-Jun activity is altered in tamoxifen-resistant cell lines. Cells were seeded at $4x10^5$ cells/ml in 6-well plates overnight. LY2 cells were cultured in relevant media supplemented with 10nM Z-(4)-hydroxytamoxifen. TR-1 cells were cultured in relevant media supplemented with 5nM Z-(4)-hydroxytamoxifen. After 24 hours, whole cell lysates were prepared and subjected to Western blot. The resulting membranes were probed with phospho-JNK (T183/Y185), total JNK, phospho-c-Jun (S73), total c-Jun, total IRAK1 and β-actin. Similar results were obtained in two independent experiments. Densitometric analysis comparing the expression of each target (LY2 relative to MCF-7, TR-1 relative to T47D) was performed using ImageJ software (Figure AIV.7).

4.2.2 Combined inhibition of IRAK1 and JNK potently inhibits 2D growth of tamoxifen-resistant ER+ breast cancer cell lines.

We proceeded to assess the impact of combined inhibition of JNK1-3 and IRAK1 activity on the growth of Tam-S and Tam-R ER+ breast cancer cell lines using a proliferation assay. Using Western blot analysis, we confirmed that JNK-IN-7 and JNK-IN-8 were both inhibiting c-Jun activation downstream of JNK (Figure 4.3). We found that JNK1-3 inhibition alone, using JNK-IN-8 at the concentration indicated (Figure 4.4), had little effect on the growth of Tam-S cell lines but significantly reduced the growth of Tam-R LY2 cells, while also impairing the growth of Tam-R TR-1 cells (Figure 4.5). However, when we targeted JNK1-3 kinases and IRAK1 with JNK-IN-7, we observed potent inhibition of 2D growth in all cell lines (Figure 4.4 and Figure 4.5). These findings imply that JNK is particularly important in maintaining the growth of Tam-R cells, while combined inhibition of IRAK1 and JNK1-3 works synergistically to potently inhibit the growth of ER+ breast cancer cells.

Subsequently, we expanded on these findings by using another combination of drugs to inhibit JNK1-3 and IRAK1 activity. Our results showed that pacritinib, which inhibits IRAK1, JAK2 and Flt3, dramatically reduced the proliferation of Tam-S and Tam-R cells as assessed on day 4 and day 7 (Figure 4.6 and Figure 4.7). Supporting what we observed previously with JNK-IN-8 (Figure 4.4 and Figure 4.5), we found that JNK1-3 inhibition alone with AS602801 significantly reduced the growth of both Tam-R cell lines (Figure 4.7). Here, the growth of Tam-S cells was also reduced by AS602801 but not to the same level as that observed for Tam-R cell lines (Figure 4.6). These results highlight the importance of JNK in maintaining the growth of Tam-R cell lines. The experimental set-up did not allow us to assess whether growth inhibition could be enhanced by combining pacritinib with AS602801, given the growth inhibition observed with pacritinib alone.

Overall, these findings support our previous work on the potential of targeting IRAK1 in ER+ breast cancer, while highlighting the potential synergy of including targeted inhibition of JNK family kinases in treating Tam-R ER+ breast cancer.

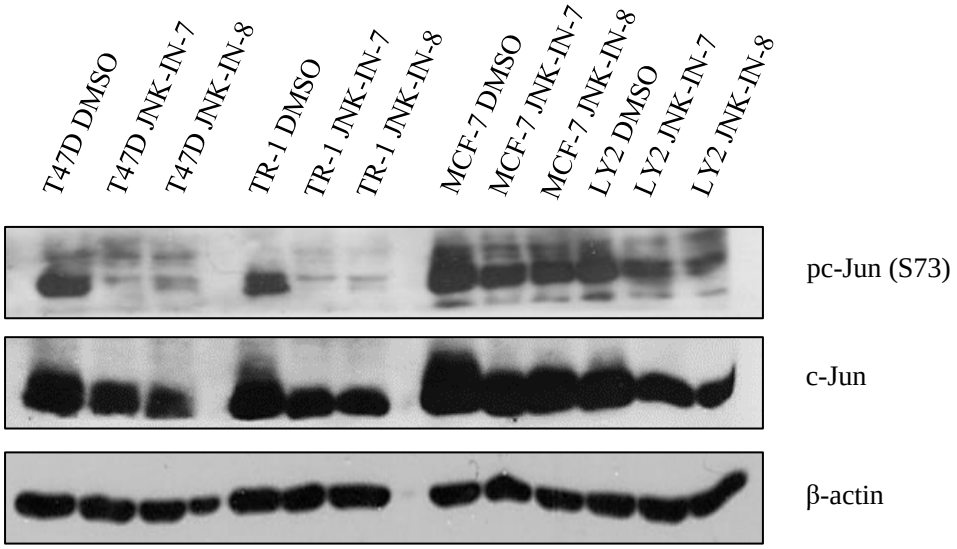

Figure 4.3. JNK-IN-7 and JNK-IN-8 inhibit downstream activation of c-Jun. Cells were seeded at $4x10^5$cells/ml in 6-well plates overnight. LY2 cells were cultured in relevant media supplemented with 10nM Z-(4)-hydroxytamoxifen. TR-1 cells were cultured in relevant media supplemented with 5nM Z-(4)-hydroxytamoxifen. Next day, cells were treated with JNK-IN-7 (1μM final concentration), JNK-IN-8 (1μM final concentration) or DMSO (vehicle control) for 24 hours. Whole cell lysates were extracted and subjected to Western blot. The resulting membranes were probed with phospho-c-Jun (S73), total c-Jun and β-actin. Similar results were obtained in two independent experiments. Figure provided by Danielle McCann (4^{th}-year undergraduate student in Dr. Marion Butler's lab).

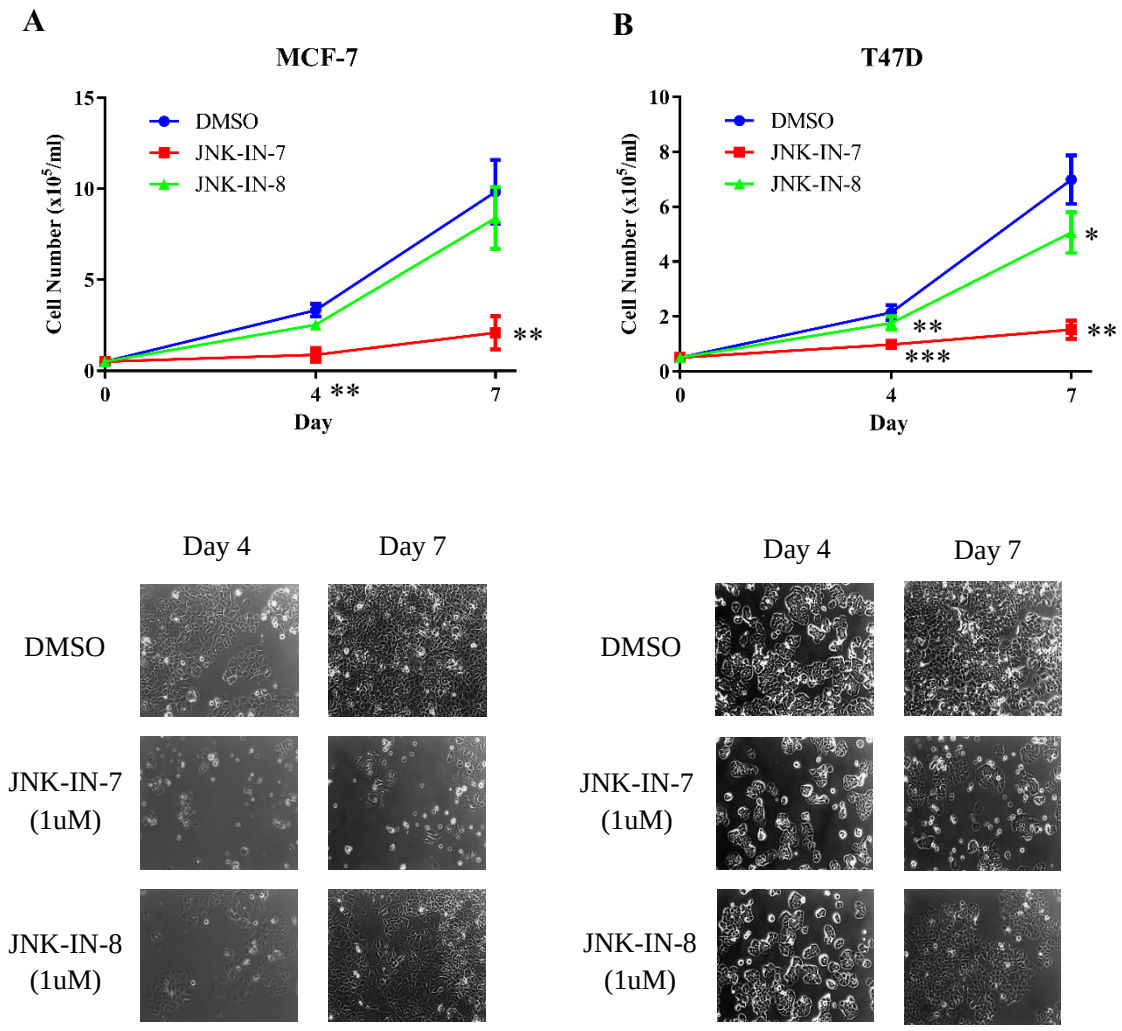

Figure 4.4. Combined targeting of IRAK1 and JNK family kinase activity potently inhibits the growth of Tam-S ER+ breast cancer cells. Cells were seeded in two 12-well plates at 4x10^{4}cells/ml in duplicate. Wells were treated with JNK-IN-7 (1μM final concentration), JNK-IN-8 (1μM final concentration) or DMSO (vehicle control) after 24 hours. Wells were counted on day 4 and day 7 using a haemocytometer. Results were obtained from at least 3 independent experiments. Images were obtained using an Optika Vision Pro camera at 10X magnification (A.) MCF-7 (B) T47D. P value was calculated using the paired Student t test. Statistically significant differences are indicated by the asterisks: *, P<0.05; **, P<0.01; ***, P<0.001.

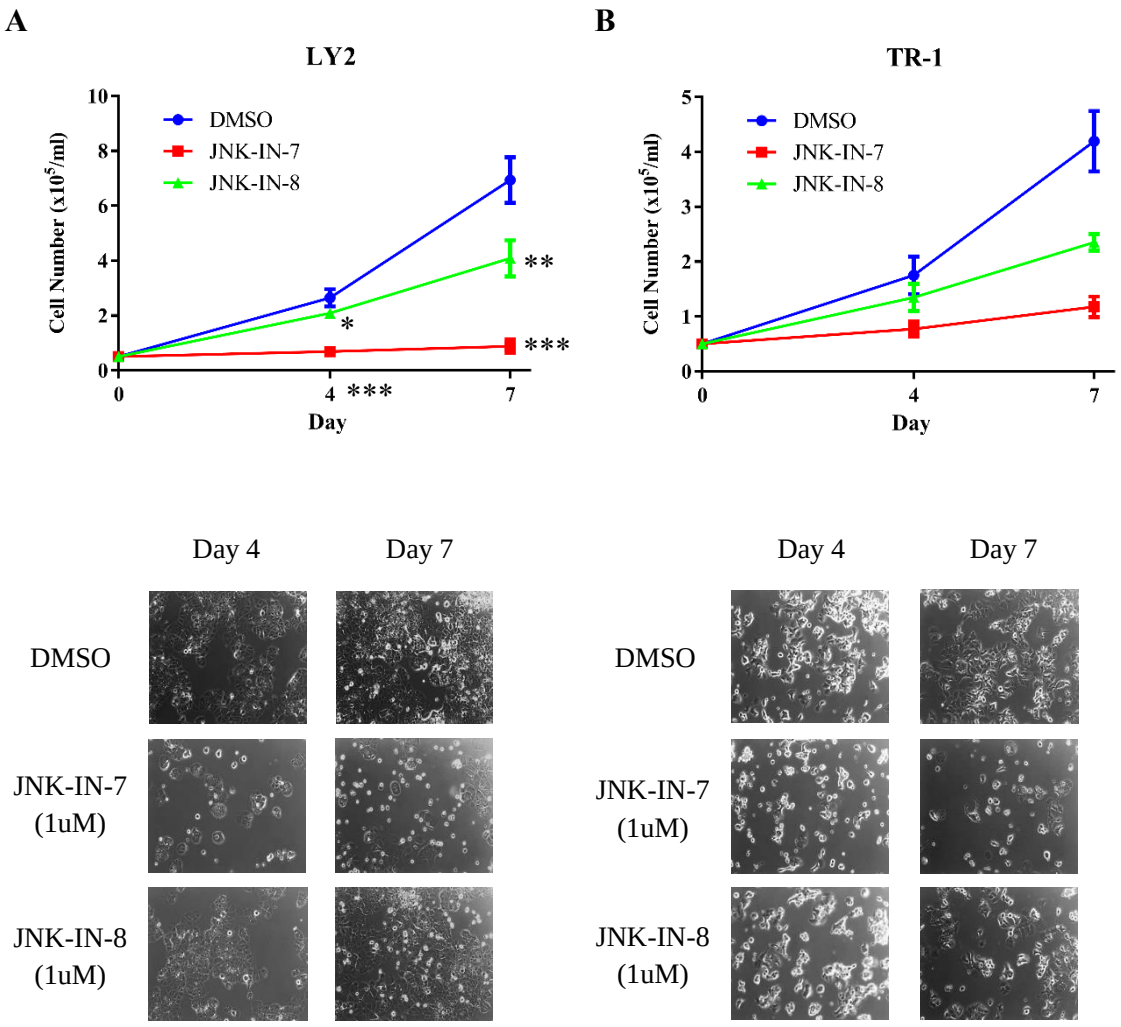

Figure 4.5. JNK inhibition alone reduces growth of tamoxifen-resistant ER+ breast cancer cells, but inhibition is significantly enhanced by combined targeting of IRAK1 and JNK family kinase activity. Cells were seeded in two 12-well plates at 4x10^{4}cells/ml in duplicate. LY2 cells were cultured in relevant media supplemented with 10nM Z-(4)-hydroxytamoxifen. TR-1 cells were cultured in relevant media supplemented with 5nM Z-(4)-hydroxytamoxifen. Wells were treated with JNK-IN-7 (1μM final concentration), JNK-IN-8 (1μM final concentration) or DMSO (vehicle control) after 24 hours. Wells were counted on day 4 and day 7 using a haemocytometer. Results were obtained from at least 3 independent experiments. Images were obtained using an Optika Vision Pro camera at 10X magnification (A.) LY2 (B) TR-1. P value was calculated using the paired Student t test.

Statistically significant differences are indicated by the asterisks: *, $P<0.05$; **, $P<0.01$; ***, $P<0.001$.

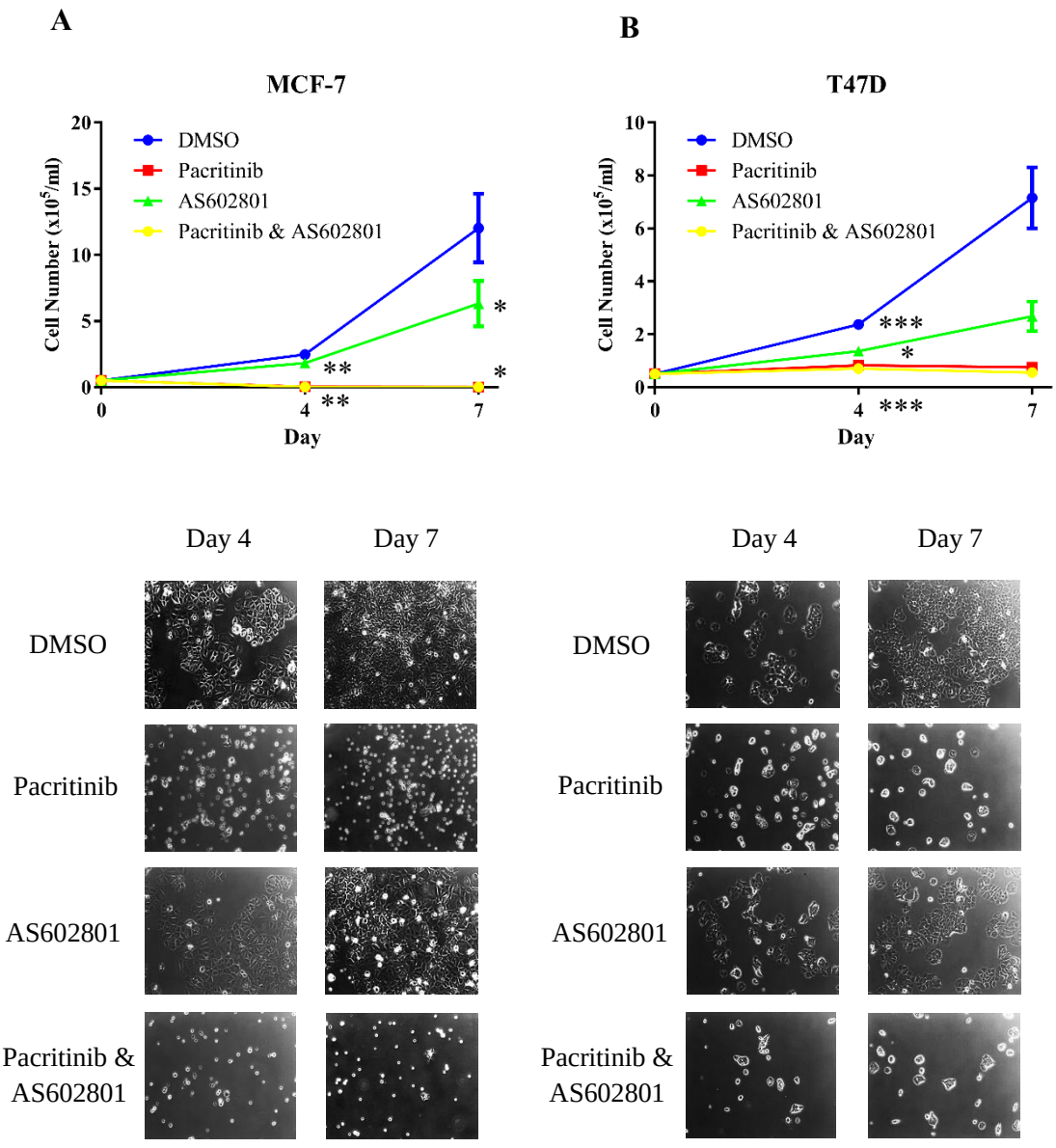

Figure 4.6. Targeting IRAK1 and JNK kinase activity results in growth inhibition of Tam-S ER+ breast cancer cells. Cells were seeded in two 12-well plates at 4x10^{4}cells/ml in triplicate. Wells were treated with pacritinib (2.5μM final concentration), AS602801 (5μM final concentration), a combination of these two drugs or DMSO (vehicle control) after 24 hours. Wells were counted on day 4 and day 7 using a haemocytometer. Results were obtained from at least 3 independent experiments. Images were obtained using an

Optika Vision Pro camera at 10X magnification (A.) MCF-7 (B.) T47D. P value was calculated using the paired Student t test. Statistically significant differences are indicated by the asterisks: *, $P<0.05$; **, $P<0.01$; ***, $P<0.001$.

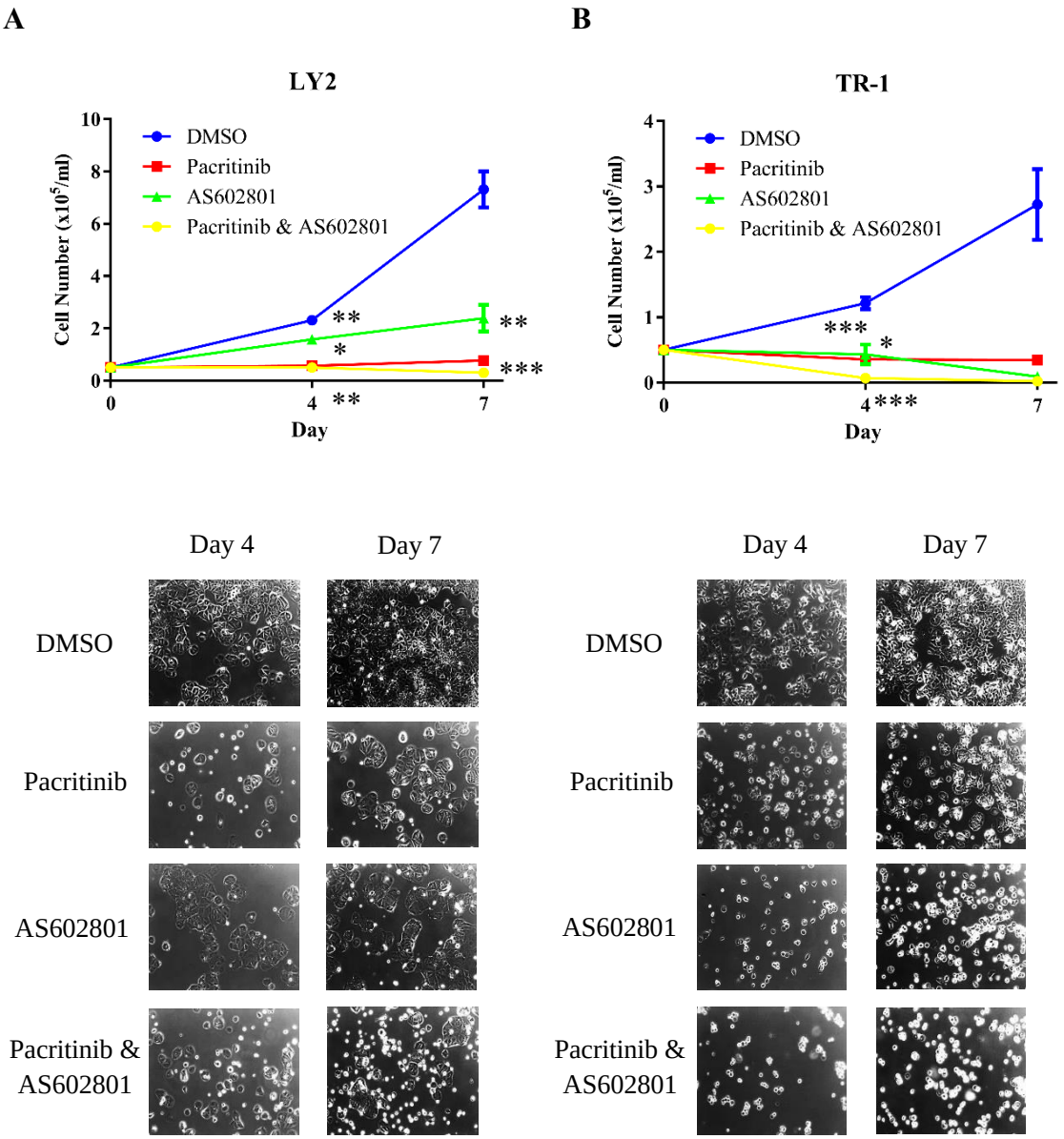

Figure 4.7. Targeting IRAK1 and JNK kinase activity individually significantly impairs the growth of tamoxifen-resistant breast cancer cells. Cells were seeded in two 12-well plates at $4x10^4$cells/ml in triplicate. LY2 cells were cultured in relevant media supplemented with 10nM Z-(4)-hydroxytamoxifen. TR-1 cells were cultured in relevant media supplemented with 5nM Z-(4)-hydroxytamoxifen. Wells were treated with pacritinib (2.5μM final concentration), AS602801 (5μM final concentration), a combination of these

two drugs or DMSO (vehicle control) after 24 hours. Wells were counted on day 4 and day 7 using a haemocytometer. Results were obtained from at least 3 independent experiments. Images were obtained using an Optika Vision Pro camera at 10X magnification (A.) LY2 (B) TR-1. P value was calculated using the paired Student t test. Statistically significant differences are indicated by the asterisks: *, $P<0.05$; **, $P<0.01$; ***, $P<0.001$.

4.2.3. Combined inhibition of IRAK1 and JNK1-3 potently inhibits 3D growth of tamoxifen-resistant ER+ breast cancer cell lines.

We next sought to assess whether our findings from the 2D proliferation assays would translate to a 3D Matrigel growth model. Cells were seeded in polyHEMA-coated 96-well plates at $5x10^4$ cells/ml in media containing 2% Matrigel. On day 4, cells were treated with the indicated inhibitors. Wells were imaged on day 7, before PrestoBlue Cell Viability reagent was added to wells and fluorescence was measured as a readout of cell viability.

In our 3D assay, we did not observe the same potent inhibition of cell growth with JNK-IN-7 at 1uM final concentration. Interestingly, at 1uM final concentration, JNK inhibition alone using JNK-IN-8 was more effective in tamoxifen-resistant cells than combined IRAK1 and JNK inhibition with JNK-IN-7 (Figure 4.9). This observation strengthens our findings in relation to JNK from our 2D experiments, further highlighting the importance of JNK to the survival of tamoxifen-resistant cells. However, when we increased the concentration of JNK-IN-7 to 10uM, the potent inhibitory effects of targeting IRAK1 and JNK1-3 in combination were highlighted again, with a pronounced reduction in 3D growth of Tam-S and Tam-R ER+ cells (Figure 4.8 and Figure 4.9). In the case of Tam-R cells, JNK-IN-7 was found to be more potent in reducing 3D growth when compared to JNK-IN-8 at this higher concentration (Figure 4.9). The increase in JNK-IN-8 concentration to 10uM did not dramatically enhance its inhibitory effects over 1uM JNK-IN-8. Taken together, these results further suggest that JNK has a significant role in maintaining the growth of tamoxifen-resistant cells but targeting JNK alone is not sufficient to potently inhibit cell growth.

Supporting what we observed at the 2D level, IRAK1 inhibition alone with pacritinib at 2.5uM final concentration resulted in significant inhibition of cell growth in both Tam-S and Tam-R ER+ breast cancer cells in our 3D Matrigel model (Figure 4.8 and Figure 4.9). Interestingly, while AS602801 at 5uM final concentration inhibited the growth of all cell lines, AS602801 had a greater impact in Tam-R cells (Figure 4.8 and Figure 4.9). This result is further evidence of the key role of JNK in supporting cell growth in tamoxifen-resistant cells. We aimed to assess the synergy of pacritinib and AS602801 but the potency of pacritinib was too high to determine whether combination treatment enhanced growth

inhibition. Reduced cell growth with dual pacritinib and AS602801 treatments was apparent from images taken, particularly in Tam-R cells (Figure 4.8 and Figure 4.9).

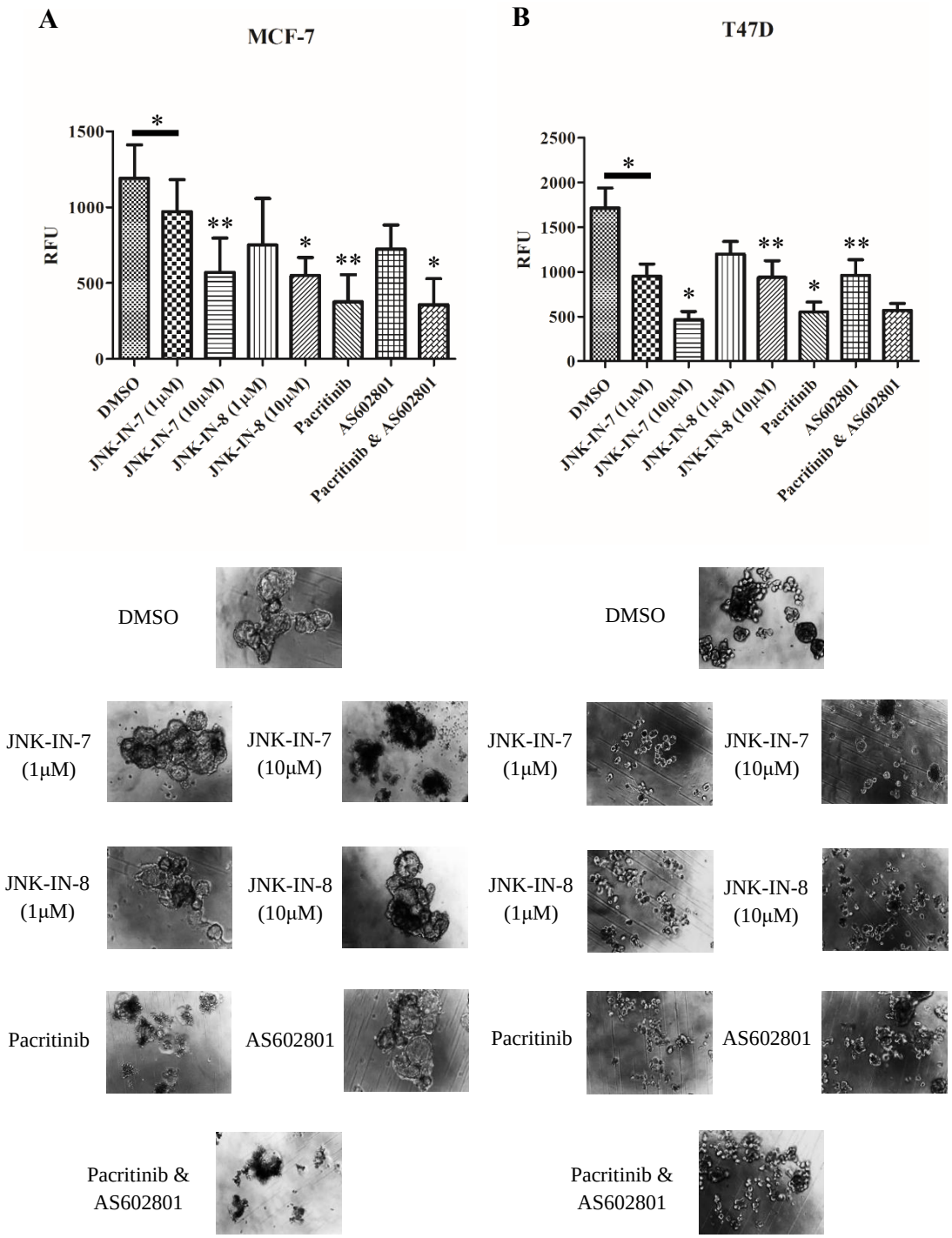

Figure 4.8. Combined targeting of IRAK1 and JNK family kinase activity significantly reduces 3D growth of Tam-S ER+ breast cancer cells. Cells were prepared in media with 2% Matrigel and plated on polyHEMA coated 96 well plates at $5x10^4$ cells/ml. Cells were treated with the indicated concentration of inhibitors or DMSO (vehicle control) on Day 4. 12µl of PrestoBlue Cell Viability reagent (Invitrogen) was added on Day 7 and fluorescence readings were taken after 7hrs using a CLARIOstar LVF Monochromator reader. Images were obtained using an Optika Vision Pro camera at 10X magnification. Results were obtained from 3 independent experiments. (A) Fluorescence readings on MCF-7 cell line (B) Fluorescence readings on T47D cell line. P value was calculated using the paired Student t test. Statistically significant differences are indicated by the asterisks: *, $P<0.05$; **, $P<0.01$.

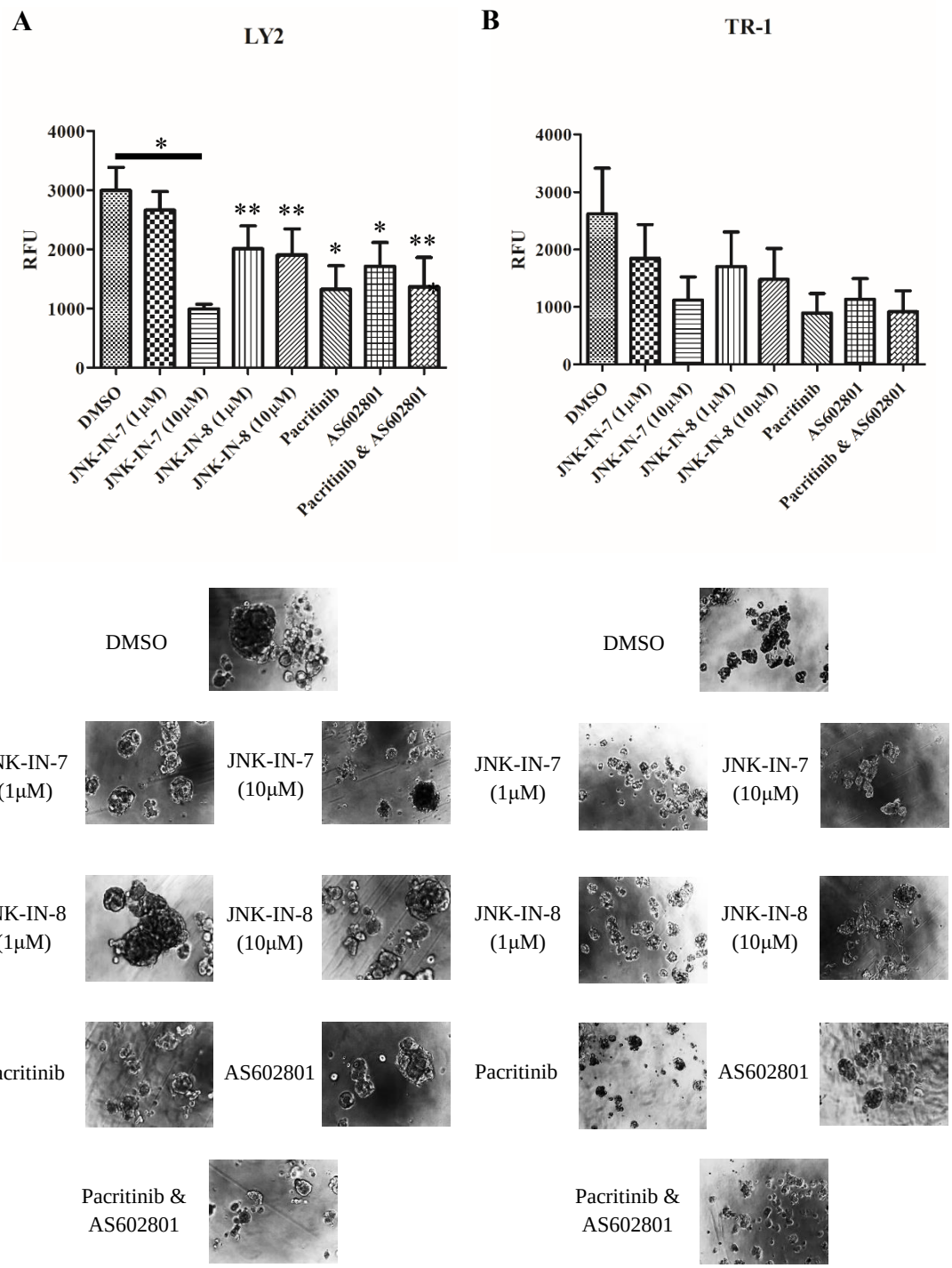
A
LY2
RFU
4000
3000
2000
1000
0
*
**
**
*
*
**
DMSO
JNK-IN-7 (1μM)
JNK-IN-7 (10μM)
JNK-IN-8 (1μM)
JNK-IN-8 (10μM)
Pacritinib
AS602801
Pacritinib & AS602801
B
TR-1
RFU
4000
3000
2000
1000
0
DMSO
JNK-IN-7 (1μM)
JNK-IN-7 (10μM)
JNK-IN-8 (1μM)
JNK-IN-8 (10μM)
Pacritinib
AS602801
Pacritinib & AS602801
DMSO
JNK-IN-7 (1μM)
JNK-IN-7 (10μM)
JNK-IN-8 (1μM)
JNK-IN-8 (10μM)
Pacritinib
AS602801
Pacritinib & AS602801
DMSO
JNK-IN-7 (1μM)
JNK-IN-7 (10μM)
JNK-IN-8 (1μM)
JNK-IN-8 (10μM)
Pacritinib
AS602801
Pacritinib & AS602801

Figure 4.9. Combined targeting of IRAK1 and JNK family kinase activity reduces 3D growth of Tam-R ER+ breast cancer cells over JNK inhibition alone. Cells were prepared in media with 2% Matrigel and plated on polyHEMA coated 96 well plates at $5x10^4$cells/ml. LY2 cells were cultured in relevant media supplemented with 10nM Z-(4)-hydroxytamoxifen. TR-1 cells were cultured in relevant media supplemented with 5nM Z-(4)-hydroxytamoxifen. Cells were treated with the indicated concentration of inhibitors or DMSO (vehicle control) on Day 4. 12µl of PrestoBlue Cell Viability reagent (Invitrogen) was added on Day 7 and fluorescence readings were taken after 7hrs using a CLARIOstar LVF Monochromator reader. Results were obtained from 3 independent experiments. (A) Fluorescence readings on LY2 cell line (B) Fluorescence readings on TR-1 cell line. P value was calculated using the paired Student t test. Statistically significant differences are indicated by the asterisks: *, $P<0.05$; **, $P<0.01$.

4.2.4. Pacritinib and AS602801 synergize to inhibit tamoxifen-resistant cell growth in 2D and 3D growth models.

We observed a clear synergistic effect when we inhibited both IRAK1 and JNK1-3 in combination with JNK-IN-7 but it was difficult to determine whether this translated to the combination of pacritinib and AS602801 due to the potency of the concentration of pacritinib that we had used for our initial analysis (Figure 4.5, Figure 4.7, Figure 4.8, Figure 4.9). To address this, MCF-7 and LY2 cells were treated with increasing concentrations of pacritinib, with or without the addition of AS602801 (5μM final concentration). Firstly, we analysed the effects of pacritinib and AS602801 on 2D growth, as done previously (Figure 4.6 and Figure 4.7). We found that AS602801 alone (5μM final concentration) potently inhibited the growth of Tam-R LY2 cells, while having a less pronounced but still significant inhibitory effect on parental MCF-7 cells (Figure 4.10). Importantly, combination treatments with pacritinib and AS602801 did enhance growth inhibition over either drug alone, with combined treatment being significantly more effective than pacritinib treatment alone in Tam-R LY2 cells (Figure 4.10 (D)). Here, AS602801 significantly increased the efficacy of low concentrations of pacritinib (Figure 4.10 (D)). Subsequently, we performed the same analysis in our 3D Matrigel growth model. We did not observe a synergistic effect of combination AS602801 and pacritinib treatment in Tam-S MCF-7 cells. However, in Tam-R LY2 cells we found that combination treatments did significantly enhance inhibition of 3D growth over the use of pacritinib alone at 1μM and 5μM pacritinib concentrations, while the combination of 5μM AS602801 and 5μM pacritinib significantly increased growth inhibition over 5μM AS602801 alone (Figure 4.11). These findings provide further support to the potential of targeting IRAK1 and JNK1-3 in combination in Tam-R cells. Blocking IRAK1 or JNK1-3 activity alone has an inhibitory effect on the growth of Tam-R cells. However, when we inhibit these targets in combination, we can significantly enhance the inhibition of Tam-R ER+ breast cancer growth.

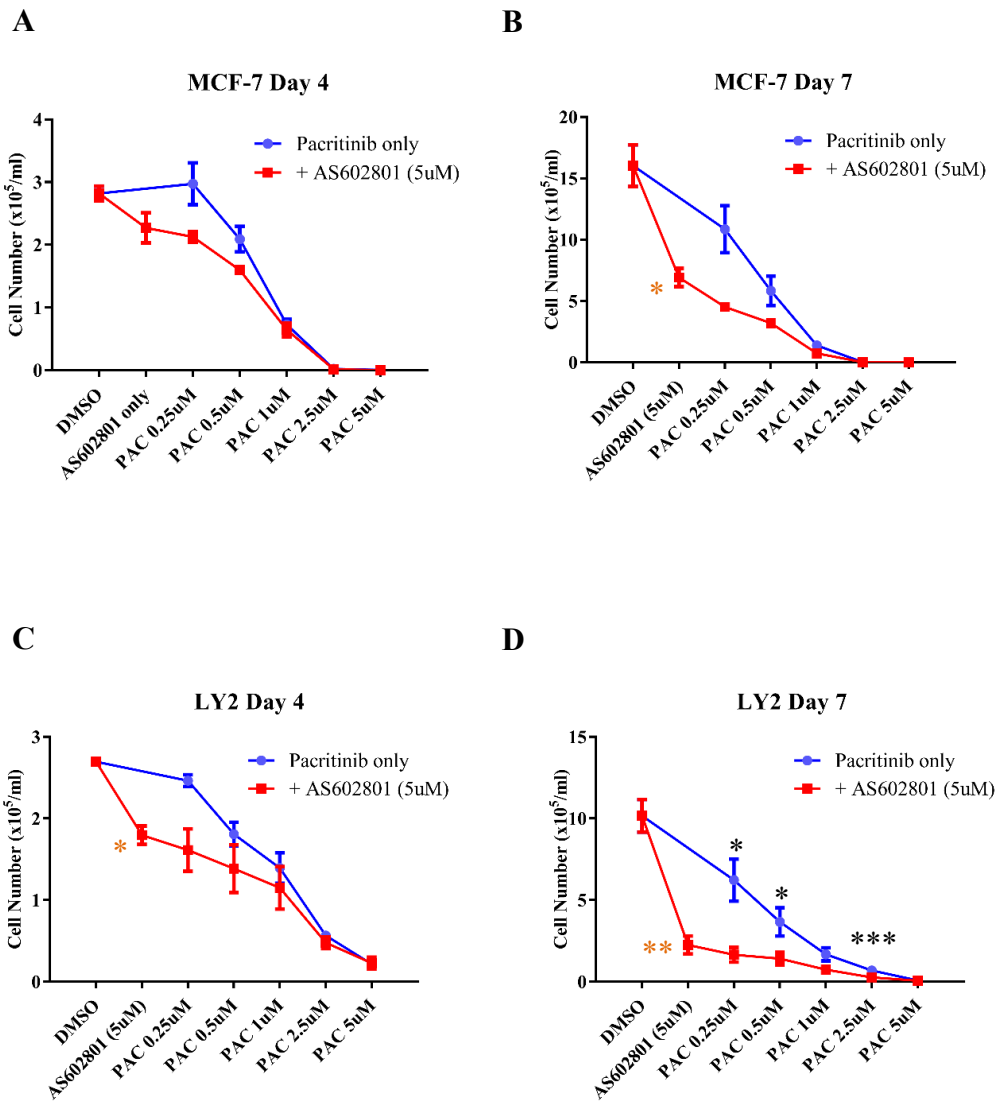

Figure 4.10. Combined targeting of IRAK1 and JNK family kinase activity enhances growth inhibition of ER+ breast cancer cells. Cells were seeded in two 12-well plates at 4x10^{4}cells/ml in duplicate. LY2 cells were cultured in relevant media supplemented with 10nM Z-(4)-hydroxytamoxifen. Wells were treated with the indicated concentrations of inhibitors or DMSO (vehicle control) after 24 hours. Wells were counted on day 4 and day 7 using a haemocytometer. Results were obtained from 3 independent experiments. (A.) MCF-7 Day 4 (B.) MCF-7 Day 7 (C.) LY2 Day 4 (D.) LY2 Day 7. P value was calculated using the paired Student t test. Statistically significant differences are indicated by the

asterisks: *, P<0.05; **, P<0.01; ***, P<0.001. (Significance testing comparing pacritinib alone vs. combination treatment is indicated by black *, comparing DMSO vs 5μM AS602801 is indicated by orange *).

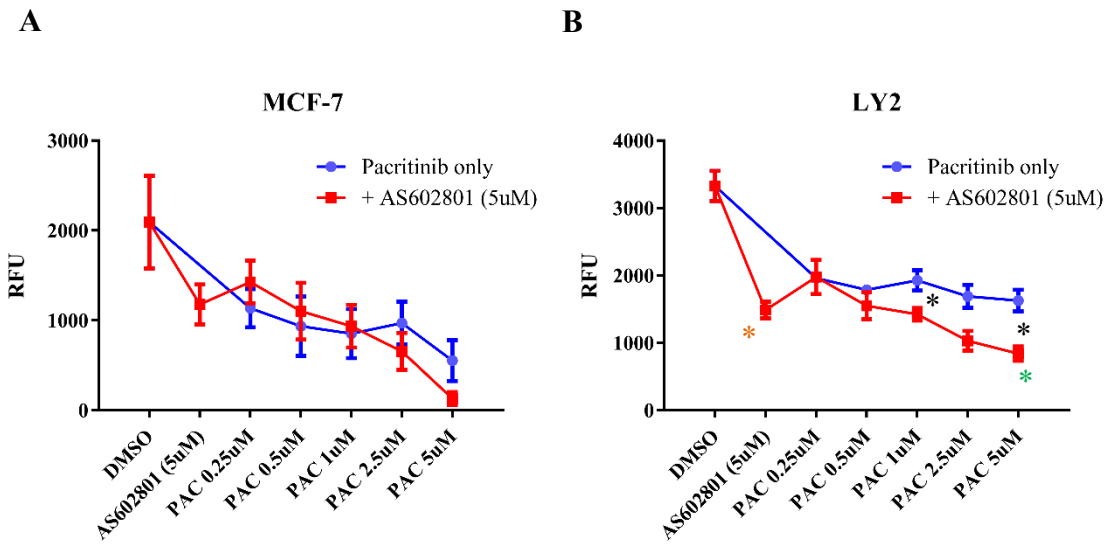

Figure 4.11. Combined targeting of IRAK1 and JNK family kinase activity reduces 3D growth of Tam-R LY2 cells over IRAK1 or JNK inhibition alone. Cells were prepared in media with 2% Matrigel and plated on polyHEMA coated 96 well plates at $5x10^4$ cells/ml. LY2 cells were cultured in relevant media supplemented with 10nM Z-(4)-hydroxytamoxifen. Cells were treated with the indicated concentration of inhibitors or DMSO (vehicle control) on Day 4. 12µl of PrestoBlue Cell Viability reagent was added on Day 7 and fluorescence readings were taken after 7hrs using a CLARIOstar LVF Monochromator reader. Results were obtained from independent experiments. (A) Fluorescence readings on MCF-7 cell line (B) Fluorescence readings on LY2 cell line. P value was calculated using the paired Student t test. Statistically significant differences are indicated by the asterisks: *, $P<0.05$. (Significance testing comparing pacritinib alone vs. combination treatment is indicated by black *, comparing DMSO vs 5µM AS602801 is indicated by orange *, comparing 5µM AS602801 vs. combination treatment is indicated by green *)

4.3. Discussion.

IRAK1 has a significant role in maintaining the growth of tamoxifen-resistant ER+ breast cancer cells. When we targeted IRAK1 through shRNA knockdown, we observed that IRAK1 knockdown reduced the growth of tamoxifen-resistant cells across 2D and 3D growth models, and re-sensitized tamoxifen-resistant cells to tamoxifen treatments (Chapter 3). IRAK1 is a kinase and as such represents a druggable target. Inhibitors are available to target the kinase activity of IRAK1.

The aim of this work was to assess the impact of drugs targeting IRAK1 on the growth of luminal A Tam-S and Tam-R breast cancer cell lines, alone and in combination with JNK inhibitors. The JNK family of kinases are primarily recognised for their role in regulating cell survival signals in response to cellular stresses. Assessing the efficacy of drugs targeting IRAK1 alone or in combination with other drugs may provide more therapeutic potential.

Initially, we examined the expression and activity levels of JNK and a downstream target of JNK, the transcription factor c-Jun, in Tam-S and Tam-R breast cancer cell lines. We found that activation of c-Jun was increased in both LY2 and TR-1 Tam-R cell lines when compared to their parental MCF-7 and T47D cells, as measured by phosphorylation at Ser73. Elevated levels of activated c-Jun have been shown in breast cancer previously, supporting tumour growth and invasion (Vleugel *et al*. 2006). Through follow-up analysis of breast cancer survival data on BreastMark (Madden *et al*. 2010), we found that high c-Jun expression correlates with significantly worse overall survival in patients that have received tamoxifen treatment (P=0.004664, n=210).

Subsequently, we found that JNK activity was altered in both Tam-R cell lines, as measured by phosphorylation at T183/Y185. Interestingly, JNK activity was reduced in Tam-R LY2 cells compared to their parental MCF-7 cells, while JNK activity was increased in Tam-R TR-1 cells compared to their parental T47D cells. The antibody used cross-reacts with JNK1-3 and as such did not show changes in the activity levels of specific JNK members. Changes in the activation of specific isoforms of JNK may be contributing to the development of tamoxifen-resistance. JNK expression was elevated in LY2 cells but

activation of p46 isoforms of JNK was almost entirely lost. In MCF-7 cells, activation of p46 and p54 isoforms was high. JNK2 has been shown to mainly target c-Jun for degradation in the absence of stimuli, while JNK1 stabilizes c-Jun and activates transcription (Fuchs *et al*. 1996). This may explain the discrepancy between JNK activation and c-Jun expression and activation that we observed in these cells. Additionally, high JNK2 expression has been associated with reduced survival of patients with basal like breast cancer (Mitra *et al*. 2011), while JNK2 has been linked to tumour migration and metastasis in murine mammary tumour models (Nasrazadani and Van Den Berg 2010, Mitra *et al*. 2011). Using the BreastMark database (Madden *et al*. 2010), we also found that high JNK2 expression correlates with significantly reduced survival of ER+ patients that have received tamoxifen treatment (P=6.346e-05, n=210). Further work targeting JNK1 and JNK2 separately would expand on our understanding of this dynamic.

Additionally, the outcome of JNK activation can vary depending on stimuli, tissue-specific roles and the isoform of JNK that is activated, with JNK being found to have both growth-promoting and tumour-suppressing roles in cancer (Wagner and Nebreda, 2009). Hyper-activation of JNK under stressful conditions can support the survival of the cell by preventing the initiation of apoptosis while the cell responds to cellular stresses. This is particularly relevant in relation to treatment resistance. Increased JNK activation in response to lapatinib treatment of TNBC and 5-fluorouracil treatment of pancreatic cancer cells has been shown to limit efficacy by impairing the initiation of apoptosis (Ebelt *et al*. 2017, Lipner *et al*. 2020). Conversely, a role for JNK in promoting mitochondrial-associated apoptosis through phosphorylation of BIM or cleavage of BID, and subsequent stimulation of cytochrome c release, has been reported (Lei and Davis 2003, Deng *et al*. 2003). Consequently, impaired JNK activity has also been linked to increased tumourigenesis in certain cancer subtypes, including breast (Cellurale *et al*. 2012). Thus, further work will be needed to fully understand the significance of the different changes we observed in JNK activity between Tam-R LY2 and TR-1 cells.

We proceeded to assess whether combined inhibition of IRAK1 and JNK would disrupt the growth of Tam-S and Tam-R ER+ breast cancer cell lines. We began by using two inhibitors that have recently been developed that inhibit the kinase activity of JNK family

kinases, JNK-IN-8 which inhibits JNK1-3 only and JNK-IN-7 which inhibits both IRAK1 and JNK1-3 activity. In this study, JNK inhibition alone with JNK-IN-8 potently inhibited the growth of Tam-R LY2 and TR-1 cells in both 2D and 3D growth models, while only modest inhibition was observed in parental MCF-7 and T47D cells. These results strongly indicate an important role for JNK in maintaining the growth of Tam-R cells.

When we proceeded to combine IRAK1 and JNK inhibition using JNK-IN-7, we saw potent inhibition of 2D (1uM) and 3D (10uM) growth across all the ER+ cell lines examined. When we imaged cells during 2D assays, we observed dense vacuolation in cells treated with JNK-IN-7 but not when cells were treated with JNK-IN-8. On review of published literature (Lee *et al*. 2016), similar images can be seen in paraptosis, an autophagic response in which JNK has a role in maintaining cell survival while the cell recovers from organelle stress. The combination of IRAK1 and JNK inhibition may be impairing this response and leading to increased paraptosis-associated cell death. To assess this, future work would need to examine the expression of ER stress markers such as CHOP, ATF4 and XBP1 (Lee *et al*. 2016). We have previously looked at the expression of total XBP1, an ERα target gene, but the role of XBP1 in ER stress responses has been associated with the splice variant XBP1s (Yoshida *et al*. 2001). Analysing the expression of XBP1s following JNK-IN-7 treatment may provide insight into the cellular stresses being triggered by this inhibitor. In future, it would also be beneficial to assess cellular apoptosis by flow cytometry to confirm that JNK-IN-7 is promoting cell death, pre-treating cells with inhibitors of cell death in Tam-S and Tam-R cells.

We proceeded to assess the efficacy of two further drugs that target IRAK1 or JNK family kinase, pacritinib and AS602801 respectively, alone or in combination. Pacritinib inhibits IRAK1, JAK2 and Flt3, and is currently in phase 3 clinical trials for the treatment of myelofibrosis, while AS602801 has previously undergone phase 2 clinical trials for endometriosis treatment (Okada *et al*. 2016, Mesa *et al*. 2017). As such, these drugs represent potential therapeutic options and are already FDA approved. We found that treating cells with pacritinib at 2.5uM final concentration, a concentration that proved to inhibit the growth of TNBC (Goh *et al*. 2017), potently inhibited the growth of Tam-S and Tam-R cell lines in this study. Due to the potency of pacritinib in our initial experiments, it

was not possible to ascertain whether combined pacritinib and AS602801 synergized to enhance growth inhibition.

We proceeded to treat MCF-7 and LY2 cells with increasing concentrations of pacritinib, starting from 0.25uM, with and without the addition of 5uM AS602801. Here, combined treatments enhanced growth inhibition of both cell lines at the 2D level and the Tam-R LY2 cells at the 3D level. Importantly, this finding further highlights the synergy of combined IRAK1 and JNK inhibition and indicates the potential to inhibit tumour growth at lower drug concentrations, which would have the potential to reduce any negative side-effects in patients undergoing treatment (Mascarenhas *et al*. 2018). Future work would need to build on this data by testing increasing concentrations of pacritinib in additional Tam-S and Tam-R cell lines and using multiple AS602801 concentrations to identify optimal synergy. Future work in the lab will move to *in-vivo* studies, given the data obtained in relation to combined IRAK1 and JNK1-3 inhibition in Tam-S and Tam-R ER+ breast cancer cell lines. Pacritinib and AS602801 have already shown inhibitory effects as single drug treatments in multiple cancer subtypes, including breast (Goh *et al*. 2017, Yamamoto *et al*. 2018). Our data would strongly imply that combined therapy could potentially reduce tumour burden and increase survival in xenograft models, using drugs that have already undergone clinical trials to assess safety and efficacy. Our results indicate that cell death is occurring in these cells following pacritinib treatments. Flow cytometry following treatments with varying concentrations of drug would also allow us to assess cell cycle and apoptosis. Future work would then involve investigating the mechanism behind these changes further. Examining how IRAK1 and JNK1-3 kinase inhibition affects ERα activity would be an important starting point, given the changes we observed in ERα following IRAK1 knockdown.

The results we have observed following pacritinib treatments support our previous work in which we used an shRNA targeting IRAK1, which significantly reduced the growth of Tam-R ER+ breast cancer cells and the Tam-S ER+ T47D cell line. The potent inhibition of Tam-S and Tam-R breast cancer cell growth by pacritinib points to a key role of the kinase activity of IRAK1 in supporting breast cancer cell growth. One major difference that we observed was in the MCF-7 cell line, where pacritinib treatment dramatically impaired cell

growth while IRAK1 knockdown had little impact. Pacritinib is however known to inhibit multiple kinases in addition to IRAK1 including JAK2 and Flt3. This prevents us from placing the efficacy of pacritinib solely on its inhibition of IRAK1 kinase function. An IRAK1 specific inhibitor would be crucial to future work, allowing us to examine the impact of inhibiting IRAK1 kinase activity only on the growth of Tam-S and Tam-R ER+ breast cancer cells. The crystal structure of IRAK1 has been published and drugs that specifically target IRAK1 have been developed but were not commercially available to us during this work (Wang *et al*. 2017). It may also be possible that results coming from IRAK1 knockdown work may not overlap fully with findings using an IRAK1 specific inhibitor, as knockdown addresses both adaptor and kinase function of IRAK1 while an IRAK1 specific inhibitor will only inhibit kinase function.

Similar to our previous work with JNK-IN-8, AS602801 treatment alone was more potent in Tam-R cells. Combining these results would strongly indicate that JNK plays an important role in the growth of Tam-R ER+ breast cancer. This is supported by our analysis of the breast cancer survival databank BreastMark which showed that high JNK2 and c-Jun expression both independently correlate with reduced survival of ER+ breast cancer patients that have received tamoxifen treatment (Figure 3.1 (C & D)). A role for JNK has been reported previously in relation to the development of resistance to lapatinib in TNBC and 5-fluorouracil in pancreatic cancer, with alterations in JNK activity allowing cancer cells to cope with cellular stresses caused by treatment (Ebelt *et al*. 2017, Lipner *et al*. 2020). Investigating whether targeted JNK inhibition can increase the sensitivity of Tam-R cells to tamoxifen will be an important part of future work.

Longer term, our findings have shown the ability of combined IRAK1 and JNK inhibition to potently impair ER+ breast cancer growth *in-vitro*, indicating the potential that these drugs may have clinically. These results are very encouraging but require further work to determine optimal treatment concentrations and to further understand the underlying mechanisms behind the potent inhibition of cell growth. This research does support progression to *in-vivo* xenograft models, to ascertain whether combined inhibition of IRAK1 and JNK can reduce tumour growth and prolong survival in animal models. This would allow us to determine whether the efficacy of these drugs translates to the *in-vivo*

level and may have the possibility to provide significant therapeutic benefit to patients with tamoxifen-resistant ER+ breast cancer. Investigating the efficacy of JNK inhibition in Tam-R xenografts is an important part of future work, with AS602801 already FDA approved.

Conclusion and Final Remarks.

IRAK1 has been extensively studied with regards to its role in innate immune responses (Flannery & Bowie 2010, Jain *et al*. 2014). In recent years, a significant role for IRAK1 in supporting tumour growth and metastasis has been identified across multiple cancer subtypes, particularly in relation to aggressive cancers (Rhyasen *et al*. 2013, Dussiau *et al*. 2015, Wee *et al*. 2015, Li *et al*. 2016). In each of these cases, targeting IRAK1 through knockdown or with an inhibitor was found to reduce tumour growth.

This study has shown that targeting IRAK1 can effectively inhibit the growth of Tam-R ER+ breast cancer cells.

This work is the first to examine the role of IRAK1 in Tam-R ER+ breast cancer. Increased levels of IRAK1 are seen in Tam-R ER+ breast cancer cell lines compared to their respective Tam-S parental cells. Our data points to a novel role for IRAK1 in ERα regulation. In Tam-R cells there are multiple signalling inputs that can modulate ERα activity to alter the transcriptional landscape regulated by ERα, which makes it difficult to unravel exactly how IRAK1 is impacting this regulation. Results coming from this study do however support a role for IRAK1 in regulating ERα activity in Tam-R ER+ breast cancer cells since increased ERα activity (S167, S118) together with an increase in ERα regulated gene expression was observed in IRAK1-deficient Tam-R cells. This was most distinctive for the ERα-regulated genes GREB1 and EGR3, which shows markedly reduced expression in Tam-R cells, but the expression of both genes increased in Tam-R cells following IRAK1 knockdown. Importantly, IRAK1 knockdown sensitized Tam-R cells to tamoxifen and we observed that the agonistic action of tamoxifen on the growth of IRAK1-deficient Tam-R cells was abrogated. This data suggests that IRAK1 is supporting the tamoxifen-resistant phenotype. Further mechanistic insight is needed to clarify how IRAK1 is regulating ERα. Co-immunoprecipitation studies to investigate whether IRAK1 directly interacts with ERα would be an important part of future work. Additionally, further mechanistic understanding of how IRAK1 is regulating ERα activity may come from our finding that Aurora-A activity is impaired in IRAK1-deficient Tam-R ER+ breast cancer cells. Aurora-A inhibitors have become a major area of cancer research due to the identified role of Aurora-A in driving aggressive tumour growth and poor patient prognoses (Zheng *et*

al. 2014, Bavetsias and Linardopoulos 2015, Thrane *et al*. 2015). Aurora-A activity has been linked to tamoxifen resistance previously, with Aurora-A capable of phosphorylating ERα at S167 and S305 (Zheng *et al*. 2014, Thrane *et al*. 2015). We did not find that impaired Aurora-A activity in Tam-R cells led to reduced S167 phosphorylation. Future work investigating the phosphorylation of ERα at S305 in IRAK1-deficient cells may provide further understanding of how IRAK1 is regulating ERα activity in Tam-R ER+ breast cancer cells.

Additionally, we observed that IRAK1 knockdown altered HER family expression levels in untreated cells and importantly following tamoxifen treatment, implicating IRAK1 in HER signalling regulation. This was an important mechanistic finding as aberrant HER family signalling has been linked to tamoxifen-resistance (Britton *et al*. 2006, Cui *et al*. 2012, Thrane *et al*. 2013, Wege *et al*. 2018). Future research into HER family activity, localisation and downstream signalling will elucidate the role of IRAK1 in this mechanism.

A key mechanistic finding from this work found that IRAK1 limits the expression of the CDK inhibitors p21 and p27 in Tam-R cells promoting cell cycle progression and tumour growth. Our research identifies IRAK1 as a potential alternative target in tamoxifen-resistant ER+ breast cancer, with IRAK1 inhibition capable of disrupting HER family signalling and Aurora-A activity, while increasing the levels p21 and p27. HER3 is a potent activator of Akt signalling, and Akt can phosphorylate p21 and p27 to impair their function (Manning and Cantley 2007, Roskoski 2014). Given the disruption of HER3 signalling we observed in IRAK1-deficient Tam-R breast cancer cells, examining Akt function in these cells may help to explain some of the downstream disruption to the cell cycle.

To build on this research further, we studied the efficacy of IRAK1 and JNK family kinase inhibition alone and in combination. JNK activity has been found to be upregulated by cancer cells in response to treatment with certain chemotherapeutics, with JNK inhibition impairing tumour growth and re-sensitizing TNBC cells to lapatinib and pancreatic cancer cells to 5-FU/FOLFOX (Ebelt *et al*. 2017, Lipner *et al*. 2020). We show that JNK activity, along with downstream c-Jun activity, is dysregulated in tamoxifen-resistant ER+ breast cancer. Targeted inhibition of JNK using two independent JNK inhibitors (JNK-IN-8 and AS602801) was found to significantly inhibit tamoxifen-resistant cell growth. However,

when JNK inhibition was combined with IRAK1 inhibition we observed potent impairment of Tam-S and Tam-R ER+ breast cancer cell growth, beyond targeting either alone. This research is the first to highlight a significant role for JNK and IRAK1 in tamoxifen-resistant breast cancer, while indicating the potential therapeutic benefits of targeting them in combination.

Overall, our data shows that targeting IRAK1 impairs the growth of Tam-R cells and re-sensitizes Tam-R cells to tamoxifen *in-vitro*, supporting the progression of this work to animal models to determine whether these results will translate to reduced tumour burden in xenograft studies.

Appendices

Appendix I: Buffers and Solutions

All the reagents were purchased from Sigma-Aldrich unless otherwise stated.

Lysis Buffer	50mM Tris-HCL (pH 7.5) 150mM NaCl 0.5% (v/v) Igepal 50mM NaF 1mM Na_3VO_4 1mM DTT 1mM PMSF COmplete Mini EDTA-free tablets, 1 tablet in 10ml (Roche Diagnostic)
4X Sample Buffer	0.25M Tris-HCL(pH 6.8) 6% (w/v) SDS (ThermoFisher Scientific) 40% (w/v) Sucrose 0.04% (w/v) Bromophenol Blue 20% (v/v) 2-mercaptoethanol
4X Laemmli Lower Tris	1.5M Tris Base 0.4% (w/v) SDS pH 8.8 with HCL
4X Laemmli Upper Tris	1.5M Tris Base 0.4% (w/v) SDS pH 6.8 with HCL
10X Running Buffer	0.25M Tris Base 1.92M Glycine 1% (w/v) SDS pH 8.3
Transfer Buffer	25mM Tris Base 192mM Glycine 15% (v/v) Methanol

	pH 8.2
10X TBS (Tris Base solution)	0.5M Tris-HCl 1.5M NaCl pH 7.5
1X TBST	10X TBS (diluted to 1X with dH_20) 0.1% Tween 20 (ThermoFisher Scientific)
Solution A	100mM Tris-HCl 2.5mM Luminol 400µM p-Coumaric acid
Solution B	100mM Tris-HCl 1:1640 (v/v) 30% Hydrogen Peroxide

Appendix II: Reagents and Product sources.

Name	Company	Product No.	Diluent	Stock Conc.	Storage
(Z)-4-hydroxytamoxifen	Tocris	3412	DMSO	51.1mM	-20^{0}C
JNK-IN-7	MedChemExpress	HY-15617	DMSO	25.3mM	-20^{0}C
JNK-IN-8	MedChemExpress	HY-13319	DMSO	25.3mM	-20^{0}C
Pacritinib (SB1518)	SelleckChem	S8057	DMSO	10mM	-20^{0}C
AS602801	MedChemExpress	HY-14761	DMSO	10mM	-20^{0}C

Table AII.1. *Reagents used during project.*

Name	Company	Product No.	Storage
Matrigel	VWR	734-0269	-20^{0}C
polyHEMA	Sigma	P3932	Room Temp. (RT)
PrestoBlue HS cell viability reagent	ThermoFisher Scientific	P50200	4^{0}C
CellTiterGlo 3D cell viability reagent	Promega	G9682	-20^{0}C
Ultra-low attachment 96 well U-bottom plates	Greiner bio-one	650970	RT
Nuclear extract kit	mybio	40010	4^{0}C
4-well inserts	IBIDI	80469	RT
Puromycin	Invivogen	ant-pr-1	-20^{0}C
L-glutamine	Sigma	G7513	-20^{0}C
Insulin	Sigma	I9278	4^{0}C
Ala-Gln	Sigma	G8541	4^{0}C

Table AII.2. *Products used during project.*

Appendix III: Real-Time PCR Primers

Specificity	Primer Sequence (5'-3')	T_m (^oC)
hIRAK1	For: AGCTGTCCAGGTTTCG	57.1
	Rev: CTGTACCCAGAAGGATGTC	57
hESR1	For: GGAGTGTACACATTTGTGTC	54.3
	Rev: CAAAGTGTCTGTGATCTTGTC	57.3
hGREB1	For: CTTGGTTTCTCTGGGAATTG	61.1
	Rev: TTCCAACAGATTAAAGGTCC	58.1
hTFF1	For: CAGAATTGTGGTTTTCCTGG	61.9
	Rev: AATTCACACTCCTCTTCTGG	58.3
hEGR3	For: TGGGAGAGAGAATGTAATGG	59.1
	Rev: ATGAGGCTAATGATGTTGTC	56.5
hFKBP4	For: AGAGTTTTGAAAAGGCCAAG	59.9
	Rev: CCTCATTGGAAAAACTAGACTC	58.4
hCCND1	For: GCCTCTAAGATGAAGGAGAC	57.1
	Rev: CCATTTGCAGCAGCTC	59.1
hCDK1	For: ACCTATGGAGTTGTGTATAAGG	56.3
	Rev: GACTGACTATATTTGGATGACG	57.7
hSIAH2	For: CTGTTTCCCTGTAAGTATGC	56.3
	Rev: GTCTTCATGTTCTGGTTTCTC	57.8
hXBP1	For: AGAGTCTGATATCCTGTTGG	55.6
	Rev: AGTTCATTAATGGCTTCCAG	58.3
hEGFR	For: TCTTAAAGACCATCCAGGAG	58.3
	Rev: ATCTGCAGGTTTTCCAAAG	59.3
hHER2	For: GCTCTTTGAGGACAACTATG	56.5
	Rev: TCAAGATCTCTGTGAGGC	56.2
hHER3	For: ATACACACCTCAAAGGTACTC	54.7
	Rev: ATCTTCTTCTTCAGTACCCAG	56.5
	For: GGAGTCTATGTAGACCAGAAC	54.3

hHER4	Rev: CACATCCTGAACTACCATTTG	59.5
hCDKN1A (p21)	For: CAGCATGACAGATTTCTACC	57.3
	Rev: CAGGGTATGTACATGAGGAG	57
hCDKN1B (p27)	For: AACCGACGATTCTTCTACTC	57.4
	Rev: TGTTTACGTTTGACGTCTTC	57.8
hGAPDH	For: ACAGTTGCCATGTAGACC	55.7
	Rev: TTGAGCACAGGGTACTTTA	55.8
	For: CTTTTGCGTCGCCAG	60.3
	Rev: TTGATGGCAACAATATCCAC	60.8

Table AIV.1. Primers for qRT-PCR, correspondent sequence and melting temperature (Tm).

Appendix IV: ImageJ analysis.

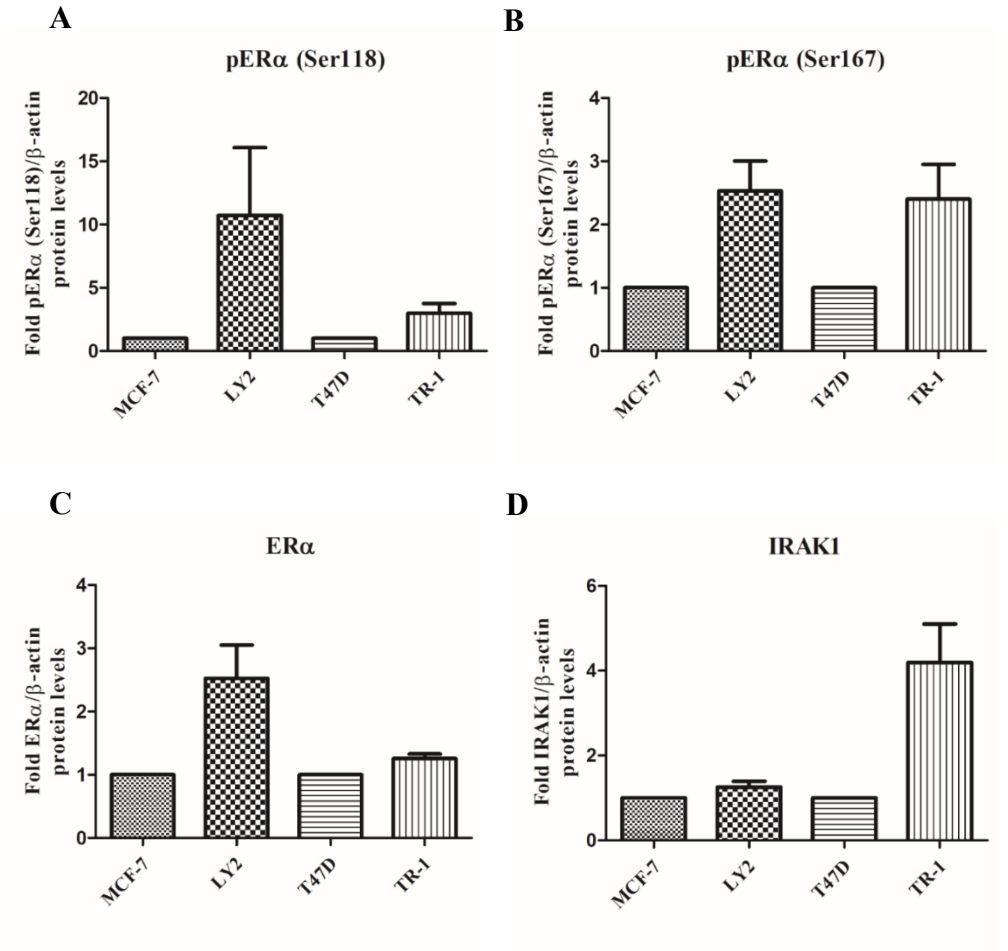

Figure AIV.1. ImageJ analysis of Western Blots from Figure 3.3. (C) (n=3). Protein levels of the indicated proteins were normalised based on β-actin levels. Protein levels in Tam-S MCF-7 cells were compared to their Tam-R subline LY2, while protein levels in Tam-S T47D cells were compared to their Tam-R subline TR-1.

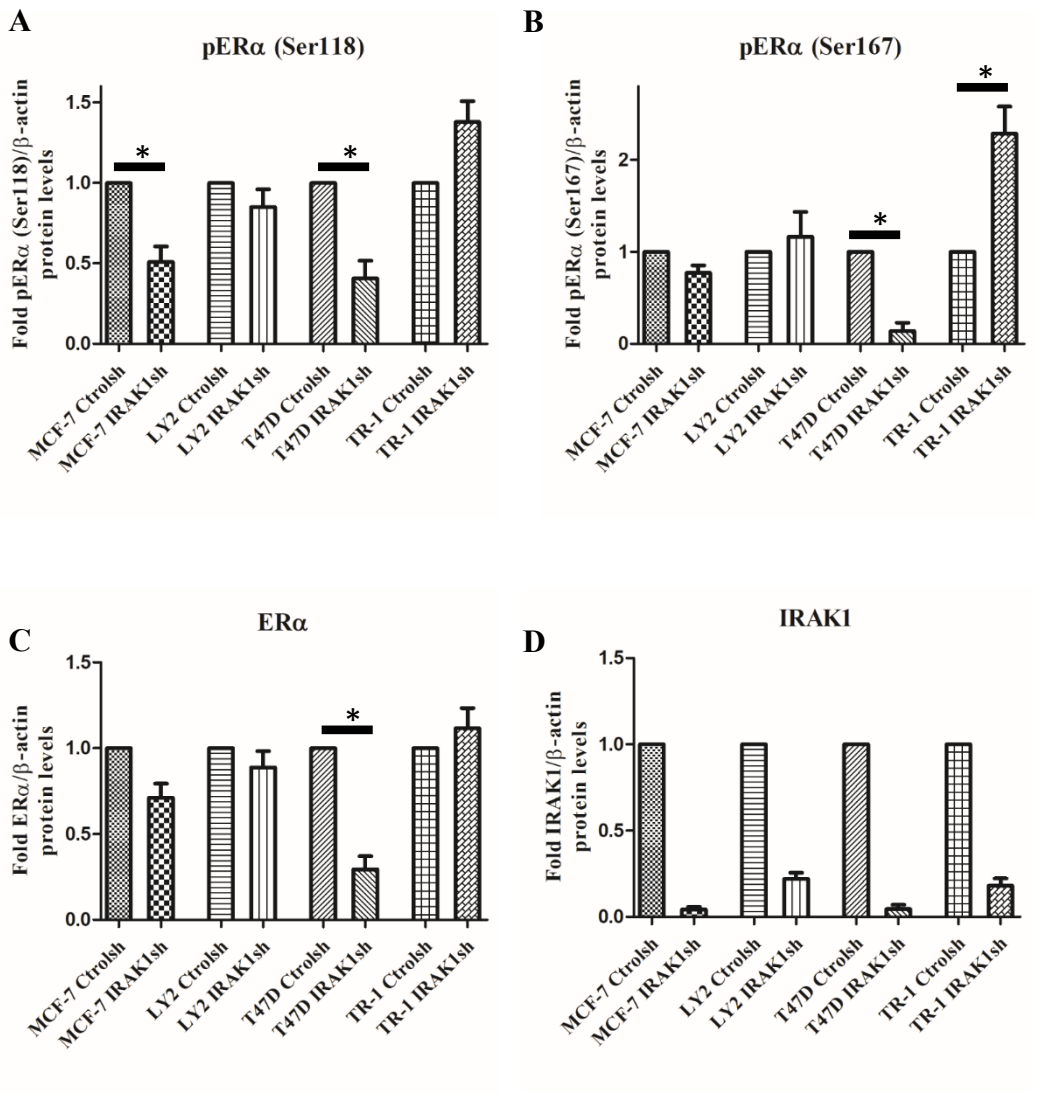

Figure AIV.2. ImageJ analysis of Western Blots from Figure 3.10. (C). (n=3). Protein levels of the indicated proteins were normalised based on β-actin levels. Protein levels in Ctrolsh cells were compared to IRAK1sh cells for each cell line. P value was calculated using the paired Student t test. Statistically significant differences are indicated by the asterisks: *, $P<0.05$.

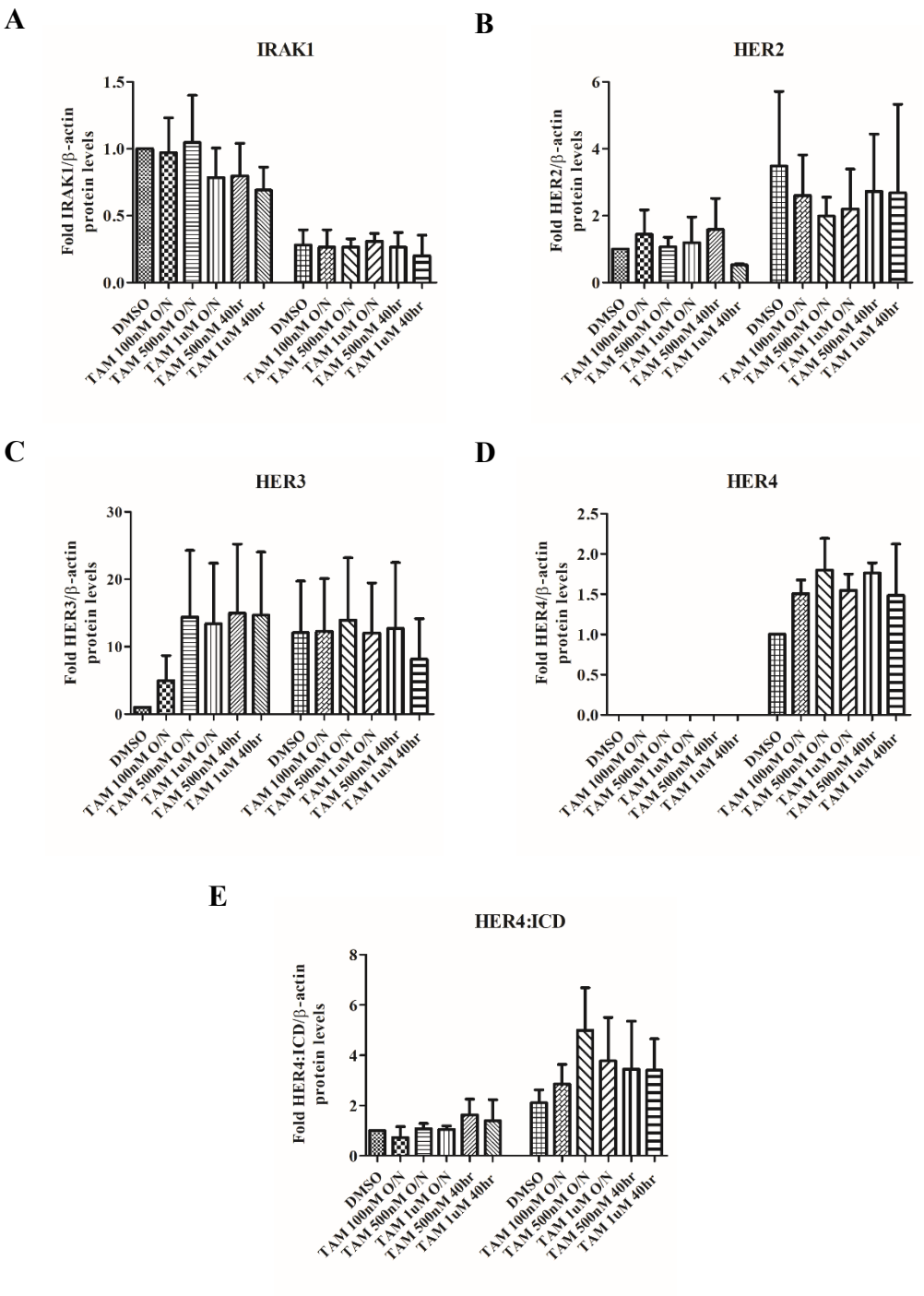

Figure AIV.3. ImageJ analysis of Western Blots on LY2 cells from Figure 3.17. (n=2). Protein levels of the indicated proteins were normalised based on β-actin levels. Protein levels in samples were analysed relative to Ctrolsh DMSO sample.

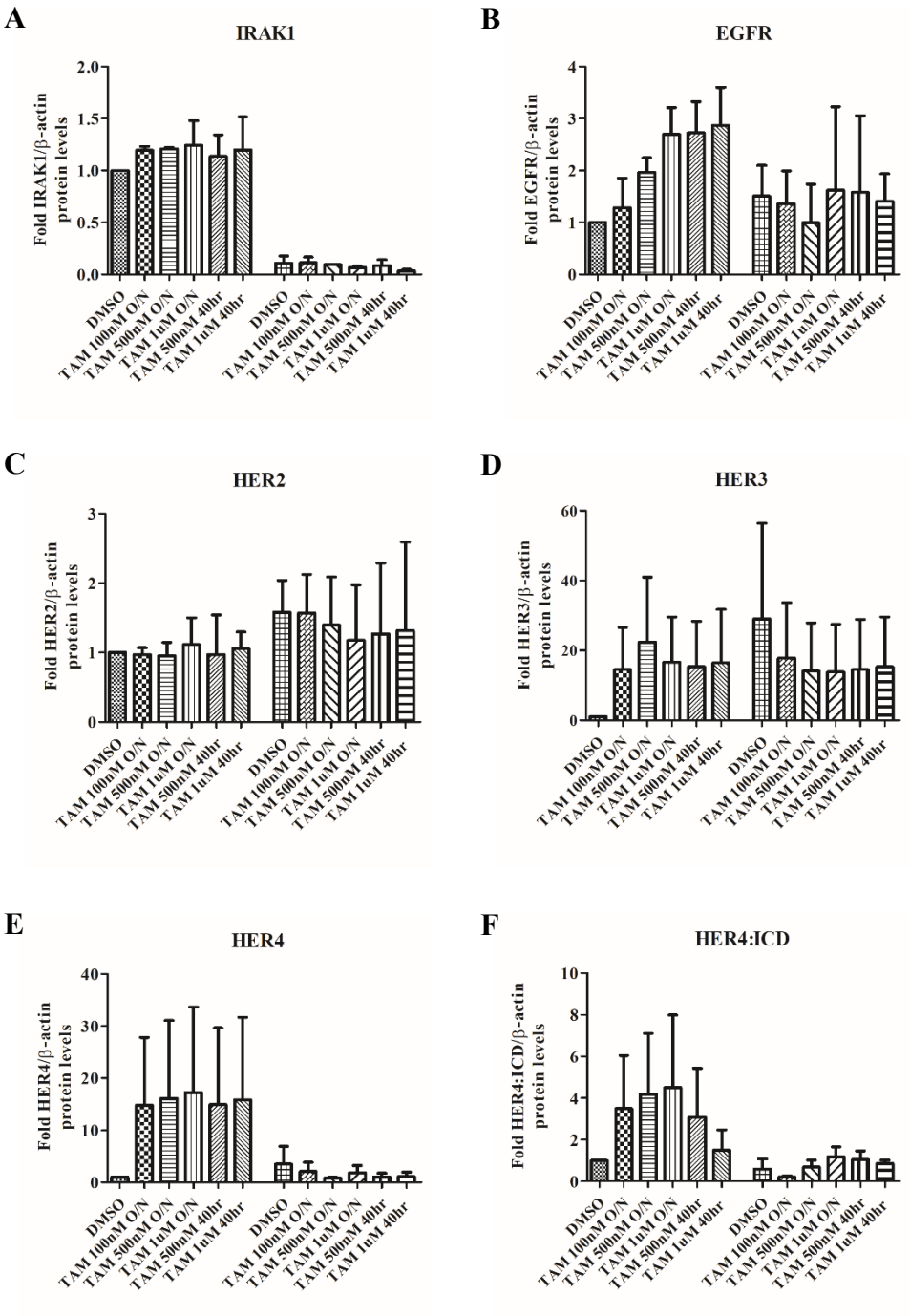

Figure AIV.4. ImageJ analysis of Western Blots on TR-1 cells from Figure 3.19. (n=2). Protein levels of the indicated proteins were normalised based on β-actin levels. Protein levels in samples were analysed relative to Ctrolsh DMSO sample.

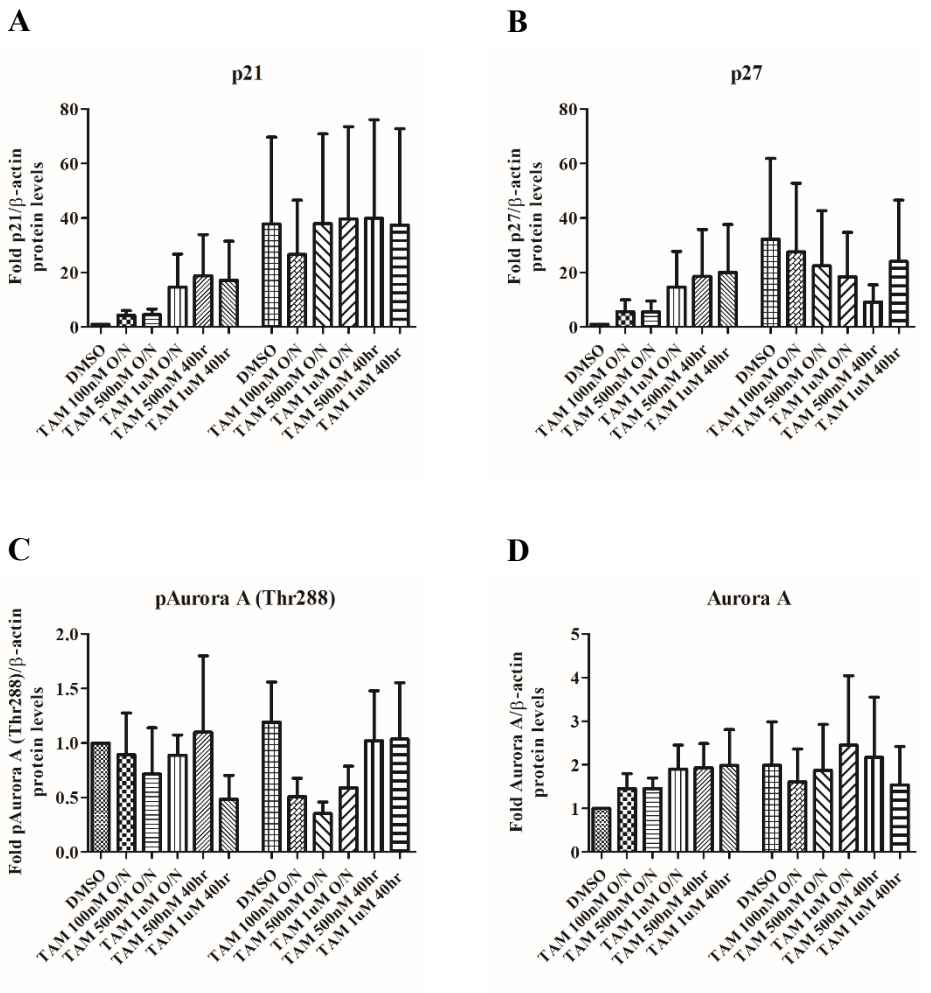

Figure AIV.5. ImageJ analysis of Western Blots on LY2 cells from Figure 3.21.(B). (n=2). Protein levels of the indicated proteins were normalised based on β-actin levels. Protein levels in samples were analysed relative to Ctrolsh DMSO sample.

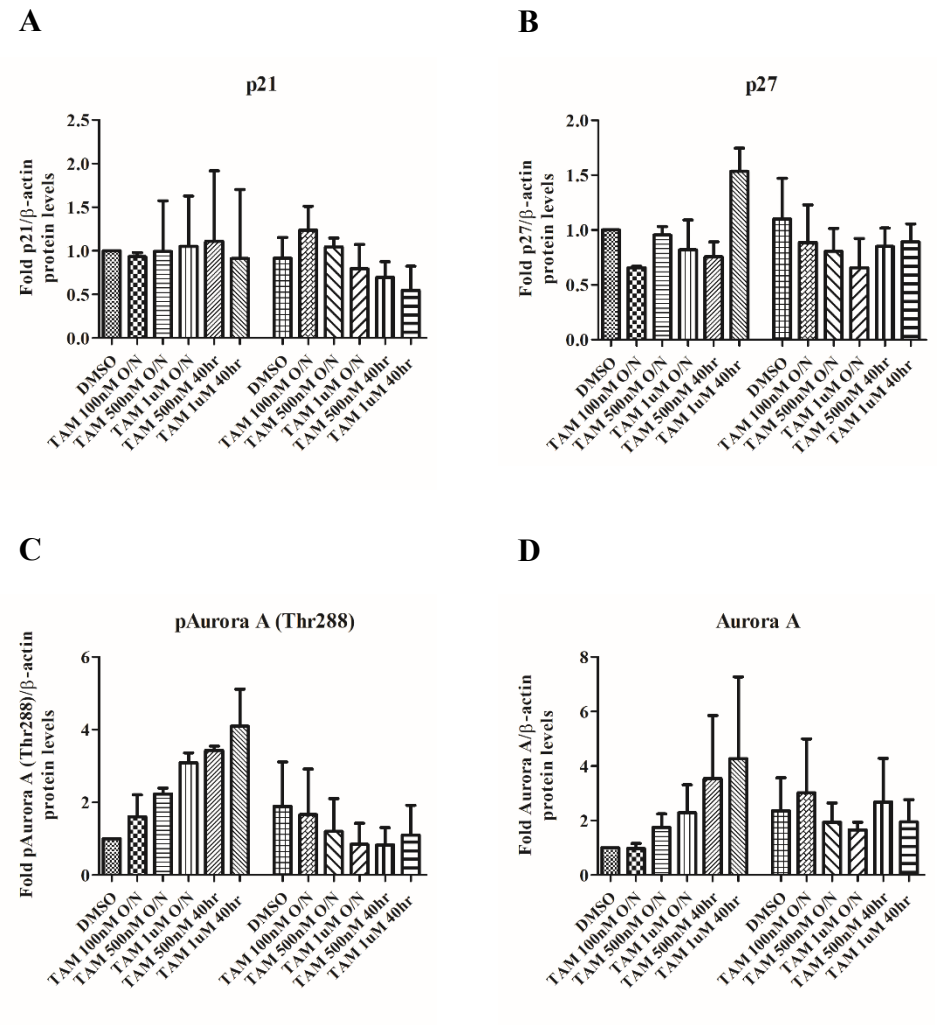

Figure AIV.6. ImageJ analysis of Western Blots on TR-1 cells from Figure 3.22.(B). (n=2). Protein levels of the indicated proteins were normalised based on β-actin levels. Protein levels in samples were analysed relative to Ctrolsh DMSO sample.

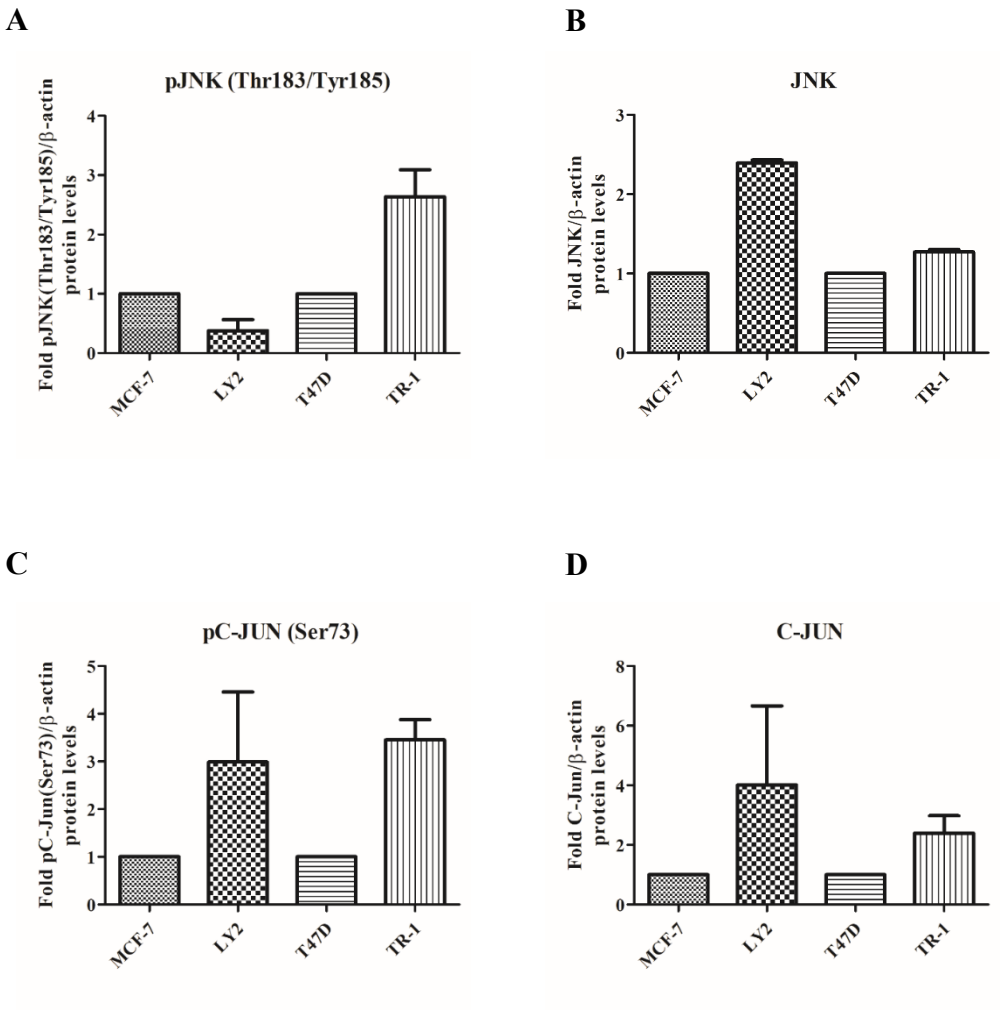

Figure AIV.7. ImageJ analysis of Western Blots from Figure 4.1. (n=2). Protein levels of the indicated proteins were normalised based on β-actin levels. Protein levels in Tam-S MCF-7 cells were compared to their Tam-R subline LY2, while protein levels in Tam-S T47D cells were compared to their Tam-R subline TR-1.

Appendix V: Confirmation of Knockdown in Proliferation Assays

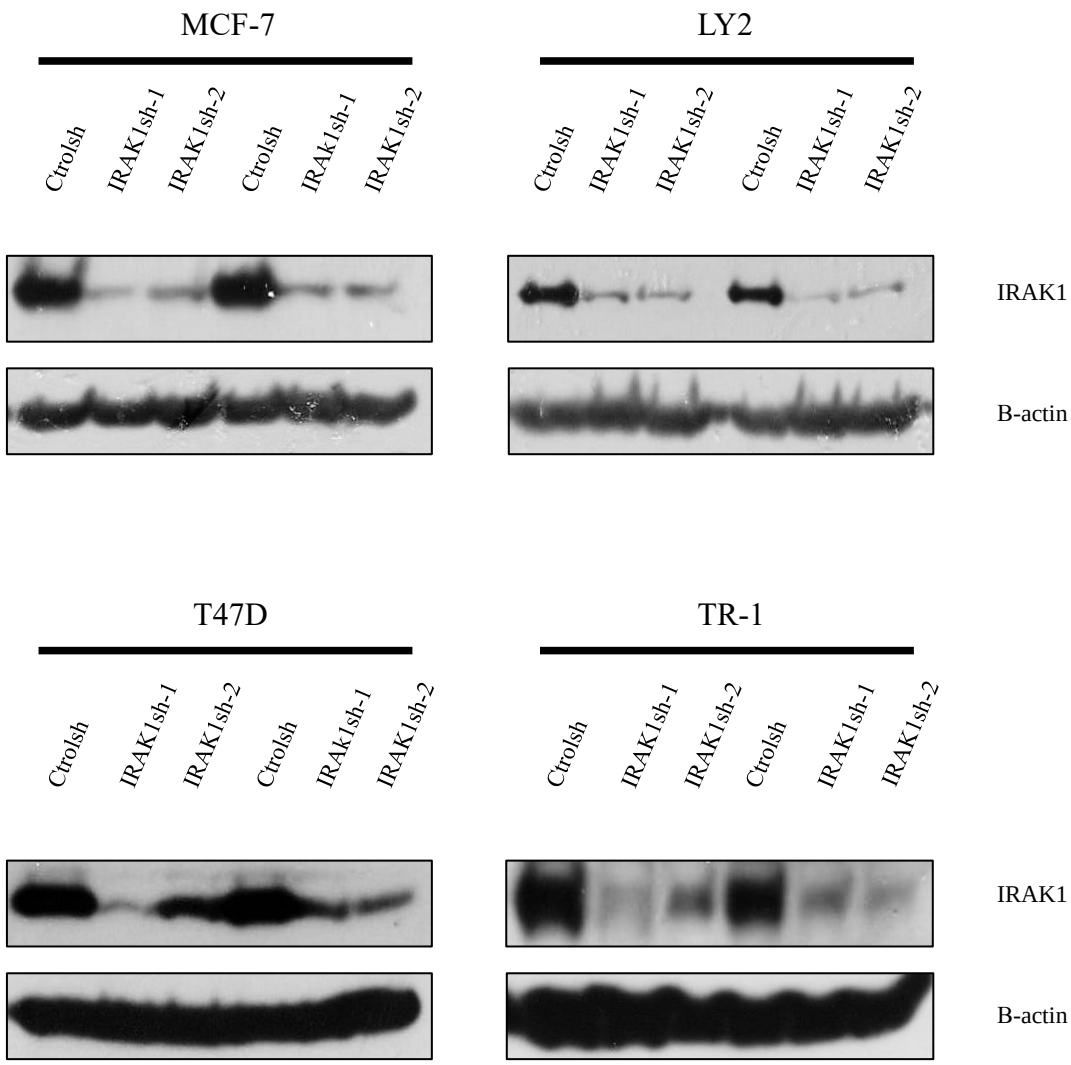

Figure AV.1. Western Blot analysis of lysates collected from proliferation assay plates confirms IRAK1 knockdown. 2X sample buffer was added to the extra well from each proliferation assay and subjected to Western blot. The resulting membranes were probed with Total IRAK1 and β-actin.

Appendix VI: Indication of correct band in pERα associated Western blots

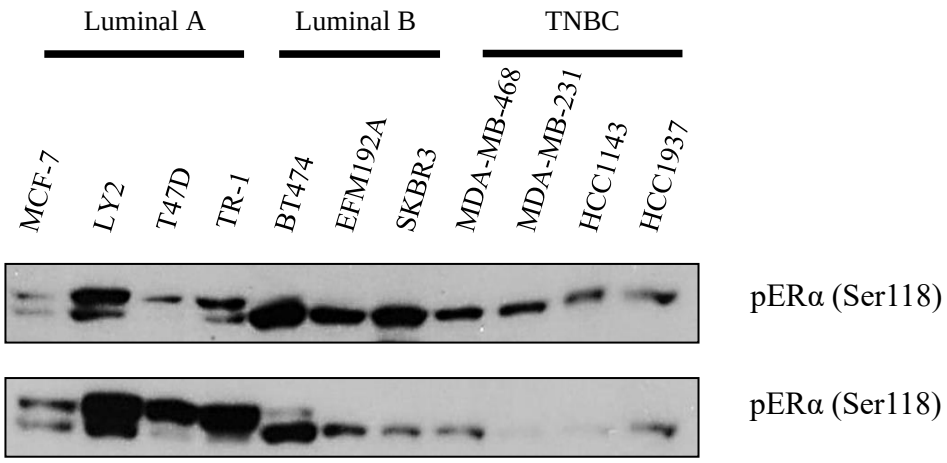

Figure AVI.1. Western Blot analysis indicates that the upper band present in pERα blots is relevant to ERα. The antibody used to analyse ERα phosphorylation at Ser118 presented a double band following Western blot analysis. Examining a panel of breast cancer cell lysates showed that the upper band was present in luminal A and ER+ luminal B cells, while the lower band was present in ER-negative TNBC cells. This highlights that the upper band is specific to ERα.

Bibliography

Ahmed, S., Sami, A. and Xiang, J., 2015. HER2-directed therapy: current treatment options for HER2-positive breast cancer. *Breast Cancer*, *22*(2), pp.101-116.

Alarcon-Vargas, D. and Ronai, Z.E., 2004. c-Jun-NH2 kinase (JNK) contributes to the regulation of c-Myc protein stability. *Journal of Biological Chemistry*, *279*(6), pp.5008-5016.

Anbalagan, M. and Rowan, B.G., 2015. Estrogen receptor alpha phosphorylation and its functional impact in human breast cancer. *Molecular and cellular endocrinology*, *418*, pp.264-272.

Anido, J., Scaltriti, M., Bech Serra, J.J., Josefat, B.S., Rojo Todo, F., Baselga, J. and Arribas, J., 2006. Biosynthesis of tumorigenic HER2 C-terminal fragments by alternative initiation of translation. *The EMBO journal*, *25*(13), pp.3234-3244.

Arasada, R.R. and Carpenter, G., 2005. Secretase-dependent tyrosine phosphorylation of Mdm2 by the ErbB-4 intracellular domain fragment. *Journal of Biological Chemistry*, *280*(35), pp.30783-30787.

Arimidex, T., 2008. Effect of anastrozole and tamoxifen as adjuvant treatment for early-stage breast cancer: 100-month analysis of the ATAC trial. *The lancet oncology*, *9*(1), pp.45-53.

Arnal, J.F., Lenfant, F., Metivier, R., Flouriot, G., Henrion, D., Adlanmerini, M., Fontaine, C., Gourdy, P., Chambon, P., Katzenellenbogen, B. and Katzenellenbogen, J., 2017. Membrane and nuclear estrogen receptor alpha actions: from tissue specificity to medical implications. *Physiological reviews*, *97*(3), pp.1045-1087.

Arnold, S.F., Obourn, J.D., Jaffe, H. and Notides, A.C., 1995. Phosphorylation of the human estrogen receptor by mitogen-activated protein kinase and casein kinase II: consequence on DNA binding. *The Journal of steroid biochemistry and molecular biology*, *55*(2), pp.163-172.

Arpino, G., Wiechmann, L., Osborne, C.K. and Schiff, R., 2008. Crosstalk between the estrogen receptor and the HER tyrosine kinase receptor family: molecular mechanism and clinical implications for endocrine therapy resistance. *Endocrine reviews*, *29*(2), pp.217-233.

Bae, S.Y., La Choi, Y., Kim, S., Kim, M., Kim, J., Jung, S.P., Choi, M.Y., Lee, S.K., Kil, W.H., Lee, J.E. and Nam, S.J., 2013. HER3 status by immunohistochemistry is correlated with poor prognosis in hormone receptor-negative breast cancer patients. *Breast cancer research and treatment*, *139*(3), pp.741-750.

Baselga, J., Albanell, J., Ruiz, A., Lluch, A., Gascón, P., Guillém, V., González, S., Sauleda, S., Marimón, I., Tabernero, J.M. and Koehler, M.T., 2005. Phase II and tumor pharmacodynamic study of gefitinib in patients with advanced breast cancer. *Journal of Clinical Oncology*, *23*(23), pp.5323-5333.

Baselga, J., Gómez, P., Greil, R., Braga, S., Climent, M.A., Wardley, A.M., Kaufman, B., Stemmer, S.M., Pêgo, A., Chan, A. and Goeminne, J.C., 2013. Randomized phase II study of the anti–epidermal growth factor receptor monoclonal antibody cetuximab with cisplatin versus cisplatin alone in patients with metastatic triple-negative breast cancer. *Journal of clinical oncology*, *31*(20), p.2586.

Basso, A.D., Solit, D.B., Chiosis, G., Giri, B., Tsichlis, P. and Rosen, N., 2002. Akt forms an intracellular complex with heat shock protein 90 (Hsp90) and Cdc37 and is destabilized by inhibitors of Hsp90 function. *Journal of Biological Chemistry*, *277*(42), pp.39858-39866.

Baud, V. and Karin, M., 2009. Is NF-κB a good target for cancer therapy? Hopes and pitfalls. *Nature reviews Drug discovery*, *8*(1), pp.33-40.

Bavetsias, V. and Linardopoulos, S., 2015. Aurora kinase inhibitors: current status and outlook. *Frontiers in oncology*, *5*, p.278.

Béguelin, W., Flaqué, M.C.D., Proietti, C.J., Cayrol, F., Rivas, M.A., Tkach, M., Rosemblit, C., Tocci, J.M., Charreau, E.H., Schillaci, R. and Elizalde, P.V., 2010. Progesterone receptor induces ErbB-2 nuclear translocation to promote breast cancer

growth via a novel transcriptional effect: ErbB-2 function as a coactivator of Stat3. *Molecular and cellular biology*, *30*(23), pp.5456-5472.

Berghoff, A.S., Bartsch, R., Preusser, M., Ricken, G., Steger, G.G., Bago-Horvath, Z., Rudas, M., Streubel, B., Dubsky, P., Gnant, M. and Fitzal, F., 2014. Co-overexpression of HER2/HER3 is a predictor of impaired survival in breast cancer patients. *The Breast*, *23*(5), pp.637-643.

Berry, M., Metzger, D. and Chambon, P., 1990. Role of the two activating domains of the oestrogen receptor in the cell-type and promoter-context dependent agonistic activity of the anti-oestrogen 4-hydroxytamoxifen. *The EMBO journal*, *9*(9), pp.2811-2818.

Bhaumik, D., Scott, G.K., Schokrpur, S., Patil, C.K., Campisi, J. and Benz, C.C., 2008. Expression of microRNA-146 suppresses NF-κB activity with reduction of metastatic potential in breast cancer cells. *Oncogene*, *27*(42), pp.5643-5647.

Bieche, I., Onody, P., Tozlu, S., Driouch, K., Vidaud, M. and Lidereau, R., 2003. Prognostic value of ERBB family mRNA expression in breast carcinomas. *International journal of cancer*, *106*(5), pp.758-765.

Blumenthal, G.M., Scher, N.S., Cortazar, P., Chattopadhyay, S., Tang, S., Song, P., Liu, Q., Ringgold, K., Pilaro, A.M., Tilley, A. and King, K.E., 2013. First FDA approval of dual anti-HER2 regimen: pertuzumab in combination with trastuzumab and docetaxel for HER2-positive metastatic breast cancer. *Clinical cancer research*, *19*(18), pp.4911-4916.

Boucher, M.J., Morisset, J., Vachon, P.H., Reed, J.C., Lainé, J. and Rivard, N., 2000. MEK/ERK signaling pathway regulates the expression of Bcl-2, Bcl-XL, and Mcl-1 and promotes survival of human pancreatic cancer cells. *Journal of cellular biochemistry*, *79*(3), pp.355-369.

Braicu, C., Buse, M., Busuioc, C., Drula, R., Gulei, D., Raduly, L., Rusu, A., Irimie, A., Atanasov, A.G., Slaby, O. and Ionescu, C., 2019. A comprehensive review on MAPK: a promising therapeutic target in cancer. *Cancers*, *11*(10), p.1618.

Brand, T.M., Iida, M. and Wheeler, D.L., 2011. Molecular mechanisms of resistance to the EGFR monoclonal antibody cetuximab. *Cancer biology & therapy*, *11*(9), pp.777-792.

Brand, T.M., Iida, M., Luthar, N., Wleklinski, M.J., Starr, M.M. and Wheeler, D.L., 2013. Mapping C-terminal transactivation domains of the nuclear HER family receptor tyrosine kinase HER3. *PLoS One*, *8*(8), p.e71518.

Brandes, L.J. and Hermonat, M.W., 1983. Receptor status and subsequent sensitivity of subclones of MCF-7 human breast cancer cells surviving exposure to diethylstilbestrol. *Cancer research*, *43*(6), pp.2831-2835.

Brasier, A.R., 2006. The NF-κB regulatory network. *Cardiovascular toxicology*, *6*(2), pp.111-130.

Breast International Group (BIG) 1-98 Collaborative Group, 2005. A comparison of letrozole and tamoxifen in postmenopausal women with early breast cancer. *New England Journal of Medicine*, *353*(26), pp.2747-2757.

Britton, D.J., Hutcheson, I.R., Knowlden, J.M., Barrow, D., Giles, M., McClelland, R.A., Gee, J.M.W. and Nicholson, R.I., 2006. Bidirectional cross talk between ERα and EGFR signalling pathways regulates tamoxifen-resistant growth. *Breast cancer research and treatment*, *96*(2), pp.131-146.

Brockmann, M., Poon, E., Berry, T., Carstensen, A., Deubzer, H.E., Rycak, L., Jamin, Y., Thway, K., Robinson, S.P., Roels, F. and Witt, O., 2013. Small molecule inhibitors of aurora-a induce proteasomal degradation of N-myc in childhood neuroblastoma. *Cancer cell*, *24*(1), pp.75-89.

Bronzert, D.A., GREENE, G.L. and LIPPMAN, M.E., 1985. Selection and characterization of a breast cancer cell line resistant to the antiestrogen LY 117018. *Endocrinology*, *117*(4), pp.1409-1417.

Buache, E., Etique, N., Alpy, F., Stoll, I., Muckensturm, M., Reina-San-Martin, B., Chenard, M.P., Tomasetto, C. and Rio, M.C., 2011. Deficiency in trefoil factor 1 (TFF1)

increases tumorigenicity of human breast cancer cells and mammary tumor development in TFF1-knockout mice. *Oncogene*, *30*(29), pp.3261-3273.

Bubici, C. and Papa, S., 2014. JNK signalling in cancer: in need of new, smarter therapeutic targets. *British journal of pharmacology*, *171*(1), pp.24-37.

Bunone, G., Briand, P.A., Miksicek, R.J. and Picard, D., 1996. Activation of the unliganded estrogen receptor by EGF involves the MAP kinase pathway and direct phosphorylation. *The EMBO journal*, *15*(9), pp.2174-2183.

Cabodi, S., Moro, L., Baj, G., Smeriglio, M., Di Stefano, P., Gippone, S., Surico, N., Silengo, L., Turco, E., Tarone, G. and Defilippi, P., 2004. p130Cas interacts with estrogen receptor α and modulates non-genomic estrogen signaling in breast cancer cells. *Journal of cell science*, *117*(8), pp.1603-1611.

Cai-McRae, X., Zhong, H. and Karantza, V., 2015. Sequestosome 1/p62 facilitates HER2-induced mammary tumorigenesis through multiple signaling pathways. *Oncogene*, *34*(23), pp.2968-2977.

Caizzi, L., Ferrero, G., Cutrupi, S., Cordero, F., Ballaré, C., Miano, V., Reineri, S., Ricci, L., Friard, O., Testori, A. and Corà, D., 2014. Genome-wide activity of unliganded estrogen receptor-α in breast cancer cells. *Proceedings of the National Academy of Sciences*, *111*(13), pp.4892-4897.

Calado, D.P., Zhang, B., Srinivasan, L., Sasaki, Y., Seagal, J., Unitt, C., Rodig, S., Kutok, J., Tarakhovsky, A., Schmidt-Supprian, M. and Rajewsky, K., 2010. Constitutive canonical NF-κB activation cooperates with disruption of BLIMP1 in the pathogenesis of activated B cell-like diffuse large cell lymphoma. *Cancer cell*, *18*(6), pp.580-589.

Campbell, R.A., Bhat-Nakshatri, P., Patel, N.M., Constantinidou, D., Ali, S. and Nakshatri, H., 2001. Phosphatidylinositol 3-Kinase/AKT-mediated activation of estrogen receptor α A new model for anti-estrogen resistance. *Journal of Biological Chemistry*, *276*(13), pp.9817-9824.

Cao, Z., Henzel, W.J. and Gao, X., 1996. IRAK: a kinase associated with the interleukin-1 receptor. *Science*, *271*(5252), pp.1128-1131.

Carey, L.A., Rugo, H.S., Marcom, P.K., Mayer, E.L., Esteva, F.J., Ma, C.X., Liu, M.C., Storniolo, A.M., Rimawi, M.F., Forero-Torres, A. and Wolff, A.C., 2012. TBCRC 001: randomized phase II study of cetuximab in combination with carboplatin in stage IV triple-negative breast cancer. *Journal of clinical oncology*, *30*(21), p.2615.

Castiglioni, F., Tagliabue, E., Campiglio, M., Pupa, S.M., Balsari, A. and Menard, S., 2006. Role of exon-16-deleted HER2 in breast carcinomas. *Endocrine-related cancer*, *13*(1), pp.221-232.

Cellurale, C., Girnius, N., Jiang, F., Cavanagh-Kyros, J., Lu, S., Garlick, D.S., Mercurio, A.M. and Davis, R.J., 2012. Role of JNK in mammary gland development and breast cancer. *Cancer research*, *72*(2), pp.472-481.

Chandarlapaty, S., Sawai, A., Scaltriti, M., Rodrik-Outmezguine, V., Grbovic-Huezo, O., Serra, V., Majumder, P.K., Baselga, J. and Rosen, N., 2011. AKT inhibition relieves feedback suppression of receptor tyrosine kinase expression and activity. *Cancer cell*, *19*(1), pp.58-71.

Chen, D., Washbrook, E., Sarwar, N., Bates, G.J., Pace, P.E., Thirunuvakkarasu, V., Taylor, J., Epstein, R.J., Fuller-Pace, F.V., Egly, J.M. and Coombes, R.C., 2002. Phosphorylation of human estrogen receptor α at serine 118 by two distinct signal transduction pathways revealed by phosphorylation-specific antisera. *Oncogene*, *21*(32), pp.4921-4931.

Chen, F., Beezhold, K. and Castranova, V., 2009. JNK1, a potential therapeutic target for hepatocellular carcinoma. *Biochimica et Biophysica Acta (BBA)-Reviews on Cancer*, *1796*(2), pp.242-251.

Chen, N., Nomura, M., She, Q.B., Ma, W.Y., Bode, A.M., Wang, L., Flavell, R.A. and Dong, Z., 2001. Suppression of skin tumorigenesis in c-Jun NH2-terminal kinase-2-deficient mice. *Cancer research*, *61*(10), pp.3908-3912.

Cheng, B.Y., Lau, E.Y., Leung, H.W., Leung, C.O.N., Ho, N.P., Gurung, S., Cheng, L.K., Lin, C.H., Lo, R.C.L., Ma, S. and Ng, I.O.L., 2018. IRAK1 augments cancer stemness and drug resistance via the AP-1/AKR1B10 signaling cascade in hepatocellular carcinoma. *Cancer research*, *78*(9), pp.2332-2342.

Cheng, J., Zhang, C. and Shapiro, D.J., 2007. A functional serine 118 phosphorylation site in estrogen receptor-α is required for down-regulation of gene expression by 17β-estradiol and 4-hydroxytamoxifen. *Endocrinology*, *148*(10), pp.4634-4641.

Cheung, L.W., Yu, S., Zhang, D., Li, J., Ng, P.K., Panupinthu, N., Mitra, S., Ju, Z., Yu, Q., Liang, H. and Hawke, D.H., 2014. Naturally occurring neomorphic PIK3R1 mutations activate the MAPK pathway, dictating therapeutic response to MAPK pathway inhibitors. *Cancer cell*, *26*(4), pp.479-494.

Chiu, C.G., Masoudi, H., Leung, S., Voduc, D.K., Gilks, B., Huntsman, D.G. and Wiseman, S.M., 2010. HER-3 overexpression is prognostic of reduced breast cancer survival: a study of 4046 patients. *Annals of surgery*, *251*(6), pp.1107-1116.

Cho, H.S., Mason, K., Ramyar, K.X., Stanley, A.M., Gabelli, S.B., Denney, D.W. and Leahy, D.J., 2003. Structure of the extracellular region of HER2 alone and in complex with the Herceptin Fab. *Nature*, *421*(6924), pp.756-760.

Chung, S.S., Giehl, N., Wu, Y. and Vadgama, J.V., 2014. STAT3 activation in HER2-overexpressing breast cancer promotes epithelial-mesenchymal transition and cancer stem cell traits. *International journal of oncology*, *44*(2), pp.403-411.

Ciupek, A., Rechoum, Y., Gu, G., Gelsomino, L., Beyer, A.R., Brusco, L., Covington, K.R., Tsimelzon, A. and Fuqua, S.A., 2015. Androgen receptor promotes tamoxifen agonist activity by activation of EGFR in ERα-positive breast cancer. *Breast cancer research and treatment*, *154*(2), pp.225-237.

Clarke, R., Liu, M.C., Bouker, K.B., Gu, Z., Lee, R.Y., Zhu, Y., Skaar, T.C., Gomez, B., O'Brien, K., Wang, Y. and Hilakivi-Clarke, L.A., 2003. Antiestrogen resistance in breast cancer and the role of estrogen receptor signaling. *Oncogene*, *22*(47), pp.7316-7339.

Comşa, Ş., Cimpean, A.M. and Raica, M., 2015. The story of MCF-7 breast cancer cell line: 40 years of experience in research. *Anticancer research*, *35*(6), pp.3147-3154.

Cross, D.A., Alessi, D.R., Cohen, P., Andjelkovich, M. and Hemmings, B.A., 1995. Inhibition of glycogen synthase kinase-3 by insulin mediated by protein kinase B. *Nature*, *378*(6559), pp.785-789.

Croston, G.E., Cao, Z. and Goeddel, D.V., 1995. NF-κB activation by interleukin-1 (IL-1) requires an IL-1 receptor-associated protein kinase activity. *Journal of Biological Chemistry*, *270*(28), pp.16514-16517.

Cui, J., Germer, K., Wu, T., Wang, J., Luo, J., Wang, S.C., Wang, Q. and Zhang, X., 2012. Cross-talk between HER2 and MED1 regulates tamoxifen resistance of human breast cancer cells. *Cancer research*, *72*(21), pp.5625-5634.

Curigliano, G., Burstein, H.J., Winer, E.P., Gnant, M., Dubsky, P., Loibl, S., Colleoni, M., Regan, M.M., Piccart-Gebhart, M., Senn, H.J. and Thürlimann, B., 2017. De-escalating and escalating treatments for early-stage breast cancer: the St. Gallen International Expert Consensus Conference on the Primary Therapy of Early Breast Cancer 2017. *Annals of Oncology*, *28*(8), pp.1700-1712.

Das, P.M., Thor, A.D., Edgerton, S.M., Barry, S.K., Chen, D.F. and Jones, F.E., 2010. Reactivation of epigenetically silenced HER4/ERBB4 results in apoptosis of breast tumor cells. *Oncogene*, *29*(37), pp.5214-5219.

Datta, S.R., Dudek, H., Tao, X., Masters, S., Fu, H., Gotoh, Y. and Greenberg, M.E., 1997. Akt phosphorylation of BAD couples survival signals to the cell-intrinsic death machinery. *Cell*, *91*(2), pp.231-241.

Dauch, D., Rudalska, R., Cossa, G., Nault, J.C., Kang, T.W., Wuestefeld, T., Hohmeyer, A., Imbeaud, S., Yevsa, T., Hoenicke, L. and Pantsar, T., 2016. A MYC–aurora kinase A protein complex represents an actionable drug target in p53-altered liver cancer. *Nature medicine*, *22*(7), pp.744-753.

Davis, R.E., Brown, K.D., Siebenlist, U. and Staudt, L.M., 2001. Constitutive nuclear factor κB activity is required for survival of activated B cell–like diffuse large B cell lymphoma cells. *The Journal of experimental medicine*, *194*(12), pp.1861-1874.

Deng, Y., Ren, X., Yang, L., Lin, Y. and Wu, X., 2003. A JNK-dependent pathway is required for TNFα-induced apoptosis. *Cell*, *115*(1), pp.61-70.

Dhamad, A.E., Zhou, Z., Zhou, J. and Du, Y., 2016. Systematic proteomic identification of the heat shock proteins (Hsp) that interact with estrogen receptor alpha (ERα) and biochemical characterization of the ERα-Hsp70 interaction. *PLoS One*, *11*(8), p.e0160312.

Dhanasekaran, D.N. and Reddy, E.P., 2008. JNK signaling in apoptosis. *Oncogene*, *27*(48), pp.6245-6251.

Dickler, M.N., Cobleigh, M.A., Miller, K.D., Klein, P.M. and Winer, E.P., 2009. Efficacy and safety of erlotinib in patients with locally advanced or metastatic breast cancer. *Breast cancer research and treatment*, *115*(1), pp.115-121.

Ding, L., Yan, J., Zhu, J., Zhong, H., Lu, Q., Wang, Z., Huang, C. and Ye, Q., 2003. Ligand-independent activation of estrogen receptor α by XBP-1. *Nucleic acids research*, *31*(18), pp.5266-5274.

Do, T.V., Xiao, F., Bickel, L.E., Klein-Szanto, A.J., Pathak, H.B., Hua, X., Howe, C., O'brien, S.W., Maglaty, M., Ecsedy, J.A. and Litwin, S., 2014. Aurora kinase A mediates epithelial ovarian cancer cell migration and adhesion. *Oncogene*, *33*(5), pp.539-549.

Drabovich, A.P., Pavlou, M.P., Schiza, C. and Diamandis, E.P., 2016. Dynamics of protein expression reveals primary targets and secondary messengers of estrogen receptor alpha signaling in MCF-7 breast cancer cells. *Molecular & Cellular Proteomics*, *15*(6), pp.2093-2107.

Dussiau, C., Trinquand, A., Lhermitte, L., Latiri, M., Simonin, M., Cieslak, A., Bedjaoui, N., Villarèse, P., Verhoeyen, E., Dombret, H. and Ifrah, N., 2015. Targeting IRAK1 in T-cell acute lymphoblastic leukemia. *Oncotarget*, *6*(22), p.18956.

Dutertre, M. and Smith, C.L., 2003. Ligand-independent interactions of p160/steroid receptor coactivators and CREB-binding protein (CBP) with estrogen receptor-α: regulation by phosphorylation sites in the A/B region depends on other receptor domains. *Molecular endocrinology*, *17*(7), pp.1296-1314.

Dutertre, S., Cazales, M., Quaranta, M., Froment, C., Trabut, V., Dozier, C., Mirey, G., Bouché, J.P., Theis-Febvre, N., Schmitt, E. and Monsarrat, B., 2004. Phosphorylation of CDC25B by Aurora-A at the centrosome contributes to the G2–M transition. *Journal of cell science*, *117*(12), pp.2523-2531.

Ebelt, N.D., Kaoud, T.S., Edupuganti, R., Van Ravenstein, S., Dalby, K.N. and Van Den Berg, C.L., 2017. A c-Jun N-terminal kinase inhibitor, JNK-IN-8, sensitizes triple negative breast cancer cells to lapatinib. *Oncotarget*, *8*(62), p.104894.

Fagan, D.H. and Yee, D., 2008. Crosstalk between IGF1R and estrogen receptor signaling in breast cancer. *Journal of mammary gland biology and neoplasia*, *13*(4), p.423.

Feng, W., Webb, P., Nguyen, P., Liu, X., Li, J., Karin, M. and Kushner, P.J., 2001. Potentiation of estrogen receptor activation function 1 (AF-1) by Src/JNK through a serine 118-independent pathway. *Molecular Endocrinology*, *15*(1), pp.32-45.

Filardo, E.J., Quinn, J.A., Bland, K.I. and Frackelton Jr, A.R., 2000. Estrogen-induced activation of Erk-1 and Erk-2 requires the G protein-coupled receptor homolog, GPR30, and occurs via trans-activation of the epidermal growth factor receptor through release of HB-EGF. *Molecular endocrinology*, *14*(10), pp.1649-1660.

Finn, R.S., Martin, M., Rugo, H.S., Jones, S., Im, S.A., Gelmon, K., Harbeck, N., Lipatov, O.N., Walshe, J.M., Moulder, S. and Gauthier, E., 2016. Palbociclib and letrozole in advanced breast cancer. *New England Journal of Medicine*, *375*(20), pp.1925-1936.

Flannery, S. and Bowie, A.G., 2010. The interleukin-1 receptor-associated kinases: critical regulators of innate immune signalling. *Biochemical pharmacology*, *80*(12), pp.1981-1991.

FLEMING, Y., ARMSTRONG, C.G., MORRICE, N., PATERSON, A., GOEDERT, M. and COHEN, P., 2000. Synergistic activation of stress-activated protein kinase 1/c-Jun N-

terminal kinase (SAPK1/JNK) isoforms by mitogen-activated protein kinase kinase 4 (MKK4) and MKK7. *Biochemical Journal*, *352*(1), pp.145-154.

Foley, J., Nickerson, N.K., Nam, S., Allen, K.T., Gilmore, J.L., Nephew, K.P. and Riese II, D.J., 2010, December. EGFR signaling in breast cancer: bad to the bone. In *Seminars in cell & developmental biology* (Vol. 21, No. 9, pp. 951-960). Academic Press.

Fuchs, S.Y., Dolan, L., Davis, R.J. and Ronai, Z.E., 1996. Phosphorylation-dependent targeting of c-Jun ubiquitination by Jun N-kinase. *Oncogene*, *13*(7), p.1531.

Fuentes, N. and Silveyra, P., 2019. Estrogen receptor signaling mechanisms. In *Advances in protein chemistry and structural biology* (Vol. 116, pp. 135-170). Academic Press.

Garcia-Echeverria, C. and Sellers, W.R., 2008. Drug discovery approaches targeting the PI3K/Akt pathway in cancer. *Oncogene*, *27*(41), pp.5511-5526.

Gassmann, M., Casagranda, F., Orioli, D., Simon, H., Lai, C., Klein, R. and Lemke, G., 1995. Aberrant neural and cardiac development in mice lacking the ErbB4 neuregulin receptor. *Nature*, *378*(6555), pp.390-394.

Ghosh, M.G., Thompson, D.A. and Weigel, R.J., 2000. PDZK1 and GREB1 are estrogen-regulated genes expressed in hormone-responsive breast cancer1, 2. *Cancer research*, *60*(22), pp.6367-6375.

Goh, J.Y., Feng, M., Wang, W., Oguz, G., Yatim, S.M.J., Lee, P.L., Bao, Y., Lim, T.H., Wang, P., Tam, W.L. and Kodahl, A.R., 2017. Chromosome 1q21. 3 amplification is a trackable biomarker and actionable target for breast cancer recurrence. *Nature medicine*, *23*(11), p.1319.

Goldhirsch, A., Winer, E.P., Coates, A.S., Gelber, R.D., Piccart-Gebhart, M., Thürlimann, B., Senn, H.J., Albain, K.S., André, F., Bergh, J. and Bonnefoi, H., 2013. Personalizing the treatment of women with early breast cancer: highlights of the St Gallen International Expert Consensus on the Primary Therapy of Early Breast Cancer 2013. *Annals of oncology*, *24*(9), pp.2206-2223.

Göthlin Eremo, A., Tina, E., Wegman, P., Stål, O., Fransén, K., Fornander, T. and Wingren, S., 2015. HER4 tumor expression in breast cancer patients randomized to treatment with or without tamoxifen. *International journal of oncology*, *47*(4), pp.1311-1320.

Gottipati, S., Rao, N.L. and Fung-Leung, W.P., 2008. IRAK1: a critical signaling mediator of innate immunity. *Cellular signalling*, *20*(2), pp.269-276.

Green, A.R., Barros, F.F., Abdel-Fatah, T.M., Moseley, P., Nolan, C.C., Durham, A.C., Rakha, E.A., Chan, S. and Ellis, I.O., 2014. HER2/HER3 heterodimers and p21 expression are capable of predicting adjuvant trastuzumab response in HER2+ breast cancer. *Breast cancer research and treatment*, *145*(1), pp.33-44.

Greger, J.G., Fursov, N., Cooch, N., McLarney, S., Freedman, L.P., Edwards, D.P. and Cheskis, B.J., 2007. Phosphorylation of MNAR promotes estrogen activation of phosphatidylinositol 3-kinase. *Molecular and cellular biology*, *27*(5), pp.1904-1913.

Gritsko, T.M., Coppola, D., Paciga, J.E., Yang, L., Sun, M., Shelley, S.A., Fiorica, J.V., Nicosia, S.V. and Cheng, J.Q., 2003. Activation and overexpression of centrosome kinase BTAK/Aurora-A in human ovarian cancer. *Clinical cancer research*, *9*(4), pp.1420-1426.

Gu, Q. and Moss, R.L., 1996. 17β-Estradiol potentiates kainate-induced currents via activation of the cAMP cascade. *Journal of Neuroscience*, *16*(11), pp.3620-3629.

Guler, G., Iliopoulos, D., Guler, N., Himmetoglu, C., Hayran, M. and Huebner, K., 2007. Wwox and Ap2γ expression levels predict tamoxifen response. *Clinical cancer research*, *13*(20), pp.6115-6121.

Guo JP, Shu SK, Esposito NN, Coppola D, Koomen JM, Cheng JQ. IKKepsilon phosphorylation of estrogen receptor alpha Ser-167 and contribution to tamoxifen resistance in breast cancer. J Biol Chem. 2010 Feb 5;285(6):3676-84. doi: 10.1074/jbc.M109.078212. Epub 2009 Nov 23. Retraction in: J Biol Chem. 2016 Oct 21;291(43):22857. PMID: 19940156; PMCID: PMC2823508.

Gupta, S., Barrett, T., Whitmarsh, A.J., Cavanagh, J., Sluss, H.K., Derijard, B. and Davis, R.J., 1996. Selective interaction of JNK protein kinase isoforms with transcription factors. *The EMBO journal*, *15*(11), pp.2760-2770.

Gupta, S., Hussain, T., MacLennan, G.T., Fu, P., Patel, J. and Mukhtar, H., 2003. Differential expression of S100A2 and S100A4 during progression of human prostate adenocarcinoma. *Journal of Clinical Oncology*, *21*(1), pp.106-112.

Gutierrez, M.C., Detre, S., Johnston, S., Mohsin, S.K., Shou, J., Allred, D.C., Schiff, R., Osborne, C.K. and Dowsett, M., 2005. Molecular changes in tamoxifen-resistant breast cancer: relationship between estrogen receptor, HER-2, and p38 mitogen-activated protein kinase. *Journal of clinical oncology*, *23*(11), pp.2469-2476.

Györffy, B., Lanczky, A., Eklund, A.C., Denkert, C., Budczies, J., Li, Q. and Szallasi, Z., 2010. An online survival analysis tool to rapidly assess the effect of 22,277 genes on breast cancer prognosis using microarray data of 1,809 patients. *Breast cancer research and treatment*, *123*(3), pp.725-731.

Hadžisejdić, I., Mustać, E., Jonjić, N., Petković, M. and Grahovac, B., 2010. Nuclear EGFR in ductal invasive breast cancer: correlation with cyclin-D1 and prognosis. *Modern pathology*, *23*(3), pp.392-403.

Han, W. and Jones, F.E., 2014. HER4 selectively coregulates estrogen stimulated genes associated with breast tumor cell proliferation. *Biochemical and biophysical research communications*, *443*(2), pp.458-463.

Herynk, M.H. and Fuqua, S.A., 2004. Estrogen receptor mutations in human disease. *Endocrine reviews*, *25*(6), pp.869-898.

Hoesel, B. and Schmid, J.A., 2013. The complexity of NF-κB signaling in inflammation and cancer. *Molecular cancer*, *12*(1), pp.1-15.

Hoskins, J.M., Carey, L.A. and McLeod, H.L., 2009. CYP2D6 and tamoxifen: DNA matters in breast cancer. *Nature Reviews Cancer*, *9*(8), pp.576-586.

Howell, A., Cuzick, J., Baum, M., Buzdar, A., Dowsett, M., Forbes, J.F., Hoctin-Boes, G., Houghton, J., Locker, G.Y. and Tobias, J.S., 2005. Results of the ATAC (Arimidex, Tamoxifen, Alone or in Combination) trial after completion of 5 years' adjuvant treatment for breast cancer. *Lancet*, *365*(9453), pp.60-62.

Howell, A., Robertson, J.F., Quaresma Albano, J., Aschermannova, A., Mauriac, L., Kleeberg, U.R., Vergote, I., Erikstein, B., Webster, A. and Morris, C., 2002. Fulvestrant, formerly ICI 182,780, is as effective as anastrozole in postmenopausal women with advanced breast cancer progressing after prior endocrine treatment. *Journal of Clinical Oncology*, *20*(16), pp.3396-3403.

Hui, L., Zatloukal, K., Scheuch, H., Stepniak, E. and Wagner, E.F., 2008. Proliferation of human HCC cells and chemically induced mouse liver cancers requires JNK1-dependent p21 downregulation. *The Journal of clinical investigation*, *118*(12), pp.3943-3953.

Hurtado, A., Holmes, K.A., Ross-Innes, C.S., Schmidt, D. and Carroll, J.S., 2011. FOXA1 is a key determinant of estrogen receptor function and endocrine response. *Nature genetics*, *43*(1), pp.27-33.

Hutcheson, I.R., Knowlden, J.M., Madden, T.A., Barrow, D., Gee, J.M., Wakeling, A.E. and Nicholson, R.I., 2003. Oestrogen receptor-mediated modulation of the EGFR/MAPK pathway in tamoxifen-resistant MCF-7 cells. *Breast cancer research and treatment*, *81*(1), pp.81-93.

Inoue, A., Omoto, Y., Yamaguchi, Y., Kiyama, R. and Hayashi, S.I., 2004. Transcription factor EGR3 is involved in the estrogen-signaling pathway in breast cancer cells. *Journal of molecular endocrinology*, *32*(3), pp.649-661.

Jain, A., Kaczanowska, S. and Davila, E., 2014. IL-1 receptor-associated kinase signaling and its role in inflammation, cancer progression, and therapy resistance. *Frontiers in immunology*, *5*, p.553.

Jiang, J., Sarwar, N., Peston, D., Kulinskaya, E., Shousha, S., Coombes, R.C. and Ali, S., 2007. Phosphorylation of estrogen receptor-α at Ser167 is indicative of longer disease-free

and overall survival in breast cancer patients. *Clinical Cancer Research*, *13*(19), pp.5769-5776.

Jing, L.I.U. and Anning, L.I.N., 2005. Role of JNK activation in apoptosis: a double-edged sword. *Cell research*, *15*(1), pp.36-42.

Jordan, C.T., Cao, L., Roberson, E.D., Duan, S., Helms, C.A., Nair, R.P., Duffin, K.C., Stuart, P.E., Goldgar, D., Hayashi, G. and Olfson, E.H., 2012. Rare and common variants in CARD14, encoding an epidermal regulator of NF-kappaB, in psoriasis. *The American Journal of Human Genetics*, *90*(5), pp.796-808.

Kaestner, P., Stolz, A. and Bastians, H., 2009. Determinants for the efficiency of anticancer drugs targeting either Aurora-A or Aurora-B kinases in human colon carcinoma cells. *Molecular cancer therapeutics*, *8*(7), pp.2046-2056.

Karin, M., Liu, Z.G. and Zandi, E., 1997. AP-1 function and regulation. *Current opinion in cell biology*, *9*(2), pp.240-246.

Katayama, H., Sasai, K., Kawai, H., Yuan, Z.M., Bondaruk, J., Suzuki, F., Fujii, S., Arlinghaus, R.B., Czerniak, B.A. and Sen, S., 2004. Phosphorylation by aurora kinase A induces Mdm2-mediated destabilization and inhibition of p53. *Nature genetics*, *36*(1), pp.55-62.

Katayama, H., Wang, J., Treekitkarnmongkol, W., Kawai, H., Sasai, K., Zhang, H., Wang, H., Adams, H.P., Jiang, S., Chakraborty, S.N. and Suzuki, F., 2012. Aurora kinase-A inactivates DNA damage-induced apoptosis and spindle assembly checkpoint response functions of p73. *Cancer cell*, *21*(2), pp.196-211.

Kato, S., Endoh, H., Masuhiro, Y., Kitamoto, T., Uchiyama, S., Sasaki, H., Masushige, S., Gotoh, Y., Nishida, E., Kawashima, H. and Metzger, D., 1995. Activation of the estrogen receptor through phosphorylation by mitogen-activated protein kinase. *Science*, *270*(5241), pp.1491-1494.

Katsha, A., Soutto, M., Sehdev, V., Peng, D., Washington, M.K., Piazuelo, M.B., Tantawy, M.N., Manning, H.C., Lu, P., Shyr, Y. and Ecsedy, J., 2013. Aurora kinase A promotes

inflammation and tumorigenesis in mice and human gastric neoplasia. *Gastroenterology*, *145*(6), pp.1312-1322.

Kawagoe, T., Sato, S., Matsushita, K., Kato, H., Matsui, K., Kumagai, Y., Saitoh, T., Kawai, T., Takeuchi, O. and Akira, S., 2008. Sequential control of Toll-like receptor–dependent responses by IRAK1 and IRAK2. *Nature immunology*, *9*(6), p.684.

Kedar, R.P., Bourne, T.H., Collins, W.P., Campbell, S., Powles, T.J., Ashley, S. and Cosgrove, D.O., 1994. Effects of tamoxifen on uterus and ovaries of postmenopausal women in a randomised breast cancer prevention trial. *The Lancet*, *343*(8909), pp.1318-1321.

Keydar, I., Chen, L., Karby, S., Weiss, F.R., Delarea, J., Radu, M., Chaitcik, S. and Brenner, H.J., 1979. Establishment and characterization of a cell line of human breast carcinoma origin. *European Journal of Cancer (1965)*, *15*(5), pp.659-670.

Kim, E.K. and Choi, E.J., 2015. Compromised MAPK signaling in human diseases: an update. *Archives of toxicology*, *89*(6), pp.867-882.

Kim, J.H., Im, K.S., Kim, N.H., Yhee, J.Y., Nho, W.G. and Sur, J.H., 2011. Expression of HER-2 and nuclear localization of HER-3 protein in canine mammary tumors: histopathological and immunohistochemical study. *The Veterinary Journal*, *189*(3), pp.318-322.

Kim, J.M., Cho, H.H., Lee, S.Y., Hong, C.P., won Yang, J., Kim, Y.S., Suh, K.T. and Jung, J.S., 2012. Role of IRAK1 on TNF-induced proliferation and NF-κB activation in human bone marrow mesenchymal stem cells. *Cellular Physiology and Biochemistry*, *30*(1), pp.49-60.

Kirkegaard, T., Witton, C.J., McGlynn, L.M., Tovey, S.M., Dunne, B., Lyon, A. and Bartlett, J.M., 2005. AKT activation predicts outcome in breast cancer patients treated with tamoxifen. *The Journal of Pathology: A Journal of the Pathological Society of Great Britain and Ireland*, *207*(2), pp.139-146.

Klingelhöfer, J., Møller, H.D., Sumer, E.U., Berg, C.H., Poulsen, M., Kiryushko, D., Soroka, V., Ambartsumian, N., Grigorian, M. and Lukanidin, E.M., 2009. Epidermal growth factor receptor ligands as new extracellular targets for the metastasis-promoting S100A4 protein. *The FEBS journal*, *276*(20), pp.5936-5948.

Knowlden, J.M., Hutcheson, I.R., Jones, H.E., Madden, T., Gee, J.M., Harper, M.E., Barrow, D., Wakeling, A.E. and Nicholson, R.I., 2003. Elevated levels of epidermal growth factor receptor/c-erbB2 heterodimers mediate an autocrine growth regulatory pathway in tamoxifen-resistant MCF-7 cells. *Endocrinology*, *144*(3), pp.1032-1044.

Kobayashi, S., Boggon, T.J., Dayaram, T., Jänne, P.A., Kocher, O., Meyerson, M., Johnson, B.E., Eck, M.J., Tenen, D.G. and Halmos, B., 2005. EGFR mutation and resistance of non–small-cell lung cancer to gefitinib. *New England Journal of Medicine*, *352*(8), pp.786-792.

Kol, A., van Scheltinga, A.G.T., Timmer-Bosscha, H., Lamberts, L.E., Bensch, F., de Vries, E.G. and Schröder, C.P., 2014. HER3, serious partner in crime: therapeutic approaches and potential biomarkers for effect of HER3-targeting. *Pharmacology & therapeutics*, *143*(1), pp.1-11.

Koong, A.C., Chauhan, V. and Romero-Ramirez, L., 2006. Targeting XBP-1 as a novel anti-cancer strategy. *Cancer biology & therapy*, *5*(7), pp.756-759.

Korobeynikov, V., Borakove, M., Feng, Y., Wuest, W.M., Koval, A.B., Nikonova, A.S., Serebriiskii, I., Chernoff, J., Borges, V.F., Golemis, E.A. and Shagisultanova, E., 2019. Combined inhibition of Aurora A and p21-activated kinase 1 as a new treatment strategy in breast cancer. *Breast cancer research and treatment*, *177*(2), pp.369-382.

Koul, H.K., Pal, M. and Koul, S., 2013. Role of p38 MAP kinase signal transduction in solid tumors. *Genes & cancer*, *4*(9-10), pp.342-359.

Koumakpayi, I.H., Diallo, J.S., Le Page, C., Lessard, L., Gleave, M., Bégin, L.R., Mes-Masson, A.M. and Saad, F., 2006. Expression and nuclear localization of ErbB3 in prostate cancer. *Clinical Cancer Research*, *12*(9), pp.2730-2737.

Kreike, B., Halfwerk, H., Armstrong, N., Bult, P., Foekens, J.A., Veltkamp, S.C., Nuyten, D.S., Bartelink, H. and van de Vijver, M.J., 2009. Local recurrence after breast-conserving therapy in relation to gene expression patterns in a large series of patients. *Clinical Cancer Research*, *15*(12), pp.4181-4190.

Kuukasjärvi, T., Kononen, J., Helin, H., Holli, K. and Isola, J., 1996. Loss of estrogen receptor in recurrent breast cancer is associated with poor response to endocrine therapy. *Journal of Clinical Oncology*, *14*(9), pp.2584-2589.

Laemmli, U.K., 1970. Cleavage of structural proteins during the assembly of the head of bacteriophage T4. *nature*, *227*(5259), pp.680-685.

Le Romancer, M., Poulard, C., Cohen, P., Sentis, S., Renoir, J.M. and Corbo, L., 2011. Cracking the estrogen receptor's posttranslational code in breast tumors. *Endocrine reviews*, *32*(5), pp.597-622.

Le Romancer, M., Treilleux, I., Leconte, N., Robin-Lespinasse, Y., Sentis, S., Bouchekioua-Bouzaghou, K., Goddard, S., Gobert-Gosse, S. and Corbo, L., 2008. Regulation of estrogen rapid signaling through arginine methylation by PRMT1. *Molecular cell*, *31*(2), pp.212-221.

Lee Y, Cho S, Seo JH, *et al*. Correlated expression of erbB-3 with hormone receptor expression and favorable clinical outcome in invasive ductal carcinomas of the breast. Am J Clin Pathol. 2007;128:1041–1049.

Lee, D., Kim, I.Y., Saha, S. and Choi, K.S., 2016. Paraptosis in the anti-cancer arsenal of natural products. *Pharmacology & therapeutics*, *162*, pp.120-133.

Lee, J.J., Loh, K. and Yap, Y.S., 2015. PI3K/Akt/mTOR inhibitors in breast cancer. *Cancer biology & medicine*, *12*(4), p.342.

Lee, K.F., Simon, H., Chen, H., Bates, B., Hung, M.C. and Hauser, C., 1995. Requirement for neuregulin receptor erbB2 in neural and cardiac development. *Nature*, *378*(6555), pp.394-398.

Lee-Hoeflich, S.T., Crocker, L., Yao, E., Pham, T., Munroe, X., Hoeflich, K.P., Sliwkowski, M.X. and Stern, H.M., 2008. A central role for HER3 in HER2-amplified breast cancer: implications for targeted therapy. *Cancer research*, *68*(14), pp.5878-5887.

Lei, K. and Davis, R.J., 2003. JNK phosphorylation of Bim-related members of the Bcl2 family induces Bax-dependent apoptosis. *Proceedings of the National Academy of Sciences*, *100*(5), pp.2432-2437.

Levine, M., Moutquin, J.M., Walton, R. and Feightner, J., 1998. Early breast cancer trialists collaborative group. Tamoxifen for early breast cancer: an overview of the randomized trials. *Lancet*, *351*, pp.1451-67.

Li, C. and Johnson, D.E., 2012. Bortezomib induces autophagy in head and neck squamous cell carcinoma cells via JNK activation. *Cancer letters*, *314*(1), pp.102-107.

Li, N., Jiang, J., Fu, J., Yu, T., Wang, B., Qin, W., Xu, A., Wu, M., Chen, Y. and Wang, H., 2016. Targeting interleukin-1 receptor-associated kinase 1 for human hepatocellular carcinoma. *Journal of Experimental & Clinical Cancer Research*, *35*(1), p.140.

Likhite, V.S., Stossi, F., Kim, K., Katzenellenbogen, B.S. and Katzenellenbogen, J.A., 2006. Kinase-specific phosphorylation of the estrogen receptor changes receptor interactions with ligand, deoxyribonucleic acid, and coregulators associated with alterations in estrogen and tamoxifen activity. *Molecular endocrinology*, *20*(12), pp.3120-3132.

Lin, C.Y., Ström, A., Vega, V.B., Kong, S.L., Yeo, A.L., Thomsen, J.S., Chan, W.C., Doray, B., Bangarusamy, D.K., Ramasamy, A. and Vergara, L.A., 2004. Discovery of estrogen receptor α target genes and response elements in breast tumor cells. *Genome biology*, *5*(9), p.R66.

Lin, S.Y., Makino, K., Xia, W., Matin, A., Wen, Y., Kwong, K.Y., Bourguignon, L. and Hung, M.C., 2001. Nuclear localization of EGF receptor and its potential new role as a transcription factor. *Nature cell biology*, *3*(9), pp.802-808.

Lipner, M.B., Peng, X.L., Jin, C., Xu, Y., Gao, Y., East, M.P., Rashid, N.U., Moffitt, R.A., Loeza, S.G.H., Morrison, A.B. and Golitz, B.T., 2020. Irreversible JNK1-JUN inhibition by JNK-IN-8 sensitizes pancreatic cancer to 5-FU/FOLFOX chemotherapy. *JCI insight*, *5*(8).

Liu, B., Ordonez-Ercan, D., Fan, Z., Edgerton, S.M., Yang, X. and Thor, A.D., 2007. Downregulation of erbB3 abrogates erbB2-mediated tamoxifen resistance in breast cancer cells. *International journal of cancer*, *120*(9), pp.1874-1882.

Liu, F., Hon, G.C., Villa, G.R., Turner, K.M., Ikegami, S., Yang, H., Ye, Z., Li, B., Kuan, S., Lee, A.Y. and Zanca, C., 2015. EGFR mutation promotes glioblastoma through epigenome and transcription factor network remodeling. *Molecular cell*, *60*(2), pp.307-318.

Liu, P.H., Shah, R.B., Li, Y., Arora, A., Ung, P.M.U., Raman, R., Gorbatenko, A., Kozono, S., Zhou, X.Z., Brechin, V. and Barbaro, J.M., 2019. An IRAK1–PIN1 signalling axis drives intrinsic tumour resistance to radiation therapy. *Nature cell biology*, *21*(2), pp.203-213.

Lo, H.W., Hsu, S.C., Ali-Seyed, M., Gunduz, M., Xia, W., Wei, Y., Bartholomeusz, G., Shih, J.Y. and Hung, M.C., 2005. Nuclear interaction of EGFR and STAT3 in the activation of the iNOS/NO pathway. *Cancer cell*, *7*(6), pp.575-589.

Lodge, A.J., Anderson, J.J., Gullick, W.J., Haugk, B., Leonard, R.C.F. and Angus, B., 2003. Type 1 growth factor receptor expression in node positive breast cancer: adverse prognostic significance of c-erbB-4. *Journal of clinical pathology*, *56*(4), pp.300-304.

Loibl, S. and Gianni, L., 2017. HER2-positive breast cancer. *The Lancet*, *389*(10087), pp.2415-2429.

Madden, S.F., Clarke, C., Gaule, P., Aherne, S.T., O'Donovan, N., Clynes, M., Crown, J. and Gallagher, W.M., 2013. BreastMark: an integrated approach to mining publicly available transcriptomic datasets relating to breast cancer outcome. *Breast cancer research*, *15*(4), p.R52.

Manning, B.D. and Cantley, L.C., 2007. AKT/PKB signaling: navigating downstream. *Cell*, *129*(7), pp.1261-1274.

Marino, M., Pallottini, V. and Trentalance, A., 1998. Estrogens cause rapid activation of IP3-PKC-α signal transduction pathway in HEPG2 cells. *Biochemical and biophysical research communications*, *245*(1), pp.254-258.

Mascarenhas, J., Hoffman, R., Talpaz, M., Gerds, A.T., Stein, B., Gupta, V., Szoke, A., Drummond, M., Pristupa, A., Granston, T. and Daly, R., 2018. Pacritinib vs best available therapy, including ruxolitinib, in patients with myelofibrosis: a randomized clinical trial. *JAMA oncology*, *4*(5), pp.652-659.

Massarweh, S., Osborne, C.K., Creighton, C.J., Qin, L., Tsimelzon, A., Huang, S., Weiss, H., Rimawi, M. and Schiff, R., 2008. Tamoxifen resistance in breast tumors is driven by growth factor receptor signaling with repression of classic estrogen receptor genomic function. *Cancer research*, *68*(3), pp.826-833.

Matsuzaki, H., Daitoku, H., Hatta, M., Tanaka, K. and Fukamizu, A., 2003. Insulin-induced phosphorylation of FKHR (Foxo1) targets to proteasomal degradation. *Proceedings of the National Academy of Sciences*, *100*(20), pp.11285-11290.

Mayer, I.A. and Arteaga, C.L., 2016. The PI3K/AKT pathway as a target for cancer treatment. *Annual review of medicine*, *67*, pp.11-28.

Mazieres, J., Peters, S., Lepage, B., Cortot, A.B., Barlesi, F., Beau-Faller, M., Besse, B., Blons, H., Mansuet-Lupo, A., Urban, T. and Moro-Sibilot, D., 2013. Lung cancer that harbors an HER2 mutation: epidemiologic characteristics and therapeutic perspectives. *Journal of clinical oncology*, *31*(16), pp.1997-2003.

Medunjanin, S., Hermani, A., De Servi, B., Grisouard, J., Rincke, G. and Mayer, D., 2005. Glycogen synthase kinase-3 interacts with and phosphorylates estrogen receptor α and is involved in the regulation of receptor activity. *Journal of Biological Chemistry*, *280*(38), pp.33006-33014.

Mesa, R.A., Vannucchi, A.M., Mead, A., Egyed, M., Szoke, A., Suvorov, A., Jakucs, J., Perkins, A., Prasad, R., Mayer, J. and Demeter, J., 2017. Pacritinib versus best available therapy for the treatment of myelofibrosis irrespective of baseline cytopenias (PERSIST-1): an international, randomised, phase 3 trial. *The Lancet Haematology*, *4*(5), pp.e225-e236.

Michalides, R., Griekspoor, A., Balkenende, A., Verwoerd, D., Janssen, L., Jalink, K., Floore, A., Velds, A., vant Veer, L. and Neefjes, J., 2004. Tamoxifen resistance by a conformational arrest of the estrogen receptor α after PKA activation in breast cancer. *Cancer cell*, *5*(6), pp.597-605.

Miettinen, P.J., Berger, J.E., Meneses, J., Phung, Y., Pedersen, R.A., Werb, Z. and Derynck, R., 1995. Epithelial immaturity and multiorgan failure in mice lacking epidermal growth factor receptor. *Nature*, *376*(6538), pp.337-341.

Miller, T.W., Pérez-Torres, M., Narasanna, A., Guix, M., Stål, O., Pérez-Tenorio, G., Gonzalez-Angulo, A.M., Hennessy, B.T., Mills, G.B., Kennedy, J.P. and Lindsley, C.W., 2009. Loss of Phosphatase and Tensin homologue deleted on chromosome 10 engages ErbB3 and insulin-like growth factor-I receptor signaling to promote antiestrogen resistance in breast cancer. *Cancer research*, *69*(10), pp.4192-4201.

Mitra, S., Lee, J.S., Cantrell, M. and Van Den Berg, C.L., 2011. c-Jun N-terminal kinase 2 (JNK2) enhances cell migration through epidermal growth factor substrate 8 (EPS8). *Journal of Biological Chemistry*, *286*(17), pp.15287-15297.

Modi, S., Stopeck, A., Linden, H., Solit, D., Chandarlapaty, S., Rosen, N., D'Andrea, G., Dickler, M., Moynahan, M.E., Sugarman, S. and Ma, W., 2011. HSP90 inhibition is effective in breast cancer: a phase II trial of tanespimycin (17-AAG) plus trastuzumab in patients with HER2-positive metastatic breast cancer progressing on trastuzumab. *Clinical Cancer Research*, *17*(15), pp.5132-5139.

Mohammed, H., D'Santos, C., Serandour, A.A., Ali, H.R., Brown, G.D., Atkins, A., Rueda, O.M., Holmes, K.A., Theodorou, V., Robinson, J.L. and Zwart, W., 2013. Endogenous purification reveals GREB1 as a key estrogen receptor regulatory factor. *Cell reports*, *3*(2), pp.342-349.

Morrison, M.M., Hutchinson, K., Williams, M.M., Stanford, J.C., Balko, J.M., Young, C., Kuba, M.G., Sánchez, V., Williams, A.J., Hicks, D.J. and Arteaga, C.L., 2013. ErbB3 downregulation enhances luminal breast tumor response to antiestrogens. *The Journal of clinical investigation*, *123*(10), pp.4329-4343.

Movérare-Skrtic, S., Börjesson, A.E., Farman, H.H., Sjögren, K., Windahl, S.H., Lagerquist, M.K., Andersson, A., Stubelius, A., Carlsten, H., Gustafsson, J.Å. and Ohlsson, C., 2014. The estrogen receptor antagonist ICI 182,780 can act both as an agonist and an inverse agonist when estrogen receptor α AF-2 is modified. *Proceedings of the National Academy of Sciences*, *111*(3), pp.1180-1185.

Muraoka-Cook, R.S., Caskey, L.S., Sandahl, M.A., Hunter, D.M., Husted, C., Strunk, K.E., Sartor, C.I., Rearick, W.A., McCall, W., Sgagias, M.K. and Cowan, K.H., 2006. Heregulin-dependent delay in mitotic progression requires HER4 and BRCA1. *Molecular and cellular biology*, *26*(17), pp.6412-6424.

Murphy, L.C., Niu, Y., Snell, L. and Watson, P., 2004. Phospho-serine-118 estrogen receptor-α expression is associated with better disease outcome in women treated with tamoxifen. *Clinical Cancer Research*, *10*(17), pp.5902-5906.

Musgrove, E.A. and Sutherland, R.L., 2009. Biological determinants of endocrine resistance in breast cancer. *Nature Reviews Cancer*, *9*(9), pp.631-643.

Muss, H.B., Tu, D., Ingle, J.N., Martino, S., Robert, N.J., Pater, J.L., Whelan, T.J., Palmer, M.J., Piccart, M.J., Shepherd, L.E. and Pritchard, K.I., 2008. Efficacy, toxicity, and quality of life in older women with early-stage breast cancer treated with letrozole or placebo after 5 years of tamoxifen: NCIC CTG intergroup trial MA. 17. *Journal of clinical oncology*, *26*(12), pp.1956-1964.

Nafi, S.N.M., Generali, D., Kramer-Marek, G., Gijsen, M., Strina, C., Cappelletti, M., Andreis, D., Haider, S., Li, J.L., Bridges, E. and Capala, J., 2014. Nuclear HER4 mediates acquired resistance to trastuzumab and is associated with poor outcome in HER2 positive breast cancer. *Oncotarget*, *5*(15), p.5934.

Nair, R., Roden, D.L., Teo, W.S., McFarland, A., Junankar, S., Ye, S., Nguyen, A., Yang, J., Nikolic, I., Hui, M. and Morey, A., 2014. c-Myc and Her2 cooperate to drive a stem-like phenotype with poor prognosis in breast cancer. *Oncogene*, *33*(30), pp.3992-4002.

Nakai, K., Hung, M.C. and Yamaguchi, H., 2016. A perspective on anti-EGFR therapies targeting triple-negative breast cancer. *American journal of cancer research*, *6*(8), p.1609.

Naresh, A., Long, W., Vidal, G.A., Wimley, W.C., Marrero, L., Sartor, C.I., Tovey, S., Cooke, T.G., Bartlett, J.M. and Jones, F.E., 2006. The ERBB4/HER4 intracellular domain 4ICD is a BH3-only protein promoting apoptosis of breast cancer cells. *Cancer research*, *66*(12), pp.6412-6420.

Nasrazadani, A. and Van Den Berg, C.L., 2011. c-Jun N-terminal kinase 2 regulates multiple receptor tyrosine kinase pathways in mouse mammary tumor growth and metastasis. *Genes & cancer*, *2*(1), pp.31-45.

Ngo, V.N., Young, R.M., Schmitz, R., Jhavar, S., Xiao, W., Lim, K.H., Kohlhammer, H., Xu, W., Yang, Y., Zhao, H. and Shaffer, A.L., 2011. Oncogenically active MYD88 mutations in human lymphoma. *Nature*, *470*(7332), pp.115-119.

Ni, C.Y., Murphy, M.P., Golde, T.E. and Carpenter, G., 2001. γ-Secretase cleavage and nuclear localization of ErbB-4 receptor tyrosine kinase. *Science*, *294*(5549), pp.2179-2181.

Ni, H., Shirazi, F., Baladandayuthapani, V., Lin, H., Kuiatse, I., Wang, H., Jones, R.J., Berkova, Z., Hitoshi, Y., Ansell, S.M. and Treon, S.P., 2018. Targeting myddosome signaling in Waldenström's macroglobulinemia with the interleukin-1 receptor-associated kinase 1/4 inhibitor R191. *Clinical Cancer Research*, *24*(24), pp.6408-6420.

Okada, M., Kuramoto, K., Takeda, H., Watarai, H., Sakaki, H., Seino, S., Seino, M., Suzuki, S. and Kitanaka, C., 2016. The novel JNK inhibitor AS602801 inhibits cancer stem cells in vitro and in vivo. *Oncotarget*, *7*(19), p.27021.

O'leary, B., Finn, R.S. and Turner, N.C., 2016. Treating cancer with selective CDK4/6 inhibitors. *Nature reviews Clinical oncology*, *13*(7), pp.417-430.

Onate, S.A., Tsai, S.Y., Tsai, M.J. and O'Malley, B.W., 1995. Sequence and characterization of a coactivator for the steroid hormone receptor superfamily. *Science*, *270*(5240), pp.1354-1357.

Osborne, C.K. and Schiff, R., 2011. Mechanisms of endocrine resistance in breast cancer. *Annual review of medicine*, *62*, pp.233-247.

Osborne, C.K., Bardou, V., Hopp, T.A., Chamness, G.C., Hilsenbeck, S.G., Fuqua, S.A., Wong, J., Allred, D.C., Clark, G.M. and Schiff, R., 2003. Role of the estrogen receptor coactivator AIB1 (SRC-3) and HER-2/neu in tamoxifen resistance in breast cancer. *Journal of the National Cancer Institute*, *95*(5), pp.353-361.

Osborne, C.K., Shou, J., Massarweh, S. and Schiff, R., 2005. Crosstalk between estrogen receptor and growth factor receptor pathways as a cause for endocrine therapy resistance in breast cancer. *Clinical cancer research*, *11*(2), pp.865s-870s.

Osborne, C.K., Wakeling, A. and Nicholson, R.I., 2004. Fulvestrant: an oestrogen receptor antagonist with a novel mechanism of action. *British journal of cancer*, *90*(1), pp.S2-S6.

Otto, T., Horn, S., Brockmann, M., Eilers, U., Schüttrumpf, L., Popov, N., Kenney, A.M., Schulte, J.H., Beijersbergen, R., Christiansen, H. and Berwanger, B., 2009. Stabilization of N-Myc is a critical function of Aurora A in human neuroblastoma. *Cancer cell*, *15*(1), pp.67-78.

Pahl, H.L., 1999. Activators and target genes of Rel/NF-κB transcription factors. *Oncogene*, *18*(49), pp.6853-6866.

Park, K.J., Krishnan, V., O'Malley, B.W., Yamamoto, Y. and Gaynor, R.B., 2005. Formation of an IKKα-dependent transcription complex is required for estrogen receptor-mediated gene activation. *Molecular cell*, *18*(1), pp.71-82.

Paruchuri, V., Prasad, A., McHugh, K., Bhat, H.K., Polyak, K. and Ganju, R.K., 2008. S100A7-downregulation inhibits epidermal growth factor-induced signaling in breast cancer cells and blocks osteoclast formation. *PloS one*, *3*(3), p.e1741.

Pawlowski, V., Révillion, F., Hebbar, M., Hornez, L. and Peyrat, J.P., 2000. Prognostic value of the type I growth factor receptors in a large series of human primary breast cancers quantified with a real-time reverse transcription-polymerase chain reaction assay. *Clinical cancer research*, *6*(11), pp.4217-4225.

Perou, C.M., Sørlie, T., Eisen, M.B., Van De Rijn, M., Jeffrey, S.S., Rees, C.A., Pollack, J.R., Ross, D.T., Johnsen, H., Akslen, L.A. and Fluge, Ø., 2000. Molecular portraits of human breast tumours. *nature*, *406*(6797), pp.747-752.

Philips, A., Chalbos, D. and Rochefort, H., 1993. Estradiol increases and anti-estrogens antagonize the growth factor-induced activator protein-1 activity in MCF7 breast cancer cells without affecting c-fos and c-jun synthesis. *Journal of Biological Chemistry*, *268*(19), pp.14103-14108.

Planas-Silva, M.D., Shang, Y., Donaher, J.L., Brown, M. and Weinberg, R.A., 2001. AIB1 enhances estrogen-dependent induction of cyclin D1 expression. *Cancer research*, *61*(10), pp.3858-3862.

Prest, S.J., May, F.E. and Westley, B.R., 2002. The estrogen-regulated protein, TFF1, stimulates migration of human breast cancer cells. *The FASEB Journal*, *16*(6), pp.592-594.

Pulvino, M., Liang, Y., Oleksyn, D., DeRan, M., Van Pelt, E., Shapiro, J., Sanz, I., Chen, L. and Zhao, J., 2012. Inhibition of proliferation and survival of diffuse large B-cell lymphoma cells by a small-molecule inhibitor of the ubiquitin-conjugating enzyme Ubc13-Uev1A. *Blood, The Journal of the American Society of Hematology*, *120*(8), pp.1668-1677.

Raman, M., Chen, W. and Cobb, M.H., 2007. Differential regulation and properties of MAPKs. *Oncogene*, *26*(22), pp.3100-3112.

Renoir, J.M., Marsaud, V. and Lazennec, G., 2013. Estrogen receptor signaling as a target for novel breast cancer therapeutics. *Biochemical pharmacology*, *85*(4), pp.449-465.

Rexer, B.N. and Arteaga, C.L., 2012. Intrinsic and acquired resistance to HER2-targeted therapies in HER2 gene-amplified breast cancer: mechanisms and clinical implications. *Critical Reviews™ in Oncogenesis*, *17*(1).

Rhyasen, G.W., Bolanos, L., Fang, J., Jerez, A., Wunderlich, M., Rigolino, C., Mathews, L., Ferrer, M., Southall, N., Guha, R. and Keller, J., 2013. Targeting IRAK1 as a therapeutic approach for myelodysplastic syndrome. *Cancer cell*, *24*(1), pp.90-104.

Riethmacher, D., Sonnenberg-Riethmacher, E., Brinkmann, V., Yamaai, T., Lewin, G.R. and Birchmeier, C., 1997. Severe neuropathies in mice with targeted mutations in the ErbB3 receptor. *Nature*, *389*(6652), pp.725-730.

Rincón, M. and Davis, R.J., 2009. Regulation of the immune response by stress-activated protein kinases. *Immunological reviews*, *228*(1), pp.212-224.

Ring, A. and Dowsett, M., 2004. Mechanisms of tamoxifen resistance. *Endocrine-related cancer*, *11*(4), pp.643-658.

Robertson, J.F., Bondarenko, I.M., Trishkina, E., Dvorkin, M., Panasci, L., Manikhas, A., Shparyk, Y., Cardona-Huerta, S., Cheung, K.L., Philco-Salas, M.J. and Ruiz-Borrego, M., 2016. Fulvestrant 500 mg versus anastrozole 1 mg for hormone receptor-positive advanced breast cancer (FALCON): an international, randomised, double-blind, phase 3 trial. *The Lancet*, *388*(10063), pp.2997-3005.

Robertson, J.F., Llombart-Cussac, A., Rolski, J., Feltl, D., Dewar, J., Macpherson, E., Lindemann, J. and Ellis, M.J., 2009. Activity of fulvestrant 500 mg versus anastrozole 1 mg as first-line treatment for advanced breast cancer: results from the FIRST study. *Journal of Clinical Oncology*, *27*(27), pp.4530-4535.

Robertson, J.F., Osborne, C.K., Howell, A., Jones, S.E., Mauriac, L., Ellis, M., Kleeberg, U.R., Come, S.E., Vergote, I., Gertler, S. and Buzdar, A., 2003. Fulvestrant versus anastrozole for the treatment of advanced breast carcinoma in postmenopausal women: a prospective combined analysis of two multicenter trials. *Cancer*, *98*(2), pp.229-238.

Rokicki, J., Das, P.M., Giltnane, J.M., Wansbury, O., Rimm, D.L., Howard, B.A. and Jones, F.E., 2010. The ERα coactivator, HER4/4ICD, regulates progesterone receptor expression in normal and malignant breast epithelium. *Molecular cancer*, *9*(1), p.150.

Roskoski Jr, R., 2010. RAF protein-serine/threonine kinases: structure and regulation. *Biochemical and biophysical research communications*, *399*(3), pp.313-317.

Roskoski Jr, R., 2012. ERK1/2 MAP kinases: structure, function, and regulation. *Pharmacological research*, *66*(2), pp.105-143.

Roskoski Jr, R., 2014. The ErbB/HER family of protein-tyrosine kinases and cancer. *Pharmacological research*, *79*, pp.34-74.

Ross-Innes, C.S., Stark, R., Teschendorff, A.E., Holmes, K.A., Ali, H.R., Dunning, M.J., Brown, G.D., Gojis, O., Ellis, I.O., Green, A.R. and Ali, S., 2012. Differential oestrogen receptor binding is associated with clinical outcome in breast cancer. *Nature*, *481*(7381), pp.389-393.

Russo, R.C., Beguelin, W., Flaqué, M.D., Proietti, C.J., Venturutti, L., Galigniana, N., Tkach, M., Guzmán, P., Roa, J.C., O'brien, N.A. and Charreau, E.H., 2015. Targeting ErbB-2 nuclear localization and function inhibits breast cancer growth and overcomes trastuzumab resistance. *Oncogene*, *34*(26), pp.3413-3428.

Sabapathy, K., Hochedlinger, K., Nam, S.Y., Bauer, A., Karin, M. and Wagner, E.F., 2004. Distinct roles for JNK1 and JNK2 in regulating JNK activity and c-Jun-dependent cell proliferation. *Molecular cell*, *15*(5), pp.713-725.

Safe, S., 2001. Transcriptional activation of genes by 17β-estradiol through estrogen receptor-Sp1 interactions.

Sardi, S.P., Murtie, J., Koirala, S., Patten, B.A. and Corfas, G., 2006. Presenilin-dependent ErbB4 nuclear signaling regulates the timing of astrogenesis in the developing brain. *Cell*, *127*(1), pp.185-197.

Sarwar, N., Kim, J.S., Jiang, J., Peston, D., Sinnett, H.D., Madden, P., Gee, J.M., Nicholson, R.I., Lykkesfeldt, A.E., Shousha, S. and Coombes, R.C., 2006. Phosphorylation of ERα at serine 118 in primary breast cancer and in tamoxifen-resistant tumours is indicative of a complex role for ERα phosphorylation in breast cancer progression. *Endocrine-related cancer*, *13*(3), pp.851-861.

Scheeren, F.A., Kuo, A.H., Van Weele, L.J., Cai, S., Glykofridis, I., Sikandar, S.S., Zabala, M., Qian, D., Lam, J.S., Johnston, D. and Volkmer, J.P., 2014. A cell-intrinsic role for TLR2–MYD88 in intestinal and breast epithelia and oncogenesis. *Nature cell biology*, *16*(12), pp.1238-1248.

Scheid, M.P., Schubert, K.M. and Duronio, V., 1999. Regulation of Bad phosphorylation and association with Bcl-xL by the MAPK/Erk kinase. *Journal of Biological Chemistry*, *274*(43), pp.31108-31113.

Sengupta, S., Sharma, C.G. and Jordan, V.C., 2010. Estrogen regulation of X-box binding protein-1 and its role in estrogen induced growth of breast and endometrial cancer cells. *Hormone molecular biology and clinical investigation*, *2*(2), pp.235-243.

Shah, K.N., Bhatt, R., Rotow, J., Rohrberg, J., Olivas, V., Wang, V.E., Hemmati, G., Martins, M.M., Maynard, A., Kuhn, J. and Galeas, J., 2019. Aurora kinase A drives the evolution of resistance to third-generation EGFR inhibitors in lung cancer. *Nature medicine*, *25*(1), pp.111-118.

Shah, Y.M. and Rowan, B.G., 2005. The Src kinase pathway promotes tamoxifen agonist action in Ishikawa endometrial cells through phosphorylation-dependent stabilization of estrogen receptor α promoter interaction and elevated steroid receptor coactivator 1 activity. *Molecular endocrinology*, *19*(3), pp.732-748.

Shaulian, E. and Karin, M., 2002. AP-1 as a regulator of cell life and death. *Nature cell biology*, *4*(5), pp.E131-E136.

She, Q.B., Chen, N., Bode, A.M., Flavell, R.A. and Dong, Z., 2002. Deficiency of c-Jun-NH2-terminal kinase-1 in mice enhances skin tumor development by 12-O-tetradecanoylphorbol-13-acetate. *Cancer research*, *62*(5), pp.1343-1348.

Shou, J., Massarweh, S., Osborne, C.K., Wakeling, A.E., Ali, S., Weiss, H. and Schiff, R., 2004. Mechanisms of tamoxifen resistance: increased estrogen receptor-HER2/neu cross-talk in ER/HER2–positive breast cancer. *Journal of the National Cancer Institute*, *96*(12), pp.926-935.

Shtiegman, K., Kochupurakkal, B.S., Zwang, Y., Pines, G., Starr, A., Vexler, A., Citri, A., Katz, M., Lavi, S., Ben-Basat, Y. and Benjamin, S., 2007. Defective ubiquitinylation of EGFR mutants of lung cancer confers prolonged signaling. *Oncogene*, *26*(49), pp.6968-6978.

Siegel, R.L., Miller, K.D. and Jemal, A., 2020. Cancer statistics, 2020. *CA: a cancer journal for clinicians*, *70*(1), pp.7-30.

Sigismund, S., Avanzato, D. and Lanzetti, L., 2018. Emerging functions of the EGFR in cancer. *Molecular oncology*, *12*(1), pp.3-20.

Smith, I.E. and Dowsett, M., 2003. Aromatase inhibitors in breast cancer. *New England Journal of Medicine*, *348*(24), pp.2431-2442.

Sotgia, F., Fiorillo, M. and Lisanti, M.P., 2017. Mitochondrial markers predict recurrence, metastasis and tamoxifen-resistance in breast cancer patients: Early detection of treatment failure with companion diagnostics. *Oncotarget*, *8*(40), p.68730.

Soule, H.D., Vazquez, J., Long, A., Albert, S. and Brennan, M., 1973. A human cell line from a pleural effusion derived from a breast carcinoma. *Journal of the national cancer institute*, *51*(5), pp.1409-1416.

Sourisseau, T., Maniotis, D., McCarthy, A., Tang, C., Lord, C.J., Ashworth, A. and Linardopoulos, S., 2010. Aurora-A expressing tumour cells are deficient for homology-directed DNA double strand-break repair and sensitive to PARP inhibition. *EMBO molecular medicine*, *2*(4), pp.130-142.

Stepensky, P., Keller, B., Buchta, M., Kienzler, A.K., Elpeleg, O., Somech, R., Cohen, S., Shachar, I., Miosge, L.A., Schlesier, M. and Fuchs, I., 2013. Deficiency of caspase recruitment domain family, member 11 (CARD11), causes profound combined immunodeficiency in human subjects. *Journal of allergy and clinical immunology*, *131*(2), pp.477-485.

Studier, F.W., 1973. Analysis of bacteriophage T7 early RNAs and proteins on slab gels. *Journal of molecular biology*, *79*(2), pp.237-248.

Su, B., Luo, T., Zhu, J., Fu, J., Zhao, X., Chen, L., Zhang, H., Ren, Y., Yu, L., Yang, X. and Wu, M., 2015. Interleukin-1β/Iinterleukin-1 receptor-associated kinase 1 inflammatory signaling contributes to persistent Gankyrin activation during hepatocarcinogenesis. *Hepatology*, *61*(2), pp.585-597.

Sui, X., Kong, N., Ye, L., Han, W., Zhou, J., Zhang, Q., He, C. and Pan, H., 2014. p38 and JNK MAPK pathways control the balance of apoptosis and autophagy in response to chemotherapeutic agents. *Cancer letters*, *344*(2), pp.174-179.

Sundvall, M., Iljin, K., Kilpinen, S., Sara, H., Kallioniemi, O.P. and Elenius, K., 2008. Role of ErbB4 in breast cancer. *Journal of mammary gland biology and neoplasia*, *13*(2), pp.259-268.

Suo, Z., Risberg, B., Kalsson, M.G., Willman, K., Tierens, A., Skovlund, E. and Nesland, J.M., 2002. EGFR family expression in breast carcinomas. c-erbB-2 and c-erbB-4 receptors have different effects on survival. *The Journal of Pathology: A Journal of the Pathological Society of Great Britain and Ireland*, *196*(1), pp.17-25.

Suzuki, S., Okada, M., Shibuya, K., Seino, M., Sato, A., Takeda, H., Seino, S., Yoshioka, T. and Kitanaka, C., 2015. JNK suppression of chemotherapeutic agents-induced ROS confers chemoresistance on pancreatic cancer stem cells. *Oncotarget*, *6*(1), p.458.

Tan, M., Jing, T., Lan, K.H., Neal, C.L., Li, P., Lee, S., Fang, D., Nagata, Y., Liu, J., Arlinghaus, R. and Hung, M.C., 2002. Phosphorylation on tyrosine-15 of p34Cdc2 by ErbB2 inhibits p34Cdc2 activation and is involved in resistance to taxol-induced apoptosis. *Molecular cell*, *9*(5), pp.993-1004.

Tan, X., Lambert, P.F., Rapraeger, A.C. and Anderson, R.A., 2016. Stress-induced EGFR trafficking: mechanisms, functions, and therapeutic implications. *Trends in Cell Biology*, *26*(5), pp.352-366.

Tanaka, T., Kimura, M., Matsunaga, K., Fukada, D., Mori, H. and Okano, Y., 1999. Centrosomal kinase AIK1 is overexpressed in invasive ductal carcinoma of the breast. *Cancer research*, *59*(9), pp.2041-2044.

Tekmal, R.R., Liu, Y.G., Nair, H.B., Jones, J., Perla, R.P., Lubahn, D.B., Korach, K.S. and Kirma, N., 2005. Estrogen receptor alpha is required for mammary development and the induction of mammary hyperplasia and epigenetic alterations in the aromatase transgenic mice. *The Journal of steroid biochemistry and molecular biology*, *95*(1-5), pp.9-15.

Thor, A.D., Edgerton, S.M. and Jones, F.E., 2009. Subcellular localization of the HER4 intracellular domain, 4ICD, identifies distinct prognostic outcomes for breast cancer patients. *The American journal of pathology*, *175*(5), pp.1802-1809.

Thrane, S., Lykkesfeldt, A.E., Larsen, M.S., Sorensen, B.S. and Yde, C.W., 2013. Estrogen receptor α is the major driving factor for growth in tamoxifen-resistant breast cancer and supported by HER/ERK signaling. *Breast cancer research and treatment*, *139*(1), pp.71-80.

Thrane, S., Pedersen, A.M., Thomsen, M.B.H., Kirkegaard, T., Rasmussen, B.B., Duun-Henriksen, A.K., Laenkholm, A.V., Bak, M., Lykkesfeldt, A.E. and Yde, C.W., 2015. A kinase inhibitor screen identifies Mcl-1 and Aurora kinase A as novel treatment targets in antiestrogen-resistant breast cancer cells. *Oncogene*, *34*(32), pp.4199-4210.

Tovey, S., Dunne, B., Witton, C.J., Forsyth, A., Cooke, T.G. and Bartlett, J.M., 2005. Can molecular markers predict when to implement treatment with aromatase inhibitors in invasive breast cancer?. *Clinical cancer research*, *11*(13), pp.4835-4842.

Turner, N.C., Ro, J., André, F., Loi, S., Verma, S., Iwata, H., Harbeck, N., Loibl, S., Huang Bartlett, C., Zhang, K. and Giorgetti, C., 2015. Palbociclib in hormone-receptor–positive advanced breast cancer. *New England Journal of Medicine*, *373*(3), pp.209-219.

Turner, N.C., Slamon, D.J., Ro, J., Bondarenko, I., Im, S.A., Masuda, N., Colleoni, M., DeMichele, A., Loi, S., Verma, S. and Iwata, H., 2018. Overall survival with palbociclib and fulvestrant in advanced breast cancer. *New England Journal of Medicine*, *379*(20), pp.1926-1936.

Vader, G. and Lens, S.M., 2008. The Aurora kinase family in cell division and cancer. *Biochimica et Biophysica Acta (BBA)-Reviews on Cancer*, *1786*(1), pp.60-72.

Varešlija, D., McBryan, J., Fagan, A., Redmond, A.M., Hao, Y., Sims, A.H., Turnbull, A., Dixon, J.M., Gaora, P.O., Hudson, L. and Purcell, S., 2016. Adaptation to AI therapy in breast cancer can induce dynamic alterations in ER activity resulting in estrogen-independent metastatic tumors. *Clinical Cancer Research*, *22*(11), pp.2765-2777.

Vleugel, M.M., Greijer, A.E., Bos, R., van der Wall, E. and van Diest, P.J., 2006. c-Jun activation is associated with proliferation and angiogenesis in invasive breast cancer. *Human pathology*, *37*(6), pp.668-674.

Vollmer, S., Strickson, S., Zhang, T., Gray, N., Lee, K.L., Rao, V.R. and Cohen, P., 2017. The mechanism of activation of IRAK1 and IRAK4 by interleukin-1 and Toll-like receptor agonists. *Biochemical Journal*, *474*(12), pp.2027-2038.

von Minckwitz, G., Jonat, W., Fasching, P., du Bois, A., Kleeberg, U., Lück, H.J., Kettner, E., Hilfrich, J., Eiermann, W., Torode, J. and Schneeweiss, A., 2005. A multicentre phase II study on gefitinib in taxane-and anthracycline-pretreated metastatic breast cancer. *Breast cancer research and treatment*, *89*(2), pp.165-172.

Wagner, E.F. and Nebreda, Á.R., 2009. Signal integration by JNK and p38 MAPK pathways in cancer development. *Nature Reviews Cancer*, *9*(8), pp.537-549.

Waks, A.G. and Winer, E.P., 2019. Breast cancer treatment: a review. *Jama*, *321*(3), pp.288-300.

Wang, J., Yin, J., Yang, Q., Ding, F., Chen, X., Li, B. and Tian, X., 2016. Human epidermal growth factor receptor 4 (HER4) is a favorable prognostic marker of breast cancer: a systematic review and meta-analysis. *Oncotarget*, *7*(47), p.76693.

Wang, L., Qiao, Q., Ferrao, R., Shen, C., Hatcher, J.M., Buhrlage, S.J., Gray, N.S. and Wu, H., 2017. Crystal structure of human IRAK1. *Proceedings of the National Academy of Sciences*, *114*(51), pp.13507-13512.

Wang, R.A., Mazumdar, A., Vadlamudi, R.K. and Kumar, R., 2002. P21-activated kinase-1 phosphorylates and transactivates estrogen receptor-α and promotes hyperplasia in mammary epithelium. *The EMBO journal*, *21*(20), pp.5437-5447.

Wang, S.C., Nakajima, Y., Yu, Y.L., Xia, W., Chen, C.T., Yang, C.C., McIntush, E.W., Li, L.Y., Hawke, D.H., Kobayashi, R. and Hung, M.C., 2006. Tyrosine phosphorylation controls PCNA function through protein stability. *Nature cell biology*, *8*(12), pp.1359-1368.

Wee, Z.N., Yatim, S.M.J., Kohlbauer, V.K., Feng, M., Goh, J.Y., Bao, Y., Lee, P.L., Zhang, S., Wang, P.P., Lim, E. and Tam, W.L., 2015. IRAK1 is a therapeutic target that drives breast cancer metastasis and resistance to paclitaxel. *Nature communications*, *6*(1), pp.1-16.

Wege, A.K., Chittka, D., Buchholz, S., Klinkhammer-Schalke, M., Diermeier-Daucher, S., Zeman, F., Ortmann, O. and Brockhoff, G., 2018. HER4 expression in estrogen receptor-positive breast cancer is associated with decreased sensitivity to tamoxifen treatment and reduced overall survival of postmenopausal women. *Breast Cancer Research*, *20*(1), p.139.

Wei, Y., Zou, Z., Becker, N., Anderson, M., Sumpter, R., Xiao, G., Kinch, L., Koduru, P., Christudass, C.S., Veltri, R.W. and Grishin, N.V., 2013. EGFR-mediated Beclin 1 phosphorylation in autophagy suppression, tumor progression, and tumor chemoresistance. *Cell*, *154*(6), pp.1269-1284.

Weston, C.R. and Davis, R.J., 2007. The JNK signal transduction pathway. *Current opinion in cell biology*, *19*(2), pp.142-149.

Williams, C.C., Allison, J.G., Vidal, G.A., Burow, M.E., Beckman, B.S., Marrero, L. and Jones, F.E., 2004. The ERBB4/HER4 receptor tyrosine kinase regulates gene expression by functioning as a STAT5A nuclear chaperone. *The Journal of cell biology*, *167*(3), pp.469-478.

Wu, Y., Zhang, Z., Cenciarini, M.E., Proietti, C.J., Amasino, M., Hong, T., Yang, M., Liao, Y., Chiang, H.C., Kaklamani, V.G. and Jeselsohn, R., 2018. Tamoxifen Resistance in Breast Cancer Is Regulated by the EZH2–ERα–GREB1 Transcriptional Axis. *Cancer research*, *78*(3), pp.671-684.

Wysowski, D.K., Honig, S.F. and Beitz, J., 2002. Uterine sarcoma associated with tamoxifen use. *New England Journal of Medicine*, *346*(23), pp.1832-1833.

Xu, C., Chen, H., Wang, X., Gao, J., Che, Y., Li, Y., Ding, F., Luo, A., Zhang, S. and Liu, Z., 2014. S100A14, a member of the EF-hand calcium-binding proteins, is overexpressed in breast cancer and acts as a modulator of HER2 signaling. *Journal of Biological Chemistry*, *289*(2), pp.827-837.

Yakes, F.M., Chinratanalab, W., Ritter, C.A., King, W., Seelig, S. and Arteaga, C.L., 2002. Herceptin-induced inhibition of phosphatidylinositol-3 kinase and Akt Is required for antibody-mediated effects on p27, cyclin D1, and antitumor action. *Cancer research*, *62*(14), pp.4132-4141.

Yamamoto, M., Suzuki, S., Togashi, K., Sanomachi, T., Seino, S., Kitanaka, C. and Okada, M., 2018. AS602801, an anticancer stem cell candidate drug, reduces survivin expression and sensitizes A2780 ovarian cancer stem cells to carboplatin and paclitaxel. *Anticancer Research*, *38*(12), pp.6699-6706.

Yamashita, H., Nishio, M., Kobayashi, S., Ando, Y., Sugiura, H., Zhang, Z., Hamaguchi, M., Mita, K., Fujii, Y. and Iwase, H., 2005. Phosphorylation of estrogen receptor α serine 167 is predictive of response to endocrine therapy and increases postrelapse survival in metastatic breast cancer. *Breast cancer research*, *7*(5), p.R753.

Yamnik, R.L. and Holz, M.K., 2010. mTOR/S6K1 and MAPK/RSK signaling pathways coordinately regulate estrogen receptor α serine 167 phosphorylation. *FEBS letters*, *584*(1), pp.124-128.

Yamnik, R.L., Digilova, A., Davis, D.C., Brodt, Z.N., Murphy, C.J. and Holz, M.K., 2009. S6 kinase 1 regulates estrogen receptor α in control of breast cancer cell proliferation. *Journal of Biological Chemistry*, *284*(10), pp.6361-6369.

Yang, H., He, L., Kruk, P., Nicosia, S.V. and Cheng, J.Q., 2006. Aurora-A induces cell survival and chemoresistance by activation of Akt through a p53-dependent manner in ovarian cancer cells. *International journal of cancer*, *119*(10), pp.2304-2312.

Yang, M., Qin, X., Qin, G. and Zheng, X., 2019. The role of IRAK1 in breast cancer patients treated with neoadjuvant chemotherapy. *OncoTargets and therapy*, *12*, p.2171.

Yoshida, H., Matsui, T., Yamamoto, A., Okada, T. and Mori, K., 2001. XBP1 mRNA is induced by ATF6 and spliced by IRE1 in response to ER stress to produce a highly active transcription factor. *Cell*, *107*(7), pp.881-891.

Yu, S., Kim, T., Yoo, K.H. and Kang, K., 2017. The T47D cell line is an ideal experimental model to elucidate the progesterone-specific effects of a luminal A subtype of breast cancer. *Biochemical and biophysical research communications*, *486*(3), pp.752-758.

Zha, J., Harada, H., Yang, E., Jockel, J. and Korsmeyer, S.J., 1996. Serine phosphorylation of death agonist BAD in response to survival factor results in binding to 14-3-3 not BCL-XL. *Cell*, *87*(4), pp.619-628.

Zhang, Q., Lenardo, M.J. and Baltimore, D., 2017. 30 years of NF-κB: a blossoming of relevance to human pathobiology. *Cell*, *168*(1-2), pp.37-57.

Zhang, T., Inesta-Vaquera, F., Niepel, M., Zhang, J., Ficarro, S.B., Machleidt, T., Xie, T., Marto, J.A., Kim, N., Sim, T. and Laughlin, J.D., 2012. Discovery of potent and selective covalent inhibitors of JNK. *Chemistry & biology*, *19*(1), pp.140-154.

Zhang, Y., Guo, H., Cheng, B.C.Y., Su, T., Fu, X.Q., Li, T., Zhu, P.L., Tse, K.W., Pan, S.Y. and Yu, Z.L., 2018. Dingchuan tang essential oil inhibits the production of inflammatory mediators via suppressing the IRAK/NF-κB, IRAK/AP-1, and TBK1/IRF3 pathways in lipopolysaccharide-stimulated RAW264. 7 cells. *Drug design, development and therapy*, *12*, p.2731.

Zhao, M., Yang, M., Yang, L., Yu, Y., Xie, M., Zhu, S., Kang, R., Tang, D., Jiang, Z., Yuan, W. and Wu, X., 2011. HMGB1 regulates autophagy through increasing transcriptional activities of JNK and ERK in human myeloid leukemia cells. *BMB reports*, *44*(9), pp.601-606.

Zhao, Z.S., Lim, J.P., Ng, Y.W., Lim, L. and Manser, E., 2005. The GIT-associated kinase PAK targets to the centrosome and regulates Aurora-A. *Molecular cell*, *20*(2), pp.237-249.

Zheng, F.M., Long, Z.J., Hou, Z.J., Luo, Y., Xu, L.Z., Xia, J.L., Lai, X.J., Liu, J.W., Wang, X., Kamran, M. and Yan, M., 2014. A novel small molecule aurora kinase inhibitor attenuates Breast Tumor–Initiating cells and overcomes drug resistance. *Molecular cancer therapeutics*, *13*(8), pp.1991-2003.

Zheng, X.Q., Guo, J.P., Yang, H., Kanai, M., He, L.L., Li, Y.Y., Koomen, J.M., Minton, S., Gao, M., Ren, X.B. and Coppola, D., 2014. Aurora-A is a determinant of tamoxifen sensitivity through phosphorylation of ERα in breast cancer. *Oncogene*, *33*(42), pp.4985-4996.

Zoubir, M., Mathieu, M.C., Mazouni, C., Liedtke, C., Corley, L., Geha, S., Bouaziz, J., Spielmann, M., Drusche, F., Symmans, W.F. and Delaloge, S., 2008. Modulation of ER phosphorylation on serine 118 by endocrine therapy: a new surrogate marker for efficacy. *Annals of oncology*, *19*(8), pp.1402-1406.